Investigations into *Xpat*, a novel gene expressed in the germ plasm and primordial germ cells of *Xenopus laevis.*

Rachel Jacqueline McCormick BSc

A thesis submitted for the degree of Doctor of Philosophy

University of Warwick

Department of Biological Sciences

December 2001

Contents

Figures and Tables

Acknowledgements.

I would like to thank **Hugh Woodland** for the experimental assistance and help he has given me during the course of my PhD.

I would also like to thank **Dr. Debbie Clements** who has provided me with a great deal of help, support and good advice during my studies. She has been a source of vast amounts of scientific expertise throughout my PhD.

Thanks also go to **Dr. Maria Rex** for the great amount of support and advice she has provided over the last 4 years. She has been hugely helpful and kind and has been a fount of experimental knowledge.

I would like to thank the technical staff at Warwick University for their assistance; particular thanks go to 'Bob-the-frog' (Robert Taylor), Jean and Vanessa at the animal house and our chief technician, Steve.

I would also like to thank Emma, Chris and everyone in DB for their support and friendship over the course of my PhD, they made the experience enjoyable and worthwhile. Nads and Rich deserve a special mention for sharing a bay with me, putting up with my incessant stress levels (especially in the last 3 months) and random arm movements and also for respecting the "RNase-free zone"!

Special thanks are due to my parents for their unfailing support and encouragement over the last 25 years and to Kathryn, wise beyond her years, for listening to and supporting me throughout. Finally, extra thanks go to Lee for his love and support and the use of his computer (complete with 19" monitor), without all of these my thesis would never have been completed.

Declaration

The results presented in this thesis were obtained by the author, unless otherwise stated.

Hugh Woodland performed all injections into, and dissections of, oocytes and embryos.

All sources of information have been acknowledged by means of reference.

This work is submitted as an application for a PhD, none of this work has been used for application for any other degree.

Summary

To determine the expression pattern of XPAT (*Xenopus* primordial germ cell associated transcript) protein in *Xenopus* oocytes, XPAT-GFP fusion proteins were generated. When XPAT was amino-terminally tagged with GFP it became localised to the nuclei of stage VI *Xenopus* oocytes. However, when carboxy-terminally tagged with GFP, XPAT also translocated to the vegetal pole of stage VI oocytes. XPAT-GFP formed particles (1 to 2.5μm in diameter) which aggregated into large (10 to 50μm) granular structures at the vegetal pole. These particles looked exactly like those seen after *in situ* hybridisation to germ plasm RNAs. The granules of XPAT-GFP were larger than endogenous germ plasm granules seen in stage VI oocytes; they were more consistent with those observed in 2-cell embryos during germ plasm aggregation. Studies involving the use of the anticytoskeletal drugs colcemid, nocodazole and cytochalasin D and the microtubule stabilising agent taxol indicated that microtubular transport was important in the localisation of XPAT-GFP. Several attempts were made to raise antibodies to XPAT peptides, but at present the endogenous expression pattern of XPAT protein is unresolved.

To investigate possible domain structure of XPAT, one carboxy-terminal and three amino-terminal deletion variants of XPAT-GFP were constructed. An N-terminal deletion protein lacking the first 61 amino acids of XPAT was able to form small particles, but none of the deletion proteins exhibited vegetal localisation or formed large aggregates in *Xenopus* oocytes. The N-terminal deletion proteins all became predominantly localised to the nucleus; protein motif analysis revealed that XPAT contains a putative bipartite NLS in its carboxy-terminal region. The C-terminal deletion protein, which lacked the putative NLS, was evenly distributed throughout the nucleus and cytoplasm of *Xenopus* oocytes.

XPAT was shown to be able to bind to homopolymeric RNAs *in vitro*. When *Xpat* mRNA was depleted from stage VI *Xenopus* oocytes (by injection of an antisense oligo) levels of *DEADSouth* and *XVLG1* mRNAs decreased substantially. Overexpression of *Xpat* in oocytes caused increased levels of *DEADSouth* and *XVLG1* and more particles of *DEADSouth* were detected by *in situ* hybridisation in *Xpat*-injected oocytes than in controls. A statistically significant difference between the diameter of *Xcat-2* RNA expression domain and that of *Xdazl* and *Xpat* in control (uninjected) oocytes was also observed. These results suggest that there are distinct sets of granules within the germ plasm. However, it will be necessary to perform double *in situ* hybridisation to clarify this point.

Abbreviations

A-P	anterior-posterior
APS	Ammonium peroxidisulphate
as	antisense
ATP	adenosine triphosphate
aub	aubergine
A-V	animal-vegetal
BBR	Boehringer blocking reagent
bcd	bicoid
BCG	bacille Calmette-Guérin
BCIP	5-bromo-4-chloro-3-indoyl phosphate
BLAST	basic local alignment search tool
bp	base pairs
BRE	Bruno response element
BSA	bovine serum albumin
C-	carboxy-
capu	cappuccino
CAT	chloramphenicol acetyl transferase
cDNA	complementary deoxyribonucleic acid
Chaps	3-[(3-cholamidopropyl)-dimethyl ammonio]-1-propane sulphonate
Ci	Curie
CTD	carboxy- terminal domain
CTP	cytidine triphosphate
DAB	diamino benzamide
dATP	deoxyadenosine triphosphate
DAZ	Deleted in Azoospermia
dCTP	deoxycytidine triphosphate
dd	double-distilled
DEPC	diethyl pyrocarbonate
dGTP	deoxyguanosine triphosphate
dIF2	Drosophila translation initiation factor 2
DIG	digoxigenin-UTP

DMSO	dimethylsulfoxide
DNA	deoxyribonucleic acid
DNase	deoxyribonuclease
dNTPs	deoxynucleoside triphosphates
ds	double stranded
dTTP	deoxythymidine triphosphate
D-V	dorsoventral
EDTA	ethylene diamine tetra acetic acid
EF1α	elongation factor 1α
EGTA	ethylene glycol-bis-(β-aminoethyl ether) N,N,N',N'-tetra acetic acid
eIF4A	eukaryotic initiation factor 4A
ELISA	enzyme linked immunosorbent assay
epu	eye-piece graticule units
ER	endoplasmic reticulum
EST	express sequence tag
FITC	fluorescein isothiocyanate
FVLE1	fatvg localisation element 1
gcl	germ cell-less
GFP	green fluorescent protein
GGLE	germinal granules localisation element
GST	glutathione S-transferase
GTP	guanosine triphosphate
GV	germinal vesicle
hb	hunchback
HRP	horseradish peroxidase
IgG	Immunoglobulin G
ind	indora
IPTG	isopropyl-β-D-thiogalactoside
K	1000
Kb	kilobase pairs
kDa	kiloDalton

KH	K homology
LB	Luria-Bertani
LE	localisation element
M	molar
mago	mago nashi
MAP	multi antigenic peptide
MBP	myelin basic protein
MCLE	mitochondrial cloud localisation element
MEMFA	100mM MOPS pH7.4, 2mM EGTA, 1mM $MgSO_4$, 4%(v/v) formaldehyde
METRO	message transport organiser
MEX	muscle excess
µg	microgram
mg	milligram
µl	microlitre
ml	millilitre
µm	micrometer
µM	micromolar
mM	millimolar
MMLV	Moloney Murine Leukemia Virus
MOPS	3-[N-morpholino] propane sulphonic acid
M_r	molecular weight
mRNA	messenger ribonucleic acid
mtlrRNA	mitochondrial large ribosomal ribonucleic acid
MTOC	microtubule organising centre
mtsrRNA	mitochondrial small ribosomal ribonucleic acid
N-	amino-
NBT	nitro-blue tetrazolium
NCBI	national center for biotechnology information
NES	nuclear export sequence
ng	nanogram
nl	nanolitre
NLS	nuclear localisation signal

nM	nanomolar
nos	nanos
NRE	nanos response element
nt	nucleotide
NTMT	0.1M Tris pH9.5, 50mM $MgCl_2$, 100mM NaCl, 0.1% (v/v) Tween-20, 5mM levamisole
OCM	Oocyte culture medium
ODC	ornithine decarboxylase
oligo	oligodeoxynucleotides
ORF	open reading frame
osk	oskar
PAGE	polyacrylamide gel electrophoresis
PBS	phosphate buffered saline
PBST	phosphate buffered saline + 0.1% (v/v) Tween-20
PCR	polymerase chain reaction
pg	picogram
pgc	polar granule component
PGC	primordial germ cell
PIE	pharyngeal and intestinal excess
PMSF	phenylmethylsulphonyl fluoride
poly(A)	polyadenylic acid
poly(C)	polycytidylic acid
poly(G)	polyguanylic acid
poly(U)	polyuridylic acid
pPGC	presumptive primordial germ cell
Prrp	proline-rich RNA-binding protein
pum	pumilio
RNA	ribonucleic acid
RNAi	RNA interference
rRNA	ribosomal ribonucleic acid
RNase	ribonuclease
RRL	rabbit reticulocyte lysate
RRM	RNA recognition motif
rpm	revolutions per minute

RT	reverse transcriptase
SDS	sodium dodecyl sulphate
Spir	Spire
SSC	saline sodium citrate solution
stau	staufen
TBE(10x)	0.9M Tris.borate pH8.3, 20mM EDTA
TBS	tris buffered saline
TCE	translational control element
TE	10mM Tris.HCl pH7.5, 1mM EDTA
Tris	tris(hydroxymethyl)aminomethane
tRNA	transfer ribonucleic acid
TTP	thymidine triphosphate
Tud	Tudor
U	unit (of enzyme activity)
UTP	uridine triphosphate
UTR	untranslated region
UV	ultraviolet irradiation
V	volts
vas	vasa
VERA	Vg1 LE binding and ER association
Vg1RBP	Vg1 RNA binding protein
vls	valois
VM1	Vg1 Motif 1
(v/v)	volume/volume
(w/v)	weight/volume
Xcat	Xenopus cytoskeletal associated transcript
Xdazl	Xenopus DAZ-like
Xklp	Xenopus kinesin like protein
Xlsirts	Xenopus laevis short interspersed repeat transcripts
Xpat	Xenopus primordial germ cell associated transcript
Xpum	Xenopus pumilio
XVLG	Xenopus vasa like gene
ZBP-1	zipcode-binding protein

Abbreviations for amino acids

One-letter symbol	Three-letter abbreviation	Amino acid
A	Ala	Alanine
C	Cys	Cysteine
D	Asp	Aspartic acid
E	Glu	Glutamic acid
F	Phe	Phenylalanine
G	Gly	Glycine
H	His	Histidine
I	Ile	Isoleucine
K	Lys	Lysine
L	Leu	Leucine
M	Met	Methionine
N	Asn	Asparagine
P	Pro	Proline
Q	Gln	Glutamine
R	Arg	Arginine
S	Ser	Serine
T	Thr	Threonine
V	Val	Valine
W	Trp	Tryptophan
Y	Tyr	Tyrosine

Chapter 1: Introduction

1.1 Germ plasm and primordial germ cells

All sexually reproducing organisms arise from the fusion of two gametes. In turn, all gametes are formed from primordial germ cells (PGCs), which segregate from somatic cell lineages during early embryonic development. Ultimately germ cells give rise to all tissues in an animal; they are pluripotent. Thus, the study of germ-line development allows both the propagation of species and the differentiation of a highly specialised cell type to be investigated.

Differentiation of germ cells is often directly dependent upon the asymmetric inheritance of maternal germ cell determinants. In *Drosophila, Caenorhabditis* and *Xenopus,* such determinants are localised to a specialised region of cytoplasm, the germ plasm. Germ plasm is assembled from germ-line specific factors deposited in the egg during oogenesis. It is distinguished by the presence of specialised organelles, termed germinal granules in *Xenopus,* polar granules in *Drosophila* and P granules in *Caenorhabditis*. These granules are exclusive to germ plasm and incorporate into forming PGCs. The germinal (polar) granules are visualised by electron microscopy as electron-dense fibrillar organelles which are not bound by membranes. Germ plasm is rich in mitochondria and ribosomes and also contains RNA, protein and pigment granules (reviewed by Houston and King, 2000a). The germ granules have not been comprehensively characterised, although it is known that they contain specific RNAs that are generally not found elsewhere in the germ plasm (Strome and Wood, 1983; St. Johnston, 1995).

Many ablation, overexpression and transplantation studies have been performed which provide evidence that germ plasm is critical in the development of PGCs in *Drosophila* and *Xenopus*. Rather than discuss these experiments here, the reader is directed to a recent comprehensive review elsewhere (Houston and King, 2000a).

1.1.1 Primoridal germ cell development and migration in *Drosophila*

PGCs arise in *Drosophila* as a cluster of cells (termed pole cells) at the posterior of the blastoderm, approximately 90 to 120 minutes post-fertilisation. The arriving nuclei associate with pole plasm and are thus directed to a germ cell fate. Pole cells

cellularise in advance of the rest of the syncitial blastoderm, this process being triggered by centrioles (Raff and Glover, 1989). Pole plasm contains maternal RNAs and proteins, which are localised to the posterior pole during oogenesis by an active process requiring microtubules, and possibly microfilaments (Clark *et al.*, 1994; Pokrywka and Stephenson, 1995; Erdelyi *et al.*, 1995; Glotzer and Ephrussi, 1996). During gastrulation, pole cells become attached to the presumptive endoderm and are carried inside the embryo by the invaginations of the posterior embryo, to become located in the posterior midgut lumen. The pole cells then actively migrate posteriorly and laterally across and then along the surface of the endoderm through the gut wall and towards the developing overlying gonadal mesoderm tissue. The pole cells and somatic gonadal precursor cells then coalesce to form the gonads, which eventually contain ~20 pole cells (reviewed in Saffman and Lasko, 1999).

1.1.2 The development and migration of PGCs in *Xenopus*

The movement of germ plasm and PGCs in *Xenopus* has been followed by staining the germ plasm with lipophilic and nuclear dyes (Whitington and Dixon, 1975; Ressom and Dixon, 1988; Heasman *et al.*, 1984; Savage and Danilchik, 1993; Robb *et al.*, 1996), and using antibodies directed against cell surface antigens (Heasman and Wylie, 1983).

In the fertilised egg, germ plasm is distributed in hundreds of small cytoplasmic islands, which are distributed over a wide cortical area of the vegetal hemisphere (Whitington and Dixon, 1975; Ressom and Dixon, 1988). These islands appear to be attached to the vegetal yolk mass and they rotate with it during the first cell cycle after fertilisation (Savage and Danilchik, 1993). After cortical rotation, the islands are suddenly released from the yolk mass and begin coalescing locally and moving towards the vegetal pole (Savage and Danilchik, 1993). This aggregation continues throughout early embryonic cleavage and is dependent on microtubules (Ressom and Dixon, 1988; Savage and Danilchik, 1993). Also required is a *Xenopus* kinesin-like protein (Xklp-1), a motor protein which is found in the germ plasm throughout aggregation (Robb *et al.*, 1996). This process is not dependent on cleavage, as artificially activated eggs also show normal aggregation (Savage and Danilchik, 1993). Germ plasm thus becomes aggregated into large patches at the vegetal pole. From the 4-cell stage onwards, germ plasm ingresses into the interior of the embryo

along the cleavage furrows. Thus, by the 32-cell stage few patches of germ plasm remain at the vegetal pole and one mass of germ plasm is inherited by each of the four vegetal pole blastomeres. Ingression is dependent on cleavage, microfilaments and microtubules (Savage and Danilchik, 1993).

As cleavage continues, each patch of germ plasm becomes unequally segregated into only one of the daughter cells. By the blastula stage, the germ plasm is found in 2-6 presumptive PGCs (pPGCs) within the endodermal mass (Figure 1.1). Early in gastrulation the germ plasm becomes relocated perinuclearly (Whitington and Dixon, 1975), thereby ensuring that as cell divisions continue both daughter cells receive germ plasm and the number of pPGCs increases (Whitington and Dixon, 1975). During gastrulation and neurulation, PGCs stay in the vegetal hemisphere and follow the normal morphogenic movements of the endodermal mass, thus becoming concentrated posteriorly in the endoderm (Whitington and Dixon, 1975; Figure 1.1).

Between stages 17 and 28 (staging, according to Nieuwkoop and Faber, 1967) all PGCs coalesce into one or two clusters of cells which are located below the archenteron cavity of the endoderm. The PGCs then migrate laterally (at stage 28) and dorsally in the endoderm (between stages 31 and 36) until they reach the dorsal crest of the endoderm by stage 40. PGCs exit the endoderm and incorporate into the dorsal mesentery, which develops in the coelom at stage 41 (Whitington and Dixon, 1975). They then migrate to the gonads via the mesentery which connects the gut to the region where the mesodermal organs are forming. From stage 44 to 46, the PGCs migrate laterally from the mesentery along the abdominal wall and into the forming genital ridges (Wylie and Heasman, 1976). During migration the PGCs divide approximately 2-3 times so that 20-30 cells populate the genital ridges (Dziadek and Dixon, 1977). PGCs then migrate up the genital ridge until they reach the developing gonads, where gametogenesis then proceeds.

1.2 The intracellular localisation of mRNAs

RNA localisation is an important and common strategy used by cells to localise proteins to subcellular domains, to control protein synthesis regionally and is particularly important to asymmetrically distribute regulatory proteins into different

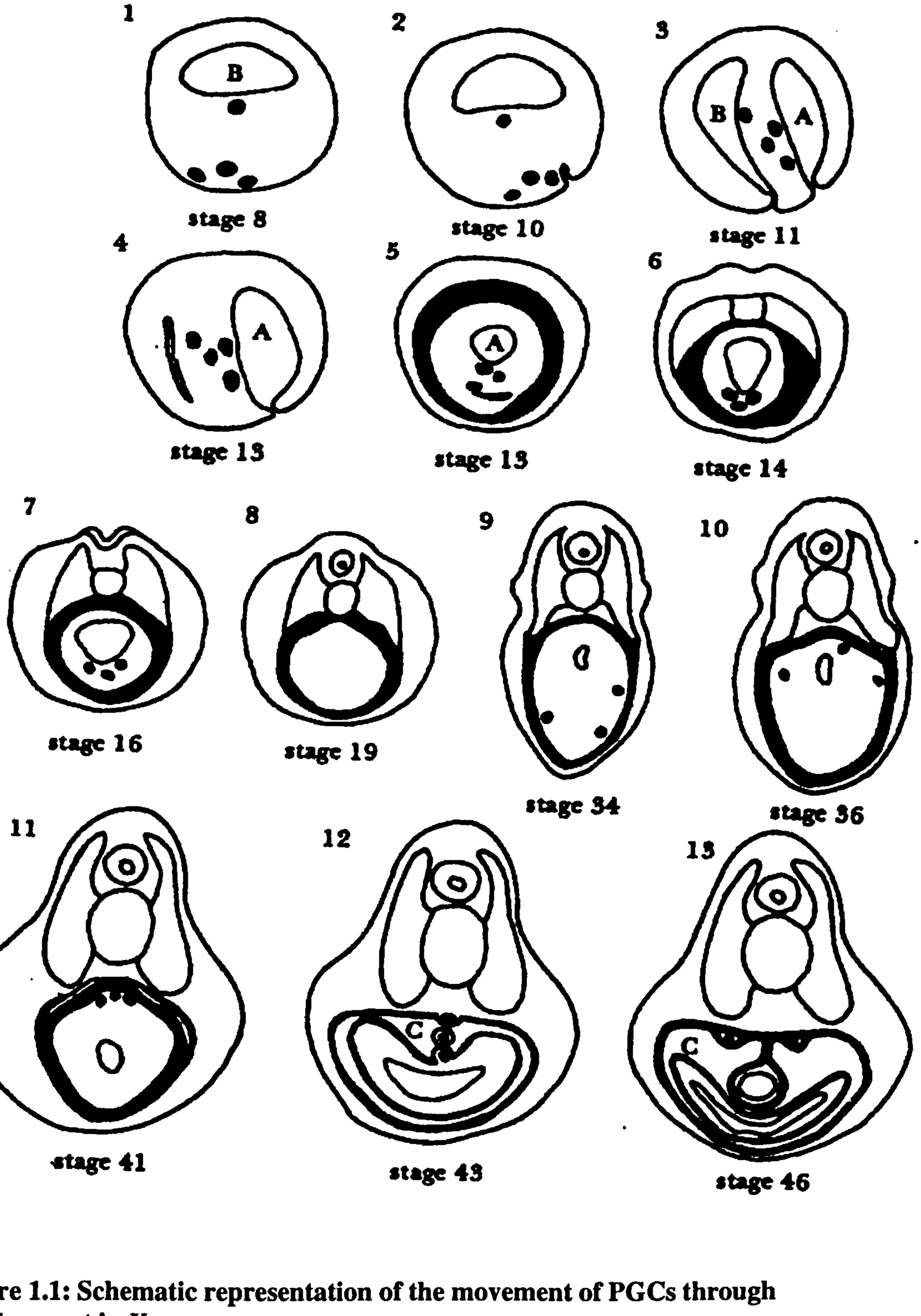

Figure 1.1: Schematic representation of the movement of PGCs through development in *Xenopus*

PGCs were followed by using a cell surface antigen. 1-4 represent longitudinal sections, 6-13 transverse sections through the hindgut region. Stages are given below. B- blastocoel, A- archenteron, C- coelom. The black dots represent PGCs. Mesoderm is represented by black shading. The PGCs are present in the endodermal mass until neurula stages. They then migrate laterally (9), and then dorsally (10-11) before leaving the endoderm and entering the mesentery (12). By stage 46 they have migrated to the genital ridges (13). Taken from Heasman and Wylie (1983).

cells during cleavage, thereby generating regional and cellular identity within the embryo (reviewed in St. Johnston, 1995; King, 1996; King *et al.*, 1999; Schnapp, 1999). There are four known methods for RNA localisation: spatial control of mRNA stability, vectorial nuclear transport, anchorage to localised binding sites and directed transport along microtubules or microfilaments (St Johnston, 1995). Whichever mechanism is used, it is critical that the localised mRNA is immobilised or anchored at the site of localisation and that its translation is coordinated with its localisation.

Significantly, initial evidence for the existence of specific localised RNAs was obtained from Ascidian eggs, where actin mRNA is enriched in the myoplasm (Jeffery *et al.*, 1983). Subsequently, many other maternal mRNAs have been shown to localise to specific regions of eggs or oocytes (for example, King and Barklis, 1985; Rebagliati *et al.*, 1985). It is now understood that RNA localisation is essential for normal embryonic development and is also used by many somatic cells to deliver proteins to discrete sites. Recently, it has been shown that the budding yeast *Saccharomyces cerevisiae* localises RNA encoding cell-fate determinants to the distal tip of daughter buds, suggesting that this mechanism is evolutionary conserved (Long *et al.*, 1997). The phenomenon of RNA localisation has been examined most extensively in oocytes and eggs. Generally oocytes and eggs are considerably larger than somatic cells, making them an easier experimental model to use, and the majority of known asymmetrically distributed RNAs localise during oogenesis and early embryogenesis (Bashirullah *et al.*, 1998). Some of the most dramatic examples of asymmetric RNA distribution during oogenesis are the specific localisation of several maternally transcribed RNAs to the anterior and posterior poles of *Drosophila* (Micklem, 1995) and *C. elegans* (Seydoux and Strome, 1999), and to the animal and vegetal poles of *Xenopus* (Smith and Williams, 1975).

The following sections summarise the steps in development and the localisation of RNAs occurring during oogenesis in *Xenopus laevis,* the species investigated in this work.

1.2.1 Morphological, subcellular and molecular changes occur during oogenesis in *Xenopus*

The development of a newly formed *Xenopus* oocyte into a fertilisable egg usually lasts 3 years, but can take as little as 9 months. During this time the oocyte undergoes a series of morphological, subcellular and molecular transformations. This process was first examined in detail and divided into six consecutive stages by Dumont (1972). Stage I oocytes arrest in diplotene and are transparent, have centrally located nuclei and do not exhibit any external signs of polarity. There is in fact only one axis that is polarised prior to fertilisation, the animal-vegetal (A-V) axis, which is set up before the onset of meiosis (Coggins, 1973). In pre-diplotene stages of oogenesis, several large mitochondrial aggregates surround the nucleus (al-Mukhtar and Webb, 1971; Kloc *et al.*, 1996) and these coalesce by stage I into a single mass called the mitochondrial cloud or Balbiani body (Balinsky and Devis, 1963) that is positioned against the future vegetal side of the nucleus (Figure 1.2). From late stage II of oogenesis, oocytes accumulate pigment and yolk and the mitochondrial cloud fragments into many islands, which move towards, and anchor at, the vegetal cortex of the oocyte (Balinsky and Devis, 1963; Tourte *et al.*, 1984; Heasman *et al.*, 1984). During this process of migration and dispersal at the vegetal pole, the mitochondrial cloud associates with granular fibrillar components of the germ plasm (Heasman *et al.*, 1984), several vegetally localised RNAs (Forristall *et al.*, 1995; Kloc and Etkin, 1995), vesicles and endoplasmic reticulum (ER) (al-Mukhtar and Webb, 1971; Billett and Adam, 1976; Tourte *et al.*, 1984). Shortly after dispersal of the mitochondrial cloud at the vegetal cortex, an ER subcompartment forms in the wedge-shaped area of the vegetal pole (Deshler *et al.*, 1997), where the components of the mitochondrial cloud were previously localised. This ER subdomain also plays a role in localisation of RNAs during oogenesis (discussed in Etkin, 1997).

Eventually, when wild-type *Xenopus* oocytes are fully grown (at stage VI), they show a striking external polarity with a dark, pigmented animal half and a light, less pigmented, vegetal hemisphere. The differences in pigmentation reflect a complex internal asymmetry at the subcellular and molecular levels. There is polarisation along the A-V axis in the distribution of organelles, with the nucleus located in the animal hemisphere. The vegetal half and/or cortex contains large yolk platelets, germ

plasm, Golgi apparatus and specialised regions of ER (Gerhart *et al.*, 1986; Hausen and Riebesell, 1991). At the molecular level, several RNAs and proteins are differentially distributed along the A-V axis.

Proteins encoded by localised maternal mRNAs are believed to direct cell-fate specification. Asymmetric cell divisions in the embryo cause localised maternal mRNAs to become segregated to particular cell groups (Forristall *et al.*, 1995), where they contribute to patterning of the mesoderm along both A-V and D-V axes (Lemaire and Gurdon, 1994). D-V axis specification also contributes to establishment of left-right asymmetry (Danos and Yost, 1995), which may also involve localised maternal factors (Lohr *et al.*, 1997). As already stated, several vegetally localised RNAs are transported with the germ plasm as part of the mitochondrial cloud in oocytes (Forristall *et al.*, 1995; Kloc and Etkin, 1995). In the embryo germ plasm is segregated into a small number of cells, which develop into PGCs (Whitington and Dixon, 1975; Ressom and Dixon, 1988; Savage and Danilchik, 1993); thus, vegetally localised RNAs in the oocyte could function as germ cell determinants (Smith and Williams, 1975). This is discussed further in Section 1.3.

1.2.1.1 Structure and function of the oocyte cytoskeleton in *Xenopus*

As mentioned previously, stage VI *Xenopus* oocytes are polarised along the A-V axis. A-V polarity also extends to the cytoskeleton, which is composed of the three major filamentous systems: microtubules (Palecek *et al.*, 1985; Gard, 1991), actin microfilaments (F-actin) (Roeder and Gard, 1994) and intermediate filaments composed of cytokeratins (Godsave *et al.*, 1984; Klymkowsky *et al.*, 1987; Torpey *et al.*, 1992; Gard *et al.*, 1997). These systems may contribute to maintenance or establishment of oocyte polarity (reviewed in Gard, 1995; Gard *et al.*, 1995; Klymkowsky, 1995). Indeed disruption of the oocyte microtubule array using nocodazole or colcemid during formation of the A-V axis blocks the vegetal localisation of maternal RNAs (Yisraeli *et al.*, 1990), and disruption of microtubules or F-actin in stage VI oocytes displaces the germinal vesicle (GV) from its normal animal pole location (Colman *et al.*, 1981; Gard, 1991, 1993; Roeder and Gard, 1994). This section details how the cytoskeleton is structured and becomes polarised during oogenesis in *Xenopus*.

Microtubules are found throughout the cytoplasm of stage I oocytes, but they are poorly ordered and there is no evidence of a microtubule organising centre (MTOC) at this stage (Gard, 1991). Starting from stage III of oogenesis, microtubules become oriented more radially, extending from the GV to the cortex of the oocyte. By stage VI the animal cytoplasm contains loose microtubule bundles which link the GV to the animal cortex, while there are fewer, less ordered microtubules extending towards the vegetal cortex (Gard, 1991). It has been suggested that the GV acts as an MTOC during the later stages of oogenesis (Gard, 1991; 1994). From stage III of oogenesis onwards, the majority of microtubules have their minus ends oriented towards the oocyte cortex and their plus ends towards the GV (Pfeiffer and Gard, 1999).

Unlike most animal cells, *Xenopus* oocytes lack centrioles and recognisable centrosomes (Gard, 1991). The maternal centrosomes are inactivated during early stage I of oogenesis before the microtubule array is polarised and prior to the establishment of A-V axis polarity (Gard, 1991). However, *Xenopus* eggs do contain a substantial amount of centrosomal components, including γ-tubulin (Stearns *et al.*, 1991). γ-tubulin was found to be concentrated near the GV surface and in the cortex of stage VI oocytes (Gard, 1994). Furthermore, γ-tubulin is asymmetrically distributed between animal and vegetal cortices of stage IV oocytes, with foci of γ-tubulin concentrated at the vegetal cortex (Gard, 1994; Gard *et al.*, 1995). This polarisation in γ-tubulin distribution coincides temporally with A-V axis formation and polarisation of the microtubule array during stage IV of oogenesis (Gard, 1994). There could, therefore, be a population of microtubules nucleated by γ-tubulin at the vegetal cortex with their minus ends at the cortex from stage IV onwards (Pfeiffer and Gard, 1999). Thus, γ-tubulin could be involved in RNA localisation to the vegetal cortex via the late pathway (see Section 1.2.2.2).

In early stage I oocytes, F-actin is found in the cortex, the GV and in a disorganised network of cables in the cytoplasm. In larger stage I oocytes, the GV and mitochondrial cloud are linked to the cortex via a dense network of actin microfilaments, but there is no evidence of a polarised distribution of F-actin (Roeder and Gard, 1994). A network of microfilaments surround the GV of stage VI oocytes

and radially oriented actin microfilaments link the animal cortex to the GV. A loose three-dimensional network of microfilaments forms in the vegetal hemisphere surrounding the yolk platelet clusters of stage VI oocytes (Roeder and Gard, 1994).

Intermediate filaments first become associated with the GV and the mitochondrial mass in previtellogenic stage I oocytes. By late stage I, they form complex networks which surround the GV and mitochondrial cloud and connect them to a network of intermediate filaments in the oocyte cortex (Godsave *et al.*, 1984; Gard *et al.*, 1997). During stage III to early stage IV, a highly interconnected network of radially oriented intermediate filaments forms, which links the cortical and perinuclear intermediate filament networks (Godsave *et al.*, 1984; Gard *et al.*, 1997). Between mid-stage IV and stage V, this network becomes polarised (Gard *et al.*, 1997), with first the animal and then the vegetal intermediate filaments becoming reoriented. Stage VI oocytes therefore contain a continuous and polarised network of intermediate filaments in their cortex. In the animal cortex, intermediate filaments form a network that is thicker and distributed in a finer mesh than the network visible at the vegetal cortex (Klymkowsky *et al.*, 1987; Gard *et al.*, 1997).

Although microtubules, microfilaments and intermediate filaments all have a distinct organisation in *Xenopus* oocytes, there is a great deal of overlap in their cytoplasmic distribution (reviewed in Gard, 1995; Gard *et al.*, 1995; Klymkowsky, 1995). Networks of all three surround the GV, are present in the cortex and link the GV to the animal cortex (Godsave *et al.*, 1984; Palacek *et al.*, 1985; Klymkowsky *et al.*, 1987; Gard, 1991; Roeder and Gard, 1994). This complex network of interactions has led to suggestions that the three cytoskeletal networks may interact or be physically associated in *Xenopus* oocytes (Gard, 1995; Klymkowsky, 1995). Indeed, confocal immunofluorescence microscopy, in combination with cytoskeletal inhibitors, was employed to demonstrate that a hierarchy of interactions between microtubules, microfilaments and intermediate filaments is necessary for A-V polarity of the oocyte cytoskeleton (Gard *et al.*, 1997).

1.2.2 RNA localisation in *Xenopus laevis* oocytes

Rebagliati *et al.* (1985) investigated how cells in different regions of embryos acquire different developmental fates by determining whether this was due to the

asymmetric distribution of specific mRNAs along the A-V axis. They demonstrated the existence of the first set of differentially localised RNAs in *Xenopus*. While most maternal RNAs were equally distributed, four were identified as being concentrated in either the vegetal (*Vg1*) or animal (*An1, An2, An3*) hemispheres. Subsequent studies revealed that although *Vg1* mRNA is uniformly distributed in stage I oocytes, it is localised to a vegetal cortical disc in stage IV oocytes (Melton, 1987). This vegetal distribution is not accompanied by any change in the RNA (Melton, 1987) and persists until oocyte maturation when *Vg1* is released from the cortex, but remains concentrated in the vegetal cytoplasm (Weeks and Melton, 1987). *Vg1* mRNA is highly enriched in a detergent insoluble fraction (Pondel and King, 1988) and is associated with the cortical cytoskeleton (Yisraeli and Melton, 1988). Vg1 protein has been implicated in the establishment of both dorsal identity (Thomsen and Melton, 1993; Joseph and Melton, 1998) and left-right asymmetry of the embryo (Hyatt *et al.*, 1996; Hyatt and Yost, 1998).

Several additional mRNAs that are either vegetally or animally localised have been described since (*An4, βTrCP, G-proteins, Oct60, PABP, PKCα, X121, Xlan4* and *Xlcaax-1* in the animal hemisphere [reviewed by Bashirullah *et al.*, 1998]; *βTrCP2*, *βTrCP3* (Hudson *et al.*, 1996), *VegT* (Zhang and King, 1996), *Xcat-2, Xcat-3 (DEADSouth)*, *Xcat-4* (Mosquera *et al.*, 1993), *Xlsirt* (Kloc *et al.*, 1993), *Xwnt-11* (Ku and Melton, 1993), *Xdazl* (Houston *et al.*, 1998) and *Xpat* (Hudson and Woodland, 1998) in the vegetal hemisphere. The *VegT* gene was independently identified as *Xombi* (Lustig *et al.*, 1996), *Antipodean* (Stennard *et al.*, 1996) and *Brat* (Horb and Thomsen, 1997) in differential or expression screens designed to isolate mesodermal patterning genes).

The animal-pole localisation of mRNAs has not been thoroughly investigated, mainly as the relative concentration of mRNAs in that hemisphere is poor (2-fold compared to >50-fold for the vegetally localised). Furthermore, unlike vegetal messages, which are cortically localised, animal localisation is rather diffuse which renders *in situ* hybridisation analysis of mRNAs technically challenging.

The first two vegetally localised clones isolated, *Vg1* and *Xcat-2*, were subjected to extensive further characterisation (Mosquera *et al.*, 1993; Forristall *et al.*, 1995; Zhou and King, 1996b). These studies showed marked differences to exist between the localisation of *Xcat-2* and *Vg1* during oogenesis. Unlike *Vg1*, *Xcat-2* is not uniformly distributed in stage I oocytes but is localised to the mitochondrial cloud. *Xcat-2* transcripts then move with the mitochondrial cloud to form a small patch at the vegetal pole at stage II. Subsequently *Xcat-2* RNA forms islands, consistent with its being a component of the germ plasm. *Xcat-2* remains cortically localised during oogenesis, its distribution being more restricted than *Vg1* (Figure 1.2). Moreover, *Xcat-2*, unlike *Vg1*, is retained in the vegetal cortex after oocyte maturation (Mosquera *et al.*, 1993). *Xcat-2* remains in a stippled pattern at the vegetal pole, in contrast to the broad ubiquitous vegetal hemisphere distribution of *Vg1*, until it disappears at blastula stages (Mosquera *et al.*, 1993; Forristall *et al.*, 1995).

These observations led to the suggestion that there are two distinct pathways for the localisation of RNAs to the vegetal cortex of *Xenopus* oocytes (Forristall *et al.*, 1995; Kloc and Etkin, 1995): the early mitochondrial cloud pathway, which localises *Xcat-2* (see Section 1.2.2.2) and a late stage III pathway which *Vg1* utilises (Melton, 1987; Yisraeli *et al.*, 1990) (see Section 1.2.2.3). These pathways are illustrated in Figure 1.2. Other RNAs which are distributed at the vegetal pole also appear to localise via one of these pathways. Transcripts which utilise the early pathway also appear to be able to localise via the late pathway (see Section 1.2.2.4).

1.2.2.1 The early pathway for vegetal RNA localisation – the METRO

The early pathway is established prior to and during stage I of oogenesis and occurs mainly during the first two stages of oogenesis. It involves the transport of various RNAs within a specific area of the mitochondrial cloud, termed the message transport organiser (METRO). The METRO-mediated localisation pathway has been divided into three steps: transport of RNAs from their site of synthesis in the GV into the mitochondrial cloud, sorting of the transcripts to specific regions within the cloud, and translocation of the entire structure to the vegetal cortex of the oocyte where the different transcripts appear to become anchored in the order *Xcat-2*, *Xlsirt* and finally *Xwnt-11* (Kloc and Etkin, 1995; Kloc *et al.*, 1996). Vegetal localisation of RNAs via the METRO is not dependent on microtubules or microfilaments.

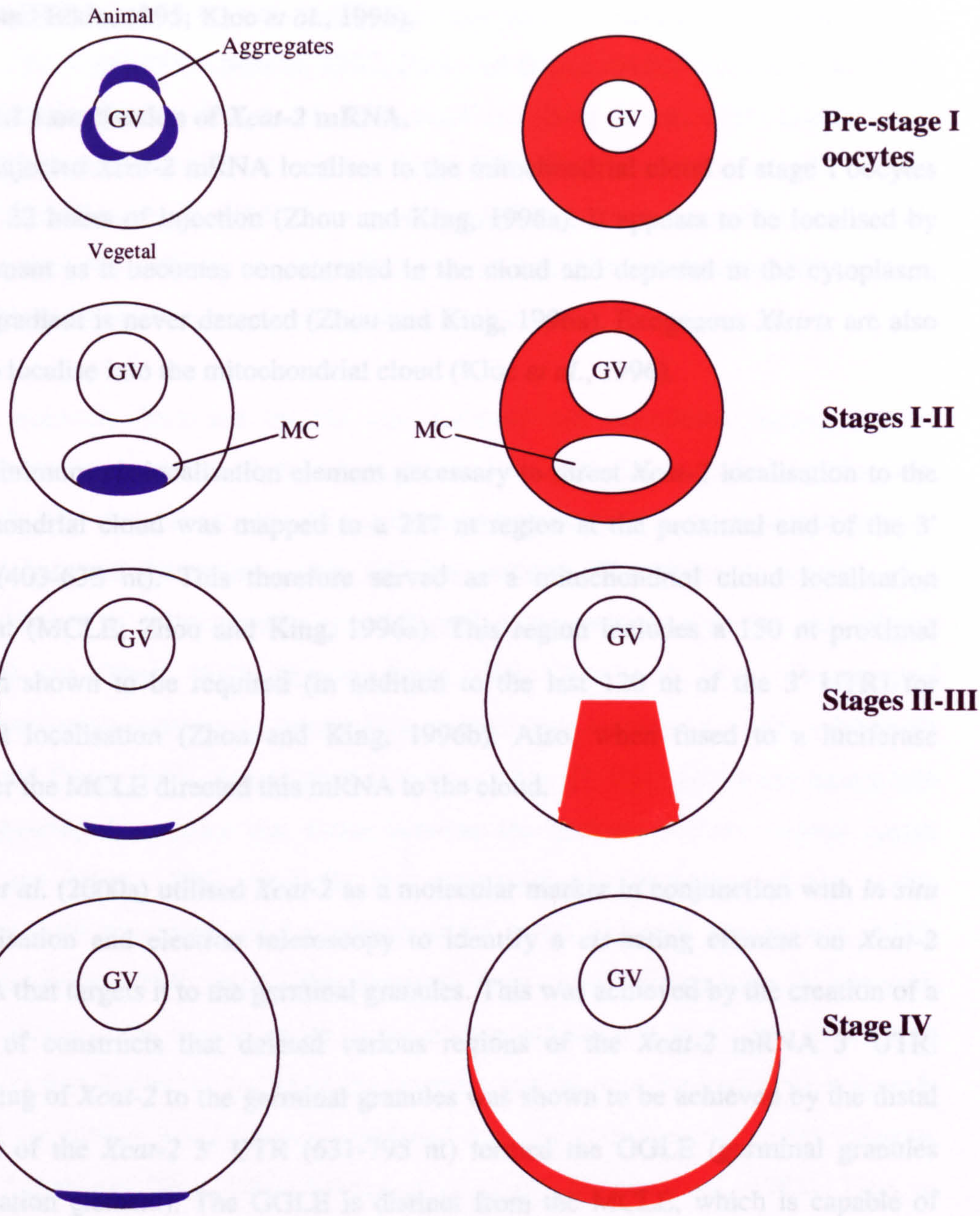

Figure 1.2: Vegetal RNA localisation pathways in *Xenopus* oocytes

Lateral views. GV, germinal vesicle; MC, mitochondrial cloud. **Early pathway**: RNAs localised via the early pathway include *Xcat-2, Xwnt-11* and *Xlsirts,* and are shown in blue in this diagram. These transcripts first associate with the mitochondrial aggregates surrounding the nucleus (GV) in pre-stage I oocytes. As the mitochondrial aggregates coalesce to form the mitochondrial cloud during stage I, early pathway RNAs localise to its future vegetal side. At late stage II of oogenesis, coincident with the fragmentation of the mitochondrial cloud, early pathway RNAs move towards the vegetal cortex in a wedge-shaped pattern and disperse in a disc-shaped region at the vegetal pole. **Late pathway:** *Vg1* RNA is localised by the late pathway and is depicted in red in this figure. *Vg1* is ubiquitously expressed in the cytoplasm of stage I and II oocytes, but is excluded from the mitochondrial cloud. During stage II-III of oogenesis, *Vg1* colocalises with an ER-subcompartment in a wedge-shaped region of the vegetal hemisphere also occupied by METRO RNAs. *Vg 1* moves to the vegetal pole during stages II-III and becomes distributed along the entire vegetal cortex during stage IV of oogenesis. (Adapted from Schnapp *et al.,* 1997; King *et al.,* 1999).

Microfilaments are, however, necessary for tight anchorage at the vegetal cortex (Kloc and Etkin, 1995; Kloc *et al.*, 1996).

1.2.2.1.1 Localisation of *Xcat-2* mRNA.

Microinjected *Xcat-2* mRNA localises to the mitochondrial cloud of stage I oocytes within 22 hours of injection (Zhou and King, 1996a). It appears to be localised by entrapment as it becomes concentrated in the cloud and depleted in the cytoplasm, yet a gradient is never detected (Zhou and King, 1996a). Exogenous *Xlsirts* are also able to localise into the mitochondrial cloud (Kloc *et al.*, 1996).

The minimum *cis*-localisation element necessary to direct *Xcat-2* localisation to the mitochondrial cloud was mapped to a 227 nt region at the proximal end of the 3′ UTR (403-630 nt). This therefore served as a mitochondrial cloud localisation element (MCLE; Zhou and King, 1996a). This region includes a 150 nt proximal domain shown to be required (in addition to the last 120 nt of the 3′ UTR) for cortical localisation (Zhou and King, 1996b). Also, when fused to a luciferase reporter the MCLE directed this mRNA to the cloud.

Kloc *et al.* (2000a) utilised *Xcat-2* as a molecular marker in conjunction with *in situ* hybridisation and electron microscopy to identify a *cis*-acting element on *Xcat-2* mRNA that targets it to the germinal granules. This was achieved by the creation of a series of constructs that deleted various regions of the *Xcat-2* mRNA 3′ UTR. Targeting of *Xcat-2* to the germinal granules was shown to be achieved by the distal 164 nt of the *Xcat-2* 3′ UTR (631-795 nt) termed the GGLE (germinal granules localisation element). The GGLE is distinct from the MCLE, which is capable of targeting *Xcat-2* to the mitochondrial cloud, but not to the germinal granules (Zhou and King, 1996a,b; Kloc *et al.*, 2000a). Thus, the 3′ UTR of *Xcat-2* possesses a compound localisation element in which the proximal 227 nt contain a *cis*-acting element (MCLE) responsible for localisation of the RNA to the mitochondrial cloud and a distal 164 nt GGLE that is necessary and sufficient to target it to the germinal granules within the cloud. The GGLE was sufficient to target a non-granule mitochondrial cloud associated RNA to the germinal granules (Kloc *et al.*, 2000a).

1.2.2.2. The late pathway for RNA localisation to the vegetal cortex

The late pathway of vegetal localisation was initially described for *Vg1* mRNA (Rebagliati *et al.*, 1995; Melton, 1987; Kloc and Etkin, 1995; Forristall *et al.*, 1995) and subsequently for *Xcat-4*, *B9*, *B12*, *VegT* and *fatvg* (King, 1995; Lustig *et al.*, 1996; Stennard *et al.*, 1996; Zhang and King, 1996; Horb and Thomsen, 1997; Zhang *et al.*, 1998; Chan *et al.*, 1999). However, since only the former has been extensively investigated, the pathway is also referred to as *Vg1*-like localisation. Other RNAs from this group behave in a similar fashion to *Vg1*.

RNAs normally localised by the late pathway are distributed homogeneously throughout the cytoplasm of stage I oocytes and are excluded from the mitochondrial cloud. In late stage II oocytes, *Vg1* mRNA aggregates into a crescent-shaped body located between the vegetal pole and the nucleus. The crescent consists of a concentration of mitochondria and ER and also contains spectrin and tubulin (Palacek and Ubbels, 1997; Kloc and Etkin, 1998; Chan *et al.*, 1999). The onset of *Vg1* localisation involves its microtubule-independent binding to an ER subdomain (Kloc and Etkin, 1998). At late stage II to early stage III, *Vg1* mRNA aggregates into a wedge-shaped structure that forms between the crescent and the vegetal cortex (Kloc and Etkin, 1995). Spatially and temporally the formation of the wedge overlaps with movement of the mitochondrial cloud (Yisraeli and Melton, 1988; Kloc and Etkin, 1994, 1995, 1998; Forristall *et al.*, 1995). From stage IV onwards, *Vg1* migrates to the vegetal cortex of the oocyte and anchors there. The localisation of *Vg1* is first limited to the tip of the oocyte's vegetal pole but over time it spreads toward the equator and becomes distributed over the entire vegetal cortex (Melton, 1987; Pondel and King, 1988; Yisraeli *et al.*, 1990; Elinson *et al.*, 1993). Thus, in comparison to the METRO RNAs, localised *Vg1* occupies a broader region of the vegetal cortex (Kloc and Etkin, 1995).

The translocation of *Vg1* to the vegetal hemisphere was shown, using cytoskeletal inhibitors and immunohistochemistry, to be dependent on cytoplasmic microtubules. Conversely, the anchoring of *Vg1* at the vegetal cortex is achieved with the involvement of cortical actin microfilaments (Yisraeli *et al.*, 1990). Thus, the oocyte cytoskeleton is critical in the localisation of transcripts by the *Vg1*-like pathway (Yisraeli *et al.*, 1990).

The anchoring step has also been demonstrated to depend upon the correct localisation of the formerly anchored *Xlsirts* transcripts (Kloc and Etkin, 1994). This dependence of *Vg1* (but not *Xcat-2*) on *Xlsirts* localisation was shown by disruption of *Xlsirts* with antisense oligodeoxynucleotides, which resulted in release of *Vg1* from the vegetal cortex.

Light and electron microscopy *in situ* hybridisation have been used to show that RNAs localised by the late pathway are excluded from the germ plasm in oocytes and embryos (Kloc *et al.*, 1998).

1.2.2.2.1 The localisation of *Vg1* RNA

After Yisraeli and Melton (1988) demonstrated that exogenous *Vg1* mRNA localises in the same way as endogenous *Vg1* in middle stage oocytes, sequences present in *Vg1* RNA that are required for its localisation became the subject of extensive searches. A 340 nt sequence from the *Vg1* 3′ UTR was found to be both necessary and sufficient to direct localisation of *Vg1* to the vegetal cortex (Mowry and Melton, 1992). Subsequently, sequence elements and protein binding sites have been discovered in this localisation element (LE) (Schwartz *et al.*, 1992; Gottlieb, 1992; Elisha *et al.*, 1995; Mowry, 1996; Deshler *et al.*, 1997; Gautreau *et al.*, 1997).

Mutational analysis of the *Vg1* LE identified an 85 nt subelement from the 5′ end of the 340 nt sequence, which when duplicated is sufficient to direct vegetal localisation (Gautreau *et al.*, 1997). Furthermore, a repeated 6 nt sequence motif (UUUCUA) called VM1 (Vg1 motif 1) was identified within the subelement that is vital for localisation (Gautreau *et al*, 1997). Point mutations within VM1 abolish *Vg1* localisation *in vivo*. VM1 is believed to act as a binding site for an essential *trans*-acting localisation factor (Gautreau *et al.*, 1997).

Transport of *Vg1* RNA is thought to begin with recognition of the RNA LE by proteins involved in localisation (Melton, 1987; Yisraeli *et al.*, 1990; Mowry, 1996). *Vg1* RNA-binding proteins (VgRBPs) with potential roles in the localisation process have been identified by their ability to specifically bind to the *Vg1* LE. There are 6 polypeptides that become cross-linked to the *Vg1* LE upon UV irradiation, named according to their molecular weights as p78, p69, p60, p40, p36 and p33 (Mowry,

1996). Two of the cross-linked proteins have been identified. p69 is Vg1RBP/Vera (Schwartz *et al.*, 1992; Havin *et al.*, 1998; Deshler *et al.*, 1998). Vg1RBP and Vera were separately isolated as two proteins, but have now been shown to be identical. This protein is highly homologous to the microfilament- and RNA-binding Zipcode binding protein (ZBP-1). ZBP-1 is involved in *β-actin* mRNA localisation in chick embryonic fibroblasts (Ross *et al.*, 1997). The predicted amino acid sequences of ZBP-1 and Vg1RBP/Vera contain five putative RNA-binding motifs: one RRM and four KH domains. p60 is a homologue of human hnRNP1 and is referred to as VgRBP60 (Cote *et al.*, 1999).

Vg1RBP/Vera associates with both *Vg1* RNA and microtubules and is necessary for their association (Elisha *et al.*, 1995). This protein also binds to a Vg1RBP binding site present in the rat *tau* RNA 3′ UTR which, upon injection, localises to the vegetal pole of stage III-IV oocytes in a distribution indistinguishable from *Vg1* RNA (Litman *et al.*, 1996). *Tau* RNA is localised in rat axons and cell bodies in a microtubule-dependent manner. This is strong evidence that Vg1RBP is involved in vegetal localisation of RNAs in oocytes. Apart from its microtubule association, an ER association of Vg1RBP was suggested by Deshler *et al.* (1997, 1998) based on the colocalisation of *Vg1* mRNA with a marker of the rough ER. Sequences necessary for Vg1RBP binding were also required for RNA localisation, implying a link between these processes (Deshler *et al.*, 1997). ER vesicles have been shown to be transported along microtubules (discussed in Deshler *et al.*, 1997), and the ER is found near to the cytoskeleton at the vegetal cortex (Elinson *et al.*, 1993).

VgRBP60 is an essential *trans*-acting localisation factor which, like Vg1RBP, directly interacts with *Vg1*'s VM1 motif and colocalises with *Vg1* in the vegetal cytoplasm. The base modifications within VM1 which specifically block VgRBP60 binding were shown to abolish *Vg1* RNA localisation *in vivo* (Cote *et al.*, 1999).

Recently, Prrp (proline-rich RNA-binding protein; Zhao *et al.*, 2001a) has been identified, which colocalises with *Vg1* at the vegetal cortex in stage IV oocytes and also interacts with *Vg1*'s LE.

Vg1RBP/Vera, VgRBP60 and Prrp all colocalise with *Vg1* RNA in the vegetal cortex in oocytes, and Vg1RBP/Vera and VgRBP60 share distribution patterns with *Vg1* RNA during localisation. These results indicate that these 3 proteins are likely to be in a complex with *Vg1* during translocation to the vegetal cortex. They could all be involved in cortical anchoring, RNA targeting and/or translational control.

1.2.2.3 Continuity between the early and late RNA localisation pathways

Kloc and Etkin (1998) first proposed a model in which the establishment of the late localisation pathway is a sequential process that involves interaction with the METRO. This proposal was based upon the observations that the initial step in *Vg1* localisation in stage II oocytes involves microtubule-independent association with the wedge-shaped subdomain of the ER, closely associated with movement of the mitcochondrial cloud. The mitochondrial cloud was also seen to overlap with a γ-tubulin–containing body that may function as an MTOC during stage III and IV of oogenesis (Kloc and Etkin, 1998).

The two vegetal localisation pathways in the *Xenopus* oocyte are not exclusive in their choice of RNA targets. Therefore, in stage III/IV oocytes, where endogenous *Xcat-2* has already localised to the vegetal cortex via the METRO, injected *Xcat-2* can also localise to the vegetal pole in a similar manner to, though not as efficiently as, *Vg1* mRNA. This process is sensitive to microtubule depolymerisation (Zhou and King, 1996b). Similarly, when *Xpat* mRNA is injected into stage III oocytes it localises in a broader domain than the germ plasm at the vegetal pole, appearing much like *Vg1*. This is in contrast to endogenous *Xpat* which localises, via the METRO, to the germ plasm (Hudson and Woodland, 1998). This indicates that there are *cis*- and *trans*-acting factors common for the two localisation pathways. However, it is not clear if there might be some long-term maintenance of *Xcat-2* and *Xpat* mRNAs in the germ plasm via continual synthesis and transport by the *Vg1* pathway.

Chan *et al.* (1999) defined a 25 nt element (FVLE1) present in the *fatvg* 3′ UTR that could direct localisation of *fatvg* through the late pathway. This element is different from any of the *Vg1* LEs. *fatvg* mRNA exhibits a localisation pattern similar, though not identical, to *Vg1*. However, some *fatvg* mRNA associates with the mitochondrial

cloud in stage II oocytes immediately before the late pathway functions. Electron microscopy *in situ* hybridisation revealed that *fatvg* RNA is localised in the germ plasm matrix, but is excluded from the germinal granules (Chan *et al.*, 2001). Thus, *fatvg* demonstrates the overall characteristic of a late pathway RNA, but also associates with the mitochondrial cloud and germ plasm, as METRO RNAs do. Thus, *fatvg* localisation also suggests there is continuity between the METRO and late pathways (Chan *et al.*, 1999, 2001).

1.3 Molecules localised to the germ plasm

The following sections summarise what is known about molecules localised to the germ plasm in the two most extensively examined species: *Drosophila* (reviewed in Gavis, 1997; Houston and King, 2000a) and *Xenopus laevis*, the system investigated in this work (Reviewed by Schnapp *et al.*, 1997; King *et al.*, 1999; Houston and King, 2000a). There are also several known genes which affect germ cell development in *Caenorhabditis elegans*. Rather than discuss these here, the reader is instead directed to recent reviews elsewhere (Wylie, 1999; Seydoux and Strome, 1999).

1.3.1 Genes involved in *Drosophila* pole cell development

The pathway of genes involved in pole cell development in *Drosophila* is summarised in Figure 1.3.

1.3.1.1 *oskar*

oskar (*osk*) is the inducer of pole plasm assembly in *Drosophila* and is critical for germ-line formation. *osk* RNA is localised to the posterior pole of the oocyte when germ plasm forms (Ephrussi *et al.*, 1991). The amount of *osk* at the posterior pole determines the number of pole cells formed (Ephrussi and Lehmann, 1992; Smith *et al.*, 1992). Replacement of the *osk* 3′ UTR with that of *bicoid (bcd)*, an RNA which localises to the anterior pole, causes *osk* to be mislocalised to the anterior of the oocyte. Ectopic pole plasm and functional pole cells form at the anterior pole and a second abdomen forms in mirror image to the posterior abdomen (Ephrussi and Lehmann, 1992).

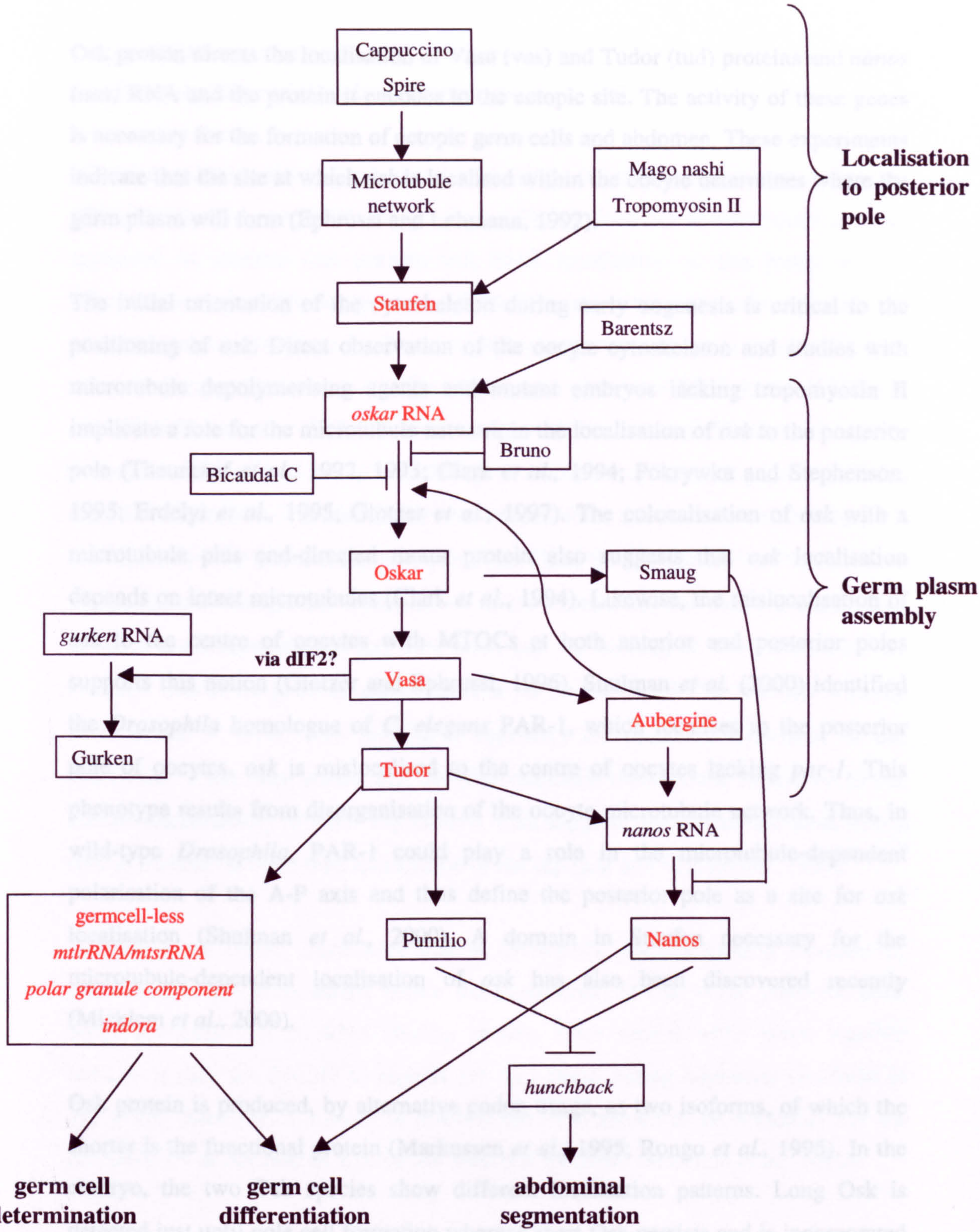

Figure 1.3: The hierarchy of genes involved in the assembly of pole plasm and abdominal segmentation in *Drosophila*

The diagram illustrates the majority of genetic interactions discussed in Section 1.3.1. Proteins are in normal type, RNAs in *italics* and putative and proven germ granule components are in red. Lines ending with arrowheads indicate positive interaction, activation or localisation, whereas lines ending with a vertical bar indicate translational repression by a *trans*-acting factor. The question mark adjacent to dIF2 is because it is unknown whether this protein is directly involved in activation of *gurken* translation by Vasa. Valois, orb and homeless have not been included in the figure as their roles in germ plasm formation are, as yet, unclear. (Adapted from Rongo and Lehmann, 1996).

Osk protein directs the localisation of Vasa (vas) and Tudor (tud) proteins and *nanos (nos)* RNA and the protein it encodes to the ectopic site. The activity of these genes is necessary for the formation of ectopic germ cells and abdomen. These experiments indicate that the site at which *osk* is localised within the oocyte determines where the germ plasm will form (Ephrussi and Lehmann, 1992).

The initial orientation of the cytoskeleton during early oogenesis is critical to the positioning of *osk*. Direct observation of the oocyte cytoskeleton and studies with microtubule depolymerising agents and mutant embryos lacking tropomyosin II implicate a role for the microtubule network in the localisation of *osk* to the posterior pole (Theurkauf *et al.*, 1992, 1993; Clark *et al.*, 1994; Pokrywka and Stephenson, 1995; Erdelyi *et al.*, 1995; Glotzer *et al.*, 1997). The colocalisation of *osk* with a microtubule plus end-directed motor protein also suggests that *osk* localisation depends on intact microtubules (Clark *et al.*, 1994). Likewise, the mislocalisation of *osk* to the centre of oocytes with MTOCs at both anterior and posterior poles supports this notion (Glotzer and Ephrussi, 1996). Shulman *et al.* (2000) identified the *Drosophila* homologue of *C. elegans* PAR-1, which localises to the posterior pole of oocytes. *osk* is mislocalised to the centre of oocytes lacking *par-1*. This phenotype results from disorganisation of the oocyte microtubule network. Thus, in wild-type *Drosophila*, PAR-1 could play a role in the microtubule-dependent polarisation of the A-P axis and thus define the posterior pole as a site for *osk* localisation (Shulman *et al.*, 2000). A domain in Staufen necessary for the microtubule-dependent localisation of *osk* has also been discovered recently (Micklem *et al.*, 2000).

Osk protein is produced, by alternative codon usage, as two isoforms, of which the shorter is the functional protein (Markussen *et al.*, 1995; Rongo *et al.*, 1995). In the embryo, the two Osk species show different localisation patterns. Long Osk is detected just until pole cell formation whereas short Osk persists and is incorporated into the pole cells. Short Osk can rescue the defects of *osk* pole plasm mutants, whereas long Osk cannot (Markussen *et al.*, 1995). Osk protein directly interacts with both Vas and Staufen proteins in a yeast two-hybrid assay (Breitwesser *et al.*, 1996) and only the functional short Osk can recruit these proteins to the posterior pole. They in turn, along with Tud and Osk itself, aid the accumulation of Osk

protein at the posterior pole (Markussen *et al.*, 1995). One of Vas's functions is in the phosphorylation of short Osk (Breitwesser *et al.*, 1996).

The correct localisation of *osk* is required for its translation (Gavis and Lehmann, 1994; Markussen *et al.*, 1995; Rongo *et al.*, 1995). Indeed *osk* remains translationally repressed in mutants that prevent *osk* RNA localisation to the posterior pole (Markussen *et al.*, 1995; Rongo *et al.*, 1995). Premature translation of *osk* outside the posterior pole is prevented by Bruno, which recognises and binds specifically to a conserved repeated sequence (the Bruno response element – BRE) in the 3′ UTR of *osk* (Kim-Ha *et al.*, 1995; Webster *et al.*, 1997; Lie and Macdonald, 1999). Translation of localised *osk* is specifically activated via an element present in the 5′ region of the mRNA. The element is only needed when the transcript is repressed via the BRE and only active at the posterior pole. Thus, the 5′ region of *osk* functions as a translational derepressor element. A direct correlation has been demonstrated between the derepression of *osk* translation and the binding of two proteins to this element. One of the proteins which binds to the 5′ end of *osk* also interacts with the BRE in the 3′ UTR. This binding is necessary for complete repression of *osk* translation. It has been shown that the BRE-mediated translational regulation of *osk* occurs independently of the 5′ cap *in vitro*. This suggests that Bruno interferes with a step in translation other than recognition of the cap (Lie and Macdonald, 1999).

Saffman *et al.* (1998) discovered that in *Drosophila* oocytes lacking *Bicaudal-C*, translation of *osk* commenced before the localisation of *osk* to the posterior pole. Since Bicaudal-C is an RNA-binding protein, these results when taken together indicate it may act directly to repress *osk* translation during oogenesis (Saffman *et al.*, 1998). Recently, a domain in Staufen has been shown to be necessary for the derepression of *osk* mRNA translation after it is localised (Micklem *et al.*, 2000).

1.3.1.2 Genes required for the localisation of *oskar*

The localisation of *osk* to the posterior pole of the oocyte and thus assembly of pole plasm material there is dependent on the activity of the following genes: *cappuccino (capu), spire (spir), staufen (stau), valois (vls), mago nashi (mago), orb, homeless* and *tropomyosin II*. These genes and their products will not be discussed further

here, but have been reviewed extensively elsewhere (Rongo and Lehmann, 1996; Rongo *et al.*, 1997).

Recently, another gene required for the localisation of *osk* mRNA has been described, *barentsz* (van Eeden *et al.*, 2001). In contrast to other defined mutations that affect this process, oocytes lacking *barentsz* exhibit no posterior localisation of *osk*, but have wild-type *bicoid* and *gurken* localisation and microtubule organisation and show no alteration in subsequent steps in pole plasm assembly. Barentsz protein colocalises with *osk* to the posterior pole and this localisation is dependent on *osk* mRNA. However, Barentsz, unlike Staufen, does not remain in the posterior pole and only colocalises with *osk* during the stages when it is being transported. Thus, Barentsz is essential for the movement of *osk* from the anterior to the posterior pole and it acts like a specific component of the *osk* localisation complex (van Eeden *et al.*, 2001).

1.3.1.3 Nanos

In *Drosophila*, the apparatus which localises the germ plasm also localises the posterior determinant in embryonic patterning, Nanos (Nos) (Wang and Lehmann, 1991; Rongo and Lehmann, 1996). In fertilised eggs, only *nos* mRNA at the posterior pole is translated (Gavis and Lehmann, 1994), which creates a gradient of Nos protein emanating from the posterior (Gavis and Lehmann, 1994; Dahanukar and Wharton, 1996).

Nos is a zinc-finger protein, which together with another protein Pumilio (Pum), acts to repress translation of maternal *hunchback (hb)* in the posterior pole allowing development of the abdomen (Barker *et al.*, 1992; Tautz and Pfeifle, 1989). Pum is an RNA-binding protein which can specifically bind the *nos* response elements (NREs) in the 3′ UTR of *hb* (Wharton and Struhl, 1991; Murata and Wharton, 1995; Zamore *et al.*, 1997). Pum is distributed throughout the embryo, yet is only able to *repress hb* translation in the posterior pole, thus it has been suggested that interaction of RNA-bound Pum with posteriorly localised *nos* mediates translational repression (Murata and Wharton, 1995). A *Xenopus* Pumilio homologue has recently been cloned and shown to bind *Xcat-2* mRNA, a homologue of *nos* (Nakahata *et al.*, 2001) (see Section 1.3.2.2).

Nos protein localised at the posterior pole of fertilised eggs incorporates into forming germ cells. Nos is present in germ cells throughout embryogenesis, but is absent from the rest of the embryo (Wang *et al.*, 1994). Nos protein is also detected in germ-line stem cells and developing cystoblasts in the adult ovary (Wang *et al.*, 1994). While not necessary for pole cell formation, maternal Nos protein is essential for the migration of germ cells to the gonads, after their exit from the posterior midgut (Forbes and Lehmann, 1998), and to prevent premature gene expression in pole cells (Kobayashi *et al.*, 1996).

In *pum* mutants, ovaries fail to maintain stem cells and all germ-line cells differentiate into egg chambers. However, Nos appears to function in differentiation of the cytoblast, the stem cell progeny (Forbes and Lehmann, 1998). Thus, it has been suggested that in germ-line development, in contrast to embryonic patterning, Nos and Pum may interact with different partners.

nos RNA is localised to the posterior pole by a large *cis*-acting signal in the *nos* 3′ UTR (Gavis and Lehmann, 1992, 1994; Gavis *et al.*, 1996). Translation of unlocalised *nos* RNA is repressed by a 90 nt translational control element (TCE) located at the proximal end of the 3′ UTR (Gavis *et al.*, 1996; Dahanukar and Wharton, 1996; Smibert *et al.*, 1996). Only a small proportion of all *nos* RNA in an embryo is localised to the posterior pole, thus indicating that restriction of Nos protein to the posterior pole must occur by translational repression (Gavis and Lehmann, 1994; Bergsten and Gavis, 1999). Bergsten and Gavis (1999) increased the number of potential sites in *nos* available for binding of translational repressors and localisation factors by using multiple copies of *nos* 3′ UTR elements in transgenes. They determined that localisation of *nos* and its translational repression are mutually exclusive; indeed RNA localisation of *nos* activates its translation by preventing *nos* RNA from interaction with translational repressors. This is achieved by a 180 nt region of the *nos* localisation element, which contains the TCE (and the +2′ element, see later; Dahanukar and Wharton, 1996; Bergsten and Gavis, 1999).

Smaug protein is distributed uniformly throughout the early *Drosophila* embryo and can bind to the *nos* TCE (*in vitro* and) *in vivo* and prevent its translation outside of

the posterior pole (Smibert *et al.*, 1996; Dahanukar *et al.*, 1999). Smaug was also shown to physically interact with Osk, which is critical for the activation of *nos* RNA. These observations indicate that Smaug is important in restricting Nos protein to the posterior of the embryo (Dahanukar *et al.*, 1999).

Genetic analysis implicates Osk, Vas and Tud in a localisation complex which anchors *nos* RNA to the posterior pole (reviewed by Gavis, 1997). Bergsten and Gavis (1999) suggested that the binding of *nos* 3′ UTR localisation elements by distinct factors promotes association of *nos* RNA with germ plasm components. Recently, Evans-Bergsten *et al.* (2001) dissected the minimal requirements for function of the *nos* localisation signal by focusing on the 88 nt +2′ element, which is located directly adjacent to the TCE (at its proximal side) within the *nos* 3′ UTR. A protein (p75) present in ovaries and embryos was found to specifically recognise a 41 nt domain within the +2′ element, that is highly conserved between *D. melanogaster* and *D. virilis*. Mutations disrupting binding of p75 to the +2′ element also disrupted *in vivo* localisation, thus implicating p75 in *nos* RNA localisation.

1.3.1.4 Aubergine

Aubergine (Aub) is a cytoplasmic protein that is related to eukaryotic translation initiation factor 2C (eIF2C) and thus may have a direct role in translational activation. Aub accumulates in pole plasm in a *vas*-dependent manner and is itself a component of the polar granules, whilst *aub* mRNA is not localised in the oocyte (Harris and Macdonald, 2001). *aub* mutants do not demonstrate efficient translation of *osk* and thus have defective pole cell formation and posterior patterning. Aub protein has a role in the posterior localisation of *nos* (Wilson *et al.*, 1996), as well as in pole cell formation (Harris and Macdonald, 2001). However, Aub's role in pole cell formation appears to be independent from its role in the activation of *osk* translation (Harris and Macdonald, 2001). This was demonstrated as *osk* translation begins before accumulation of Aub at the posterior pole, and can occur even if the Aub concentration is reduced at the posterior pole. Using *aub* embryos and an *osk-bcd* transgene, which localises anteriorally, Aub was shown to be necessary for ectopic pole cell development and therefore also likely to be involved in this process at the posterior pole (Harris and Macdonald, 2001).

There are a number of localised mRNAs that affect *Drosophila* germ cell formation, but not that of the abdomen (via *nanos*). These are discussed in the following sections.

1.3.1.5 *germcell-less*

germcell-less (gcl) encodes a protein that specifically associates with the nuclei which migrate into pole plasm and become incorporated into pole cells. Reduction of maternal *gcl* mRNA levels causes the resulting embryos to lack pole cells, yet they have a normal posterior axis (Jongens *et al.*, 1992). Similarly, transgenic mothers which overexpress *gcl* produce progeny with increased numbers of pole cells. However, these pole cells undergo fewer divisions or die before or during the formation of the cellular blastoderm. Mislocalisation of *gcl* RNA to the embryo's anterior pole causes the ectopic initiation of events similar to those seen during normal pole cell formation (Jongens *et al.*, 1994). These effects did not occur as a result of ectopic localisation of any other pole cell components but solely as a result of *gcl* concentration. Mutant embryos completely lacking *gcl* failed to establish a germ-line. *gcl* activity was shown to be required for formation of proper pole buds and pole cells and survival of pole cells (Robertson *et al.*, 1999). High-resolution, three-dimensional wide-field microscopy and immunoelectron microscopy was used to analyse the subcellular localisation of Gcl. Gcl protein was seen to associate specifically with the nuclear pores of pole cells (Jongens *et al.*, 1994). The correct localisation of Gcl to the nuclear envelope was found to be critical for formation of pole cells, but was not required to initiate and form proper pole buds (Robertson *et al.*, 1999).

1.3.1.6 *polar granule component*

An untranslated RNA, termed *polar granule component (pgc)* was identified and found to localise to polar granules. *pgc* is expressed only in female germ cells (Nakamura *et al.*, 1996). Transgenic female flies expressing antisense *pgc* RNA contained pole cells which failed to complete migration or populate the embryonic gonads; and their *nos* and *gcl* RNA and Vas protein signals were reduced in intensity. Furthermore, females that developed from these embryos frequently had ovaries which completely lacked gametes. Thus, *pgc* RNA has an essential role in the

differentiation of pole cells into functional germ cells in females (Nakamura *et al.*, 1996).

1.3.1.7 *indora*

indora (ind) mRNA is expressed specifically in pole cells within embryonic gonads. Antisense reduction of *idr* mRNA in embryos causes failure of pole cells to develop into functional germ cells in females. Thus, induction of *idr* in pole cells is, like *pgc*, necessary for correct germ-line development in females (Mukai *et al.*, 1999).

1.3.1.8 *mitochondrial rRNAs*

Mitochondrial large ribosomal RNA (mtlrRNA) localises to *Drosophila* pole plasm and injection of *mtlrRNA* into UV-sterilised embryos restores pole cell (though not functional germ cell) formation (Kobayashi and Okada, 1989). Because *mtlrRNA* is exclusively encoded by the mitochondrial genome, it appears that it is transported out of mitochondria to reach polar granules in germ plasm (Kobayashi and Okada, 1989). A combination of light and electron microscopy *in situ* hybridisation has shown that *mtlrRNA* is present outside mitochondria and localises to the polar granules within the pole plasm of early cleavage embryos. However, it does not localise to the granules of pole cells (Kobayashi *et al.*, 1993, 1994, 1995; Amikura *et al.*, 1996). The localisation of *mtlrRNA* is dependent on the function of *osk*, *vas* and *tud* genes (Ding *et al.*, 1994; Kobayashi *et al.*, 1994; 1995). The injection of anti-*mtlrRNA* ribozymes into cleavage embryos reduces *mtlrRNA* in germ plasm and inhibits pole cell formation (Iida and Kobayashi, 1998). *osk* and *gcl* mRNAs and Vas and Tud proteins are not affected in these embryos. Thus, while *mtlrRNA* has an essential role in pole cell formation (Iida and Kobayashi, 1998), it is not required for the differentiation of pole cells into functional germ cells (Kobayashi and Okada, 1989; Amikura *et al.*, 1996).

Mitochondrial small ribosomal RNA (mtsrRNA) has also been identified as a component of polar granules (Kashikawa *et al.*, 1999). The temporal and spatial distribution of *mtsrRNA* is essentially identical to that of *mtlrRNA*, and *mtsrRNA* localises on polar granules of cleavage stage embryos. As for *mtlrRNA*, *mtsrRNA* localisation is dependent on the function of *osk*, *vas* and *tud* genes (Kashikawa *et al.*, 1999). It has recently been shown that *mtsrRNA* and *mtlrRNA* both localise in

mitochondrial-type ribosomes formed on the surface of the polar granules for a short time prior to pole cell formation (Amikura *et al.*, 2001b). Ultrastructural analysis indicates that at least two mitochondrial ribosomal proteins are found in these ribosomes, as well as in mitochondria. These mitochondrial-type ribosomes are smaller than cytosolic ribosomes and are integrated into polysomes (active sites of translation) on the polar granules. Furthermore, ribosomes were only seen on polar granules when the *mtrRNAs* and proteins were present on the granules. Amikura *et al.* (2001b) proposed that translation from these mitochondrial-type ribosomes is important in formation of the *Drosophila* germ-line.

1.3.1.9 Vasa

Vas protein is detected throughout the development of the germ-line in *Drosophila.* Maternal Vas incorporates into pole cells and is distributed in embryonic gonads and in the germ-line throughout oogenesis. During mid-oogenesis, Vas protein localises to the pole plasm at the posterior pole of the oocyte, and its localisation depends upon the functions of *capu, spir, osk* and *stau* (Hay *et al.*, 1988a,b, 1990; Lasko and Ashburner, 1990; Liang *et al.*, 1994). The recruitment of other molecules to the pole plasm later in oogenesis (including *nos, pum, gcl, mtlrRNA* and Tud protein) depends on *vas* function. *vas* null embryos are defective in many aspects of oogenesis, including oocyte differentiation; *vas* females produce few or no eggs (Lasko and Ashburner, 1988). Furthermore, *vas*-null oocytes cannot efficiently accumulate *orb, Bicaudal-D, osk* or *nos,* but are still able to accumulate *gurken* mRNA. However, Gurken protein accumulation is severely reduced in *vas* ovaries. *vas* mutants show A-P and D-V axis polarity defects which appear to be linked to the reduction in Gurken protein levels (Tomancak *et al.*, 1998). Vas functions in activating *gurken* translation early in oogenesis and aids accumulation of *gurken* mRNA later in oogenesis (Styhler *et al.*, 1998; Tomancak *et al.*, 1998).

Vas is a member of the DEAD-box family of putative RNA helicases, similar to eukaryotic initiation factor 4A (eIF4A) (Hay *et al.*, 1988b). Vas has been shown to function as an ATP-dependent RNA helicase *in vitro,* and *vas* mutants that cannot bind RNA do not form polar granules (Liang *et al.*, 1994). Recruitment of Vas to the pole plasm is dependent on protein-protein interactions, but after localisation Vas binds RNA to mediate formation of germ cells (Liang *et al.*, 1994). The posterior

accumulation of Vas is mediated by its interaction with Osk protein (Breitwesser *et al.*, 1996). Recently Vas protein has been shown to directly interact with the *Drosophila* homologue of yeast translation initiation factor 2, encoded by *dIF2, in vitro and in vivo* (Carrera *et al.*, 2000). Therefore, Vas may regulate translation of germ-line mRNAs by interacting specifically with dIF2 (Carrera *et al.*, 2000).

1.3.1.10 Tudor

Vas protein is necessary for the recruitment of Tud to the polar granules. *tud* RNA is not found in the oocyte, thus the protein is apparently transported from the nurse cells (Golumbeski *et al.*, 1991). Tud protein is found in the mitochondria present in pole plasm and around cleavage stage nuclei, as well as in germ granules (Bardsley *et al.*, 1993). *tud* mutants do not form polar granules or pole cells, thus *tud*, like *osk* and *vas*, is absolutely required for determination and formation of pole cells (Boswell and Mahowald, 1985). Furthermore, as with *osk*, the number of pole cells that form in embryos is proportional to the amount of Tud protein that accumulates at the posterior pole (Bardsley *et al.*, 1993). It has recently been discovered that embryos derived from *tud* females exhibit reduced localisation of *mtlrRNA* and *mtsrRNA*. In normal embryos, Tud protein colocalises with the two *mtrRNA*s at the boundaries between polar granules and mitochondria, when *mtrRNA* transport occurs. Thus Tud appears to be required for mediating transport of *mtrRNAs* from mitochondria to polar granules (Amikura *et al.*, 2001a).

1.3.2 *Xenopus* germ plasm localised RNAs

Over the last decade, a number of RNAs that localise to the germ plasm of *Xenopus* have been identified (reviewed in Wylie, 1999; King *et al.*, 1999). However, only recently have functional studies allowed the roles of some of these RNAs to be determined (reviewed in Houston and King, 2000a; Kloc *et al.*, 2001).

1.3.2.1 *Xcat-2*

Xcat-2 (*Xenopus cytoskeletal associated transcript 2*) was originally isolated and characterised by Mosquera *et al.* (1993) (see Section 1.2.2). *Xcat-2* mRNA was seen, by *in situ* hybridisation, to localise to the mitochondrial cloud and it moves with the cloud material to the vegetal cortex early in oogenesis (Forristall *et al.*, 1995). *Xcat-2* mRNA has a distribution pattern entirely consistent with it being a germ plasm

component (Forristall *et al.*, 1995; Kloc *et al.*, 1998). Indeed Kloc *et al.* (1998) showed that, at the ultrastructural level, *Xcat-2* mRNA is localised on the germinal granules themselves.

Xcat-2 encodes a protein that is a member of the CCHC RNA-binding family of Zinc finger proteins, and is closely related to Nos (Mosquera *et al.*, 1993). Xcat-2 protein is able to bind RNA in an *in vitro* assay (MacArthur *et al.*, 1999). Using an Xcat-2 specific antibody, MacArthur *et al.* (1999) showed that *Xcat-2* is translationally repressed during oogenesis and is not expressed until early embryogenesis. Indeed, *Xcat-2* RNA was found to be tightly associated with a dense complex in oocytes, consistent with its translationally repressed state. Replacing the *Xcat-2* 3′ UTR with that of *β-globin* did not alleviate this translational inhibition, thus the 3′ UTR does not appear to be involved in the translational repression of *Xcat-2* mRNA. Xcat-2 protein is expressed during blastulation and gastrulation, which coincides temporally with the movement of germ plasm to a perinuclear location and subsequent symmetric segregation of germ plasm and increase in pPGC numbers (MacArthur *et al.*, 1999).

1.3.2.2 Xpum

The *Xenopus* homologue of Pumilio has been recently identified (Nakahata *et al.*, 2001). Nakahata *et al.* (2001) isolated a cDNA clone encoding a protein homologous (78% identity) to *Drosophila* Pumilio in the domain defining this family. A monoclonal antibody was raised against the Pumilio domain, and it was able to cross react with the *Xenopus* homologue of Pumilio (Xpum) in oocytes and eggs. This protein can bind to the NRE of *Drosophila hb* mRNA, as can *Drosophila* Pum. Using UV-crosslinking studies it was shown that, like Pum, Xpum can specifically bind to the 3′ UTR of *cyclin B1* mRNA. Furthermore, Xpum physically associates with Xcat-2 (the *Xenopus* Nanos homologue) in an *in vitro* protein pull-down assay (Nakahata *et al.*, 2001). However, as Xcat-2 protein is absent from oocytes and eggs (MacArthur *et al.*, 1999), Xcat-2 was undetectable in anti-Xpum immunoprecipitates from oocytes extracts. Thus, it is not yet known whether Xpum acts together with a Nanos homologue to control mRNA translation in oocytes. Although the role of

Xpum is unknown at present, Nakahata *et al.* (2001) hypothesised that Xpum is important in translational control of *cyclin B1* mRNA, as in *Drosophila.*

1.3.2.3 *DEADSouth*

DEADSouth (Xcat-3) was originally isolated in a screen for vegetally localised maternal RNAs (Elinson *et al.*, 1993; Moquera *et al.*, 1993). It was later shown, by *in situ* hybridisation analysis of oocytes and early embryos that *DEADSouth* RNA localises to the vegetal cortex via the mitochondrial cloud early in oogenesis, is expressed in a pattern characteristic of germ plasm and is a germ-line specific RNA (MacArthur *et al.*, 2000). Multiple sequence analysis of DEADSouth indicated that it is more like the RNA-dependent helicase eIF4A than other developmentally important DEAD-box proteins (MacArthur *et al.*, 2000). Preliminary experiments suggest that *DEADSouth,* unlike *Xcat-2,* is not localised to the germinal granules themselves but is found in the cytoplasm surrounding them (M. L. King unpublished observations, cited in Houston and King, 2000a).

1.3.2.4 *Xdazl*

Xdazl mRNA is expressed in the germ plasm from early oocytes until the neurula stage (Houston *et al.*, 1998). *Xdazl* mRNA localisation in the oocyte is restricted first to the mitochondrial cloud and then to the vegetal cortex (Houston *et al.*, 1998). Xdazl protein is first detected in blastulae (Houston and King, 2000b) and is seen in PGCs in the endoderm until early tailbud stages (stage 22). Within the cell, Xdazl protein is cytoplasmic and localised to the germ plasm (Houston and King, 2000b). *Xdazl* RNA must therefore be under translational control, like *Xcat-2* (Houston and King, 2000b; MacArthur *et al.*, 1999). Xdazl is an RNA-binding protein homologous to the human Deleted in Azoospermia (DAZ) and related proteins in many species and contains a consensus RNP domain (Houston *et al.*, 1998). As *Xdazl* encodes an RNA-binding protein (Houston *et al.*, 1998) and the protein is cytoplasmic (Houston and King, 2000b), possible roles for Xdazl include regulation of translation, RNA transport, RNA storage or regulation of RNA stability. *Xdazl* mRNA was depleted from stage VI *Xenopus* oocytes and these oocytes fertilised by the host-transfer technique. *Xdazl*-depletion caused PGC numbers to be greatly reduced; this loss of PGCs occurs at the late tailbud stage, at or near the time when PGCs normally begin their dorsal migration. PGCs lacking *Xdazl* appear laterally but do not migrate

dorsally. *Xdazl* can act as the functional homologue of *Drosophila* boule, a protein required for meiotic entry during spermatogenesis (Houston *et al.*, 1998).

1.3.2.5 *mitochondrial rRNAs*

Mitochondrial large rRNA (mtlrRNA) was shown to be a component of the germ plasm in *Xenopus* from 4-cell to blastula stage (Kobayashi *et al.*, 1998). Electron microscopy *in situ* hybridisation revealed that the *mtlrRNA* signal was present within the germinal granules during these stages (Kobayashi *et al.*, 1998).

Recently, *mtsrRNA* has also been identified as a common component of the germinal granules in *Xenopus* embryos (Kashikawa *et al.*, 2001). *mtsrRNA* has a distribution pattern identical to that of *mtlrRNA*, namely it is localised on the surface of the germinal granules from 4-cell to blastula stage and then disappears until the end of gastrulation. Kloc *et al.* (2000b) re-examined the distribution of *mtlrRNA* and *mtsrRNA* and found that, contrary to the findings of Kobayashi *et al.* (1998), the mitochondrial rRNAs are located in close proximity to the germinal granules but are not major components of the granules themselves. In fact the majority of *mtlrRNA* and *mtsrRNA* was found to be present within mitochondria and, to a lesser extent, the germ plasm matrix (Kloc *et al.*, 2000b). The temporal distribution of the *mitochondrial rRNAs* (4-cell to blastulae) coincides with the inheritance of germ plasm by only one daughter cell. This may indicate a role for *mtlrRNA* or *mtsrRNA* in restricting the association of germ plasm to one pole of the mitotic spindle during cleavage at these stages. However, this is purely speculative and it is not yet known whether these RNAs are functional in germ plasm.

1.3.2.6 *Xlsirts*

Xlsirts are a family of interspersed repeat transcripts from *Xenopus laevis* that have in common a 79- to 81- nucleotide sequence tandemly repeated 3-13 times. Each of the *Xlsirts* possesses unique flanking sequences on each side of the tandem repeat unit. The transcripts do not contain start codons and do not appear to be translated (Kloc *et al.*, 1993). *Xlsirt* RNA is first localised in the mitochondrial cloud in early stage II oocytes and is then distributed in island-like structures at the vegetal pole by stage III, thus colocalising with the germ plasm. At the ultrastructural level, *Xlsirts* is detected within the germ plasm, but is not associated with germinal granules in stage

II-IV oocytes (Kloc *et al.*, 1998). In embryos *Xlsirts* remains associated with the germ plasm. Recently four proteins were shown, using UV-crosslinking studies, to interact with the *Xlsirts* localisation signal in the vegetal cortex of stage V-VI oocytes. The evidence suggests that one of the proteins is Vg1RBP/Vera (Bubunenko and King, 2001).

1.3.2.7 *XVLG1*

Besides *Xdazl,* the only other molecule with a defined role in germ plasm in *Xenopus* is the *Xenopus Vasa-like gene-1 (XVLG-1)* (Komiya *et al.,* 1994; Ikenishi *et al.,* 1996; Ikenishi and Tanaka, 1997). XVLG1 shares 8 highly conserved amino acid regions (with the exception of 1 amino acid in 1 of these regions), with the DEAD-box family of proteins, and it is most similar to *Drosophila* Vasa (Komiya *et al.,* 1994). *XVLG-1* RNA is expressed in adult testis and ovaries, as well as in pPGCs from late gastrula (stage 12) to hatching tadpole stage (stage 33/34) and in some of the PGCs at stages 49-50 (Komiya *et al.*, 1994; Ikenishi and Tanaka, 2000). *In situ* hybridisation analysis of *Xenopus* oocytes reveals that *XVLG-1* RNA is present in stage I-III oocytes, but is barely detectable in stage IV-VI oocytes. It was detected throughout the cytoplasm except in the mitochondrial cloud of stage I oocytes. XVLG-1 protein is present in the germ plasm from gastrula stage 12, but is also found around the somatic cell nuclei (Ikenishi *et al.,* 1996). The protein remains in association with PGCs until stage 46 and in somatic cells until stage 42, although the amount of protein is much greater in germ-line cells than in somatic cells (Ikenishi *et al.*, 1996). Injection of an anti-XVLG1 antibody revealed that the presence of XVLG-1 protein is necessary for the differentiation of germ plasm-containing cells into PGCs during and after stages 37/38 (Ikenishi and Tanaka, 1997). However, injection of antibody into somatic cells had no effect on their development. Therefore, like its homologue in *Drosophila*, XVLG-1 is important in germ-line development.

1.3.2.8 *Xwnt-11*

Xwnt-11 encodes a secreted protein related to the Wnt family and its mRNA is vegetally localised (Ku and Melton, 1993). *Xwnt-11* RNA is translocated to the vegetal cortex via the METRO pathway during stage I of oogenesis and is found in the germ plasm during oogenesis and embryonic development. However, like *Xlsirts*

and *DEADSouth, Xwnt-11* is not detected on the germinal granules (Kloc *et al.*, 1998). The presence of *Xwnt-11* in the germ plasm led Kloc *et al.* (1998) to suggest that a Wnt-directed signalling pathway could aid specification of the germ cell lineage.

1.3.2.9 *Xpat*

Xpat (Xenopus primordial germ cell associated transcript) encodes a novel protein and its RNA is localised to the germ plasm and PGCs of *Xenopus* throughout oogenesis and early embryogenesis. *Xpat* mRNA expression persists longer than any other known *Xenopus* germ plasm transcripts, and can be detected by *in situ* hybridisation in PGCs of stage 40 tadpoles (Hudson and Woodland, 1998). *Xpat* RNA has been demonstrated, using electron microscopy *in situ* hybridisation, to be localised on the germinal granules (Etkin, 2000). *Xpat* is discussed further in Section 1.4.

1.3.3 The role of localised molecules in germ plasm

The maternal localisation of RNAs coding for RNA-binding proteins appears to be a common theme in germ cell determination. RNAs for *nanos* and *vasa* are well known components of *Drosophila* pole plasm, and they encode proteins that are implicated in RNA-binding. Specifically in *Xenopus, Xcat-2* (a *nanos*-like gene, Mosquera *et al.*, 1993), *DEADSouth* (a translation initiation factor-like putative RNA helicase, MacArthur *et al.*, 2000) and *Xdazl* (which contains an RNP domain and is the functional homologue of *Drosophila boule,* Houston *et al.*, 1998) are also expressed in the germ plasm and have putative RNA-binding roles.

How the inheritance of RNAs coding for RNA-binding proteins establishes the germ-line is still unclear, but it has been hypothesised that the mechanism may involve germ cell-specific regulation of mRNA stability or splicing, or translational repression. There appears to be a role for translational control (activation or repression) of maternal mRNAs in germ-line specification. For example, the Nanos/Pumilio complex is involved in translational repression of *hunchback* RNA in *Drosophila* (Murata and Wharton, 1995), and translational suppression by Nanos is necessary for entry of PGCs into the *Drosophila* gonad (Kobayashi *et al.*, 1996). Germ plasm components also appear to be subjected to this translational control

mechanism, Nanos protein is never detected in *Drosophila* oocytes, and injected *nanos* RNA is not translated in the oocyte (Gavis and Lehmann, 1994). Different *cis*-elements in the 3′ UTR of *nanos* are responsible for localisation and control of translation (Gavis *et al.*, 1996; Dahanuka and Wharton, 1996). Like *nanos*, *Xcat-2* is also translationally repressed during oogenesis and is not translated until early embryogenesis (MacArthur *et al.*, 1999). The recent discovery of a Pumilio homologue in *Xenopus* indicates that its function as a translational regulator could also be conserved in *Xenopus*.

The germ plasm may act as a protective enclave from signals involved in somatic cell lineage determination (Dixon, 1994). Transcriptional repression in PGCs may act to protect these cells from a somatic cell fate. Germ-line blastomeres in *C. elegans*, in contrast to somatic cells, were found to be lack newly transcribed mRNAs during early cleavage stages (Seydoux *et al.*, 1996). This transcriptional suppression was demonstrated to require PIE-1 protein, a germ-line specific factor which, when ectopically expressed in somatic blastomeres, could also repress transcription in these cells (Seydoux *et al.*, 1996). PIE-1 was found to specifically block phosphorylation of RNA polymerase II large subunit carboxy-terminal domain (CTD), which is normally phosphorylated during eukaryotic mRNA transcription (Seydoux and Dunn, 1997). A sequence element in PIE-1 that is required for PIE-1 to function as a transcriptional repressor *in vitro* resembles the CTD of RNA polymerase II (Batchelder *et al.*, 1999). PIE-1 may therefore act to block transcription in germ-line blastomeres by targeting factors that can bind to the CTD (Batchelder *et al.*, 1999). A period of transcriptional repression has also been observed in *Drosophila* pole cells (Seydoux and Dunn, 1997; Van Doren *et al.*, 1998), which indicates that a general block in transcription may be a conserved feature of germ cell specification.

1.4 The germ granule mRNA *Xpat*

Xpat (Xenopus primordial germ cell associated transcript) was isolated from a cDNA library screen designed to isolate mRNAs specific to vegetal poles of *Xenopus* gastrula embryos (Hudson and Woodland, 1998). *In situ* hybridisation analysis of *Xpat* revealed that it is localised at the vegetal pole of early stage I oocytes and associates with the mitochondrial cloud during oogenesis. *Xpat* mRNA is specifically

localised to the germ plasm throughout oogenesis and embryogenesis (see Figure 1.4) and, unlike any other known germ plasm RNAs, *Xpat*'s expression persists after gastrulation until stage 40 (Figure 1.4). Thus, the expression of *Xpat* mRNA ceases at the time when PGCs are known to enter the dorsal mesentery (Hudson and Woodland, 1998). It is thought that all the *Xpat* mRNA localised in embryos is purely maternal, as Northern blots indicate that no zygotic transcription of *Xpat* occurs (Hudson and Woodland, 1998).

Hudson and Woodland (1998) also demonstrated that the large ~3 kb 3′ UTR of *Xpat* is both necessary and sufficient to localise injected *Xpat* mRNA to the vegetal pole in stage III oocytes. The injected *Xpat* mRNA, unlike endogenous *Xpat*, localised in a domain that was broader than the germ plasm at the vegetal pole, appearing similar to the distribution of *Vg1*. Furthermore, exogenous *Xpat* mRNA did not localise to the vegetal pole in stage V or VI oocytes, thus it only localises at stages where the late pathway has been shown (by Yisraeli and Melton, 1988) to be active. Thus, whilst endogenous *Xpat* localises via the METRO, exogenous *Xpat* can localise via the late pathway of RNA localisation (see Section 1.2.2). Exogenous XPAT protein was shown to have no effect on the localisation of injected *Xpat* mRNA (Hudson and Woodland, 1998).

Xpat is a novel clone which encodes a predicted protein of 303 amino acids, with a molecular weight of 35kDa. When it was isolated, *Xpat* was found to have no convincing homology to any known proteins (Hudson and Woodland, 1998). Recent searches, performed in November 2001 using the NCBI BLAST database, revealed that the 3′UTR has a 140 bp region (a repetitive element) which appears in the *Silurana tropicalis* Zinc-finger transcription factor *Slug* gene and smaller parts of this region are present in the *X. laevis cerberus* 3′ UTR, the *X. borealis type I cytoskeleton actin* mRNA and the *X. laevis VhVI* gene for immunoglobulin heavy chain as well as many other *Xenopus* mRNAs. Small 20 bp regions of the 5′ UTR have homology to various clones of human DNA sequences and others, but nothing of note in the EST databases (other than *X. laevis* clones and various short sequence matches). The nucleotide sequence of the ORF has only limited regions of homology – over ~20-30 bp regions - to various human and *Drosophila* genomic DNA

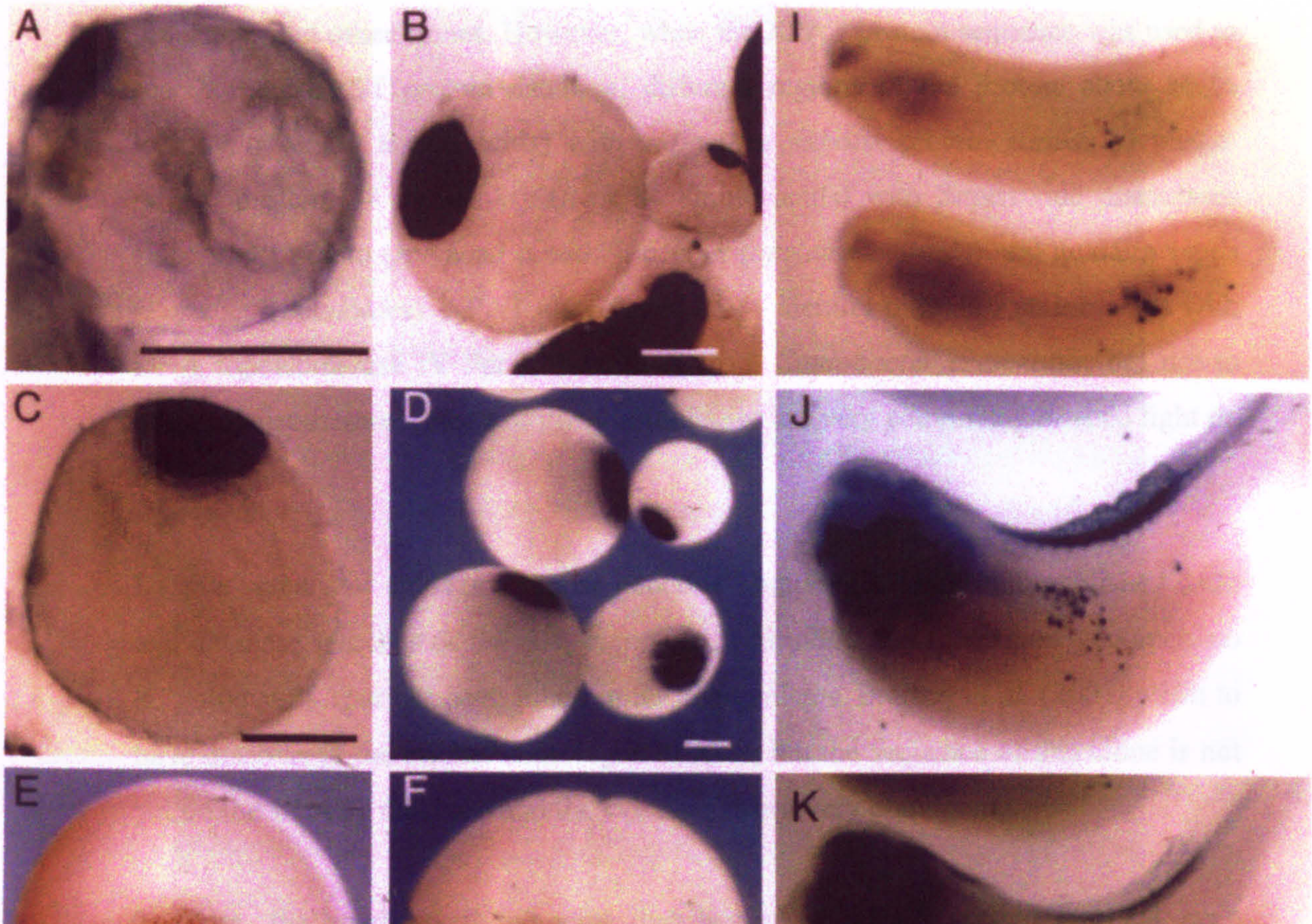

Figure 1.4: Localisation of *Xpat* mRNA assessed by *in situ* hybridisation

(A-D) Stage I-III oocytes (Dumont, 1972); *Xpat* transcripts are localised to the vegetal pole from stage I (A), remaining there during stages II (B, C) and III (D). (E, F) In cleavage stage embryos the signal takes on a granular appearance in a small disc at the vegetal pole. During gastrulation (stage 10.5, G) the cells that contain *Xpat* move inside, and remain there through neurulation (stage 14, H) until tailbud (stage 26, I). At stage 35 (J) they have begun to move anteriorly and dorsally in the endodermal mass. This continues through stage 37 (K), until they are most dorsal by stage 40 (L). (G-L) Embryos are cleared. Scale bar = 100μm. (Taken from Hudson and Woodland, 1998).

sequences and other clones. However, when the XPAT protein sequence was used to search the BLAST protein database, different regions of the protein show 34 % identity (over 50 amino acids) with a *Bacillus subtilis* protein similar to phage-related protein, 34 % identity (over 84 amino acids) with Superoxide dismutases from sweet potato (*Ipomoea batatas*), pepper (*apsicum annuum*) and quaking aspen (*Populus tremuloides*). XPAT also shared 25 % identity over 116 amino acids with DNA topoisomerase IV Par C subunit A from *Caulobacter crescentus*, but not to other topoisomerases. None of these homologies are very convincing or shed light on *Xpat* function.

Despite screens of chick and mouse genomic libraries (R. Hames, unpublished data) and database searches of the now complete *Drosophila* and *C. elegans* genomes, no homologue of *Xpat* has been found in these organisms. Bradley *et al.* (2001) claim to have discovered the cricket homologue of *Xpat*, but the sequence of this clone is not yet on the BLAST database and the evidence is not very convincing.

To date, the spatial and temporal distribution of XPAT protein has not been investigated. There is no doubt that establishing the distribution of the protein that it encodes will be critical in delineating the role of the *Xpat* gene. It will also be important to determine whether destruction of *Xpat* affects the localisation of other transcripts and, if so, where *Xpat* lies within the hierarchy of localisation proposed by Kloc and Etkin (1995). Lastly, it will be vital to find out how ablation of *Xpat* affects PGC differentiation and behaviour.

1.5 Aims of this study

- To determine the expression pattern and localisation properties of XPAT protein in *Xenopus.*
- To investigate the effect that destruction of *Xpat* mRNA has on other germ plasm components *in vivo*.
- To determine the effect that overexpression of *Xpat* mRNA has on other germ plasm transcripts.
- To determine the role of *Xpat* in development of the amphibian germ-line.

Chapter 2: Materials and Methods

2.1 DNA manipulation

All enzymes were purchased from Gibco BRL unless otherwise stated.

DNA was stored either in water or in EB buffer (10 mM Tris-HCl, pH 8.5) at -20°C.

2.1.1 Agar plates and cultures

Cells were plated on LB agar (10 g bacto-tryptone, 5 g bacto-yeast extract, 10 g NaCl, 15 g bacto agar per litre) and grown in LB cultures as above (with no agar). Ampicillin was used at a final concentration of 0.1 mg/ml where appropriate.

2.1.2 Agarose gels

Agarose gels were made using 1 x TBE (89 mM Tris, 89 mM boric acid, 10 mM EDTA pH 8.0) using between 0.6 and 2 % agarose, depending upon the size separation required. DNA was stained by addition of ethidium bromide to 0.1 µg/ml. Loading dye (6 x TBE, 5 % (v/v) glycerol; bromophenol blue and xylene cyanol were added to achieve desired colour) was used at 1:6 concentration. 1 Kb DNA Ladder (Gibco BRL) was used to observe size separation, typically 0.5 µg was loaded per lane on a gel.

2.1.3 Restriction digestions and ligations

DNA was digested with restriction enzymes according to the manufacturer's recommendations. Double digestions were carried out with the React Buffers (Gibco BRL) recommended. Restriction digestion was used to check all constructs made. DNA was quantified using an Ultraspec III spectrophotometer (Pharmacia) and associated software.

Ligations were carried out using T4 DNA ligase according to Sambrook *et al.* (1989). A molar ratio of 3:1, insert: vector was used for all ligations. Approximately 200 ng of vector DNA was used and the amount of insert adjusted accordingly. In cases where the amount of insert was limited, the amount of vector was reduced to fit the ratio above. Vector was dephosphorylated using bacterial alkaline phosphatase (1 U/µl, Boehringer Mannheim). Generally, 0.5 U was added for the final 1 hour of

digestion and then another 0.5 U was added for the final 30 minutes of digestion. DNA was then gel purified (see Section 2.1.5). Insert DNA was also isolated by gel purification.

2.1.4 Transformations

2.1.4.1 The RbCl Transformation Procedure

DNA transformations were made into *Escherischia coli* DH5α (ϕ80d*lacZ*ΔM15, *recA*1, *endA*1, *gyrA*96, *thi*-1, *hsd*R17 (r_K-, m_K+), *supE*44, *relA*1, *deo*R, Δ[*lacZYA-argF*]U169) cells, unless otherwise stated.

A single colony was inoculated from an LB plate into 10 ml of LB broth. This was shaken overnight at 37°C. The overnight was then subcultured 1:100 in LB+ 20 mM $MgSO_4$ (typically 250 ml). Cells were grown to OD_{590}=0.4-0.6 (~2-3 hours). They were then centrifuged at 5,000 rpm for 5 minutes at 4°C. The pellet was gently resuspended in 0.4 of the original volume (100 ml for a 250 ml subculture) in ice cold TFBI (30 mM KOAc (potassium acetate), 100 mM RbCl, 10 mM $CaCl_2$, 50 mM $MnCl_2$, 15 % glycerol, final pH 5.8). This was incubated on ice for 5 minutes, centrifuged at 5,000 rpm for 5 minutes at 4°C and the pellet gently resuspended in 1/25 original volume cold TFB2 (10 mM MOPS, 75 mM $CaCl_2$, 10 mM RbCl, 15 % glycerol, final pH 6.5). For 250 ml subculture 10 ml of TFB2 was used. This was then incubated on ice for 15-60 minutes, aliquoted 100 µl/tube and quick frozen on dry ice and stored at -70°C.

To transform, an aliquot was thawed on ice, the DNA was added and the cells incubated for 30-120 minutes on ice. The reaction was then heat shocked at 42°C for 90 seconds, incubated on ice for 5-10 minutes, and then diluted 6-fold in LB medium and grown for 30 minutes at 37°C. The transformation was then plated on LB medium containing ampicillin and grown overnight at 37°C.

2.1.4.2 The calcium chloride method for transformation

For cells other than DH5α, competency was obtained by use of the calcium chloride method (from Sambrook *et al.,* 1989). For example, BL21 (F-, *omp*T, *hsd*S_B [r_B^-, m_B^-]*dcm*, *gal*) and AD202 (F-, *ara*D139, DE(*arg*F-*lac*)U169, *omp*T1000::kan, LAM-, *flh*D5301, *fru*A25, *rel*A1, *rps*L150(*str*R), *rbs*R22, *deo*C1) cells were treated in this way for bacterial expression of proteins (Section 2.7).

2.1.5 Gel purifications and DNA preparations

Gel purification was carried out upon gel slices, excised with a clean razor blade, using a Qiagen QIAquick Gel Extraction kit.

DNA minipreps were performed from 5-10 mls of culture using Qiagen Qiaprep plasmid minipreparation kit, according to manufacturer's recommendations.

2.1.6 Production of glycerol stocks

Glycerol stocks of overnight cultures of bacteria were made by adding 0.5 ml 30 % glycerol to 0.5 ml bacterial culture, vortexing and rapidly freezing on dry ice. Glycerols were stored at -70°C.

2.2 PCR

Primers were made as in Section 2.3.1. New primers were tested alone and in pairs to test for non-specific background bands caused by amplification from one primer. In all PCRs, unless otherwise stated, *Taq* DNA polymerase was used (5 U/µl, Gibco BRL) with 1 x PCR buffer. 10 x PCR buffer (200 mM Tris-Cl pH 8.4, 500 mM KCl), W1 detergent and 50 mM $MgCl_2$ were purchased with the *Taq*. dNTPS were purchased from Amersham. Paraffin oil was placed over each PCR to prevent evaporation. Each PCR is set out as follows: initial denaturation (optional), cycling of denaturation, annealing, extension, and final extension (optional). Unless otherwise stated, PCRs were analysed on agarose gels (see Section 2.1.2).

2.2.1 RT-PCR

Reverse transcriptions (RTs) were carried out as follows: 0.5 µg total RNA was made up to 20.1 µl with ddH_2O and heated to 75°C for 5 minutes. The following were then added: random hexamers (6-mer random oligos [$pd(n)_6$], Pharmacia Biotech) to 3.3 µM, PCR buffer to 1 x, $MgCl_2$ to 3 mM, RNAse inhibitor (Amersham Pharmacia Biotech) to 1 U/µl. After incubation at 37°C for 5 minutes, 400 U MMLV reverse transcriptase (200 U/µl, Gibco BRL) were added to each tube and incubated at 37°C for a further 60 minutes. 'No enzyme' and 'no RNA' reactions acted as controls for the PCR. Samples were then heated to 95°C for 5 minutes and 1 µl typically used in each PCR.

PCRs were performed by mixing the following components: 1 x PCR buffer, 1.5 mM $MgCl_2$, 200 µM of each dNTP (dATP, dCTP, dGTP and dTTP), 0.05 % W1, 0.25 µM each primer, 1 U (0.2 µl) *Taq* polymerase and water added to 19 µl. cDNA was added to this mixture.

PCR conditions were as follows: 94°C -1 minute, 55°C -30 seconds, 72°C -30 seconds for 1 cycle, followed by: 94°C -30 seconds, 55°C -1 minute, 72°C -1 minute for 25-30 cycles and finally 72°C for 5 minutes. 25 cycles were used for *EF1α*, 28 cycles for *Xpat*, and 30 cycles for all other primer pairs. Linearity curves were run for every marker in every experiment by dilution of a cDNA sample. Three negative controls were also run for every marker: 'no enzyme' (–RT), 'no RNA' (–RNA) and a water control (–cDNA).

Primers for each clone were as shown in Table 2.1 below.

Table 2.1: Primers used for RT-PCR analysis

Where primers are taken from other sources, references are shown.

Transcript	Primers
Xpat:	5' GCTGTGTCCGATGTAATG 3' 5' GCTGCTCTGCTATGTGAT 3'
ODC:	5' GGAGCTGCAAGTTGGAGA 3' 5' TCAGTTGCCAGTGTGGTC 3' (Bassez *et al.*, 1990)
EF1α:	5' CAGATTGGTGCTGGATATGC 3' 5' CACTGCCTTGATGACTCCTA 3'
VegT:	5' CGAGGCTAACCAAGGCTTGA 3' 5' TCCGGCACTGTAGCAATGTC 3'
Xcat-2:	5' TGACTCATGGAGCGACTACT 3' 5' TCAGACGGTGAGACGTGTAT 3'
Xcat-3:	5' TTGGCTGACTAAGCACTTGA 3' 5' CTTGCACAACGGTACTAGAA 3'
Xdazl:	5' ATGGCGATTCAGCAGATTCC 3' 5' ATTGGCTCCAGAAGCAGACA 3'
XVLG-1:	5' GGATCGTCCACGTTCTTATG 3' 5' AGGCGGAGGAATATAGGTCA 3'
fatvg:	5' TCACTTCAGTGGCCTTAACC 3' 5' AGCCAGCTCTTCATCTGTTG 3'
Vg1	5' GACCGCTAACGATGAGTG 3' 5' AGGAATGTCTTCTGGCTC 3'
β-catenin:	5' TTGGCTCACCAGTTGACTCT 3' 5' AGCACACGGATAGCACCTTA 3'

2.2.2 PCRs used to generate fragments for cloning into DNA constructs

N.B. In all primers, nucleotides in lower case indicate sequence that is not present in the gene, that is restriction sites and anchors.

2.2.2.1 Xpat ORF PCR for construct for oocyte expression

This PCR was used to generate the ORF of Xpat with *Hind*III sites on the ends to enable cloning into the *Hind*III site of pSPJC2L for overexpression in oocytes.

Primers were as follows:

5'gactgaaagcttATGGCTTTGAAGGCAGAAGAC 3'

5'ctgaggaagcttTCAAAATCTTAACAAAAACTTAAAC 3'

PCR reactions were made as follows for each 25 µl reaction: 1 µl template (approx. 0.5 ng), 0.2 µM of each primer, 2.5 U Pwo DNA polymerase (5 U/µl, Roche Molecular Biochemicals), 1 x PCR buffer (10 x: 100 mM Tris-Cl, pH 8.85, 250 mM KCl, 50 mM $(NH_4)_2SO_4$, 20 mM $MgSO_4$, Roche Molecular Biochemicals), 200 µM

of each dNTP. Cycling conditions were: 94°C -30 seconds, 50°C -30 seconds, 72°C -90 seconds, for 5 cycles, 94°C -30 seconds, 60°C -30 seconds, 72°C -90 seconds, for 25 cycles and 72°C for 5 minutes.

2.2.2.2 Xpat ORF PCR for construct for GST fusion protein expression

This PCR was used to generate the ORF of Xpat with *Bgl*II sites on the ends to enable cloning into the *Bam*H1 site of pGEX-2T for overexpression in bacteria.

Primers were as follows:

5' gccgagatctATGGCTTTGAAGGCAGAAG 3'

5' gccgagatctCAGGCCAACATCCCACCAAG 3'

PCR reaction and cycling conditions were as in Section 2.2.2.1

2.2.2.3 Xpat UTRORF PCR for construct to determine translatability of *Xpat* in presence of a morpholino oligonucleotide *in vitro*

The following PCR was used to generate the 5' UTR + ORF of *Xpat* to clone between the *Bgl*II and *Hind*III sites of pSPJC2L.

Reaction and cycling conditions were as in Section 2.2.2.1 with the following primers:

5' gccgagatctTGCAGCCTGTGTCTGAATG 3'

5' ctgaggaagcttTCAAAATCTTAACAAAAACTTAAAC 3'

2.2.2.4 GFP PCR for construct to generate XPAT-GFP fusion proteins

Primers were designed to generate the ORF of GFP to insert between the *Bgl*II and *EcoR1* sites of pSPJC2L.

Reaction and cycling conditions were as in Section 2.2.2.1 with the following primers:

5' gccgagatctATGAGTAAAGGAGAAGAAC 3'

5' gccggaattcTTATTTGTATAGTTCATCCAT 3'

The resulting construct was called pSPJC2L-cGFP.

2.2.2.5 XPAT-GFP fusion protein constructs

This PCR was used to generate the ORF of Xpat (without the STOP codon) with *Bgl*II sites on the ends to enable cloning into the *Bgl*II site of pSPJC2L-cGFP for expression in oocytes.

Reaction and cycling conditions were as in Section 2.2.2.1 with the following primers:

5' gccgagatctATGGCTTTGAAGGCAGAAG 3' (XPATGFP-1)

5' gccgagatctCAGGCCAACATCCCACCAAG 3' (XPATGFP-8)

2.2.2.6 Deletion constructs of Xpat-GFP

These PCRs were to make Xpat-GFP constructs which, when translated, lack amino acids at the C-terminus or N-terminus of XPAT. Primers were designed to generate regions of the ORF of XPAT to insert into the *Bgl*II site of pSPJC2L-cGFP.

A) To make NDEL-1 -a deletion of the first 61 amino acids of XPAT

Reaction and cycling conditions were as in Section 2.2.2.1, with the following primers:

5'gccgagatctATGCAGCAGTGGCAGCTC 3'

and XPATGFP-8.

B) To make NDEL-2 –a deletion of the first 92 amino acids of XPAT

Reaction and cycling conditions were as in Section 2.2.2.1, with the following primers:

5'gccgagatctATGAACTCATTAAGTGGCAC 3'

and XPAT GFP-8.

C) To make NDEL-3 –a deletion of the first 159 amino acids of XPAT

Reaction and cycling conditions were as in Section 2.2.2.1, with the following primers:

5' gccgagatctATGCCTGCCACAAGCACTC 3'

and XPATGFP-8.

D) To make CDEL-1 –a deletion of the last 128 amino acids of XPAT

Reaction and cycling conditions were as in Section 2.2.2.1, with the following primers:

5' gccgagatctAGTGCTTGTGGCAGGCATC 3'

and XPATGFP-1.

2.2.2.7 Xpat and GFP ORF PCRs to make GFP-XPAT

A) GFP ORF PCR.

Primers were designed to generate the ORF of GFP (without the STOP codon) to insert between the *BglII* and *HindIII* sites of pSPJC2L.

PCR reaction and cycling conditions were as in Section 2.2.2.1 with the following primers:

5' gccgagatctATGAGTAAAGGAGAAGAAC 3'

5' gactgaaagcttTTTGTATAGTTCATCCATGC 3'

The resulting construct was called pSPJC2L-NGFP.

B) XPAT ORF PCR

This PCR was used to generate the ORF of *Xpat* with *Hind*III sites on the ends to enable cloning into the *Hind*III site of pSPJC2L-NGFP for expression in oocytes.

Reaction and cycling conditions were as in Section 2.2.2.1 with the following primers:

5'gactgaaagcttATGGCTTTGAAGGCAGAAGAC 3'

5'ctgaggaagcttTCAAAATCTTAACAAAAACTTAAAC 3'

2.2.2.8 Xpat ORF PCR for Myc-XPAT fusion protein expression

This PCR was used to generate the ORF of *Xpat* to clone in-frame between the *Bgl*II and *Xho*I sites of pCS3+MT. This vector contains 6 myc epitope tags.

Reaction and cycling conditions were as in Section 2.2.2.1 with the following primers:

5' gcgcagatctCGATGGCTTTGAAGGCAGAAGAC 3'

5' gcgcctcgagTCAAAATCTTAACAAAAACTTAAAC 3'

2.2.2.9 PCR to generate a template for transcription of dsXpat RNA

This PCR was used to generate the ORF of Xpat with T7 promoter sequences on both ends. Thus, transcription of this PCR product with T7 RNA polymerase generated dsXpat RNA.

Primers were as follows:

5'taatacgactcactatagggagaccacGGCTTTGAAGGCAGAAGAC 3'

5' taatcagactcactatagggagaccacTCAAAATCTTAACAAAAACTTAAACC 3'

PCR reactions were made as follows for each 25 µl reaction: 1 µl template (approx. 1ng), 1 x PCR buffer, 1.5 mM $MgCl_2$, 200 µM of each dNTP (dATP, dCTP, dGTP and dTTP), 0.05 % W1, 0.25 µM each primer, 2.5 U (0.5 µl) *Taq* polymerase.

Cycling conditions were: 94°C -20 seconds, 50°C -20 seconds, 72°C -20 seconds, for 5 cycles, 94°C -20 seconds, 60°C -20 seconds, 72°C -20 seconds, for 25 cycles and 72°C for 5 minutes.

2.2.3 PCR to generate template for Xpat ORF *in situ* hybridisation probe

This PCR was used to generate the ORF of Xpat with T7 promoter sequence on its 3' end. Transcription of this PCR product with T7 RNA polymerase generated antisense *Xpat* mRNA. Primers used were as follows:

5' gccgagatctATGGCTTTGAAGGCAGAAG 3' (XPATGFP-1)

5' taatcagactcactatagggagaccacTCAAAATCTTAACAAAAACTTAAACC 3'

PCR reaction and cycling conditions were as in Section 2.2.2.9.

2.2.4 SP6/internal primer PCRS on colonies

Each 20 µl reaction comprised the following: 1 x PCR buffer, 0.25 µM of each primer, 1 U Taq polymerase, 1.5 mM $MgCl_2$, 0.05 % W1, 200 µM of each dNTP and a scraping from a colony.

Conditions were as follows: 94°C- 1 minute, 55°C- 30 seconds, 72°C- 30 seconds for one cycle, and then 94°C -30 seconds, 55°C- 1 minute, 72°C- 1 minute for 30 cycles and finally 72°C- 5 minutes for one cycle.

Primers used to check for the presence of an insert following a ligation and transformation were: SP6 and the specific downstream primer used in the PCR step of the cloning strategy. Thus, the downstream primer varied depending on which construct had been made.

2.3 Sequencing

2.3.1 Sequencing

All constructs made were completely sequenced on both strands using Sequenase Version 2.0 (USB/Amersham Life Science), with 10 μCi [α-^{35}S]-dATP per reaction. 2-3 μg of dsDNA template was used for each reaction in 20 μl of water. To denature the DNA, 5 μl of 1 M NaOH/1 mM EDTA was added and the reaction was incubated at room temperature for 5 minutes. DNA was precipitated by addition of 10 μl 5 M ammonium acetate and 70 μl ethanol, left at -20°C for 20 minutes and recovered by centrifugation at 13K rpm for 15 minutes. Templates were then resuspended in 7 μl water. The reactions were then carried out exactly as specified by the manufacturers on microtitre plates. 1 pmol of all primers were used in the reactions. For many sequencing reactions SP6, T3 and T7 primers were used (depending on which vector the construct was in). All constructs were also sequenced using the PCR primers that they were constructed with (Section 2.2.2). The following primers were then used to complete sequencing:

XPAT-SEQ1 5' GTGCATTACATCGGACACAG 3'

SEQXPAT2A 5' CCTGCCCAGAAACCTAATGA 3'

SEQXPAT2B 5'CCCAAAGGAGAAACGGAAGA 3'

Primers were manufactured commercially by Gibco BRL.

In some cases, regions of sequence were verified using automated cycle sequencing, using the ABI PRISM™ Dye Terminator Cycle Sequencing Ready Reaction Kit with AmpliTaq® DNA polymerase, FS (Perkin Emer) on the 373A DNA Sequencer (Applied Biosystems). In all cases, automated sequencing was performed by Lesley Ward.

2.3.2 Sequencing gels

0.4 mm gels were poured and used in a 40 cm gel apparatus. 6 % Acrylamide gels were used, containing Acrylamide: NN-methylenebisacrylamide in the ratio 19:1 respectively, 1 x TBE, 42% urea (w/v) and run in 1 x TBE. 800 μl 10 % (w/v) APS and 140 μl TEMED were added per 100 mls of gel, just before pouring. Gels were run at 40 watts, fixed in 10 % (v/v) methanol, 10 % (v/v) acetic acid, vacuum dried at 80°C and autoradiographed.

2.4 RNA manipulation

2.4.1 Small scale preparation of RNA from 5-10 embryos or oocytes for use in RT-PCR (Section 2.2.1)

All centrifugations were carried out at 13K rpm.

Material was homogenised in 500 µl of XT buffer (0.3 M NaCl, 20 mM Tris-HCl pH 7.5, 1 mM EDTA, 1 % SDS). 180 µg Proteinase K (Boehringer Mannheim) was added to give a final concentration of 0.36 mg/ml, and incubated at 37°C for 15 minutes. The homogenate was then extracted with an equal volume of phenol; separation was obtained by a 10 minute centrifugation. The upper phase was then phenol-chloroform (1:1) extracted; this time separation was obtained with a 5 minute spin.

RNA (and DNA) was precipitated at -20°C for 30 minutes with 2 volumes of ethanol and 5 µg of glycogen. Nucleic acids were recovered by centrifugation for 20 minutes. Pellets were redissolved in 90 µl 1 x DNase I buffer (10 x: 200 mM Tris-Cl pH 8.3, 500 mM NaCl, 25 mM $MgCl_2$) diluted in ddH_2O. 50 U Ribonuclease inhibitor (Amersham Pharmacia Biotech) and 20 U RNase-free DNAse I (Boehringer Mannheim) were added. Digestion was carried out for 30 minutes at 37°C, with vortexing every 10 minutes to ensure the pellet was resuspended. Samples were further proteinase digested at 37°C for 20 minutes, with addition of 360 µl XT buffer and 120 µg proteinase K. The samples were then extracted in one volume of phenol, followed by one volume of phenol:chloroform (1:1). RNA was precipitated using 2 volumes of ethanol at room temperature for 30 minutes and recovered with a 20 minute spin. RNA pellets were then washed with 70 % ethanol and resuspended in 20 µl of ddH_2O (2-4 µl/oocyte).

2.4.2 RNA labelling with digoxigenin-UTP by *in vitro* transcription with T7 and T3 RNA polymerases (for use in whole mounts- Section 2.5)

Templates for digoxigenin-UTP (DIG) labelling transcriptions were prepared by linearising 1-4 µg of the appropriate plasmid DNA with restriction enzymes for 2 hours at 37°C. In cases where *EcoR*1 and *Xho*1 did not cut internally, they were used for antisense (T7 RNA polymerase) and sense (T3 RNA polymerase) transcript template production respectively. In other cases templates were linearised with

*Cla*1, (*Xdazl,* antisense) or *Hind*III (*Xcat*-2, antisense). The template for making Xpat ORF was generated by PCR as described in Section 2.2.3. A fraction of the digested sample was run on an agarose gel to check for complete digestion. The DNA was then purified using the Qiagen QIAquick Gel Extraction Kit, with the following modifications to the manufacturer's recommendations: 3 volumes of Buffer QG (Qiagen) and 1 volume of isopropanol was added to the digested DNA and the DNA was then applied to the QIAquick column as instructed in the manufacturer's recommendations, which were then followed as usual. The purified DNA was eluted into 30 µl EB (10 mM Tris-Cl, pH 8.5). DNA was checked again on an agarose gel.

RNA was transcribed using the DIG RNA Labelling Mix (Boehringer Mannheim). Typically, when transcribing the antisense strand, T7 polymerase (Gibco BRL) was used and to transcribe the sense strand, T3 polymerase (Gibco BRL) was used.

Each 20 µl RNA labelling reaction comprised: 0.5 µg linearised DNA template, 1 x DIG RNA labelling mix (10 x: 10 mM ATP, 10 mM CTP, 10 mM GTP, 6.5 mM UTP, 3.5 mM DIG-11-UTP, pH 7.5, Boehringer Mannheim), 1 x T3/T7 transcription buffer (5 x: 200 mM Tris-Cl (pH 7.9), 30 mM $MgCl_2$, 10 mM spermidine-$(HCl)_3$, Gibco BRL), 50 U RNA polymerase (Gibco BRL), 50 U Ribonuclease Inhibitor (Amersham Pharmacia Biotech). This was incubated at 37°C for 2 hours, after which samples were DNAse treated by addition of 2 U RNAse-free DNAse I (Boehringer Mannheim) for 15 minutes, and the RNA was precipitated with 1/10 volume 8 M LiCl and 3 volumes ethanol, left at -20°C for 2 hours and recovered by centrifugation at 13K rpm for 15 minutes. RNA pellets were then washed with 70 % ethanol and resuspended in 100 µl hybridisation buffer (Section 2.5) and used as a 100 x stock. RNAs were checked on 0.8% agarose gels before and after DNAse treatment.

2.4.3 *In vitro* transcription of mRNA

To produce a template, the ORF (or ORF + UTR in certain cases) required was PCR amplified (Section 2.2.2) and cloned into the appropriate restriction site of pSPJC2L (Cook *et al.,* 1993). Templates were linearised by restriction digestion and checked on agarose gels for completion of digestion. Templates were purified using gel extraction (Section 2.1.5).

In vitro transcription of RNA for microinjection, or for use in *in vitro* translation (Section 2.6.2), was performed with Ambion SP6 mMessage mMachine™ kit. The manufacturer's instructions were followed and the LiCl method for RNA precipitation was chosen for the subsequent ease of resuspension. RNAs were checked on 0.8 % agarose gels after resuspension and RNA yields were quantified by determination of the UV light absorbance at 260 nm, using an Ultraspec III spectrophotometer (Pharmacia) and associated software.

2.5 Whole mount *in situ* hybridisation

Oocytes and embryos were collected at various stages and vitelline membranes removed manually from embryos with forceps, or enzymatically (according to Islam and Moss, 1996). Embryos were fixed overnight at 4°C or for 1-2 hours at room temperature in MEMFA (100 mM MOPS pH 7.4, 2 mM EGTA, 1 mM $MgSO_4$, 4 % formaldehyde). Embryos and oocytes were then dehydrated through an ethanol series for storage in 100 % ethanol at -20°C. This method is based on that of Harland (1991).

Embryos and oocytes were rehydrated through an ethanol series to PBST (PBS [136 mM NaCl, 2.6 mM KCl, 10 mM Na_2HPO_4, 1.76 mM KH_2PO_4 pH 7.2] + 0.1 % (v/v) Tween-20). Embryos were then treated with 3 µg/ml proteinase K (Boehringer Mannheim) for 5-10 minutes, oocytes were treated with 50 µg/ml for 5-10 minutes. The embryos/oocytes were then washed in PBST twice for 5 minutes. A 20 minute fixation in 4 % formaldehyde in PBST and then five 5 minute washes in PBST followed this. Embryos/oocytes were equilibrated in hybridisation buffer (50 % (v/v) formamide, 5 x SSC, 1 mg/ml Type II Torula Yeast RNA (Sigma), 100 µg/ml Heparin (Sigma sodium salt grade 1A from porcine intestinal mucosa), 2 % (w/v) BBR, 0.1 % (v/v) Tween-20, 0.1 % (w/v) CHAPS), by placing in 50 % hybridisation buffer in PBST until oocytes/embryos sank, then in hybridisation buffer until they sank. Fresh hybridisation buffer was added and embryos and oocytes were pre-hybridised at 60°C for 5-6 hours. Hybridisation was carried out over-night at 52°C, by replacing the prehybridisation buffer with fresh hybridisation mix, containing 1/100 of DIG labelled RNA probe denatured for 5 minutes at 70°C, giving a final concentration of approximately 1 µg/ml.

The following day embryos and oocytes were washed in: 2 x SSC, 0.3 % CHAPS, at 60°C for 3 x 20 minutes. RNAse digestion was carried out for 30 minutes with 20 µg/ml RNAse A in 2 x SSC, 0.3 % CHAPS at 37°C. The following washes were subsequently carried out: [2 x SSC, 0.3 % CHAPS] at room temperature for 10 minutes; [0.2 x SSC, 0.3 % CHAPS] at 60°C for 2 x 30 minutes; [PBST, 0.3 % CHAPS] at 60°C for 2 x 10 minutes; [PBST] at room temperature for 10 minutes; [PBST, 0.5 % BBR] at room temperature for 15 minutes. A 1/2000 anti-DIG antibody (DIG Nucleic Acid Detection Kit, Boehringer Mannheim) dilution in PBST, 0.5 % BBR was placed on the embryos/oocytes and they were incubated for 16 hours at 4°C.

Oocytes and embryos were then washed at room temperature for 5 hours, with hourly changes of PBST. This was followed by an overnight wash in PBST at room temperature.

Two 5 minute washes were then carried out with NTMT (0.1M Tris pH 9.5, 50mM $MgCl_2$, 100 mM NaCl, 0.1 % (v/v) Tween-20, 5 mM levamisole). Then, colour reaction reagents were added to fresh NTMT: 10 µl BCIP-NBT/ml (Boehringer Mannheim). Reactions were left to develop at 4°C in the dark. Reactions were stopped by a quick wash in TE buffer and samples were fixed in MEMFA for 1-2 hours at room temperature or over-night at 4°C.

After hybridisation, oocytes were washed in PBST and photographed on Kodak Ektachrome 160T film using a Stemi SVII (Zeiss) dissecting microscope.

2.6 *In vitro* translation of proteins

2.6.1 Coupled *in vitro* Transcription and Translation

This was performed using the TNT® SP6 Coupled Reticulocyte Lysate System (Promega). Each 50 µl reaction comprised the following: 25 µl TNT® rabbit reticulocyte lysate, 2 µl TNT® Reaction Buffer, 1 µl TNT® SP6 RNA polymerase, 20 µM Amino Acid Mixture Minus Methionine (Promega), 1 µg DNA template, 50 U ribonuclease inhibitor (Amersham Pharmacia Biochem), 2 µl ^{35}S-methionine (1,200 Ci/mmol at 10 mCi/ml). Reactions were incubated at 30°C for 90 minutes.

Typically 2.5 µl out of each 50 µl reaction were loaded onto 12 % acrylamide gels to analyse the products of translation (Section 2.9.2).

2.6.2 *In vitro* translation of mRNA

This was performed using the Rabbit Reticulocyte Lysate System, Nuclease Treated (Promega). Each 50 µl reaction comprised the following: 35 µl rabbit reticulocyte lysate (Promega), 20 µM Amino Acid Mixture, Minus Methionine (Promega), 2 µl ^{35}S-methionine (1,200 Ci/mmol at 10 mCi/ml), 10-500 ng mRNA substrate in water (transcribed using mMessage mMachine™, Ambion, as in Section 2.4.3) and 50 U Ribonuclease Inhibitor (100 U/µl, Amersham Pharmacia Biochem). Reactions were incubated at 30°C for 90 minutes. Typically 2.5 µl out of each 50 µl reaction were loaded onto 12 % acrylamide gels to analyse the products of translation (Section 2.9.2).

2.6.3 *In vitro* RNA homopolymer binding assays

In vitro RNA homopolymer binding assays were performed exactly as described in Swanson and Dreyfuss (1988). Briefly, mRNAs were translated in reticulocyte lysate (Promega) in the presence of ^{35}S-methionine (as described in Section 2.6.2) and added to Sepharose-conjugated RNA homopolymers (polyguanylic acid on Sepharose 4B, polyadenylic acid on Sepharose 4B, polycytidylic acid on 4 % beaded agarose, polyuridylic acid on polyacrylhydrazido-agarose, all from Sigma) or dsDNA (on cellulose, also from Sigma) in binding buffer (100 mM-2 M NaCl, 0.5 % Triton X-100). Following binding and washing, the beads were resuspended in 50 µl SDS loading buffer, boiled for 3 minutes at 95°C and run on 12 % SDS-PAGE gels as described in Section 2.9.2.

2.7 Production of XPAT-GST fusion proteins in bacteria

Constructs for these experiments were made as described in Section 2.2.2.2.

The ORF was cloned into pGEX-2T. pGEX-2T with no insert was used as a GST-only control throughout. Overnight cultures were diluted 1/10 in fresh LB and ampicillin and grown for 2 hours at 37°C. Cultures were then induced to express GST- XPAT (or GST) by addition of IPTG to a concentration of 0.1mM and grown at 37°C for a further 2 hours. Bacterial strains used were DH5α, BL21 and AD202

(genotypes given in Section 2.1.4.2), which all gave similar results for GST-XPAT. Samples were centrifuged at 3K rpm for 10 minutes and pellets resuspended in 1 ml PBS containing 0.1 mM PMSF. This was incubated on ice for 20 minutes and then the bacteria were lysed by sonication at 6 μm wavelength for 4 x 30 seconds. 100 μl was taken as a total protein sample and the remaining sample was centrifuged at 13K rpm for 15 minutes at 4°C. The supernatant was taken off (this is the soluble protein fraction) and the pellet was resuspended in 1 ml 0.5 % SDS.

2.8 Immunisations and Preparation of Serum

2.8.1 Production of MAP peptides

20-30 μg of MAP peptide was made, purchased and purified for immunisation by Alta Bioscience (School of Biochemistry, The University of Birmingham). Peptides were supplied lyophilised and were resuspended in PBS.

2.8.2 Immunisations

Rabbits and mice were immunised with the desired peptide in complete non-ulcerative Freunds adjuvant (Morris) (Guildhay Ltd). Complete Freunds adjuvant was prepared by adding 10 doses of intradermal BCG vaccine BP, resuspended in 0.4 ml PBS, to 20 mls Freunds. Subsequently, boosts were carried out in incomplete non-ulcerative Freunds. For the primary injection and boosts 500 μg MAP peptide was injected into each rabbit, and 5 μg into each mouse. Rabbits and mice were injected every 4 weeks and test bleeds taken 10-14 days after each injection.

2.8.3 Preparation of serum

Blood was heated to 37°C for 15 minutes, clots that formed were detached by ringing with a Pasteur pipette and the blood left overnight at 4°C to contract further. Serum was taken and spun at 13K for 5 minutes, aliquoted and stored at -20°C.

2.8.4 Enzyme Linked Immunosorbent Assay (ELISA)

This assay was used to detect the binding of antibody to peptide, to determine if there was an immune response by the rabbit/mouse to the MAP peptide. MAP peptides were diluted to final concentration of 1 μg/ml in coating solution (50 mM sodium carbonate pH 9.6). 150 μl of the peptide solution was put into the wells of a

polystyrene 96-well microtitre plate (Nunc). A complete column of wells was coated for each peptide. The wells of column 1, the blank, were all coated with coating buffer only. The plate was incubated overnight at 4°C to coat.

The coating buffer was removed from the wells and the wells were filled to capacity (320 µl) with blocking solution (0.5 % (w/v) gelatin in 1 x PBS [10 x PBS, 150 mM pH 7.2: 80 g NaCl, 2 g KCl, 11.5 g Na_2HPO_4, 2 g KH_2PO_4 per litre]). The plate was then incubated at 37°C for 30 minutes. The blocking solution was removed and the wells were washed 3 times with 0.1 % v/v Tween-20 in PBS. Rabbit or mouse serum was diluted in the range 1/1000-1/4000, and normal rabbit or mouse serum was used at 1/1000.Each well used was then filled with 150 µl of antibody solution. The top row was reserved for normal serum so that a measure against each peptide could be obtained. The plate was incubated at 37°C for 30 minutes.

The antibody solutions were removed and the wells washed 5 times with 0.1 % (v/v) Tween-20 in PBS. Each well used was then filled with 150 µl of horseradish peroxidase-conjugated goat anti-rabbit IgG (Bio-RAD laboratories) or horseradish peroxidase-conjugated rabbit anti-mouse IgG (Sigma), diluted 1/3000 with PBS. The plate was incubated at 37°C for 30 minutes. The secondary antibody solution was removed and the wells were washed 5 times with 0.1 % v/v Tween-20 in PBS. Colour was then developed by addition of 150 µl/well of substrate (per 25 ml: 5 mg o-Phenylenediamine (OPD) tablets (5 mg/tablet, Sigma), 0.74 % (w/v) Na_2HPO_4, 0.225 (w/v) citric acid and 10 µl 30% H_2O_2). Colour was allowed to develop for 30 minutes in the dark and was terminated by the addition of 100 µl 2M H_2SO_4. The absorbance at 490 nm was recorded.

2.9 Protein Analysis

2.9.1 Protein extraction

All samples were diluted in 2 x loading dye (to give final concentration 1 x dye: 50 mM Tris-Cl pH 6.8, 1 % 2-mercaptoethanol, 2 % SDS, 0.1 % bromophenol blue, 10 % glycerol). Samples were heated at 95°C for 5 minutes before loading.

• *Oocytes and embryos*; samples were homogenised in 10-20 µl per oocyte (or embryo) of Barth's saline containing 1 mM PMSF, and insoluble proteins removed

by centrifugation at 13K rpm for 5 minutes. Various volumes were loaded, typically the equivalent of 1/3 oocyte per lane of mini gel.

• *Bacteria*: pellets were resuspended in 1 x loading dye and various amounts were loaded, typically around 0.05-0.2 ml of induced culture.

2.9.2 Protein gels

Gels were made with a 12 % acrylamide (37.5:1 acrylamide:NN-methylenebisacrylamide respectively) resolving gel (0.375 M Tris-Cl pH 8.8, 0.1% SDS, 0.1 % APS, 4 µl TEMED/10 mls gel) and 5 % (37.5:1) acrylamide stacking gel (126 mM Tris-HCl pH 6.8, 0.1 % SDS, 0.1 % APS, 5 µl TEMED/5 ml gel) and run in Tris-glycine buffer (40 mM Tris, 253 mM glycine, 0.1 % SDS). The gels were run at 100 volts. Pre-stained size markers were loaded onto each gel: See Blue™Plus2 Pre-Stained Standards (NOVEX™ Novel experimental technology).

Gels were stained with 0.2 % Coomassie blue in 10 % acetic acid and 40 % methanol, and destained in 10 % glacial acetic acid and 40 % methanol.

Gels were dried under vacuum at 80°C.

2.9.3 Western Blotting

Gels were run as in Section 2.9.2. All materials used in the blot were soaked in 1 x western transfer buffer (40 mM Tris, 194 mM glycine, 20 % Analar grade methanol) prior to use. Blots were set up as follows: cathode side- 3 sheets of Whatman paper, gel, nitrocellulose membrane (Hybond™-C, Amersham), 3 sheets Whatman paper, in a Mini Trans-blot® Electrophoretic Transfer Cell (Bio-rad) apparatus. Blots were run for 1 hour at 100 volts on a magnetic stirrer to recircularise buffer.

Membranes were rinsed in TBS (10 mM Tris pH 8.0, 150 mM NaCl) and blocked in 5 % Marvel milk powder in TBST (10 mM Tris-Cl, pH 8.0, 150 mM NaCl, 0.1 % (v/v) Tween-20) for 1-2 hours. Primary antibodies (serum) were placed on blots in TBST/5 % Marvel and left overnight, shaking at 4°C.

4 x 5 minute washes in TBST were performed at room temperature. Secondary antibody (Goat Anti-Rabbit IgG (H + L) Horseradish Peroxidase Conjugate, Bio-Rad

Laboratories; or Rabbit Anti-Mouse IgG (whole Molecule) Peroxidase Conjugate, Sigma) was diluted 1/3000 in 5 % Marvel milk powder in TBST and incubated at room temperature for >2 hours. Membranes were then washed for 2 x 5 minutes with TBST and 2 x 5 minutes in TBS. Finally filters were rinsed in 100 mM Tris-Cl pH 7.5 and then the substrate added for the horseradish peroxidase enzyme [3,3' diaminobenzidine (DAB) tetrahydrochloride tablets (Sigma) at 0.5 mg/ml] in 100 mM Tris-Cl pH 7.5 and 12 µl 30 % hydrogen peroxide added for every 10 mg of DAB used. Reactions were left to develop colour for up to 5 minutes and the reaction stopped by washing extensively in TBST.

2.9.4 Immunoprecipitations

For radioactive immunoprecipitations, oocytes were prepared as described in Section 2.10.6. Oocytes were homogenised in 200 µl of ice cold EBC lysis buffer (150 mM NaCl, 1 % NP-40, 50 mM Tris pH 8.0, 2 mM EDTA, 1 mM PMSF, 1 mM DTT), and the volume made up to 500 µl (per 10 oocytes) with EBC. Debris was removed by a 5 minute centrifugation at 13K rpm. The lysate was removed. 10 µl were removed for analysis on an SDS PAGE gel to test for incorporation of ^{35}S-methionine and overexpression of proteins in oocytes. To the lysate, various dilutions of serum were added, usually between 1/100 and 1/500: Monoclonal Anti-c-myc clone 9E10 (Sigma) was used at 1/100 dilution. Samples were then incubated on ice for 1 hour. 40 µl of protein-A Sepharose beads (50% slurry in PBS) were added per 500 µl lysate and the samples were incubated at 4°C with rotation for 1 hour. The Sepharose was allowed to settle under gravity and the supernatant was removed. The beads were then washed 3 times in NETN0.1 buffer (20 mM Tris-Cl pH 8.0, 100 mM NaCl, 1 mM EDTA, 0.5 % NP-40). The final wash was removed to leave ~50 µl total volume (of beads + buffer). An equal volume of 2 x SDS loading dye was added and the samples heated at 95°C for 3 minutes prior to gel analysis.

2.9.5 Whole mount immunocytochemistry

This was performed as described in Sive *et al.* (2000) with the following modifications: the primary antibody, GFP (FL) rabbit polyclonal antibody (200 µg/ml, Santa Cruz Biotechnology), was used at a 1/100 dilution. Secondary antibody: Goat Anti-Rabbit IgG (H + L) Horseradish Peroxidase Conjugate (Bio-Rad

Laboratories) was diluted 1/200 in PBT; or Goat Anti-Rabbit IgG (whole molecule) FITC conjugate (Sigma) was diluted 1/50 in PBT. At the end of the protocol, oocytes were fixed in Bouin's (9.25 % formaldehyde (v/v), 5 % (v/v) glacial acetic acid) overnight at room temperature, washed for 5 x 20 minutes in 70 % ethanol buffered with PBST and then bleached. Bleaching was performed in bleaching solution (1 % (v/v) H_2O_2, 5% formamide (v/v), 0.5 x SSC) exactly as described in Sive *et al.* (2000).

2.10 Embryo and Oocyte Culture and Manipulation

Embryos were staged according to Nieuwkoop and Faber (1967).

2.10.1 Embryo culture and dissection

Female frogs were injected with 50-100 U follicle stimulating hormone (FSH) 48-144 hours prior to laying and 600 U human chorionic gonadotrophin (HCG) 16 hours prior to laying. Frogs were placed in Barth's saline (88 mM NaCl, 1.0 mM KCl, 2.5 mM $NaHCO_3$, 15 mM Tris-Cl pH 7.6, 0.3 mM $Ca(NO)_2$, 0.41 mM $CaCl_2$, 0.82 mM $MgSO_4$) for laying and eggs removed into small dishes of Barth's saline. Testes were manually dissected and placed into Barth's saline. Eggs were flooded in water after wiping with split testis and allowed to fertilise for 30 minutes. Jelly was removed by a 10 minute treatment in 2 % (w/v) cysteine pH 8.0 and then washed three times in 0.1 x Barth's saline. For culturing gentomycin was added to 10 µg/ml.

Embryos were dissected in Barth's saline, after manual removal of vitelline membranes.

2.10.2 Embryo injection

Embryos were injected, usually bilaterally at the two cell stage, with various amounts of mRNA (Section 2.4.3) in 6 % Ficoll (w/v in 0.1 x Barth's saline) using a micromanipulator and fine drawn out capillary tube. Injected embryos were then transferred to 0.1 x Barth's saline for culturing.

2.10.3 Oocyte injection

Stage VI oocytes were dissected from ovaries, injected with various amounts of mRNA or 10-15 ng of antisense oligonucleotide and cultured in Barth's saline at 18°C.

Table 2.2 Oligonucleotides used for antisense experiments

Where oligos are taken from other sources, references are shown.

Primer Name	Primer sequence
asXpat-1	5' TTGACCATCTGAAGACCG 3'
asXpat-2	5' GAACATCACTACAGGTGC 3'
asXpat-3	5' CACAAGCACTCCACGGAA 3'
asXpat-4	5' AGTGGCAGCTCTTAGAAG 3'
asXpat-5	5' GTTGAGGACACGTCAGGA 3'
asXpat-6	5' GCTGAGAACACTACCGTT 3'
asXpat-7	5' TGAAGACCGATGTAGCAG 3'
asXpat-8	5' CCAGTTGATCCAGAGCTT 3'
asXpat-9	5' CCTCGCTACAGATGGCTA 3'
asXpat-10	5' CACGTCAGGATAGAGCTT 3'
asXpat-11	5' TCCAACTACGAGCCACAT 3'
asXpat-12	5' TTCTGCCTTCAAAGCCATAGA 3'
asVegT	5' CAGCAGCATGTACTTGGC 3' (Zhang *et al.*, 1998)

Antisense oligonucleotides were used to deplete *Xpat* mRNA or *VegT* mRNA at injection doses of 10-15 ng per oocyte. These oligonucleotides were synthesised in a more stable modified form in which the 5' and 3' terminal four bases were linked by phosphorothioate linkages instead of the conventional phosphodiester bonds (*asXpat1-11* and *asVegT*, INTERACTIVA biotechnologie GmbH; *asXpat12*, Gibco BRL). The sequences of the antisense oligonucleotides used are shown in Table 2.2.

Morpholino antisense oligodeoxynucleotides were also used to prevent the translation of specific proteins. Morpholino oligos have substitutions of the riboside moieties with nitrogen-containing morpholine moieties and are phosphorodiamidate linked (Summerton & Weller, 1997). All morpholinos used were 25-mers and had the following sequences:

Xpat morpholino: 5' ATTCTCATTCTCAGCAGCAAAAGGA 3',

Xsox17β morpholino: 5' TGATTCGGAGTGCTGTGGTGATTAG 3',

Standard control morpholino: 5' CCTCTTACCTCAGTTACAATTTATA 3' (Gene Tools LLC). Morpholino oligos were resuspended in sterile filtered water and injected in doses of 10-50 ng per oocyte.

2.10.4 Culturing of oocytes in growth conditions and drug treatments

Oocytes of the stages required were dissected and injected. Oocytes were cultured in OCM (oocyte culture medium), as previously described in Yisraeli and Melton, (1988): 0.5 x Leibowitz L-15 medium (Gibco BRL), 1 mM L-glutamine, 1 µg/ml insulin, 15 mM Hepes pH 7.8, 50 U/ml nystatin, 100 µg/ml gentamycin, 100 U/ml penicillin-streptomycin, 10 % (v/v) vitellogenin-containing frog serum (prepared as in Yisraeli and Melton, 1988). Occasionally, instead of 10 % (v/v) vitellogenin-containing frog serum, purified vitellogenin to a final concentration of 5 mg/ml was used (purified as described in Kloc & Etkin, 1999).

Cytoskeletal inhibitors were added to the media when oocytes were injected and were replaced daily. The inhibitors were dissolved in DMSO (except demecolcemine, which was dissolved in ethanol) at the following stock concentrations: cytochalasin D (Sigma) 2 mM, paclitaxel (Sigma) 5 mg/ml, demecolcemine (Sigma) 10 mM, nocodazole (Sigma) 1 mg/ml. Cytochalasin D and nocodazole were stored at -20°C, whilst paclitaxel and demecolcemine were stored at +4°C. The cytoskeletal inhibitors were used at the following working concentrations: cytochalasin D 2 µM, paclitaxel 5 µg/ml, demecolcemine 10 µM, nocodazole 1 µg/ml.

2.10.5 Oocyte dissection

Oocytes were dissected in Barth's saline. A manual dissection procedure was used to remove nuclei (as described in Woodland and Adamson, 1977). For oocyte bisection, oocytes were first fixed by heating to 75-85 °C in Barth's saline for 30 seconds. They were then cut open using a scalpel.

2.10.6 Photography

Oocytes expressing GFP constructs were photographed using a Leica (MZFLIII) DC100 dissecting microscope and digital camera. Pictures of oocytes at a higher

magnification (x 100 to x 400) were taken using a Nikon (UFX-II) Optiphot microscope and the Leica digital camera.

2.10.7 Production of protein in oocytes and protein analysis

This method was used to test *in vitro* transcribed mRNAs (Section 2.4.3) and for immunological procedures (Section 2.9.4). Oocytes were injected and cultured ± ^{35}S-methionine label to assess the translatability of the message prior to overexpression studies and to make radioactively labelled proteins.

Stage VI oocytes were dissected from ovaries, injected with mRNA and cultured overnight in Barth's saline with 10-15 µCi ^{35}S-methionine (10 µCi/µl, 1000 Ci/mmol) per 8 oocytes. For protein analysis of transcribed messages oocytes were typically homogenised in 20 µl/oocyte of: Barth's saline, 1 mM PMSF, 0.5 µg/ml leupeptin. Insoluble material was removed by centrifugation at 13K rpm for 5 minutes. The extract of approximately 1/3 of an oocyte was loaded onto each lane of a protein gel (Section 2.9.2), gels were dried and autoradiographed to visualise production of protein.

Chapter 3: Investigation of the dynamics of XPAT localisation using XPAT tagged with green fluorescent protein (GFP)

3.1 An introduction to GFP and the use of GFP fusion constructs in expression studies

The introduction of green fluorescent protein (GFP) from the jellyfish *Aequorea victoria* as an endogenous fluorescent tag promises to provide both an innocuous means of rendering target proteins visible and of providing information about cytoskeletal function in living cells. Initial studies have been encouraging in showing that GFP and fusion constructs of GFP with a variety of cellular proteins remain fluorescent in a variety of cell types and species. The fusion proteins also behaved in a manner similar to the native proteins.

GFP (reviewed by Tsien, 1998) was discovered by Shimomura *et al.* (1962), but the gene was not cloned until 30 years later (Prasher *et al.*, 1992). The crystal structure of GFP was recently determined at 1.9 angstrome resolution (Ormo *et al.*, 1996; Yang *et al.*, 1996) and this revealed that the protein consists of an 11-stranded β-barrel structure (the β-can) that surrounds a single central α-helix. The chromophore is formed by the spontaneous cyclisation of residues Ser-65, Tyr-66 and Gly-67, followed by oxidation of the α-β bond of Tyr-66 (Heim *et al.*, 1994; Inouye and Tsuji, 1994). This autocatalytic post-translational reaction occurs in ~4 hours in native GFP (Heim *et al.*, 1994; Inouye and Tsuji, 1994). The chromophore forms from the central α-helix and is contained at almost the exact centre of the β-can (Ormo *et al.*, 1996; Yang *et al.*, 1996; Brejc *et al.*, 1997). Many of the physical properties of GFP (such as resistance to heat, urea, detergents and formaldehyde fixation) result from the insulation of the chromophore inside the β-barrel.

The isolated chromophore and intact GFP both absorb light maximally at ~390 nm with a smaller peak of absorption at 480nm (Morise *et al.*, 1974; Cody *et al.*, 1993). However, only intact GFP emits green light, the emission sprectrum peaking at 508nm (Morise *et al.*, 1974). The GFP gene contains all the information required for the formation of the chromophore. Thus, no Cnidaria-specific biosynthetic pathways or

agents such as antibodies, cofactors or substrates are necessary for its activity (Chalfie *et al.*, 1994).

Ludin *et al.* (1996) modified previously developed epitope tag vectors to incorporate GFP in two different forms suitable for its addition to target proteins at either N- or C-terminus. They showed that when MAP2 protein was tagged using such a vector it retained its phenotypic effects on transfected cells, which could be visualised in the living state.

The main purpose of using GFP-tagged proteins is to study dynamic events and their regulation *in vivo* using non-intrusive techniques. As a reporter, GFP has considerable advantages compared with the other conventional ones in that substrates and pre-treatment are not required for observation of the fluorescence in intact organs or tissue. Also, the analysis can be carried out on a real-time basis without killing animals or cells.

When injected into *Xenopus* oocytes, GFP-tagged proteins can be visualised in the living cells using standard fluorescent microscopy techniques. To investigate where XPAT protein is localised within the *Xenopus* oocyte, it was decided to make XPAT: GFP chimeras to visualise XPAT distribution. Two constructs were made incorporating GFP as a fluorescent tag at the N- terminus (in GFP-XPAT) or C-terminus (in XPAT-GFP) of the encoded fusion protein.

3.2 The production of Xpat::GFP chimeras

3.2.1 Resequencing of Xpat cDNA

During construction of Xpat-GFP, it became apparent that there must be some errors in the original Xpat cDNA sequence (Hudson and Woodland, 1998), since all attempts to make Xpat-GFP generated an XPAT-sized protein product (35kDa) in an *in vitro* transcription and translation reaction (Figure 3.2.E) and not a product of the expected size for XPAT-GFP (65kDa). However, the GFP in the vector alone (prior to the additional ligation of Xpat) translated well and at the correct size (30kDa), as shown in Figure 3.2.E. It seemed likely therefore that there was an error in the sequence at the 3′ end of the Xpat ORF near to the predicted STOP codon, and so the Xpat ORF

was resequenced. This was done using both manual and automatic sequencing reactions on both strands of the cDNA using primers spanning the length of the ORF. The correct cDNA and protein sequences of Xpat are shown in Figure 3.1, with alterations from the published Xpat sequence (Hudson and Woodland, 1998) highlighted in red. As predicted, there was an error in the sequence at the 3′ region of Xpat's ORF and in fact the actual XPAT protein is a 293 amino acid polypeptide, 10 amino acids shorter than the 303 amino acid-polypeptide originally predicted.

Figure 3.1: Corrected cDNA and predicted protein sequence of Xpat

```
   TGCAGCCTGTGTCTGAATGAATCCTCCTTTTGCTGCTGAGAATGAGAATTTTAGATGTGT
 1 ---------+---------+---------+---------+---------+---------+ 60
   ACGTCGGACACAGACTTACTTAGGAGGAAAACGACGACTCTTACTCTTAAAATCTACACA

   TCAAATTTAAAGGCTTTCAGGATAGCCCAGACTAGAGAATCTCTATGGCTTTGAAGGCAG
61 ---------+---------+---------+---------+---------+---------+ 120
   AGTTTAAATTTCCGAAAGTCCTATCGGGTCTGATCTCTTAGAGATACCGAAACTTCCGTC

                                                 M  A  L  K  A  E -

   AAGACTCTTTTGATATTTACTCCCAGTTGATCCAGAGCTTCTGCAGATATGCTGAGAACA
121 ---------+---------+---------+---------+---------+---------+ 180
   TTCTGAGAAAACTATAAATGAGGGTCAACTAGGTCTCGAAGACGTCTATACGACTCTTGT

     D  S  F  D  I  Y  S  Q  L  I  Q  S  F  C  R  Y  A  E  N  T -

   CTACCGTTTCAGAAAGCCAATCCCCAGCTTTCAATGCACAAAAGGAATTCCAAACTTGTC
181 ---------+---------+---------+---------+---------+---------+ 240
   GATGGCAAAGTCTTTCGGTTAGGGGTCGAAAGTTACGTGTTTTCCTTAAGGTTTGAACAG

     T  V  S  E  S  Q  S  P  A  F  N  A  Q  K  E  F  Q  T  C  Q -

   AAGACCATGCATGCTGTACACACTCTGAAGCCCATACGCACATTTTGATGCAGCAGTGGC
241 ---------+---------+---------+---------+---------+---------+ 300
   TTCTGGTACGTACGACATGTGTGAGACTTCGGGTATGCGTGTAAAACTACGTCGTCACCG

     D  H  A  C  C  T  H  S  E  A  H  T  H  I  L  M  Q  Q  W  Q -
```

```
    AGCTCTTAGAAGAACAGTGGGAGTACATTGACCATCTGAAGACCGATGTAGCAGCCCTGA
301 ---------+---------+---------+---------+---------+---------+ 360
    TCGAGAATCTTCTTGTCACCCTCATGTAACTGGTAGACTTCTGGCTACATCGTCGGGACT

      L   L   E   E   Q   W   E   Y   I   D   H   L   K   T   D   V   A   A   L   K -

    AACAGTTGCTGCATGGTTTCATGAACTCATTAAGTGGCACTGACAGTGGCATGGAGGGTA
361 ---------+---------+---------+---------+---------+---------+ 420
    TTGTCAACGACGTACCAAAGTACTTGAGTAATTCACCGTGACTGTCACCGTACCTCCCAT

      Q   L   L   H   G   F   M   N   S   L   S   G   T   D   S   G   M   E   G   T -

    CAAATCATTTTCTTCCTCCCCACCAAAACCCAACTTTGCTTAAAGATGAGGAAATTGTTG
421 ---------+---------+---------+---------+---------+---------+ 480
    GTTTAGTAAAAGAAGGAGGGGTGGTTTTGGGTTGAAACGAATTTCTACTCCTTTAACAAC

      N   H   F   L   P   P   H   Q   N   P   T   L   L   K   D   E   E   I   V   A -

    CAAGTGCTCTAAACAGGCCAAGCGTTGATATCAATGGATTTGAAGAGAACATCACTACAG
481 ---------+---------+---------+---------+---------+---------+ 540
    GTTCACGAGATTTGTCCGGTTCGCAACTATAGTTACCTAAACTTCTCTTGTAGTGATGTC

      S   A   L   N   R   P   S   V   D   I   N   G   F   E   E   N   I   T   T   G -

    GTGCCCAAATCCATGCAGCATTTACCAAAAGCCCCAAAAAGATGCCTGCCACAAGCACTC
541 ---------+---------+---------+---------+---------+---------+ 600
    CACGGGTTTAGGTACGTCGTAAATGGTTTTCGGGGTTTTTCTACGGACGGTGTTCGTGAG

      A   Q   I   H   A   A   F   T   K   S   P   K   K   M   P   A   T   S   T   P -

    CACGGAAATCTGAAGTTCTGTGGAGCTGCAGTCCGACCCTCGCTACAGATGGCTATTTTA
601 ---------+---------+---------+---------+---------+---------+ 660
    GTGCCTTTAGACTTCAAGACACCTCGACGTCAGGCTGGGAGCGATGTCTACCGATAAAAT

      R   K   S   E   V   L   W   S   C   S   P   T   L   A   T   D   G   Y   F   M -

    TGCTTCCTGACATTATCCTAAATCCCCTGGATGGAAAGAAGCTAGTTTCCATGCTGCGCA
661 ---------+---------+---------+---------+---------+---------+ 720
    ACGAAGGACTGTAATAGGATTTAGGGGACCTACCTTTCTTCGATCAAAGGTACGACGCGT

      L   P   D   I   I   L   N   P   L   D   G   K   K   L   V   S   M   L   R   S -
```

```
    GCTCCAACTACGAGCCACATCGTTTTGCAGAGCTTCTGTTTCAACATCACGTTCCCCATT
721 ---------+---------+---------+---------+---------+---------+ 780
    CGAGGTTGATGCTCGGTGTAGCAAAACGTCTCGAAGACAAAGTTGTAGTGCAAGGGGTAA

      S   N   Y   E   P   H   R   F   A   E   L   L   F   Q   H   H   V   P   H   S -

    CCCTCTTCCAACTGTGGGCTAACAAAGTGAACTTTGATGGTTCCAGAGGGAAACTTGGCC
781 ---------+---------+---------+---------+---------+---------+ 840
    GGGAGAAGGTTGACACCCGATTGTTTCACTTGAAACTACCAAGGTCTCCCTTTGAACCGG

      L   F   Q   L   W   A   N   K   V   N   F   D   G   S   R   G   K   L   G   L -

    TGCCCAGAAACCTAATGATAGACATCTTGCACCAAACATCCAAAAGGTTTGTCTTGGGCC
841 ---------+---------+---------+---------+---------+---------+ 900
    ACGGGTCTTTGGATTACTATCTGTAGAACGTGGTTTGTAGGTTTTCCAAACAGAACCCGG

      P   R   N   L   M   I   D   I   L   H   Q   T   S   K   R   F   V   L   G   P -

    CAAAGGAGAAACGGAAGATTAAGACAAGGTTGAATTTGTTGTTGAGGACACGTCAGGATA
901 ---------+---------+---------+---------+---------+---------+ 960
    GTTTCCTCTTTGCCTTCTAATTCTGTTCCAACTTAAACAACAACTCCTGTGCAGTCCTAT

      K   E   K   R   K   I   K   T   R   L   N   L   L   L   R   T   R   Q   D   R -

    GAGCTTGGTGGGATGTTGGCCTGTAGGCAAAGGTTTAAGTTTTTGTTAAGATTT
961 ---------+---------+---------+---------+---------+----  1014
    CTCGAACCACCCTACAACCGGACATCCGTTTCCAAATTCAAAAACAATTCTAAA

      A   W   W   D   V   G   L   .
```

3.2.2 The production of XPAT-GFP and GFP-XPAT

In order to incorporate GFP as a fluorescent tag at the N- or C- terminus of XPAT, the pSPJC2L vector (Cook *et al.*, 1993) was modified to accept cloned cDNA fragments to be expressed in frame with GFP.

In order to construct GFP-Xpat, the coding region for GFP was amplified by PCR using primers that created 5′ *Bgl*II and 3′ *Hind*III sites. The resulting PCR fragment was cloned into the *Bgl*II and *Hind*III sites of pSPJC2L, creating pSPJC2L-NGFP. The region encoding the Xpat ORF was amplified from a cDNA library clone with

primers creating 5′ and 3′ *Hind*III sites. The resulting fragment was cloned into the *Hind*III site of pSPJC2L-NGFP, generating GFP-Xpat, Xpat tagged with GFP at its N-terminus. This clone is illustrated in Figure 3.2A.

To construct Xpat-GFP, the GFP coding sequence was amplified using primers designed to create a 5′ *Bgl*II and a 3′ *Eco*R1 site. Finally, the resulting fragment was cloned into the *Bgl*II and *Eco*R1 sites of pSPJC2L to generate pSPJC2L-cGFP. This vector thus contained restriction sites that could be used to create mRNA encoding proteins tagged with GFP at the C-terminus. Fluorescently tagged Xpat was prepared using this vector containing GFP. The region containing Xpat's ORF was amplified from a cDNA library clone with primers creating 5′ and 3′ *Bgl*II sites. The resulting fragment was cloned into the *Bgl*II site of pSPJC2L-cGFP generating Xpat-GFP. This clone is shown in Figure 3.2.B.

Once constructs were made, restriction digestion was used to confirm that the inserts were present and that the orientation of Xpat was correct. This was necessary because Xpat was generated with *Hind*III on both ends of the PCR product (in GFP-Xpat) and with *Bgl*III on both ends of its PCR product (in Xpat-GFP) thus it could be ligated into the construct in either of two possible orientations. Figure 3.2.C and 3.2D show restriction digests on GFP-Xpat and Xpat-GFP, respectively; the digests are consistent with Xpat having inserted in the correct orientation, in-frame with GFP, in both constructs.

Following restriction digestion, *in vitro*-coupled transcription and translation reactions were performed using Xpat-GFP or GFP-Xpat DNA as a template. A fraction of each reaction was resolved by SDS-PAGE, alongside translations of both Xpat and GFP. An autoradiograph of this gel is shown in Figure 3.2.F, and indicates that both XPAT-GFP and GFP-XPAT have an apparent molecular weight of approximately 65kDa, the expected size for these chimeras. In 3.2.F, it is not obvious that XPAT-GFP and GFP-XPAT are exactly the same size, since they are not in adjacent lanes of the gel. A further protein gel was run to clarify the sizes of both proteins, an autoradiograph of this gel is shown in 3.2.G. As this figure shows, XPAT-GFP and GFP-XPAT are identical in size, as expected.

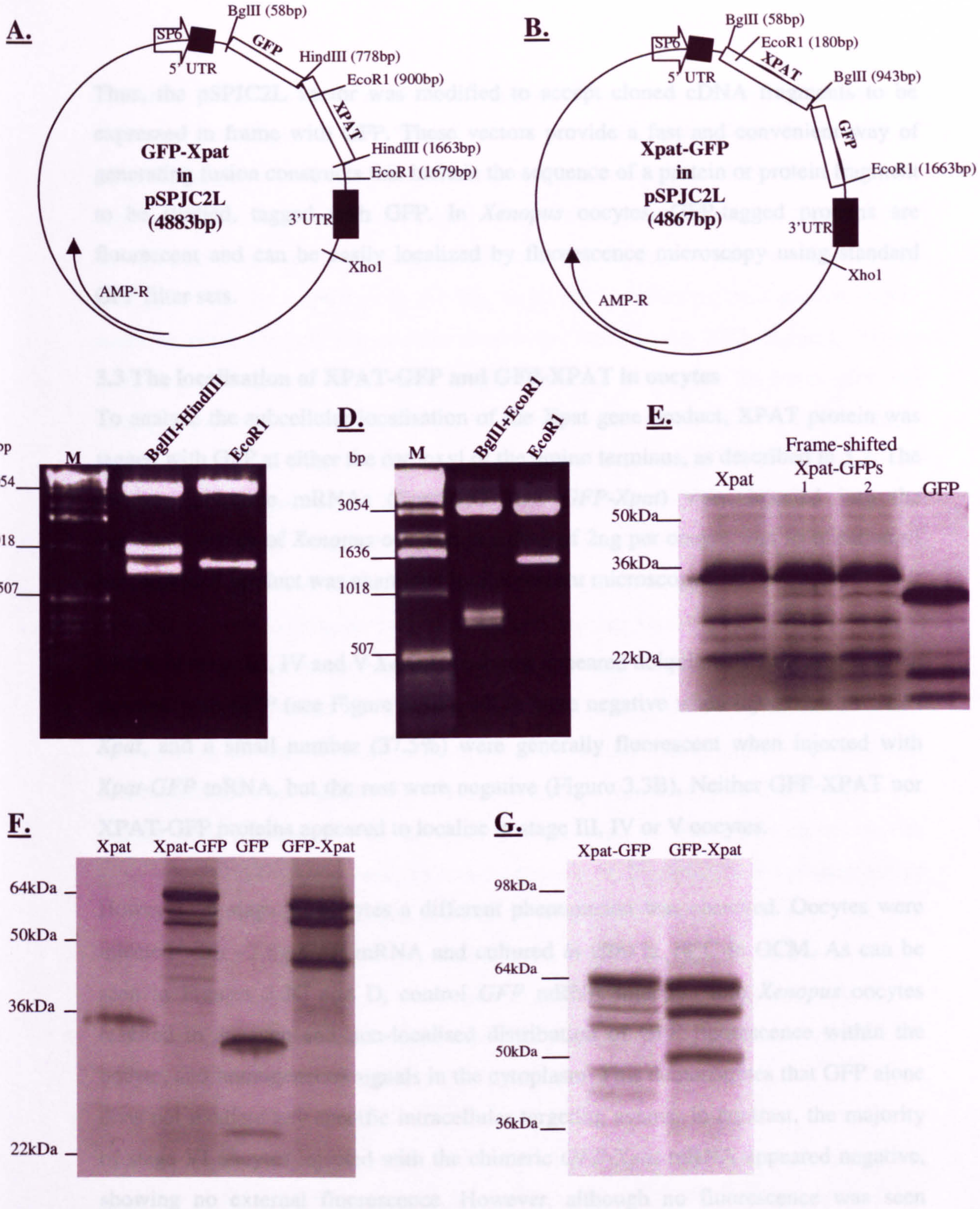

Figure 3.2: Cloning of Xpat-GFP and GFP-Xpat.

(A) Vector map of GFP-Xpat in pSPJC2L, with positions of restriction enzyme sites marked. (B) The vector map of Xpat-GFP in pSPJC2L with restriction enzyme sites marked. The 3' and 5'UTRs present in pSPJC2L vector are *globin* UTRs. (C) 1% agarose gel of restriction enzyme digests on GFP-Xpat DNA; *Bgl*II and *Hind*III double digest was used to confirm the presence of GFP and Xpat inserts in the clone, and *Eco*R1 was used to confirm the orientation of Xpat in the clone (see map in A for details). (D) 1% agarose gel of restriction enzyme digests on Xpat-GFP DNA; *Bgl*II and *Eco*R1 double digest was used to confirm the presence of GFP and Xpat inserts in the clone, and the orientation of Xpat in the clone was confirmed by *Eco*R1 digestion (see map in B for details). (E) Autoradiograph of 12% acrylamide gel of *in vitro* transcription and translation reactions (performed using rabbit reticulocyte lysate) using Xpat, GFP and 2 original attempts to generate Xpat-GFP cDNA as a template. (F) and (G) show autoradiographs of 12% SDS-PAGE gels of (rabbit reticulocyte lysate) *in vitro* transcription and translation reactions using Xpat, GFP, GFP-Xpat and Xpat-GFP DNA as templates.

Thus, the pSPJC2L vector was modified to accept cloned cDNA fragments to be expressed in frame with GFP. These vectors provide a fast and convenient way of generating fusion constructs that include the sequence of a protein or protein fragment to be studied, tagged with GFP. In *Xenopus* oocytes, GFP-tagged proteins are fluorescent and can be easily localized by fluorescence microscopy using standard GFP filter sets.

3.3 The localisation of XPAT-GFP and GFP-XPAT in oocytes

To analyse the subcellular localisation of the Xpat gene product, XPAT protein was tagged with GFP at either the carboxyl or the amino terminus, as described in 3.2. The resultant chimeric mRNAs (*Xpat-GFP* and *GFP-Xpat*) were injected into the equatorial region of *Xenopus* oocytes, at a dose of 2ng per oocyte, and localisation of the translated product was examined by fluorescent microscopy.

69.6% of stage III, IV and V *Xenopus* oocytes appeared ubiquitously fluorescent when injected with *GFP* (see Figure 3.3A), 100% were negative when injected with *GFP-Xpat*, and a small number (37.5%) were generally fluorescent when injected with *Xpat-GFP* mRNA, but the rest were negative (Figure 3.3B). Neither GFP-XPAT nor XPAT-GFP proteins appeared to localise in stage III, IV or V oocytes.

However, in stage VI oocytes a different phenomenon was observed. Oocytes were injected with ~2 ng *GFP* mRNA and cultured *in vitro* at 18°C in OCM. As can be seen in Figures 3.3C and D, control *GFP* mRNA injection into *Xenopus* oocytes resulted in an even and non-localised distribution of GFP fluorescence within the oocyte, and homogeneous signals in the cytoplasm. This demonstrates that GFP alone does not mediate any specific intracellular targeting events. In contrast, the majority of stage VI oocytes injected with the chimeric *GFP-Xpat* mRNA appeared negative, showing no external fluorescence. However, although no fluorescence was seen localising externally, dissected nuclei were fluorescent - highlighting that GFP-tagged XPAT is localised to the nucleus of *Xenopus* oocytes (Figure 3.3J and Section 3.3.3).

Localisation of XPAT-GFP protein was also observed in stage VI *Xenopus* oocytes. On day 1 (18 hours after injection), the fusion protein was expressed principally in an

equatorial domain around the point of injection. There was diffuse fluorescence in some oocytes (Figure 3.3E shows four such oocytes, expressing XPAT-GFP in equatorial region), but also small granules, ~1-2 μm in diameter which could easily be seen in a dissecting stereomicroscope (as seen in the oocyte shown in Figure 3.3F). By 42 hours after injection in many oocytes most of the fluorescence was found at, or just lateral to, the vegetal pole. At this stage the fluorescence was predominantly punctate, but at the pole the granules were larger (see Figures 3.3G, H and I). Figure 3.3G is a photograph of the same oocyte shown in 3.3F taken 24 hours later and clearly shows that the particles of XPAT-GFP protein expression have grown larger during this period. Figure 3.3H shows an oocyte expressing XPAT-GFP in small granules at the vegetal pole 42 hours after injection of *Xpat-GFP* mRNA. Figure 3.3I shows an enlarged view of an oocyte expressing XPAT-GFP in granules, this photograph clearly shows how the small particles appear to be aggregating into larger granules towards the vegetal pole of the oocyte. By day 3 (66-72 hours after injection) the granules had, in many cases, aggregated into large structures (of between 10-50 μm across) exactly like the granules seen by *in situ* hybridisation to germ plasm RNAs, and also with some monoclonal antibodies raised against unknown germ plasm constituents (Denegre *et al,* 1997). These granules were seen at or just lateral to the vegetal pole (Figures 3.4 A, B, C, D and E). Figure 3.4A shows three oocytes expressing XPAT-GFP in granules at the vegetal pole. Figure 3.4B is a photograph of an oocyte expressing fluorescent granules of XPAT-GFP protein. However, 3.4C is a good example of an oocyte expressing even larger aggregates of fusion protein granules at its vegetal pole. A direct view of the vegetal pole of this oocyte is shown in Figure 3.4D. A different oocyte that is expressing large granules of XPAT-GFP protein, again at its vegetal pole, is shown in Figure 3.4E.

In order to get a better perception of exactly what was happening to the particles and granules of XPAT-GFP protein in oocytes, a higher magnification microscope was used (Figures 3.4 F and G). Figure 3.4F shows a higher magnification view (x200) of the vegetal region localisation of XPAT-GFP protein after 18hours in culture, small granules of XPAT-GFP are clearly visible. Figure 3.4G is a high power photograph (200x magnification) of large granules of XPAT-GFP protein formed 42 hours after injection. These photographs confirm that the small punctate particles of XPAT-GFP

(Opposite) Figure 3.3: Expression of XPAT-GFP, GFP and GFP-XPAT in *Xenopus* oocytes

Oocytes were injected with 2 ng of *Xpat-GFP*, *GFP* or *GFP-Xpat* mRNA and cultured *in vitro* in OCM at 18°C. Localisation of protein was examined by fluorescent microscopy after various times in culture. (A) Stage III and IV oocytes injected with *GFP* mRNA. (B) Stage IV oocytes injected with *Xpat-GFP* mRNA. (C) Stage VI oocytes shown 18 hours post-injection with *GFP* mRNA. (D) Oocytes expressing GFP, 42 hours after injection. (E)+(F) Stage VI oocytes 18 hours after injection with *Xpat-GFP* mRNA. (G) Shows the oocyte in (F) 42 hours after *Xpat-GFP* injection. (H) Another oocyte expressing small granules of XPAT-GFP protein, at its vegetal pole 42 hours after mRNA injection. (I) A vegetal view of granules of XPAT-GFP forming in a stage VI *Xenopus* oocyte, 42 hours after injection with mRNA. (J) Two stage VI oocytes injected with *GFP-Xpat* mRNA, showing no external fluorescence after 42hours in culture. In (A) and (B) the scale bars represent 200µm. In (C) –(J) each oocyte is ~1.2mm in diameter.

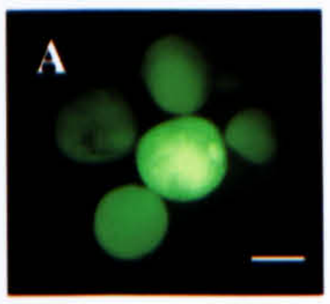
A

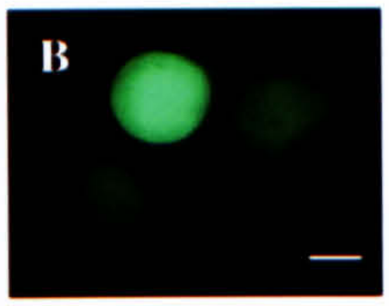
B

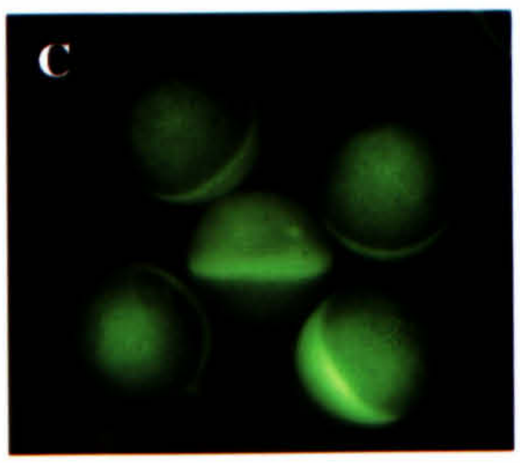
C

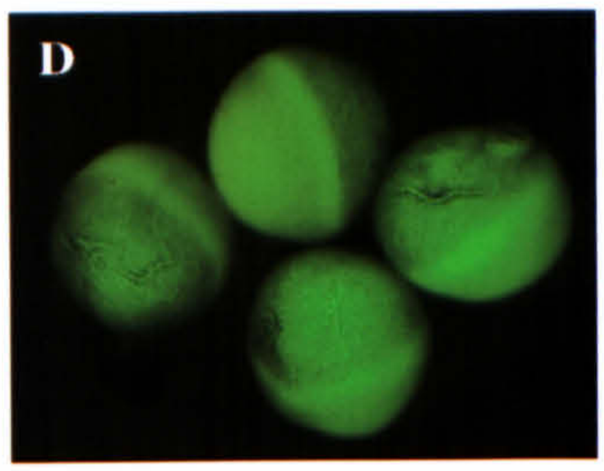
D

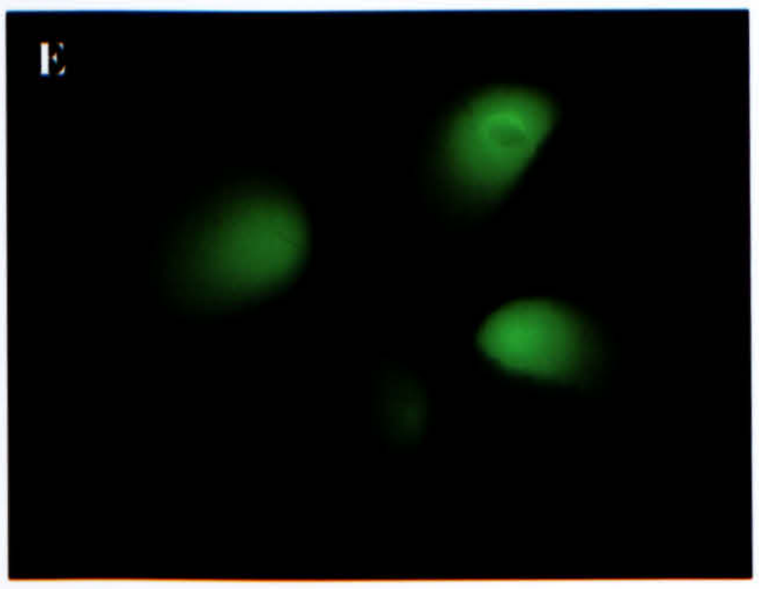
E

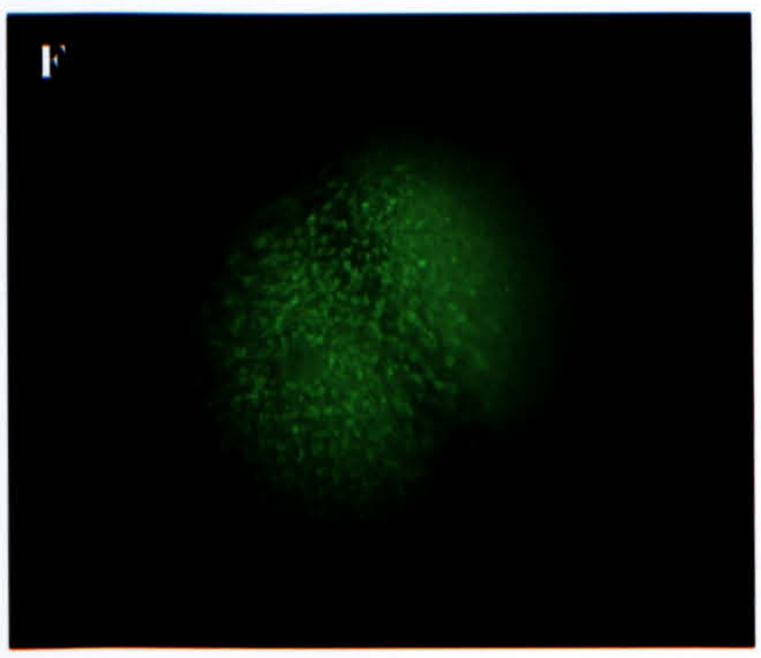
F

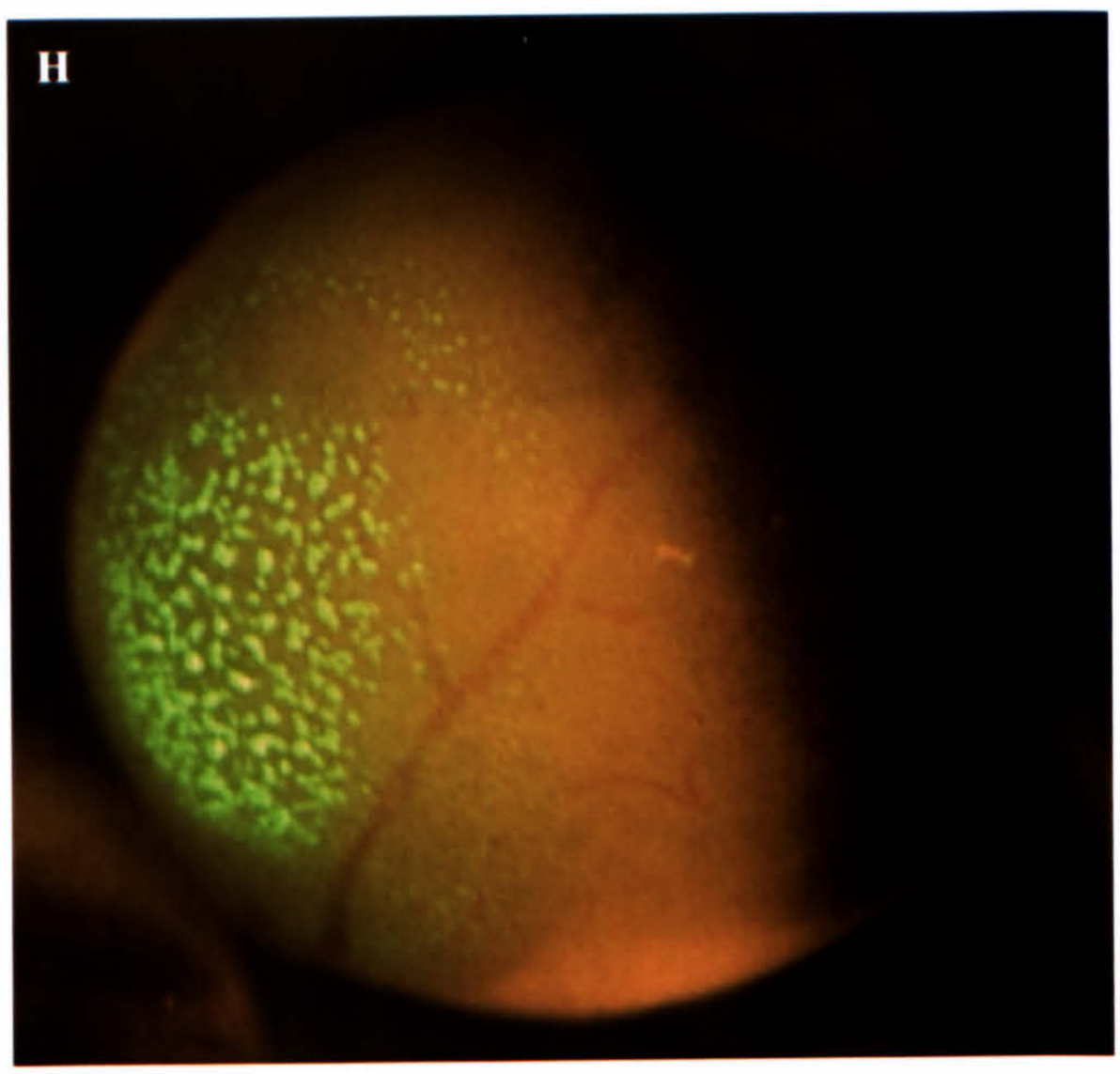
H

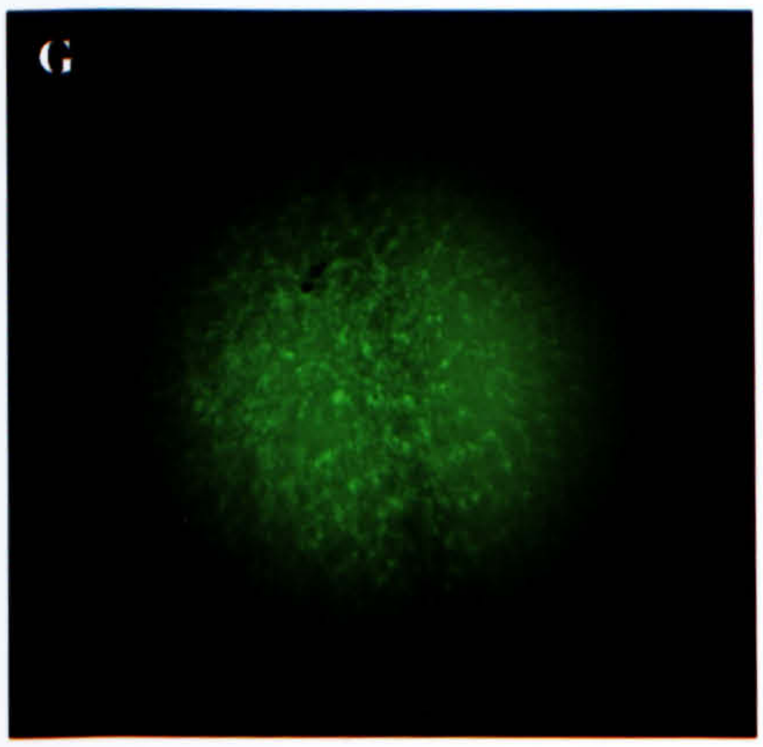
G

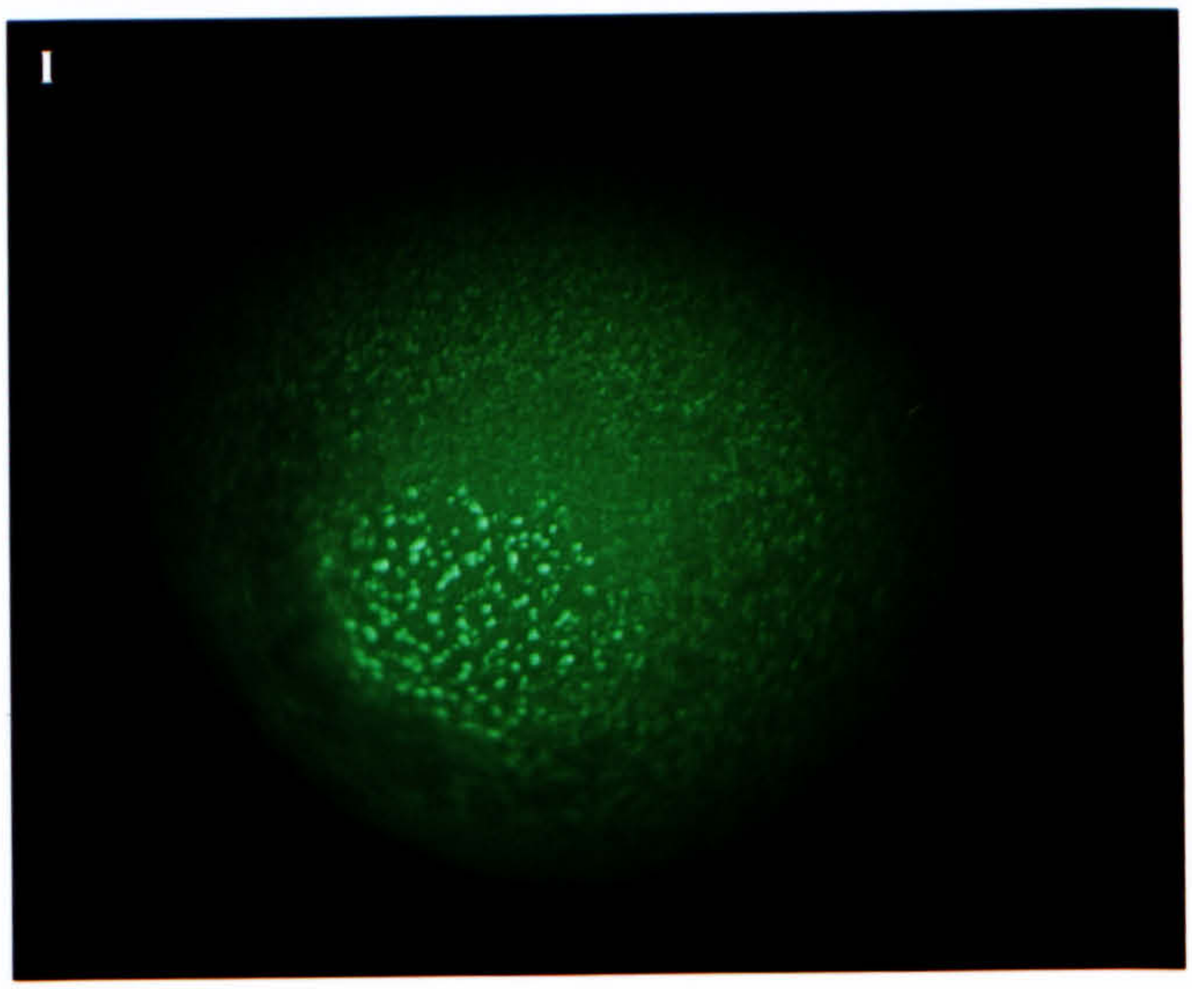
I

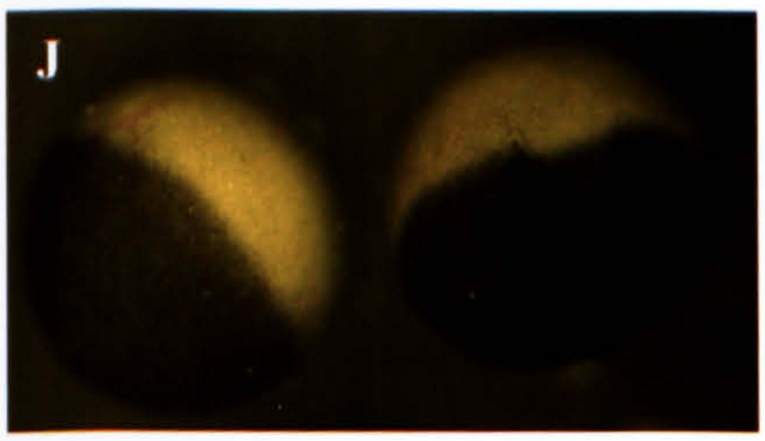
J

protein are aggregating into larger structures (shown particularly well in Figure 3.4G). Thus, after 3 days, XPAT-GFP appears to be distributed in a similar way to germ plasm itself.

The striking localisation of fluorescence from XPAT-GFP in particulate structures in the vegetal hemisphere of oocytes, compared to the lack of localisation of unfused GFP, demonstrates that the XPAT domain of the fusion protein is in fact responsible for the targeting and localisation of this fluorescence.

Two separate experiments were then performed using stage VI *Xenopus* oocytes. *GFP-Xpat, Xpat-GFP* or *GFP* alone were injected into either the animal region or the vegetal region of an oocyte and oocytes were then cultured *in vitro* for up to three days. The oocytes were then scored for localisation of fluorescence. Table 3.1 shows the numbers of oocytes that showed vegetal localisation. The experiments summarised in this table were done concomitantly under identical conditions.

Table 3.1 The localisation of XPAT-GFP versus GFP-XPAT in stage VI *Xenopus* oocytes

Time post-injection	*GFP* injected Vegetally	*GFP-Xpat* injected vegetally	*Xpat-GFP* injected vegetally	*GFP* injected animally	*GFP-Xpat* injected animally	*Xpat-GFP* injected animally
Day 1 18 hours	G: 93.5% –: 6.5% *N=77*	V: 19.3% E: 14.0% –: 66.7% *N=57*	V: 39.7% E: 29.3% –: 31.0% *N=58*	G: 86.0% –: 14.0% *N=57*	V: 3.9% E/A: 17.7% –: 78.4% *N=51*	V: 10.9% E/A: 47.8% –: 41.3% *N=46*
Day 2 42 hours	G: 86.2% –: 13.8% *N=58*	V: 9.6% E: 1.9% –: 88.5% *N=52*	V: 41.8% E: 27.3% –: 30.9% *N=55*	G: 85.2% –: 14.8% *N=54*	V: 4.2% E/A: 4.2% –: 91.6% *N=48*	V: 23.8% E/A: 23.8% –: 52.4% *N=42*
Day 3 66 hours	G: 74.5% –: 25.5% *N=47*	V: 8.7% E: 0% –: 91.3% *N=23*	V: 25% E: 35.7% –: 39.3% *N=28*	G: 57.1% –: 42.9% *N=28*	V: 7.4% E: 0% –: 92.6% *N=27*	V 22.7% E/A: 27.3% –: 50.0% *N=22*

G = general fluorescence, – = no fluorescence, V= vegetal fluorescence, E= equatorial fluorescence, A= animal fluorescence, N= number of oocytes scored. Oocytes that died were removed from culture and discarded, thus affecting scores.

As Table 3.1 shows, 18 hours after vegetal injection of *Xpat-GFP*, ~40% of oocytes show vegetal fluorescence, by day 3 this decreases to 25%. However, 18 hours post vegetal injection of *GFP-Xpat,* 19% of oocytes show vegetal fluorescence, this number decreasing to 9% by day 3. 18 hours after a vegetal injection of *GFP*, used as a control, 94% of oocytes showed a general fluorescence throughout the oocyte. On

(Opposite) Figure 3.4: Expression of XPAT-GFP in *Xenopus* oocytes

Stage VI *Xenopus* oocytes were injected with 2 ng of *Xpat-GFP* mRNA and cultured *in vitro* in OCM at 18°C. After 66 hours (unless otherwise stated) the localisation of XPAT-GFP was examined by fluorescent microscopy. (A) Three oocytes expressing granules of XPAT-GFP at their vegetal poles. (B) An oocyte expressing granules of XPAT-GFP protein. (C) An oocyte showing aggregation of granules of XPAT-GFP protein. (D) A vegetal view of the oocyte in (C) showing aggregating granules. (E) Another stage VI oocyte expressing granules of XPAT-GFP protein at its vegetal pole. (F) A high magnification photograph (x200) of an oocyte 18 hours after injection with *Xpat-GFP* mRNA, showing small fluorescent granules visible at the vegetal pole. (G) A high magnification photograph (x200) of large granules of XPAT-GFP protein formed at the vegetal pole of an oocyte 42 hours after injection with mRNA. In (A) –(E) each oocyte is ~1.2mm in diameter. The scale bar in (F) and (G) represents 50 μm.

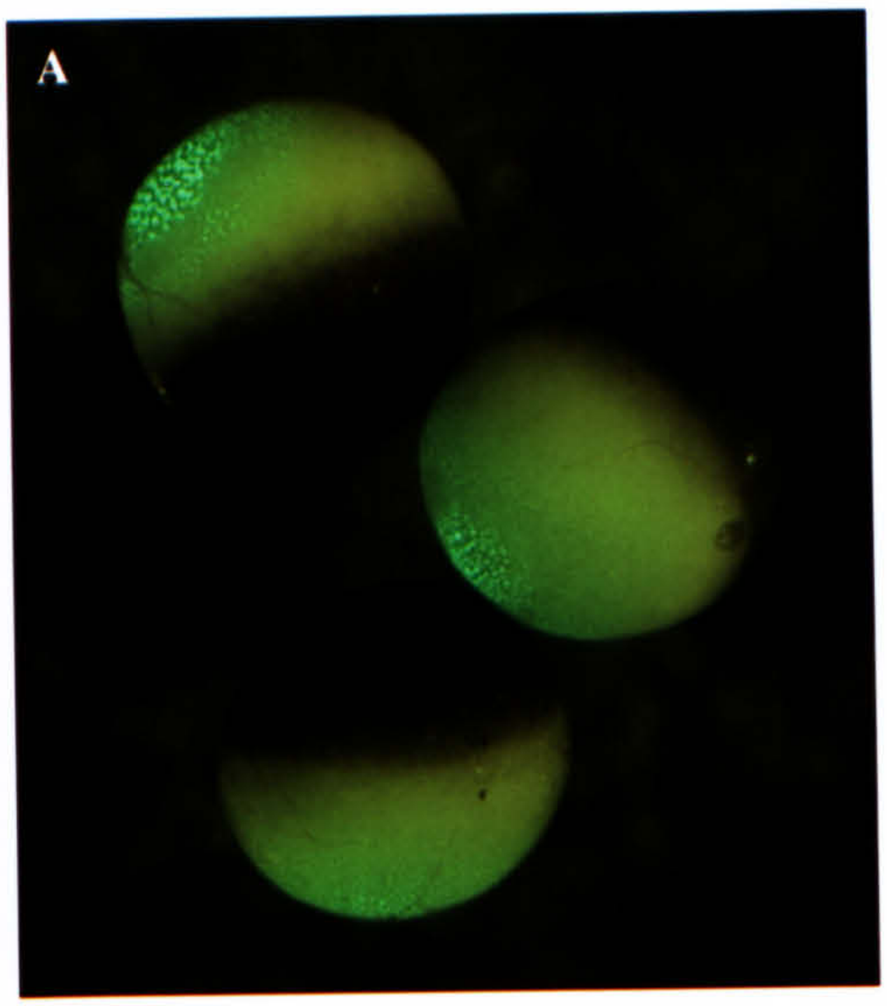
A

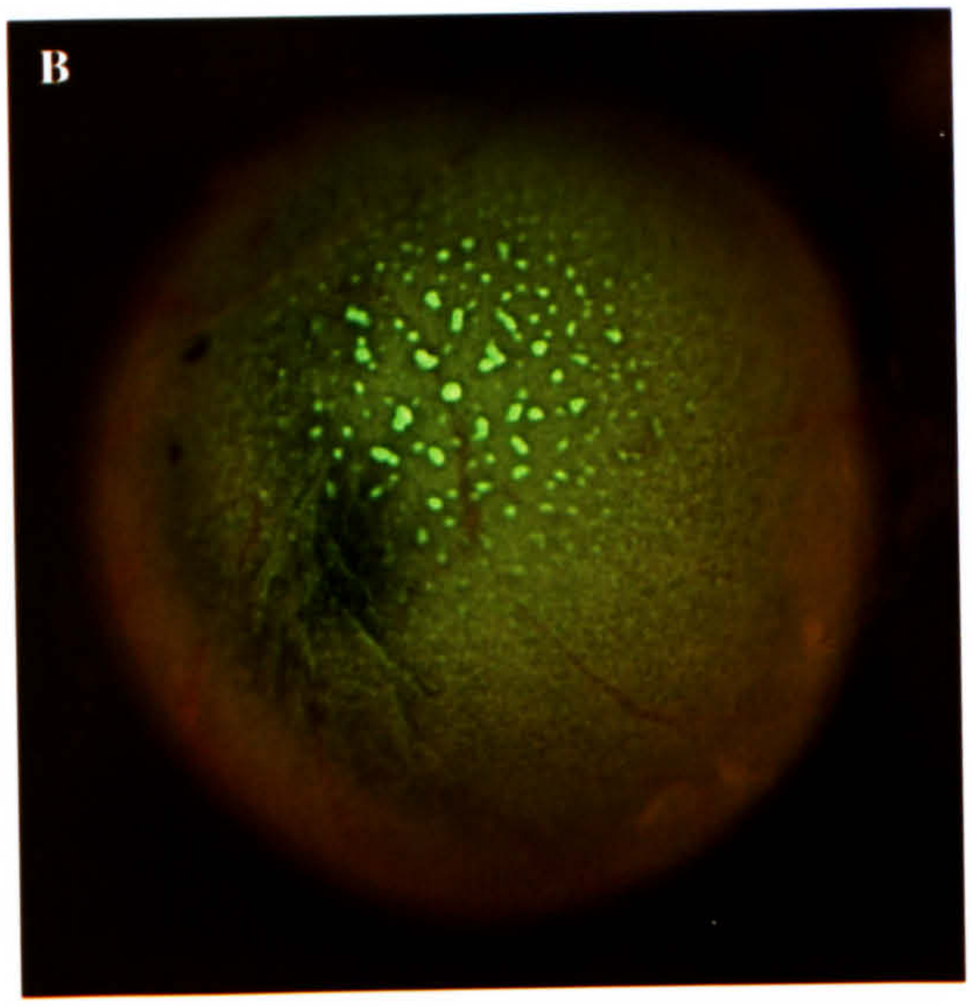
B

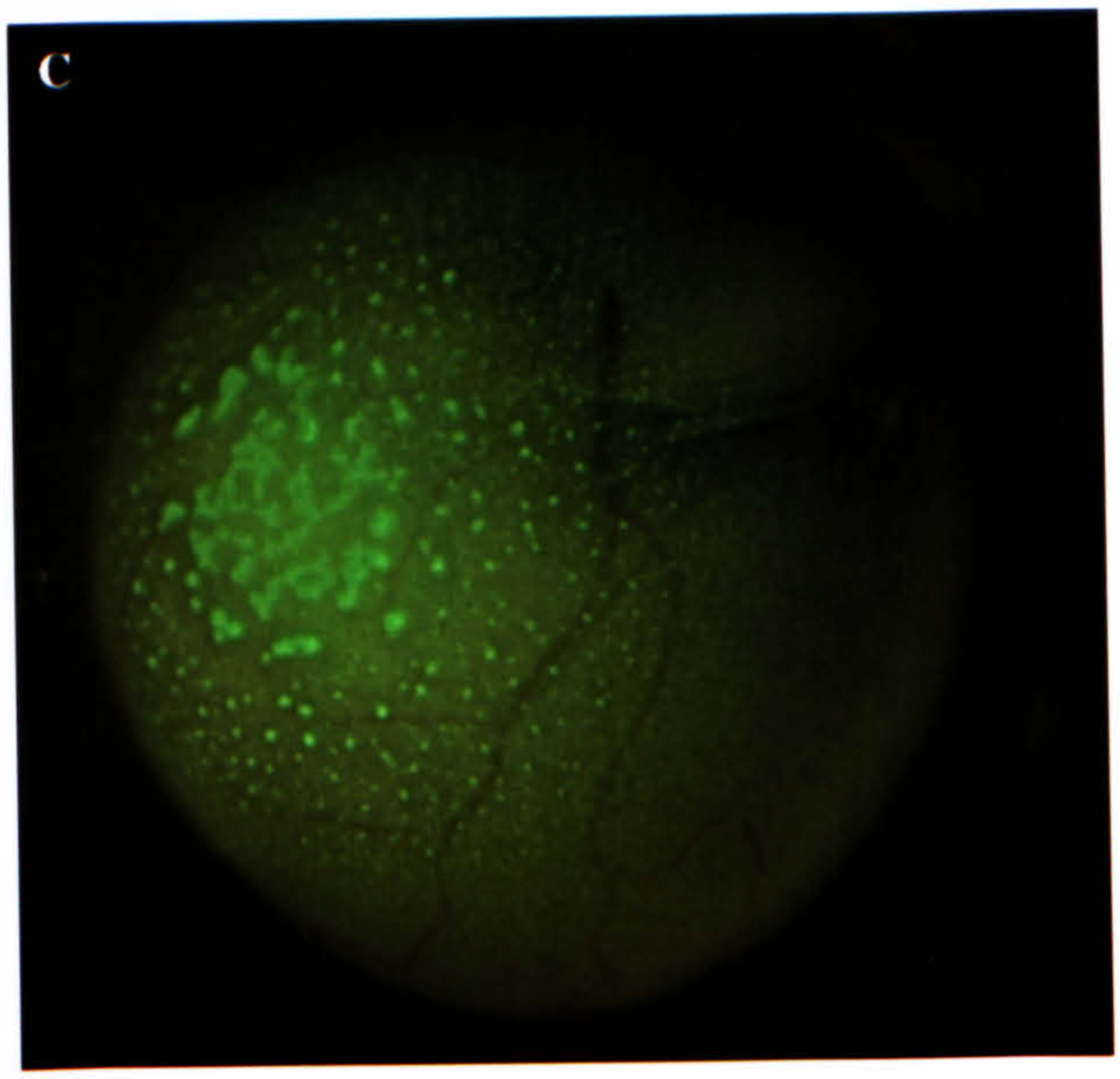
C

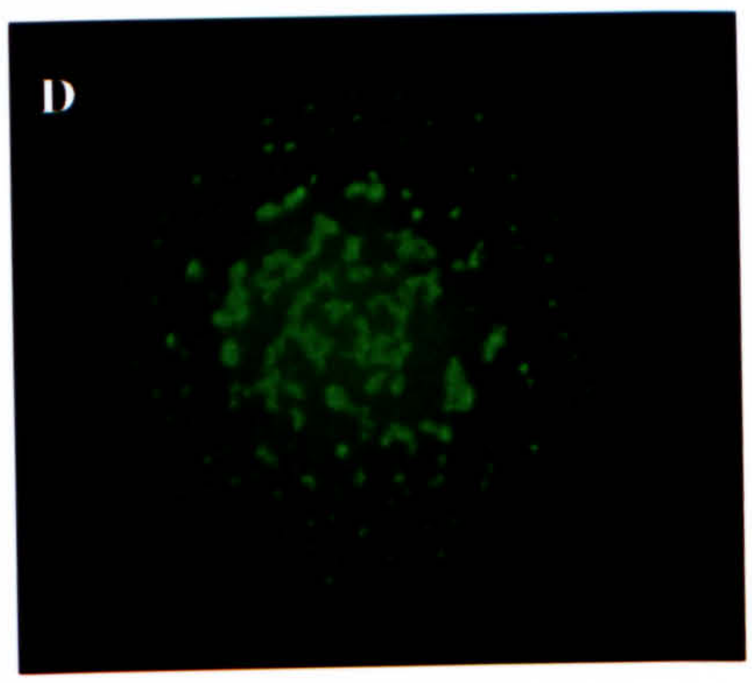
D

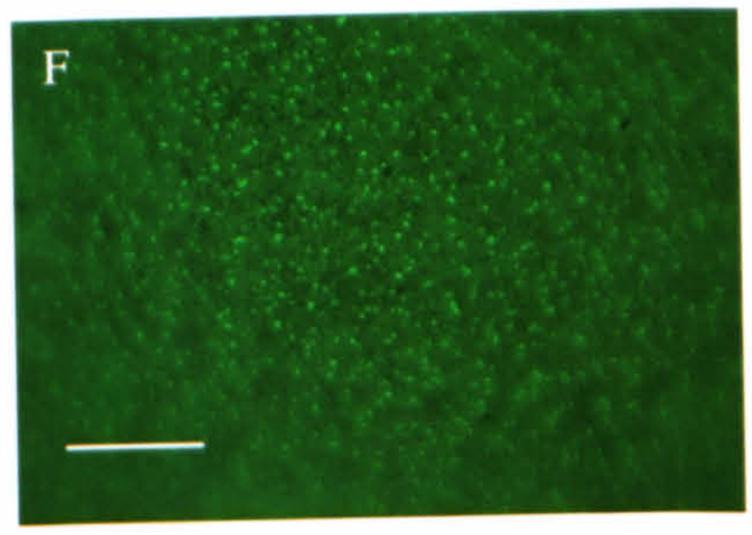
F

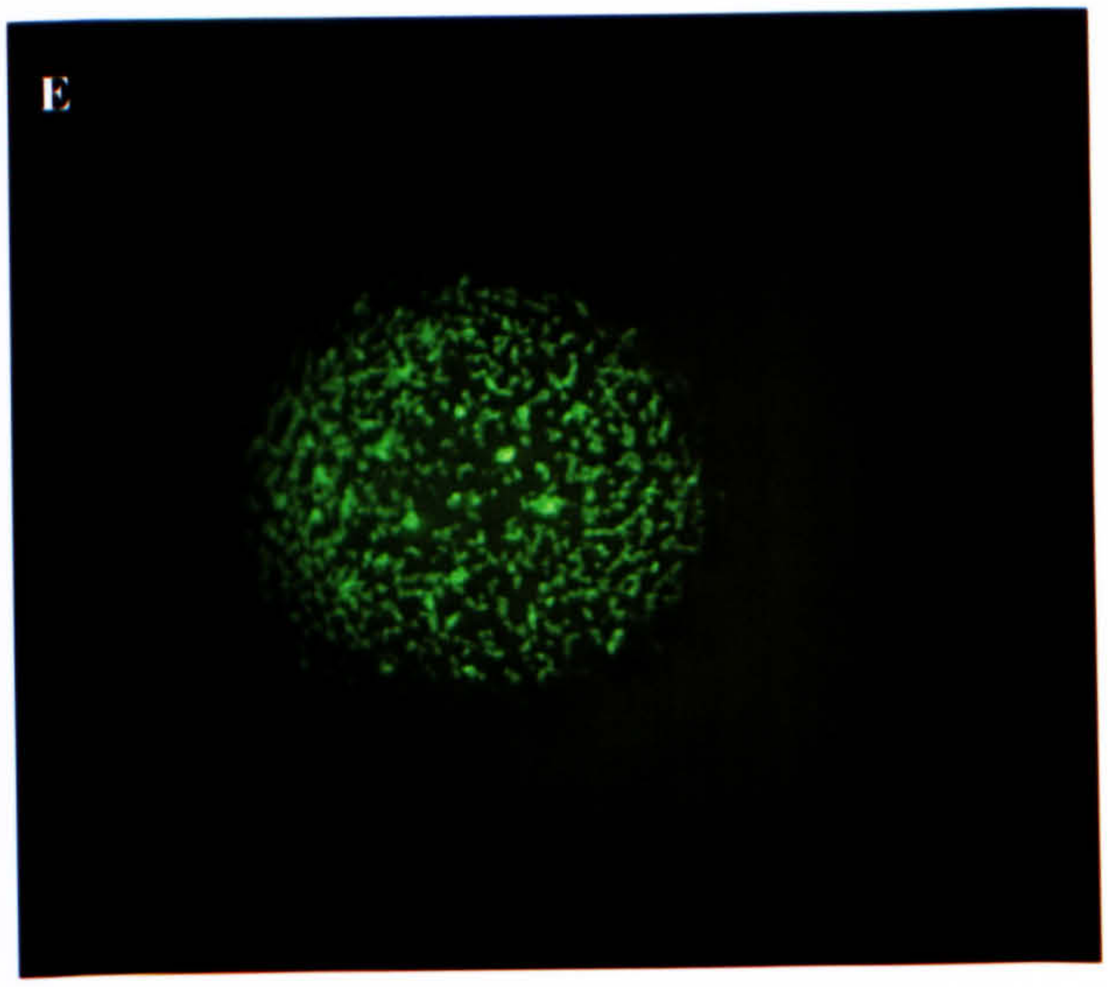
E

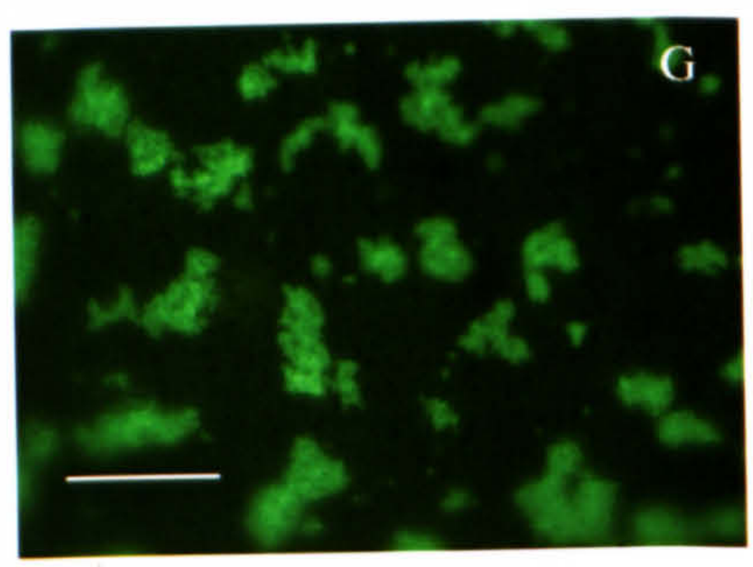
G

day 3, this figure reduces to 75%. This reduction is probably related to the health of the oocytes, since the remaining 25% are apparently negative.

It was also decided to determine the effect of injecting RNA into the animal pole of the oocyte. 86% of these oocytes show general fluorescence 18 hours post *GFP* injection. By day 3, however, this reduces to 57% (again likely due to the health of the oocytes). In comparison, 18 hours after animal injection of *GFP-Xpat*, 78% of oocytes are negative, 18% show equatorial or animal fluorescence and 4% are vegetal. By day 3, 7% show vegetal expression and 93% appear negative.

18 hours after an animal injection of *Xpat-GFP*, 41% of oocytes are negative, 48% show equatorial/animal injection and 11% show vegetal localisation of XPAT-GFP. By day 3, 50% of oocytes are negative, 23% show equatorial or animal expression whereas 27% now have vegetal localisation, and, as previously described, this is granular. Thus, the localisation of XPAT-GFP appears to be dynamic, capable of moving from animal to vegetal pole. Indeed, a very similar proportion of oocytes injected (in the animal pole) with *Xpat-GFP* achieve localisation to the vegetal pole by day 3 compared with oocytes injected vegetally with *Xpat-GFP* (23% compared with 25%).

It is worth noting that following an animal injection (compared with a vegetal injection), a greater proportion of oocytes are negative. This is true of *GFP*, *GFP-Xpat* or *Xpat-GFP* injection. By day 3, 43% of oocytes injected animally with GFP were negative whereas only 26% of those oocytes injected vegetally with GFP were negative. This is because there is a risk of injecting the RNA into oocyte nucleus rather than into the cytoplasm, which could stop translation (Braddock *et al.*, 1989).

Thus, the results for XPAT-GFP seemed most encouraging. In other literature, C-terminal GFP tags are used (rather than N-terminal ones) in the majority of experiments in order to see the expected localisation; for example, Xenf (Nakatani *et al.*, 2000) and APC (Mimori-Kiyosue *et al.*, 2000) in *Xenopus* A6 epithelial cells, XFD (Pownall *et al.*, 1998) and $GABA_A$ (Chappel *et al.*, 1998) in *Xenopus* oocytes, and Dishevelled (Miller *et al.*, 1999) in oocytes and fertilised eggs. On the other hand, Sayers *et al.* (1997) used GFP-insositol 1,4,5-trophosphate which localises to the

animal pole and perinuclear region of *Xenopus laevis* oocytes. However, the C-terminal region of this protein is functional as a channel (ES) domain. Mishima and Nishida (1999) used both C- and N-terminal GFP tagged versions of X coronin. Both constructs gave consistent localisation to same place as seen previously in fixed immuno-fluorescent staining. Likewise, Ludin *et al.* (1996) used both orientations and saw that both were visible for MAD2C. For every example stated, no authors indicated failure of any fusion protein to localise in the expected manner.

3.3.1 The effect of injection site on localisation of XPAT-GFP in *Xenopus* oocytes

Since it seems from the results in Table 3.1, discussed in Section 3.2, that the location of the site of injection (animal versus vegetal) has an effect on both vegetal localisation and on number (and percentage) of oocytes that appear negative. It was decided to examine this further, using greater numbers of oocytes for XPAT-GFP. XPAT-GFP was further pursued, whereas GFP-XPAT was not because the localisation of XPAT-GFP seemed more promising.

Larger numbers of oocytes in several different experiments were injected in either the vegetal half (towards the vegetal pole but not directly at the vegetal pole since this could directly disrupt the germ plasm), the animal half (Section 3.2) or at the equatorial region of the oocyte. These oocytes were then cultured *in vitro* for up to 3 days and then scored for the localisation of the fluorescence. The results from these experiments were pooled and are recorded in Table 3.2.

Table 3.2 The location of the injection site affects the localisation of XPAT-GFP

Time post injection	*Xpat-GFP* injected animally	*Xpat-GFP* injected equatorially	*Xpat-GFP* injected vegetally
Day 1 **18 hours**	V: 10.9% E/A: 47.8% –: 41.3% *N=46*	V: 13.2% E: 61.6% –: 25.2% *N=357*	V: 53.15% E: 22.8% –: 24.05% *N=79*
Day 2 **42 hours**	V: 23.8% E/A: 23.8% –: 52.4% *N=42*	V: 23.5% E: 51.2% –: 25.3% *N=293*	V: 41.8% E: 27.3% –: 30.9% *N=55*
Day 3 **66 hours**	V: 22.7% E/A: 27.3% –: 50% *N=22*	V: 31.0% E: 44.4% –: 24.6% *N=329*	V: 42.4% E: 4.8% –: 52.9% *N=210*

V= vegetally fluorescent, E= equatorially fluorescent, A= animally fluorescent, – = no fluorescence, N= number of oocytes scored.

For the experiments described next, which are summarised in Table 3.2, greater numbers of oocytes were scored on day 3 than on days 1 and 2 because some oocytes were not analysed for 3 days before assessing the localisation.

As previously described in 3.2, oocytes injected with *Xpat-GFP* animally showed ~11% vegetal localisation on day 1. This figure rises to 24% on day 2 and 23% on day 3. Numbers of negative oocytes were 41% on day 1, 52% on day 2 and 50% on day 3. *Xpat-GFP* appears to be translated at the site of injection, so fluorescence is seen here and then the XPAT-GFP appears to translocate towards the vegetal pole.

With an injection into the equatorial region (Table 3.2), day 1 sees 13% vegetal localisation, on day 2 this rises to 24% and by day 3 it increases to 31%. Thus, each day sees increasing numbers of oocytes showing vegetal localisation. This is possibly because the XPAT-GFP protein is moving to its "correct" location in the oocyte, which takes time, but there is less distance to travel from the equatorial region than from the animal pole. It is also interesting to note that the number of negative oocytes is less in the sample injected equatorially; by day 3 only 25% are negative (compared with 50% in animally injected oocytes).

In those oocytes injected in the vegetal pole, day 1 sees 53% of oocytes showing vegetal expression, a high percentage as would be expected at the site of injection. Oocytes injected in the equatorial region and in the animal pole also show fluorescence in the region of injection – 62% of oocytes injected in the equator still show fluorescence here 18 hours later; and 48% of those oocytes injected at the animal pole still show animal or equatorial fluorescence 18 hours after injection. Thus, as previously suggested, *Xpat-GFP* appears to be translated at the site of injection, so fluorescence is firstly seen here and then the XPAT-GFP appears to translocate towards the vegetal pole.

On day 2, 42% of oocytes that had been injected in the equator show vegetal localisation and on day 3 this percentage stays about the same. However, the number of negative oocytes increases with the length of time the oocytes are in culture; on day 1 24% are negative, by day 2 this is 31% and on day 3 53% are negative. This is probably related to the health of the oocytes as prolonged times in culture seem to

lead to some deterioration. Also, if oocytes do not show XPAT-GFP localisation in the vegetal region they tend, by day 3, to be negative.

Thus, it seems that vegetal injection gives a higher percentage of vegetally localised XPAT-GFP throughout the experiments at any given time but, for example, on day 3 43% of oocytes show vegetal fluorescence after a vegetal pole injection, compared with 31% vegetal after an equatorial injection and 23% vegetal after an injection in the animal pole. This is to be expected since *Xpat-GFP* is translated at the injection site; if oocytes are injected at the vegetal pole (where XPAT seems to localise) then the fluorescence will remain in the vegetal region, whereas animal or equatorial injected *Xpat-GFP* is translated and then the protein has to translocate to the vegetal pole. However, there are fewer negative oocytes on day 2 and day 3 after an equatorial injection compared to a vegetal injection. It seems that equatorial injection causes *Xpat-GFP* to be translated at the injection site and then the protein translocates vegetally over time.

3.3.2 The effect of culture medium on localisation of XPAT-GFP in oocytes

It was decided to determine whether or not the culture medium used had any effect on XPAT-GFP localisation in oocytes. This was done because stage III and IV oocytes need serum in their medium in order for mRNA to be localised (Yisraeli and Melton, 1988). It was thus interesting to determine whether the localisation of XPAT-GFP protein also needs serum. The results shown are a compendium of data from a number of experiments. Each experiment showed the same trend although the proportions in each category varied. The oocytes were injected equatorially and cultured in either oocyte culture medium (OCM) (made up of 50% Leibowitz medium containing 10% vitellogenin containing-frog serum), or simply 50% Leibowitz medium. Oocytes were scored daily for the localisation of fluorescence, the results of these experiments are summarised in Table 3.3.

Table 3.3: The effect addition of serum to the culture medium had on the localisation of XPAT-GFP and GFP in *Xenopus* oocytes

Time Post-injection	*GFP* injected – serum	*GFP* injected + serum	*Xpat-GFP* injected – serum	*Xpat-GFP* injected + serum
Day 1 18 hours	G: 89.1% –: 10.9% *N=55*	G: 88.3% –: 11.7% *N=60*	V: 35.3% E: 15.7% –: 49.0% *N=51*	V: 18.9% E: 58.5% –: 22.6% *N=53*
Day 2 42 hours	G: 77.8% –: 22.2% *N=54*	G: 93.1% –: 6.9% *N=58*	V: 22.2% E: 22.2% –: 55.6% *N=45*	V: 44.2% E: 28.9% –: 26.9% *N=52*
Day 3 66 hours	G: 55.6% –: 44.4% *N=27*	G: 71.4% –: 28.6% *N=28*	V: 36.5% E: 2.8% –: 60.7% *N=107*	V: 35.5% E: 12.2% –: 52.3% *N=107*

G= general fluorescence, – = no external fluorescence, V= vegetal fluorescence, E= equatorial fluorescence, N= number of oocytes scored. mRNA was injected equatorially into stage VI oocytes.

Unfused *GFP* was injected into oocytes as a control. As a general trend, the percentage of these injected oocytes showing fluorescence decreases with time. This is true whether these oocytes are cultured with or without serum in the medium. Likewise, the number of negative oocytes (those showing no external fluorescence) increases with time in culture, from 11% on day 1 to 44% on day 3 (with no serum) and from 12% on day 1 to 29% on day 3 (with serum in the medium). However, fewer oocytes are negative after 2 or 3 days in culture when serum is in the medium than when it is not (Table 3.3).

Similar trends are seen in *Xpat-GFP* injected oocytes. The number of negative oocytes increases with time in culture both with and without serum. However, fewer negative oocytes are seen in the sample cultured with serum than in the sample cultured without it (Table 3.3). For example, 49% of oocytes were negative without serum compared with 23% negative with serum; by day 3, 61% are negative with no serum compared with 52% with it. The presence of serum in the medium also has an obvious effect on vegetal localisation of XPAT-GFP. In the presence of serum 19% of oocytes show vegetal localisation on day 1, this increases to 44% on day 2 and by day 3 this figure is 36%. However, without serum, 35% of oocytes show vegetal localisation on day 1, dipping to 22% on day 2 and finally rising to 37% on day 3.

Thus, on day 2, 22% of oocytes show vegetal expression (without serum) and 44% show vegetal expression (with serum). But, by day 3 the numbers of oocytes showing vegetal localisation of XPAT-GFP are very similar whether serum is in the medium or not. Thus, the main effect of serum in OCM is to reduce the number of oocytes showing no external fluorescence (for *GFP* or *Xpat-GFP* injected oocytes).

It was decided, on the basis of these results, that to obtain the greatest numbers of oocytes with vegetal fluorescence, vegetal injection followed by culture in serum-containing medium is necessary. However, to obtain greater numbers of oocytes expressing XPAT-GFP in any region, equatorial injection and then culture in serum-containing medium is necessary. Thus, serum was used in OCM for all subsequent experiments and either vegetal or equatorial injection was used depending on the aim of each experiment.

3.3.3 The nuclear localisation of XPAT-GFP and GFP-XPAT

Since a great proportion of the oocytes injected with *GFP-Xpat, Xpat-GFP* and even *GFP* appeared to show no fluorescence after 3 days in culture (that is, were scored as negative), it was decided to determine whether the GFP fusion proteins were still present or were no longer being translated. One possible explanation for the large numbers of apparently negative oocytes was that the fluorescence was actually present in the nucleus. To determine whether this was true, nuclei were removed from several oocytes, which had been injected with *Xpat-GFP* or *GFP-Xpat* and yet appeared negative. All nuclei removed from externally fluorescent oocytes were positive for fluorescence, whether cultured with or without serum. Those nuclei removed from apparently negative *GFP-Xpat* injected oocytes and *Xpat-GFP* injected oocytes were all fluorescent too. Figure 3.5 (B and C) shows a nucleus removed from a *GFP-Xpat* injected oocyte and Figure 3.5D shows a nucleus removed from an *Xpat-GFP*-injected oocyte. Both of these nuclei are fluorescent and thus contain GFP fusion protein.

In total, 11/11 nuclei from superficially negative *Xpat-GFP* injected oocytes, 2/2 nuclei from positive *Xpat-GFP* oocytes, 11/11 nuclei from superficially negative *GFP-Xpat* and 3/3 nuclei from *GFP* injected oocytes were fluorescent. Interestingly, stage IV and V oocytes injected with *Xpat-GFP*, which appeared negative and showed no localisation, also had positive nuclei (2/2 nuclei were positive); Figure 3.5A shows the nucleus from one such oocyte.

It was also decided that it would be interesting to look inside *Xpat-GFP* and *GFP* injected oocytes to determine if granules and particles were purely superficial or not. To do this, oocytes were fixed by heating to 75-85°C in Barth's saline for 30 seconds and then cut open using a scalpel. Figure 3.5 shows oocytes dissected in this way. Figure 3.5E shows an oocyte that expressed GFP and was bisected; the nucleus of this oocyte was fluorescent as was the rest of the oocyte. Figure 3.5F shows an oocyte that expressed XPAT-GFP protein in particles (rather than granules) at the vegetal pole and was cut in two. It could be seen that these particles were mainly, but not totally, superficial and were also visible under the surface of the oocyte, as if moving towards the pole. An oocyte expressing particles of XPAT-GFP protein at its equator was cut in half (Figure 3.5G). It was obvious that these particles were present inside the oocyte in the cytoplasm of the vegetal region, thus they were not purely superficial. Figure 3.5H shows an oocyte expressing small granules of XPAT-GFP protein at its equator. When this oocyte was bisected (Figure 3.5I) it could be seen that these granules were quite superficial and seemed to be present just at the oocyte's surface. In contrast, when the oocyte shown in Figure 3.5J, expressing particles of XPAT-GFP just lateral to the vegetal pole, was bisected (Figure 3.5K) it could be seen that these particles were not all superficial. There were small particles of XPAT-GFP protein present inside the oocyte under the surface in the vegetal region. Again, the nucleus was fluorescent and thus contained XPAT-GFP protein. Thus, small particles of XPAT-GFP are present fairly widely in a gradient from the surface of the oocyte, whereas larger granules are predominantly superficial with a few more-internal, but in the same region of the cell.

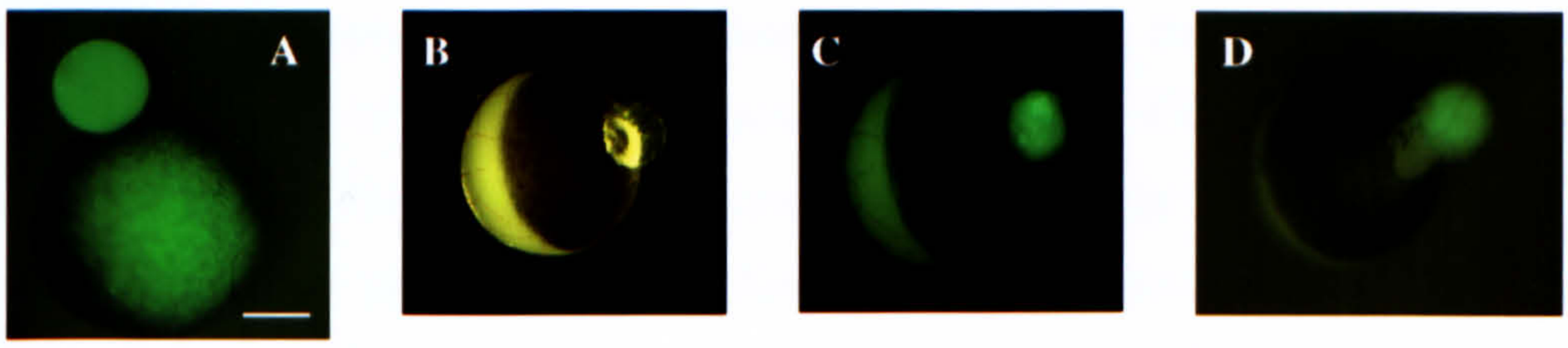

Figure 3.5:To determine where XPAT-GFP, GFP and GFP-XPAT proteins localise inside *Xenopus* oocytes following microinjection of mRNA.

(A) Stage IV oocyte injected with *Xpat-GFP* which has had its nucleus removed. (B) Stage VI oocyte injected with *GFP-Xpat* which has had its nucleus removed. (C) Same oocyte as in as (B) but photographed under UV light. (D) Stage VI oocyte injected with *Xpat-GFP* with its nucleus removed. (E) Stage VI oocyte injected with GFP, cut in half. (F) Bisected stage VI oocyte expressing XPAT-GFP protein in particles at the vegetal pole. (G) Bisected stage VI oocyte expressing Xpat-GFP protein in granules lateral to vegetal pole, the granules are not totally superficial. (H)Stage VI oocyte expressing XPAT-GFP protein in small granules at equator. (I) Oocyte seen in (H) bisected , particles are quite superficial in this oocyte. (J) Stage VI oocyte expressing XPAT-GFP protein in small granules lateral to the vegetal pole. (K) Oocyte shown in (J) cut in half, illustrating that not all XPAT-GFP particles are superficial. In (A) the scale bar represents 200 µm. In (B)-(K) the diameter of each oocyte is ~1.2 mm.

3.4 To confirm the subcellular localisation of GFP-XPAT and XPAT-GFP by *in vivo* radiolabelling

Visual examination emphasises the particulate forms of XPAT; thus, it was decided to use a second approach to investigate the localisation of XPAT-GFP, GFP-XPAT and indeed XPAT itself within the *Xenopus* oocyte. To this end, stage VI *Xenopus* oocytes were injected with 20 ng of mRNA for *Xpat, GFP, GFP-Xpat* or *Xpat-GFP*. The oocytes were then cultured overnight at 18 °C in the presence of ^{35}S-methionine. This is taken up by oocytes and radiolabels all newly translated proteins. The following day, nuclei were removed from some of these oocytes and homogenised (N fraction) and the remaining cytoplasm and membranes were homogenised and centrifuged to give a cytosol (soluble, Cs) fraction and a cytoplasm insoluble (pellet- Ci) fraction. Some oocytes were homogenised whole to give an oocyte total protein (T) fraction. These fractions were then resolved on an acrylamide gel, alongside control (uninjected) oocyte fractions that were prepared in the same way. The gels were then subjected to autoradiography. An additional band of the expected size was seen in fractions from each of the injected oocyte samples when compared with control oocyte fractions. Figure 3.6 shows autoradiographs of these protein gels.

Nuclei were removed from oocytes using a manual dissection procedure (as described by Woodland and Adamson, 1977). Several studies have indicated that this manual enucleation method yields nuclei with virtually undetectable levels of cytoplasmic contamination (including Bonner, 1975; Woodland and Adamson, 1977; Braddock *et al.*, 1994). For example, it was determined that manual enucleation yields expected nucleus: cytoplasm concentration ratios for injected proteins: BSA was enriched in the cytoplasmic fraction, whereas histones were concentrated in the nuclear fraction (Bonner, 1975; Woodland and Adamson, 1977). Similarly, Braddock *et al.* (1994) manually dissected nuclei out of *Xenopus* oocytes and ran the resulting fractions on a gel. They then used western blot analysis and probed with antibodies to nucleoplasmin (a nucleus specific protein) and CAT (a cytoplasmic protein whose RNA had been injected into the cytoplasm). They demonstrated that the fractions were not contaminated, as nucleoplasmin was located specifically in the nucleus, whereas CAT could be detected in the cytoplasmic but not in the nuclear fraction (Braddock *et al.*, 1994).

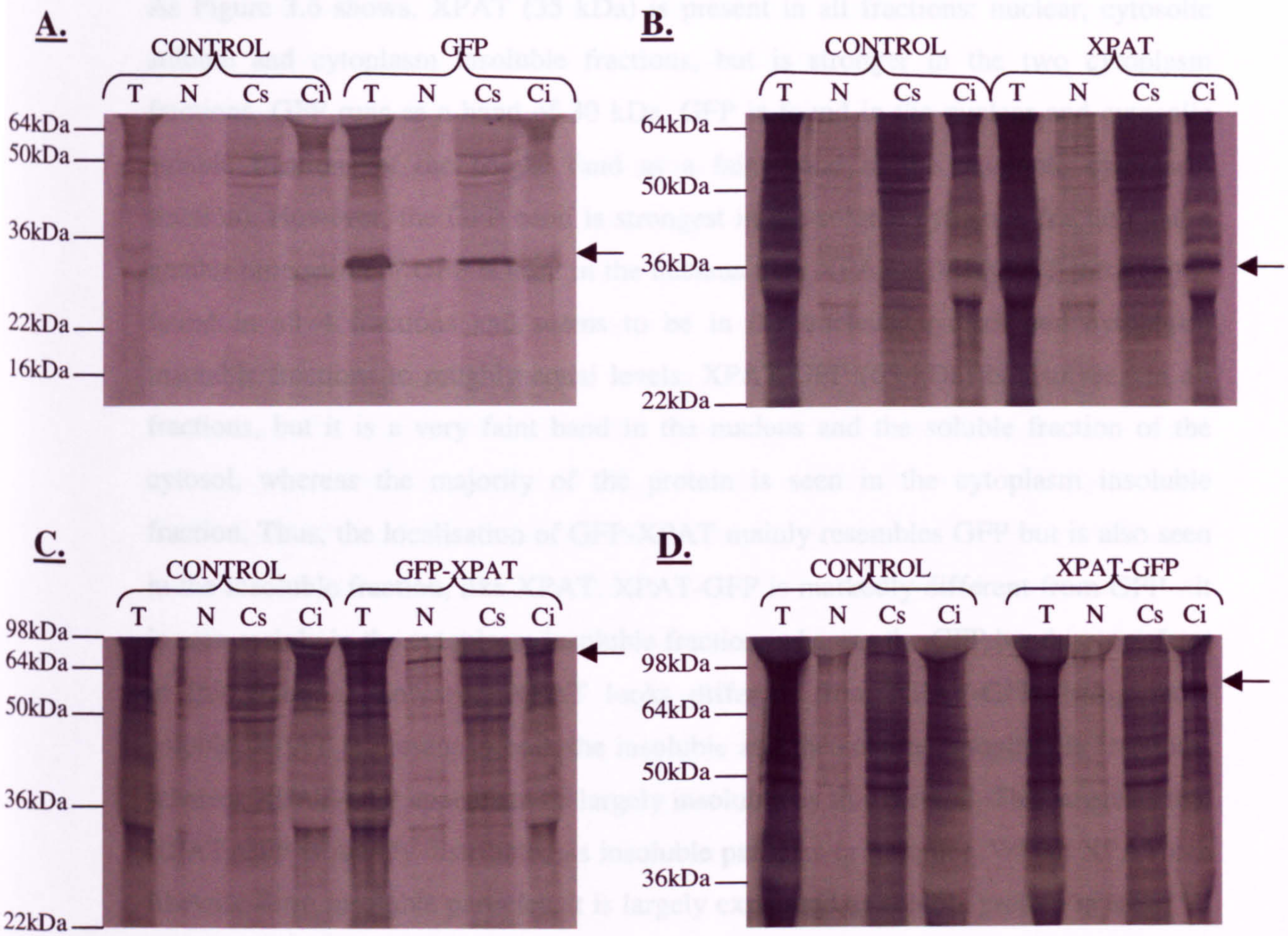

Figure 3.6: To determine the subcellular localisation of GFP-XPAT and XPAT-GFP by *in vivo* radiolabelling.

Stage VI *Xenopus* oocytes were injected with 20ng of *GFP, Xpat*, *GFP-Xpat* or *Xpat-GFP* mRNA or left uninjected. They were cultured over-night in the presence of ^{35}S-methionine. The following day, oocytes were homogenised to give a Total protein sample (T), nuclei were removed from oocytes to give a nuclei (N) fraction. The remaining membranes and cytoplasm were homogenised and centrifuged to give a cytosol soluble fraction (Cs) and a pellet of insoluble cytoplasm (Ci). These fractions were resolved by SDS-PAGE, ensuring equal amounts of each protein sample were loaded (equivalent to 1/3 of an oocyte per lane). On each gel all 4 control (uninjected) oocyte fractions were run along side 4 fractions from one of the injected oocytes. Gels were then autoradiographed, and these autoradiographs are shown: (A) GFP, (B) XPAT, (C) GFP-XPAT, (D) XPAT-GFP.

As Figure 3.6 shows, XPAT (35 kDa) is present in all fractions: nuclear, cytosolic soluble and cytoplasm insoluble fractions, but is stronger in the two cytoplasm fractions. GFP runs as a band of 30 kDa. GFP is found in the nuclear and cytosolic soluble fractions of the oocyte (and as a faint band in the insoluble cytoplasm fraction). However, the GFP band is strongest in the soluble cytosolic fraction and a greater proportion of GFP is seen in the nucleus than XPAT. GFP-XPAT (65 kDa) is found in all 4 fractions and seems to be in the nucleus, cytosol and cytoplasm insoluble fractions to roughly equal levels. XPAT-GFP (65 kDa) is also seen in all fractions, but it is a very faint band in the nucleus and the soluble fraction of the cytosol, whereas the majority of the protein is seen in the cytoplasm insoluble fraction. Thus, the localisation of GFP-XPAT mainly resembles GFP but is also seen in the insoluble fraction, like XPAT. XPAT-GFP is markedly different from GFP - it is seen mainly in the cytoplasm insoluble fraction, whereas the GFP band is very faint in this fraction. However, XPAT looks different from XPAT-GFP, being more soluble. XPAT is present in both the insoluble and the soluble cytoplasmic fractions, whereas XPAT-GFP appears to be largely insoluble by this method. This suggests that XPAT-GFP is mainly distributed as insoluble particles or granules. Whilst XPAT can likewise form insoluble particles, it is largely expressed as soluble protein in stage VI oocytes, at least when overexpressed.

The oocyte nucleus occupies about 4% of the aqueous volume of the cell (Bonner, 1975), so an evenly distributed protein should show this distribution. XPAT shows close to a 50:50 nucleus:cytoplasm distribution, which is what histone nuclear proteins show using this method (Woodland and Adamson, 1977). However, the distribution of XPAT-GFP is clearly seen as a partitioning between nucleus and cytoplasm in sectioned oocytes. Unlike GFP, the perinuclear region is fluorescence-free, unless the XPAT-GFP remains nuclear and close to the nucleus on one side. It seems clear that the XPAT-GFP is either nuclear and non-particulate or particulate and in a limited, mainly peripheral, part of the cytoplasm. Presumably, it is limited by binding to cytoplasmic components, likely the cytoskeleton, and this prevents translocation to the nucleus. The particulate material in the cytoplasm would be pelleted and hence present in the cytoplasmic insoluble fraction. GFP and GFP-XPAT do not form particles, so are not concentrated in the insoluble fraction; they are diffusely in all cytoplasm (as long as it persists on the case of GFP-XPAT) and so are

not anchored and are free to enter the nucleus. It is notable that XPAT contains a putative bipartite nuclear localisation signal (see Chapter 5).

3.5 *In situ* hybridisations to *GFP* in oocytes expressing XPAT-GFP and GFP

XPAT-GFP protein localises near the point of mRNA injection in stage VI *Xenopus* oocytes (Section 3.2.1). *Xpat-GFP* mRNA has *globin* UTRs and *globin* mRNA moves very slowly in *Xenopus* oocytes; Drummond *et al.* (1985) observed little movement of RNA from the animal half to the vegetal half even 48 hours after injection. In contrast, similar amounts of mRNA were present in both halves 48 hours after vegetal pole injection (Drummond *et al.*, 1985). In order to determine what actually happens to the *Xpat-GFP* mRNA following its injection into oocytes, *in situ* hybridisation analysis was performed. Stage VI *Xenopus* oocytes were injected equatorially with 2ng *Xpat-GFP* or *GFP* mRNA, cultured in OCM at 18°C and fixed at intervals. *In situ* hybridisation was then performed to determine a time course of the localisation of injected mRNA. As a control for this experiment, oocytes that had been injected with *GFP* mRNA were also concomitantly hybridised *in situ*. For this experiment, a GFP riboprobe was used, as this was specific for the injected mRNA.

Figure 3.7 shows photographs of the *in situ* hybridisation analysis of oocytes injected with *Xpat-GFP* or *GFP*. Two hours after injection, the *GFP* mRNA could be seen as a purple patch around the site of injection; *Xpat-GFP* mRNA was always seen as a small 50µm diameter spot, whereas *GFP* mRNA was often seen in a broader patch at this stage, up to ~250µm across. 18hours after injection (Figure 3.7), both *GFP* and *Xpat-GFP* mRNA domains broaden, *GFP* injected oocytes showed patches of *GFP* mRNA up to 550µm across, whereas *Xpat-GFP* remains a bit tighter in localisation- only a maximum of 350µm in diameter. Thus, it is already obvious that *Xpat-GFP* mRNA is localising differently to *GFP* mRNA.

By day 2, 42 hours post-injection, the two mRNAs were quite different in localisation, as Figure 3.7 shows. *GFP* was still localised in a wider domain, in patches of up to ~650µm. Whereas *Xpat-GFP* seemed to be in much smaller areas, of which there were many in any one oocyte. These patches were generally ~75µm across and spread from the equatorial to the vegetal region in the same way that the XPAT-GFP protein

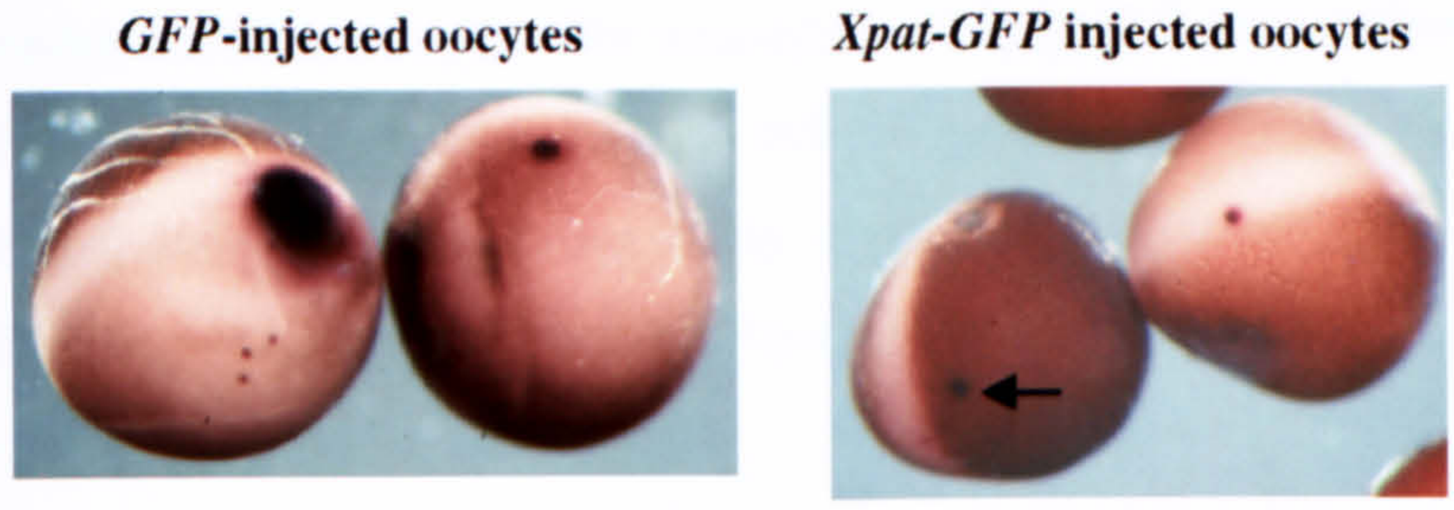

Figure 3.7: *In situ* hybridisation analysis of injected mRNA in *Xenopus* oocytes.

Stage VI oocytes were injected equatorially with 2 ng of either *GFP* or *Xpat-GFP* mRNA, and then cultured *in vitro* in OCM at 18ºC. Oocytes were then fixed after various times in culture and *in situ* hybridisation analysis, using a *GFP* riboprobe, was performed to provide a time course for exogenous mRNA localisation. Oocytes were not bleached, however those hybridised *in situ* after 72 hours were all placed into Murray's clearing agent and then methanol before being photographed, thus they appear different in colour to the other oocytes. Exogenous *GFP* mRNA is localised in a much wider domain than *Xpat-GFP* mRNA. The diameter of each stage VI oocyte is ~1.2 mm.

is localising. Similarly, on day 3 (66 hours post-injection) *GFP* was still seen in large patches (of approximately the same size as those seen on day 2), whereas *Xpat-GFP* localisation varies between oocytes. For example, in Figure 3.7, two different oocytes are shown- one shows a patch of *Xpat-GFP* mRNA localisation on the equator of the oocyte (~400μm) and a second shows many small areas of staining in the vegetal pole- resembling the particles of XPAT-GFP protein localisation.

At present, it is unclear where XPAT-GFP protein is located in relation to its mRNA as it was necessary to bleach oocytes after *in situ* hybridisation to detect the signal efficiently. Bleaching affects fluorescence of the GFP, so it can no longer be seen under the microscope. *In situ* hybridisation with antisense *GFP* riboprobe then subsequent whole-mount immunostaining for GFP was attempted on oocytes overexpressing XPAT-GFP. Unfortunately, due to time constraints, this procedure was only performed twice. When an HRP-conjugated secondary antibody was used to detect GFP, this resulted in over-staining, which meant the *in situ* hybridisation signal was masked. Using an FITC-conjugated secondary antibody for immunostaining meant the oocytes could not be bleached (as this would quench fluorescence) and, as the *in situ* hybridisation signal was weak, no conclusions could be drawn from this experiment. Thus, this procedure needs to be optimised to determine whether *Xpat GFP* mRNA and protein colocalise in oocytes. One hypothesis would be that *Xpat-GFP* mRNA is in the same location as the protein it encodes.

Interestingly, *Xpat-GFP* and *GFP* mRNAs localise in completely different ways. The only difference in the mRNAs themselves is the addition of sequence encoding *Xpat*'s ORF, as the *GFP* mRNA is transcribed from exactly the same vector as *Xpat-GFP*. Thus the *Xpat* ORF (as this is the only *Xpat* sequence in this construct) has an effect on localisation of the mRNA. This is different from results gained previously in stage III and IV oocytes when it was determined that the 3'UTR of *Xpat* directs mRNA localisation (Hudson and Woodland, 1998).

3.6 The effect of XPAT-GFP on the endogenous germ plasm in oocytes

Stage VI *Xenopus* oocytes were injected with 2ng of *Xpat-GFP* or *GFP* mRNA, cultured in OCM at 18°C and after 18 hours and 72 hours in culture, oocytes were removed and fixed. Then *in situ* hybridisation analysis was performed using *Xcat-2* as a riboprobe. This was done in order to determine whether the injection and expression of XPAT-GFP affects the endogenous germ plasm in oocytes and also to check whether increasing time in culture affects the germ plasm. *Xcat-2* was used as a marker of germ plasm in this experiment. The results of these *in situ* hybridisations are shown in Figure 3.8.

After 18hours in culture, both *Xpat-GFP* and *GFP*-injected oocytes show *Xcat-2* is expressed in particles in a disc shape on the vegetal pole. Thus, XPAT-GFP has not affected endogenous germ plasm after 18 hours. Similarly, after 72 hours in culture, both *Xpat-GFP* and *GFP*-injected oocytes still show *Xcat-2* expression, in the same pattern and location and as strongly as before. Thus, XPAT-GFP has not affected the germ plasm in stage VI oocytes. However, the diameter of the *Xcat-2* expression domain in *Xpat-GFP*-injected oocytes appears smaller than that in *GFP*-injected oocytes after 72 hours in culture.

In order to ascertain whether or not there was a statistically significant difference between the size of *Xcat-2* expression domain in *Xpat-GFP* and *GFP*-injected oocytes, the Student's T test was performed. An eye-piece graticule (calibrated using a micrometer slide) in a dissecting microscope was used to measure the diameter of the *Xcat-2* expression domain in oocyte. Oocytes were injected with 2ng of *GFP* or *Xpat-GFP* mRNA, cultured in vitro for 72 hours, then fixed, *in situ* hybridised with *Xcat-2* probe and the diameter of the expression domain measured. Table 3.4 shows the mean diameter of expression domain of *Xcat-2* in GFP-injected oocytes, in oocytes expressing XPAT-GFP in the equatorial region and oocytes expressing XPAT-GFP in granules at the vegetal pole. (For raw data see Appendix 1).

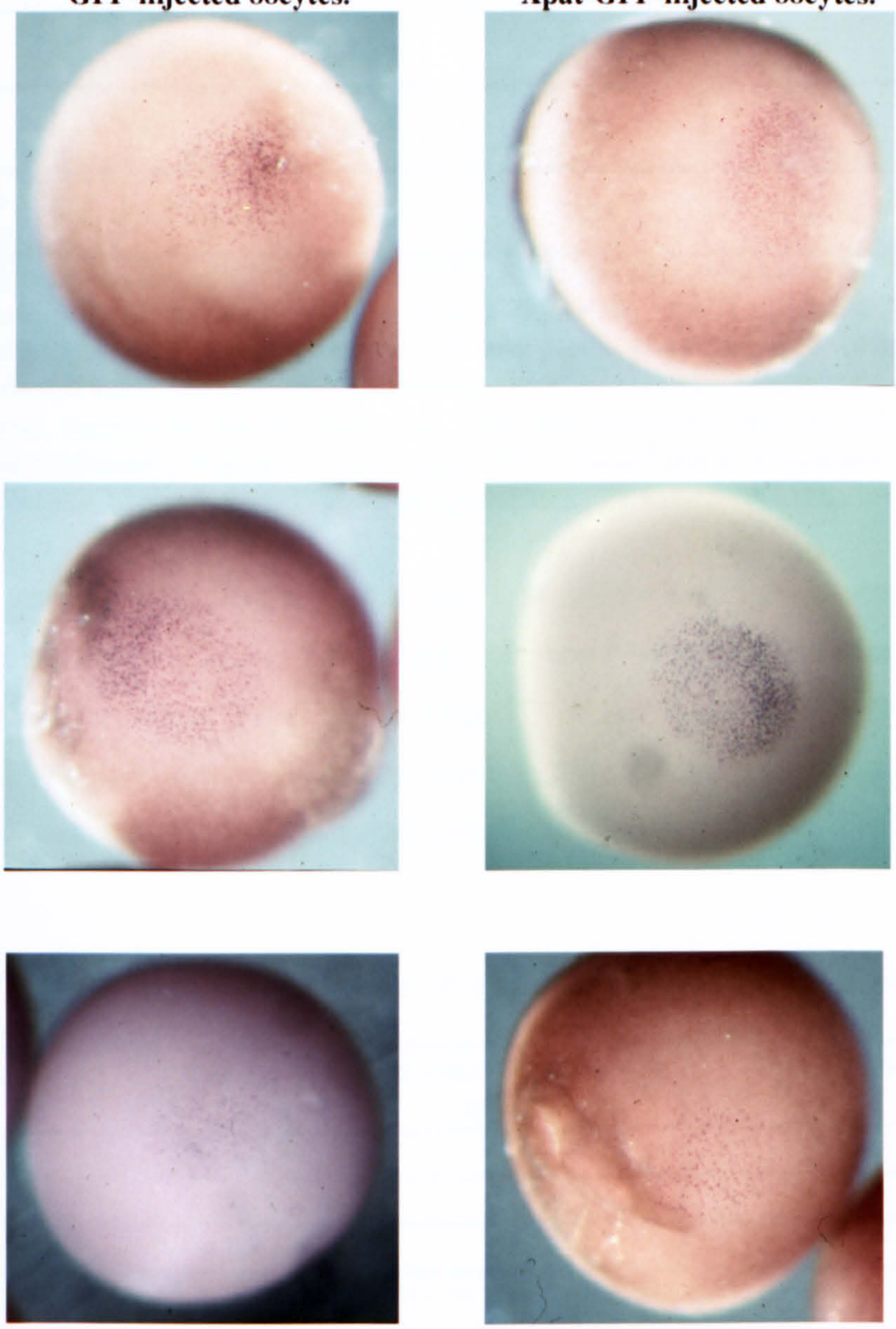

Figure 3.8: *In situ* hybridisation to *Xcat-2* or *Xpat* in oocytes that had been injected with *GFP* or *Xpat-GFP* mRNA.

Stage VI *Xenopus* oocytes were injected equatorially with 2 ng of *Xpat-GFP* or *GFP* mRNA and cultured *in vitro* in 50 % Leibowitz medium at 18°C for up to 72 hours. Oocytes were then fixed and *in situ* hybridisation analysis performed. *Xcat-2* was used as a marker of the germ plasm. A riboprobe specific for *Xpat*'s 3´UTR was used to detect purely endogenous *Xpat* mRNA; as the injected *Xpat-GFP* mRNA contains only *Xpat*'s ORF and not any UTR sequence. The diameter of each oocyte is ~1.2 mm.

Table 3.4 The means and variance of the diameter of *Xcat-2* expression in *Xenopus* oocytes

Oocyte expression	Mean (epu)	Mean (μm)	Variance	Number of oocytes (n)
GFP	20.9	522.5	11.5	14
XPAT-GFP equatorially	17.9	447.5	5.54	11
XPAT-GFP in vegetal granules	13.7	342.5	1.56	3

Oocytes were injected with 2ng of *GFP* or *Xpat-GFP* mRNA and then cultured *in vitro* for 3 days. Oocytes were hybridised *in situ* with an *Xcat-2* riboprobe. The diameter of *Xcat-2* expression domain was then measured using an eye-piece graticule in a dissecting microscope. The first column shows mean (Σdiameters / n) in epu (eye piece graticule units), where n is the total number of oocytes measured. This was converted into μm (after the graticule had been calibrated). Variance is $(\Sigma\text{diameters})^2/n - \text{mean}^2$ and is a measure of the differences in the means. The raw data is shown in Appendix 1.

The means and variance were then converted into T values for use in the Student's T test. This test compares two sets of data. Table 3.5 shows which sets of data were compared, T values and critical T values. The critical T value is taken at the 95% level of significance for the appropriate degrees of freedom from statistical tables (degrees of freedom= total number of oocytes (for both sets of data)-2).

Table 3.5: T values for the Student's T-test comparing *Xcat-2* diameter (measured after *in situ* hybridisation)

Oocytes/injection	T value	Critical T value at 95% level	Significant?
GFP cf XG eq	2.606	2.069	√
GFP cf XG gran	6.217	2.131	√
XG eq cf XG gran	4.15	2.179	√

In situ hybridisation was performed after 3 days in culture. GFP= GFP injected oocytes, XGeq= oocytes expressing XPAT-GFP in particles at the equatorial region, XG gran= oocytes expressing XPAT-GFP in granules at vegetal pole, √= statistically significant.

As Table 3.5 shows, there is a statistically significant difference between the size of the *Xcat-2* expression pattern in oocytes expressing GFP and oocytes expressing XPAT-GFP equatorially in particles. Likewise there is also a statistical significance between the diameter of *Xcat-2* expression domain in oocytes expressing GFP and oocytes expressing XPAT-GFP vegetally in granules. Thus, it appears that, 72hours after injection, XPAT-GFP does have an effect on *Xcat-2* localisation in oocytes when

compared with *Xcat-2* localisation in *GFP* injected oocytes. Also, a statistically significant reduction in size of *Xcat-2* expression domain was seen in oocytes expressing XPAT-GFP in granules at the vegetal pole, compared with oocytes expressing XPAT-GFP equatorially in small particles.

It is worth noting that no observable difference in diameter of *Xcat-2* expression domain was seen in oocytes 18 hours after injection with *Xpat-GFP* compared with *GFP* injection. Thus, the formation of vegetal granules of XPAT-GFP protein after 3 days in culture affects *Xcat-2* expression, as does formation of equatorial particles of XPAT-GFP. That is, localisation of XPAT-GFP in oocytes affects endogenous germ plasm. Similarly, in many oocytes expressing large granules of XPAT-GFP at their vegetal poles, the oocyte's pigment granules are visibly highly disrupted in the area where XPAT-GFP is localised.

Some oocytes which had been injected with *Xpat-GFP* and *GFP* were cultured *in vitro* for 72 hours and then *in situ* hybridised with a probe specific for the 3' UTR of *Xpat*. This was done to determine whether overexpressing XPAT-GFP has any effect on the localisation of the endogenous *Xpat* mRNA. A UTR probe was used since *Xpat-GFP* contains the ORF of *Xpat* and thus the probe was specific for endogenous *Xpat*. Figure 3.8 shows the results of these *in situ* hybridisations. As this figure shows, overexpression of XPAT-GFP does not affect endogenous *Xpat* localisation. *Xpat* is expressed in particles in the vegetal pole in both *GFP* and *Xpat-GFP* injected oocytes. It is worth noting that the *Xpat* UTR *in situ* hybridisation probe works less well than *Xpat* ORF *in situ* hybridisation probe which is why, in Figure 3.9, the signal is weaker than in Figures 7.3 and 7.6 (see later).

It will be interesting to determine whether XPAT-GFP colocalises with the endogenous germ plasm. Experiments to ascertain this were attempted using *in situ* hybridisation to various germ plasm mRNAs (*DEADSouth, Xcat-2* and *Xdazl*) and subsequent immunostaining of GFP. Due to time constraints, this was attempted on only two occasions. Because of the technical difficulties outlined above (at the end of Section 3.5) – namely, detection of HRP-conjugated antibodies causing over-staining and weak *in situ* hybridisation signal - it was impossible to draw any conclusions from these experiments.

3.7 The localisation of XPAT-GFP in *Xenopus* embryos

2-cell *Xenopus* embryos were injected bilaterally in the vegetal region with 0.5ng of *GFP* or *Xpat-GFP* mRNA, and then cultured *in vitro* in 10% Barth's saline. Figure 3.9 shows photographs of embryos expressing GFP or XPAT-GFP protein. Figure 3.9A shows stage 12 embryos that had been injected with *GFP*. This figure shows GFP expression is patchy, in regions of the embryo fated to become epidermis. 3.9B shows stage 12 embryos injected with *Xpat-GFP* and shows XPAT-GFP protein is expressed only in regions of the epidermis. XPAT-GFP is expressed less strongly than GFP and in smaller patches- almost in a stripe around the embryo. 3.9C is a photograph of a stage 18 embryo which is expressing XPAT-GFP in a band around the epidermis. Figures 3.9D and E show the embryo in 3.9C bisected, the XPAT-GFP protein expression is very superficial just on the surface of the embryo. This result is very strange, the *Xpat-GFP* mRNA was injected into the vegetal area of 2-cell embryos and yet the protein is expressed in the epidermis. It appears that XPAT-GFP could be localised in cell nuclei (Figure 3.9C shows this clearly). These results are reproducible as the experiment has been performed twice and the same results were obtained each time.

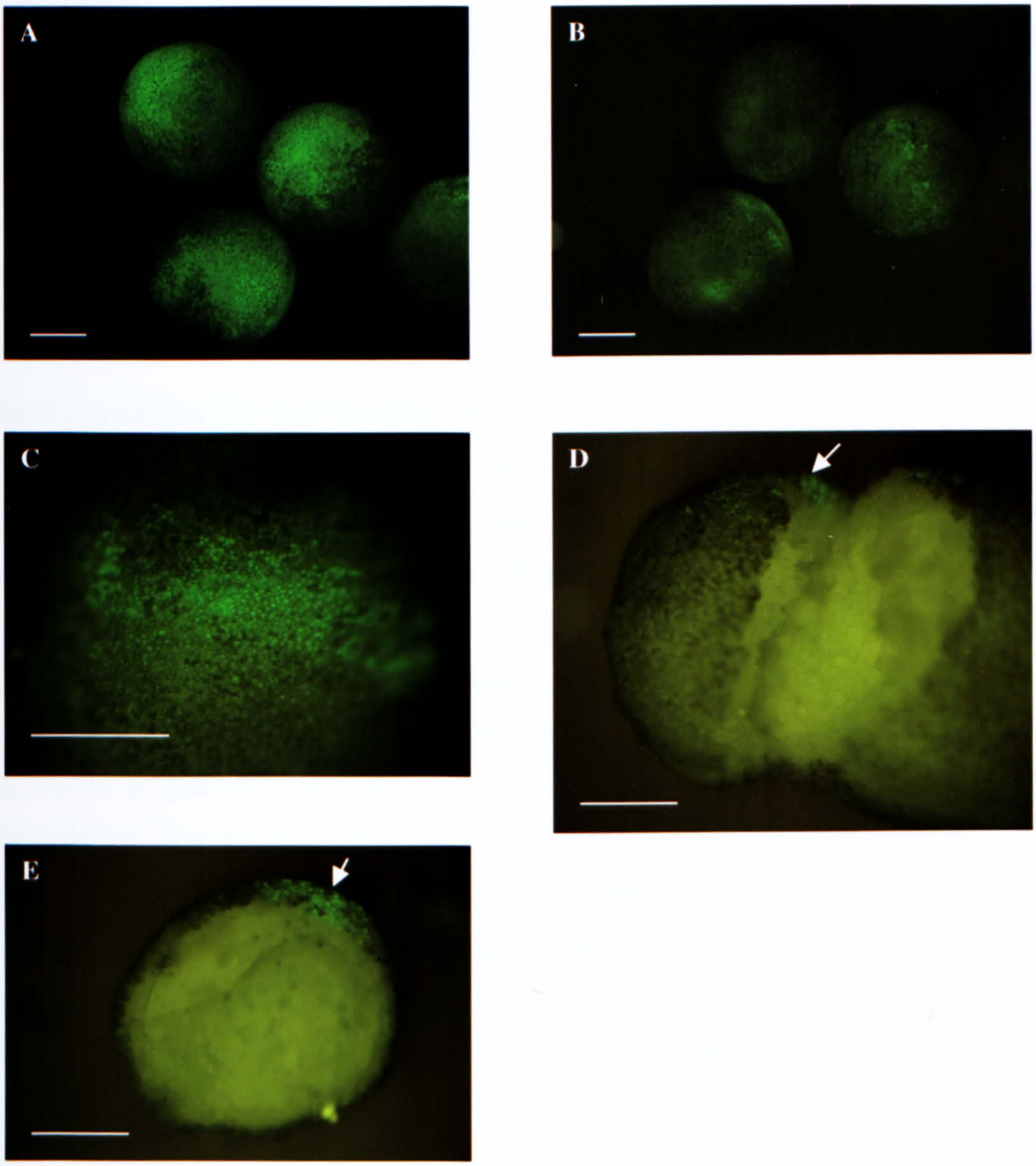

Figure 3.9 Localisation of XPAT-GFP and GFP in *Xenopus* embryos.

2-cell embryos were injected bilaterally in the vegetal region with 0.5 ng of *Xpat-GFP* or *GFP* mRNA and then allowed to develop *in vitro* in 10 % Barth's saline. (**A**) Shows 3 stage 12 *Xenopus* embryos which had been injected with *GFP* mRNA, GFP expression is patchy in regions of embryos fated to become epidermis. (**B**) Shows 3 stage 12 *Xenopus* embryos which had been injected with *Xpat-GFP* mRNA, XPAT-GFP is expressed only in regions of epidermis. (**C**) Shows a stage 18 *Xenopus* embryo which had been injected with *Xpat-GFP*, and is expressing fusion protein in a band around the epidermis. (**D**) and (**E**) illustrate that XPAT-GFP expression is very superficial. (**D**) Shows the embryo from (C) bisected and (**E**) shows a closer view of the embryo in (D), arrows highlight XPAT-GFP fluorescence. The scale bar in each photograph represents 500 µm.

3.8 Discussion

GFP fusion constructs now seem to be so well trusted that the live cell imaging of GFP-tagged proteins is used to generate primary data for determining the cellular localisation of products from newly cloned genes (Matus, 2001). Thus, to determine where XPAT protein localises *in vivo*, XPAT was fused (at either its carboxy- or amino- terminus) with GFP, and the resulting chimeric proteins were expressed in *Xenopus* oocytes.

GFP-XPAT localised to the nucleus of stage VI *Xenopus* oocytes; whereas XPAT-GFP, in addition to being present in the nucleus, formed small (1 to 2.5 μm) particles which aggregated into large granular structures (of 10-50 μm diameter) at the vegetal pole. XPAT-GFP was transported to the vegetal pole of full-grown oocytes, but whether as particles, or as soluble protein existing in equilibrium with particles, cannot be said. The former seems more likely. The particles of XPAT-GFP looked exactly like those seen after *in situ* hybridisation to germ plasm RNAs and the granules resembled those seen after immunostaining of fertilised eggs with some monoclonal antibodies raised against unknown germ plasm constituents (Denegre *et al.*, 1997). In *Xenopus*, extensive aggregation of the germ plasm islands begins at the onset of the first cleavage and continues throughout the early cleavage divisions (Ressom and Dixon, 1988; Savage and Danilchik, 1993). Savage and Danilchik (1993) performed detailed studies on germ plasm aggregation in *Xenopus* embryos and ascertained that shortly after fertilisation the cytoplasmic islands of germ plasm were distributed in a widespread pattern, with granules averaging 11.9 μm in size. In the 2-cell embryo, granules averaged 26.8 μm in size and by the 4-cell stage the germ plasm patches had an average size of 78.5 μm (Savage and Danilchik, 1993). Thus, XPAT-GFP granules, which ranged from 10 to 50 μm in diameter in stage VI oocytes, were similar in size to patches of germ plasm observed in 2-cell *Xenopus* embryos.

The pattern of XPAT-GFP distribution can hardly be accidental and, although the distribution of the endogenous XPAT protein is not yet known, it seems likely that it is a germ granule component at some point. It would be a good candidate to support formation of granules of germ plasm mRNAs at late stages of oogenesis and/or could

potentially aid aggregation during early embryogenesis. At some stage the protein may also have a nuclear function.

Xpat-GFP mRNA is translated at the site of its injection and XPAT-GFP protein must be anchored there - otherwise it would diffuse widely, like GFP. Similarly, *Xpat-GFP* mRNA is much more tightly localised than *GFP* in stage VI oocytes. This could be because of cytoplasmic binding of the mRNA or of the nascent peptides. It will be interesting to determine whether *Xpat-GFP* mRNA and the protein it encodes colocalise in oocytes. This is currently being investigated by R. Hames, a Ph.D student in H.R. Woodland's laboratory. Since GFP-XPAT does not localise, it would also be useful to know the distribution of this mRNA after injection. Little expression of XPAT-GFP protein was seen in smaller (stage III-V) oocytes, even though the injected mRNA contained no *Xpat* UTRs. These data suggest that either the ORF has regulatory sequences, which is most unusual, or XPAT is unstable in some embryonic cells, at least when overexpressed.

It will be important to determine how XPAT forms small granules, how it translocates to the vegetal pole and how it forms large aggregates there. In reticulocyte lysates translated XPAT-GFP does not form granules nor does it do so in the nucleus. This suggests that aggregate formation depends on the proteins with which XPAT interacts. (RNAs could be involved, but this does not seem likely because in a vast cell, like a *Xenopus* oocyte, transcription can have little impact during the course of the experiment [Woodland, 1982]. Also, suitable RNA targets for the binding of large amounts of protein made in an injection experiment are unlikely to exist in the equator of the cell). The fact that particles form suggests that, if interacting proteins exist, they are abundant cellular components.

The observation that XPAT-GFP can form granules, whereas GFP-XPAT cannot, indicates that the orientation of the GFP in the fusion protein is critical to its function and suggests that XPAT is likely to be made up of different domains. For example, it is possible that having a GFP tag at the amino terminus of XPAT (as in GFP-XPAT) masks an essential localisation domain, thus preventing XPAT from forming granules and/or localising to the vegetal pole. Likewise, since GFP-XPAT is present solely in the nucleus this indicates a nuclear localisation signal (NLS) is likely to be in the

carboxy-terminal half of XPAT (indeed there is a putative bipartite NLS in XPAT- see Chapter 5). Alternatively, the location of GFP could have an effect on the overall structure of XPAT, or hinder an interaction it is normally involved in.

Chapter 4: The effect of cytoskeletal inhibitors on the localisation of XPAT-GFP

4.1 Introduction

Drugs which disrupt microtubules and microfilaments (including nocodazole, colchicine and cytochalasin B) were shown to perturb the establishment and the stabilisation, respectively, of *Vg1* mRNA localisation in the *Xenopus* oocyte (Yisraeli *et al.*, 1990; Kloc and Etkin, 1995). In mammalian cells disruption of actin filaments prevent *actin* mRNA localisation, while disruption of microtubules has no effect (Sundell and Singer, 1991). These studies suggest that the cytoskeleton is required for mRNA localisation. It is plausible, therefore, that the cytoskeleton may also be involved in protein localisation.

To determine whether or not microtubules and microfilaments have a role in XPAT-GFP localisation and in the formation of granules of XPAT-GFP, evidence was accrued through observation of the effects of the anticytoskeletal drugs colcemid, nocodazole and cytochalasin D. To this end, oocytes injected with *Xpat-GFP* mRNA were cultured *in vitro* in OCM in the presence of the microtubule inhibitors nocodazole, an agent that causes microtubule depolymerisation, or colcemid, which binds to soluble tubulin and prevents the polymerisation into microtubules. Cytochalasin D was employed to assess the role of microfilaments, as this drug prevents actin assembly at the barbed ends of microfilaments.

To expand this analysis, some oocytes were cultured in the presence of taxol, a drug that promotes microtubule polymerisation by stabilising microtubules. Oocytes that have been treated with nocodazole become virtually devoid of microtubules in cortices of both hemispheres of oocytes. Conversely, oocytes treated with taxol show striking enrichments of cortical microtubules in both hemispheres (Canman and Bement, 1997).

Nocodazole has been previously used to depolymerise *Xenopus* oocyte microtubules at concentrations of between 3 and 66 μM (Yisraeli *et al.*, 1990; Kloc and Etkin, 1995; Canman and Bement, 1997; Gard *et al.*, 1997). 3 μM nocodazole was shown to cause complete depolymerisation of cortical microtubules - after 48 hours no

microtubules were detected (Gard *et al.*, 1997). Yisraeli *et al.* (1990) determined that nocodazole was equally effective at microtubule disruption over a 10-fold range of concentrations (3-30 μM). Similarly, 10-53 μM concentrations of colcemid have been previously used to effectively disrupt oocyte microtubules (Colman *et al.*, 1981; Peter *et al.*, 1991; Gard *et al.*, 1997). 53 μM colcemid causes complete depolymerisation of microtubules (Gard *et al.*, 1997) and 10 μM has been shown to cause exactly the same morphological changes observed with much higher concentrations (up to 53 μM; Peter *et al.*, 1991).

Cytochalasin D has been used to effectively disrupt oocyte microfilaments at doses of between 2 and 10 μM (Peter *et al.*, 1991; Canman and Bement, 1997). 2 μM cytochalasin D was observed to cause similar effects to 50 μM cytochalasin B (Peter *et al.*, 1991), which depolymerises both cytoplasmic and cortical F-actin in stage VI oocytes (Colman *et al.*, 1981; Roeder and Gard, 1994).

Concentrations of between 5 and 30 μM taxol have been previously used effectively (Jessus *et al.*, 1988; Canman and Bement, 1997). Jessus *et al.* (1988) showed that an external taxol concentration of 5 μM was sufficient to promote tubulin polymerisation in stage VI *Xenopus* oocytes.

4.2 Expression of GFP in oocytes treated with anti-cytoskeletal drugs

To analyse the effect of anticytoskeletal drugs on stage VI *Xenopus* oocytes and on their expression of GFP, *GFP* mRNA was injected into the equatorial region of oocytes at a dose of 2 ng per oocyte. The oocytes were then cultured *in vitro* at 18°C in OCM in the presence of the appropriate cytoskeletal inhibitor for up to 3 days. All concentrations of inhibitors were chosen based on previous reports in which these drugs were effective in oocytes (Jessus *et al.*, 1988; Peter *et al.*, 1991; Gard *et al.*, 1997– see Section 4.1). Thus, nocodazole was added to a final concentration of 3 μM, colcemid at 10 μM, cytochalasin D at a concentration of 2 μM and taxol to 5 μM. The oocytes were all examined for phenotypic changes, which would indicate that the cytoskeletal inhibitors had disrupted their respective monomers, and the localisation of GFP was examined by fluorescent microscopy in order to determine the effect of the drugs on GFP fluorescence. As previously described in Section 3.3,

and shown in Figure 4.1B, control oocytes expressed GFP in an even and non-localised distribution after 42 hours in culture.

Those oocytes expressing GFP that were cultured in the presence of cytochalasin D showed diffuse fluorescence (Figure 4.1D). The oocytes appeared mottled, and the pigment was rearranged but this is a general observation when oocytes are incubated in cytochalasin D (Figure 4.1C, Peter *et al.*, 1991). No particles of GFP were observed in any of the oocytes.

GFP-injected oocytes that were cultured in OCM containing colcemid also displayed general fluorescence (Figure 4.1F). The nuclei in these oocytes were visible under the surface (Figure 4.1E) and were fluorescent (Figure 4.1F). This was also seen in *Xpat-GFP*-injected oocytes, as the disruption of microtubules causes the nucleus to be displaced towards the surface (Colman *et al.*, 1981; Peter *et al.*, 1991). Again, the fluorescence was diffuse and non-particulate.

GFP-injected oocytes that were cultured in the presence of nocodazole also showed general, non-localised, diffuse fluorescence as the four oocytes shown in Figure 4.1H illustrate. Like the colcemid-treated oocytes, nuclei in these oocytes became displaced and were clearly visible under the surface at the animal pole (Figure 4.1G). The nuclei were highly fluorescent as Figure 4.1H illustrates, but the contrast with the surrounding area is because the nucleus displaces pigment.

Oocytes expressing GFP that were incubated in taxol-containing OCM showed general and diffuse fluorescence; Figure 4.1J shows four such oocytes. The pigment of these oocytes was highly disrupted and had a mottled appearance (Figure 4.1I), a known effect of taxol on *Xenopus* oocytes (Heidemann and Gallas, 1980). There was no evidence that GFP formed granules or appeared to localise in a network of particles (as XPAT-GFP does in Figure 4.2J). Figure 4.1K shows a higher magnification view of a GFP-expressing oocyte incubated in the presence of taxol. This photograph shows that the visible fluorescence was totally diffuse and non-localised.

Figure 4.1 (Opposite): Expression of GFP in oocytes treated with cytoskeletal inhibitors
Stage VI *Xenopus* oocytes were each injected with 2 ng of *GFP* mRNA and cultured *in vitro* at 18°C for 42 hours in OCM containing a working concentration of 3 μM nocodazole, 10 μM colcemid, 2 μM cytochalasin D, 5 μM taxol or no drug. Oocytes were then observed using light or fluorescence microscopy. (A) to (E) were visualised using light microscopy, and (F) to (K) were photographed using fluorescence microscopy.

(A) Control oocytes, cultured without cytoskeletal inhibitors.

(B) Four control oocytes expressing GFP evenly throughout cytoplasm.

(C) Oocytes cultured in the presence of cytochalasin D. The oocytes exhibit mottling on their surface as the drug has caused pigment rearrangement.

(D) Oocytes treated with cytochalasin D showed general GFP expression, pigment rearrangement by the drug caused mottling on oocyte surface.

(E) Oocytes cultured in the presence of colcemid. The oocytes' nuclei are visible under the surface of the animal pole (arrowed). Usually the nucleus is anchored by microtubules, but colcemid treatment has disrupted the microtubule network.

(F) Four oocytes treated with colcemid showing general GFP expression. The nuclei are highly fluorescent and visible under surface of animal pole (one such nucleus is arrowed).

(G) Oocytes treated with nocodazole. As in colcemid-treated oocytes, the cell nuclei have been displaced and are clearly visible through the animal pole surface (arrowed).

(H) Four oocytes cultured in presence of nocodazole express GFP in a non-localised manner. The nuclei have been displaced, are fluorescent and are clearly visible through the surface of the animal pole (one such nucleus is arrowed).

(I) Oocytes cultured in presence of taxol, a microtubule stabiliser. The drug causes pigment rearrangement, apparent as mottling on the oocytes' surfaces.

(J) Four oocytes treated with taxol expressing GFP generally. The pigment of these oocytes is highly disrupted.

(K) View of an oocyte treated with taxol clearly shows that no particles of GFP are visible on the surface of the oocyte, and the fluorescence is diffuse.

The diameter of all oocytes shown is ~1.2 mm.

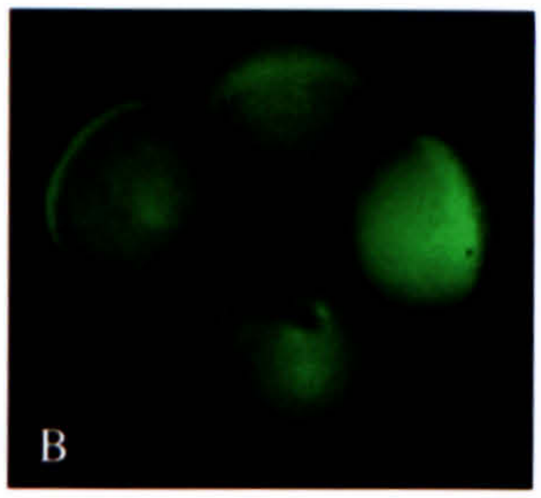

Control

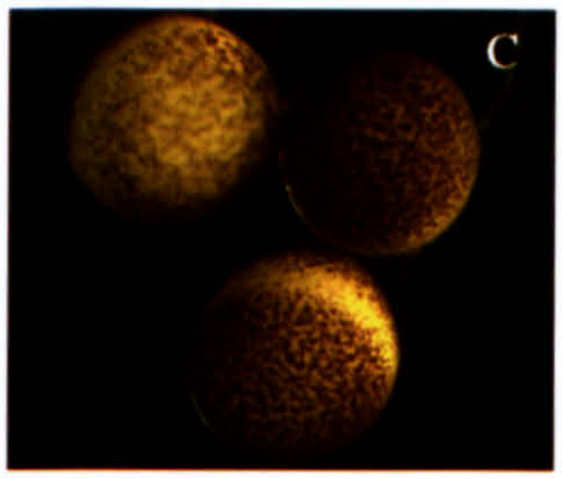

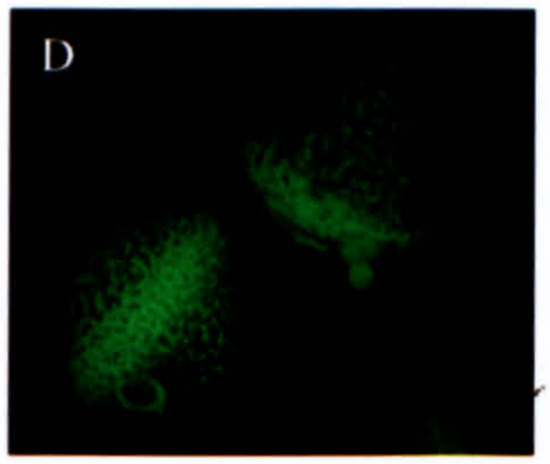

Cytochalasin D

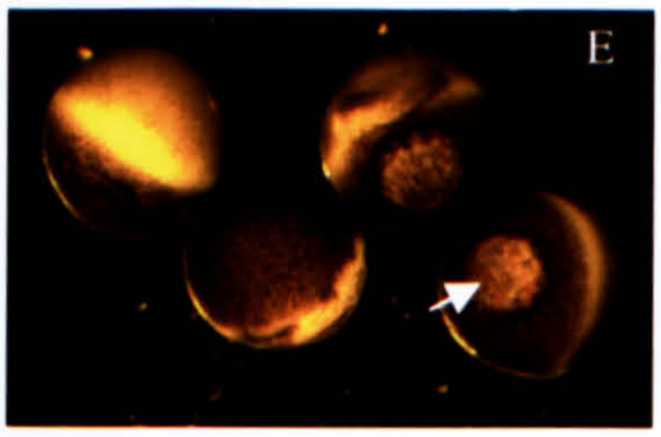

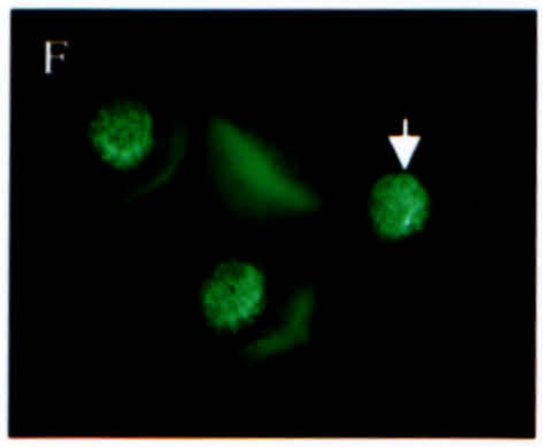

Colcemid

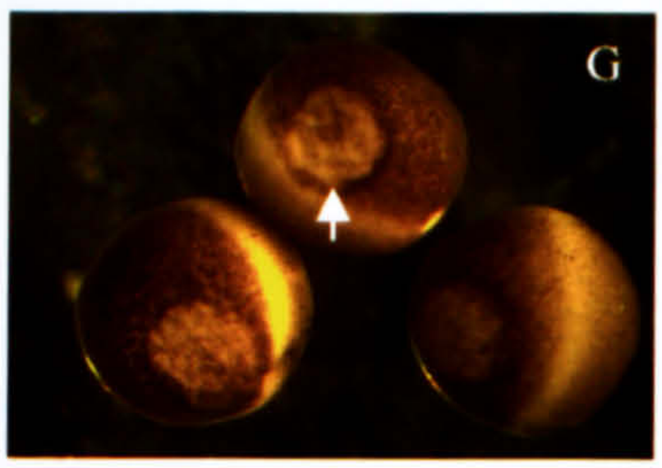

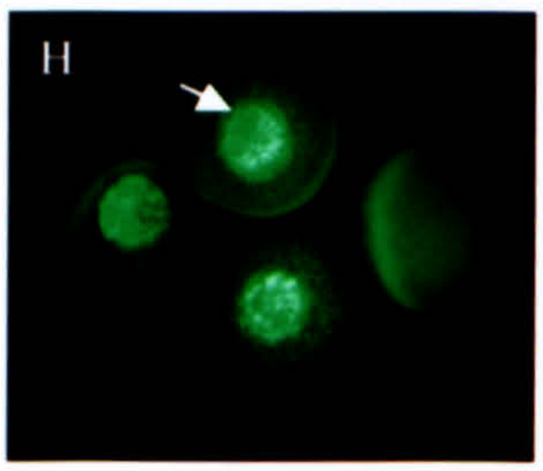

Nocodazole

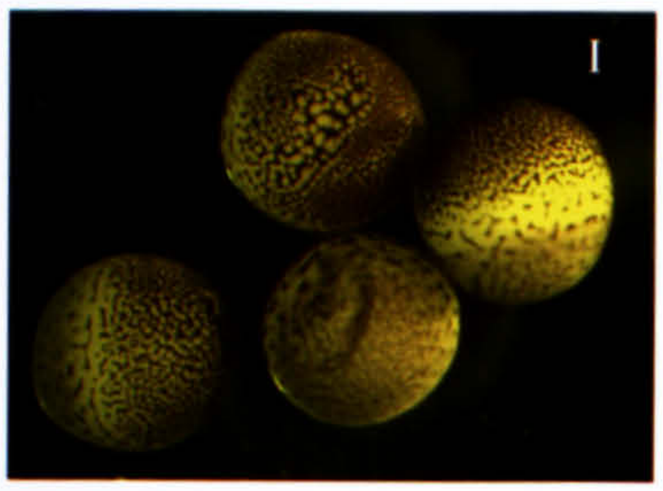

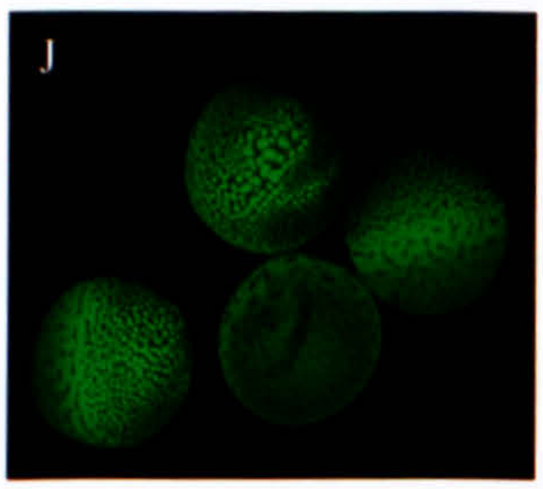

Taxol

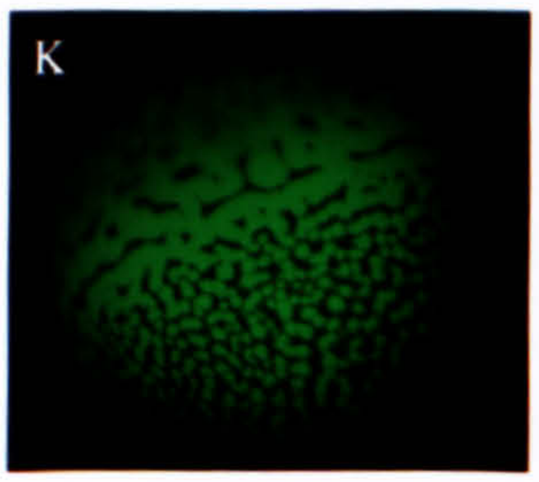

Thus, while the cytoskeletal inhibitors had no effect on GFP localisation, the oocytes showed obvious signs of pigment disruption or nuclei displacement, as *Xpat-GFP* injected oocytes did when cultured in the presence of anti-cytoskeletal drugs (see Section 4.3). These obvious phenotypic alterations indicate that the drugs are working and are thus disrupting their intended polymers.

4.3 The localisation of XPAT-GFP in oocytes treated with anti-cytoskeletal drugs

To analyse the effect of anticytoskeletal drugs on the localisation of XPAT-GFP, *Xpat-GFP* mRNA was injected into the equatorial region of *Xenopus* oocytes at a dose of 2 ng per oocyte. The oocytes were then cultured *in vitro* at 18°C in OCM in the presence of the appropriate cytoskeletal inhibitor for up to 3 days. As for the *GFP*-injected oocytes (Section 4.2), nocodazole was added to a final concentration of 3 μM, colcemid at 10 μM, cytochalasin D at a concentration of 2 μM and taxol at 5 μM. Some oocytes were treated with both cytochalasin D and colcemid, each at the concentration stated above. The localisation of the translated product was examined by fluorescent microscopy, and the oocytes were all scored for localisation of fluorescence. The results from three experiments were pooled and are recorded in Table 4.1. The experiments summarised in this table were done under identical conditions.

As shown in Table 4.1, XPAT-GFP protein localised in stage VI *Xenopus* oocytes that were cultured with no drugs. On day 1, 18 hours after injection, the fusion protein was expressed principally in an equatorial domain around the point of injection (47.0%). There was diffuse fluorescence in the majority of oocytes, but also some small granules of ~2.5 μm in diameter. 14.6% of oocytes expressed XPAT-GFP in small particles at the vegetal pole (Figures 4.2A and B). The remaining 38.4% of oocytes showed no external fluorescence and were thus scored as negative, although the nuclei of these oocytes do contain XPAT-GFP (see Section 4.4).

By 42 hours after injection, 25.8% of control oocytes expressed XPAT-GFP at, or just lateral to, the vegetal pole. 49.2% of oocytes still expressed XPAT-GFP in a domain around the equatorial injection site and the remaining 25.0% of oocytes were

Table 4.1: The localisation of XPAT-GFP in stage VI *Xenopus* oocytes following culture in the presence of cytoskeletal inhibitors

	Control	Cytochalasin D	Colcemid	Nocodazole	Taxol	Cytochalasin D + Colcemid
Day 1	V=14.6% E=47.0% –=38.4% n=164	V=16.5% E=63.3% –=20.2% n=79	V=9.1% E=40.3% –=50.6% n=77	V=9.6% E=41.1% –=49.3% n=73	V=4.25% E=31.9% –=51.05% G=12.8% n=47	 –=33.3% G=66.7% n=15
Day 2	V=25.8% E=49.2% –=25.0% n=124	V=15.7% E=33.3% –=19.6% G=31.4% n=51	V=24.1% E=24.1% –=46.3% G=5.5% n=54	V=15.1% E=24.5% –=26.4% G=34.0% n=53	V=3.6% E=50.0% –=14.3% G=32.1% n=28	 N/D
Day 3	V=33.6% E=40.2% –=26.2% n=122	V=28.6% E=10.7% –=46.4% G=14.3% n=28	V=15.0% E=17.5% –=55.0% G=12.5% n=40	V=21.05% E=21.05% –=34.2% G=23.7% n=38	V=35.1% –=19.3% G=45.6% n=57	 –=50% G=50% n=14

V=vegetal fluorescence, E=equatorial fluorescence, –=no external fluorescence,
G=general fluorescence, n= number of oocytes scored.

scored as negative. At this stage the fluorescence was mostly punctate, but at the vegetal pole the granules were larger.

As summarised in Table 4.1, 66 hours after injection with *Xpat-GFP*, 40.2% of control oocytes still showed equatorial fluorescence around the injection site. 33.6% of oocytes showed localisation at the vegetal pole and the remaining 26.2% were negative. Those oocytes showing fluorescence expressed large granular aggregates of XPAT-GFP at the vegetal pole (of between 30 and 50 μm in diameter) and smaller particles up to 2.5 μm at the equator. Figure 4.3A is a photograph of three oocytes expressing XPAT-GFP in granules at the vegetal pole.

4.3.1 The effect of cytochalasin D treatment on localisation of XPAT-GFP

When oocytes were incubated in the presence of cytochalasin D, as summarised in Table 4.1, 18 hours after injection XPAT-GFP was expressed principally in an equatorial domain around the injection site (63.3% of oocytes). When oocytes incubated in cytochalasin D were compared with control oocytes, a higher proportion of them showed equatorial expression. Indeed, a much higher percentage of oocytes incubated with cytochalasin D (compared to control oocytes) showed fluorescence, as only 20.2% were scored as negative. 16.5% of oocytes incubated in the presence of cytochalasin D expressed XPAT-GFP at the vegetal pole. The fluorescence was diffuse in some oocytes (Figure 4.2C) but some small granules of up to 2.5 μm in diameter were seen in most oocytes expressing XPAT-GFP vegetally. One such oocyte, expressing small granules of XPAT-GFP is shown in Figure 4.2D.

15.7% of XPAT-GFP-expressing oocytes that had been treated with cytochalasin D showed fluorescence at the vegetal pole in small granules 42 hours after injection. These granules were not as large as those seen in control oocytes or as regular. Larger (up to 10 μm) granules were seen at the vegetal pole, and smaller (1μm) particles surrounded them, but the oocytes were abnormal in pigmentation (and possibly starting to die), and localisation was not identical to that seen in control oocytes. 33.3% of oocytes incubated in cytochalasin D still showed equatorial expression of XPAT-GFP, in small particles. 31.4% of oocytes showed a diffuse, general fluorescence and the remaining 19.6% were negative.

Of those oocytes injected with *Xpat-GFP* and incubated in cytochalasin D, 10.7% were fluorescent at the equator, 14.3% showed general fluorescence and 28.6% showed vegetal localisation of XPAT-GFP 66 hours after mRNA injection. The remaining 46.4% were negative. In all oocytes that fluoresced, the fluorescence was mainly diffuse with only a few 2.5-10 μm granules at the vegetal pole in those oocytes exhibiting vegetal localisation. Figure 4.3B shows three cytochalasin D-treated oocytes exhibiting general XPAT-GFP fluorescence.

Thus, vegetal localisation and particle formation do not require microfilament function. Some particles coalesced into larger aggregates in the presence of cytochalasin D, but the aggregates appeared less regular and were not as large as granules seen in control oocytes (10 μm compared to 50 μm in controls). It is an issue whether any residual microfilament function remains in oocytes treated with cytochalasin D.

4.3.2 Localisation of XPAT-GFP in oocytes treated with colcemid

Oocytes cultured in the presence of colcemid also showed XPAT-GFP localisation after 18 hours in culture. As shown in Table 4.1, a high proportion of oocytes (40.3%) expressed XPAT-GFP in an equatorial domain around the injection site. The majority of the fluorescence in these oocytes was diffuse and non-particulate as shown in the three oocytes in Figure 4.2E. 9.1% of oocytes expressed XPAT-GFP at the vegetal pole. These oocytes contained a small number of fluorescent particles (1 to 2 μm across) as seen in the oocyte shown in Figure 4.2F. However, a higher proportion of these oocytes showed no external fluorescence compared with control oocytes, indeed 50.6% of colcemid-perturbed oocytes were scored as negative on day one.

As summarised in Table 4.1, 24.1% of those oocytes incubated in the presence of colcemid showed vegetal localisation 42 hours after injection. In these oocytes a few small particles of XPAT-GFP (up to 2 μm in diameter) were seen at the vegetal pole, but most of the external fluorescence was diffuse. 24.1% of the colcemid-treated oocytes still showed fluorescence at the equator around the injection site, and

Figure 4.2 (Opposite) Localisation of XPAT-GFP in oocytes treated with anti-cytoskeletal drugs
Stage VI *Xenopus* oocytes were each injected at their equator with 2 ng of *Xpat-GFP* mRNA and cultured *in vitro* for 18 hours in OCM containing a final concentration of 3 μM nocodazole, 10 μM colcemid, 2 μM cytochalasin D, 5 μM taxol or no inhibitor. The localisation of XPAT-GFP in oocytes was examined by fluorescent microscopy.

(A) Two control oocytes, the arrowed oocyte is expressing XPAT-GFP in a region just lateral to the vegetal pole, the other oocyte is expressing XPAT-GFP equatorially.

(B) A single oocyte expressing XPAT-GFP in small granules at the vegetal pole.

(C) Five oocytes treated with cytochalasin D expressing XPAT-GFP equatorially or vegetally (arrowed).

(D) An oocyte, treated with cytochalasin D, expressing XPAT-GFP in small granules at the vegetal pole.

(E) Three oocytes treated with colcemid expressing XPAT-GFP equatorially or vegetally (arrowed).

(F) Vegetal view of an oocyte treated with colcemid. This oocyte is expressing small particles of XPAT-GFP.

(G) Four oocytes treated with nocodazole, expressing XPAT-GFP in equatorial domains.

(H) An example of a nocodazole-treated oocyte expressing XPAT-GFP in small granules in vegetal pole.

(I) Three oocytes treated with taxol. These oocytes contain small particles of XPAT-GFP, as the closer view in (J) illustrates.

(J) Vegetal view of an oocyte treated with taxol, small particles of XPAT-GFP are visible and appear to be in networks at the vegetal pole.

(K) An oocyte treated with both cytochalasin D and colcemid shows no localisation of XPAT-GFP and no granules are visible.

(L) An oocyte treated with cytochalasin D and colcemid contains very few particles of XPAT-GFP.

All oocytes shown are ~1.2 mm in diameter.

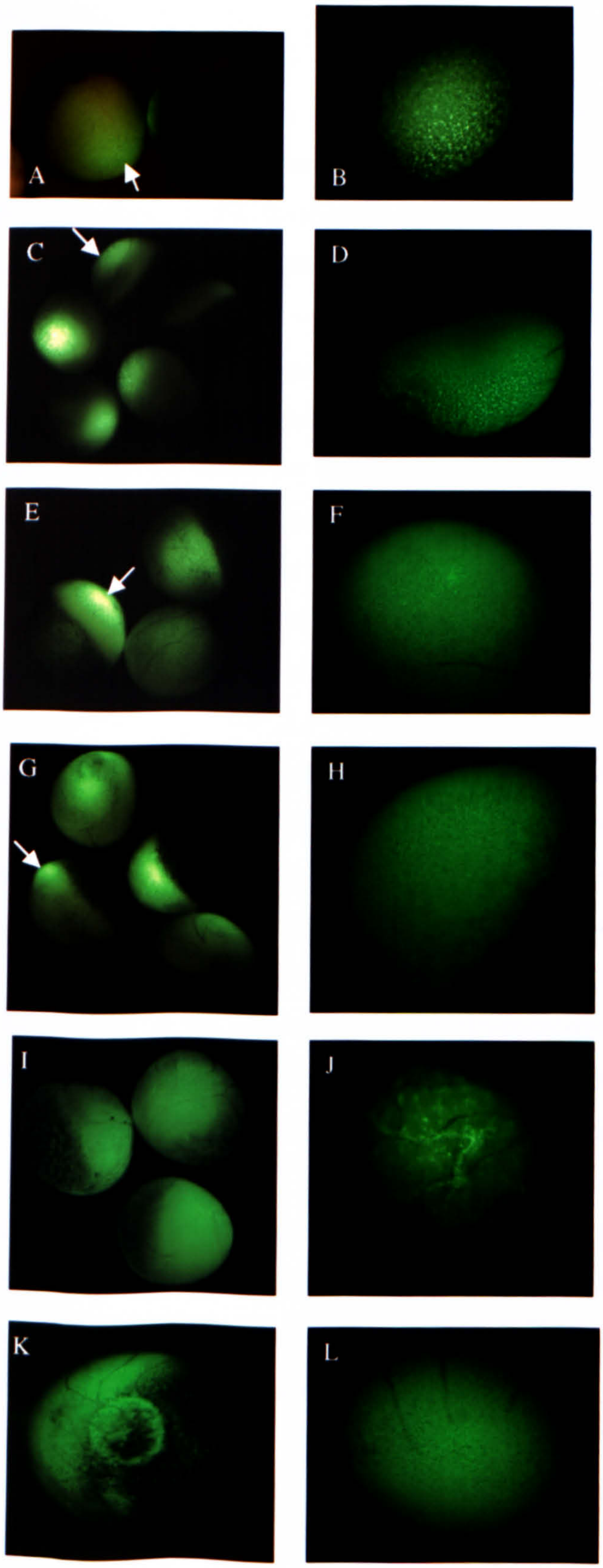

Control

Cytochalasin D

Colcemid

Nocodazole

Taxol

Cytochalasin D + Colcemid

5.5% exhibited general fluorescence. The remaining 46.3% of these oocytes were scored as negative.

Oocytes incubated in the presence of colcemid were mostly (55%) negative for XPAT-GFP fluorescence after 3 days in culture. 15% of oocytes showed vegetal XPAT-GFP localisation, 17.5% fluoresced equatorially and 12.5% were generally fluorescent (Table 4.1). The fluorescence in all positive oocytes was diffuse with only a few particles of up to 1μm visible at the very vegetal pole. However, there were particles present inside those oocytes that exhibited external fluorescence (this is shown later, in Section 4.4). Figure 4.3C shows four oocytes expressing XPAT-GFP in a general way- the nuclei are fluorescent and visible under the surface at the animal pole in all of these oocytes which indicates that colcemid treatment is working. These results suggest that vegetal transport depends, at least in part, on microtubule function, but particle formation seems relatively resistant. It is an issue whether any microtubule function remains in oocytes treated with colcemid.

4.3.3 The effect of nocodazole treatment on XPAT-GFP localisation

As summarised in Table 4.1, 41.1% of *Xpat-GFP*-injected oocytes that were incubated in the presence of nocodazole expressed XPAT-GFP in a domain around the equatorial injection site 18 hours after injection. The fluorescence in these oocytes was diffuse, as shown in the four oocytes in Figure 4.2G. 9.6% of oocytes expressed XPAT-GFP at the vegetal pole. The fluorescence in these oocytes was mostly diffuse but some particles (1 to 2 μm in diameter) were visible, as the oocyte in Figure 4.2H illustrates. The remaining 49.3% were scored as negative.

As Table 4.1 indicates, 15.1% of those oocytes incubated in nocodazole, showed vegetal fluorescence after 42 hours in culture. In these oocytes, like those treated with colcemid, a few 1 μm particles of XPAT-GFP could be seen at the vegetal pole, but the majority of the fluorescence was diffuse. 24.5% of these oocytes showed equatorial fluorescence and 34.0% were generally fluorescent. In all these oocytes, the fluorescence was diffuse and not granular. The remaining 26.4% of oocytes showed no external fluorescence.

66 hours after mRNA injection, 21.05% of XPAT-GFP-expressing oocytes that had been treated with nocodazole showed vegetal localisation, 21.05% showed equatorial fluorescence and 23.7% were generally fluorescent. The remaining 34.2% of oocytes were scored as negative. The fluorescence in all positive oocytes was highly diffuse, only the oocytes showing vegetal localisation expressed small (1 μm) particles at the very vegetal pole. Figure 4.3D shows six fluorescent oocytes that were incubated in nocodazole. The nuclei in all six oocytes were highly fluorescent and visible under the animal pole surface.

Thus, as might be expected, nocodazole gives results broadly like those for colcemid.

4.3.4 Localisation of XPAT-GFP in oocytes treated with taxol

18 hours after injection, of the oocytes incubated in taxol: 31.9% showed equatorial fluorescence, 4.25% expressed XPAT-GFP at the vegetal pole, 12.8% were generally fluorescent and the remaining 51.05% showed no external fluorescence and were thus scored as negative (Table 4.1). In all oocytes exhibiting external fluorescence, the fluorescence was mainly diffuse but contained some small (1-2 μm) particles as seen in the three oocytes shown in Figure 4.2I. One such oocyte is shown at a higher magnification in 4.2J; from this photograph it is obvious that there are small particles (up to 2 μm in diameter) of XPAT-GFP that appear to be forming networks of tracks of fluorescence. These networks were easily visible under a dissecting stereomicroscope.

Only 3.6% of XPAT-GFP-expressing oocytes showed vegetal localisation after 42 hours when treated with taxol. 50% of oocytes showed equatorial fluorescence, 32.1% general expression and the remaining 14.3% were negative (Table 4.1). In those oocytes showing equatorial fluorescence, the fluorescence was diffuse. However, in oocytes expressing XPAT-GFP vegetally or generally small particles were visible that appeared to form networks of fluorescent tracks. Association with tracks suggests that the particles associate with microtubule tracts. This does not exclude the possibility that the tubules orient another cytoskeletal component. Clearly particles form, supporting the idea that microtubules are not needed for their formation. The reduction in vegetal localisation, coupled with the considerable

pigment re-organisation, suggests that taxol effects are stronger than those of the microtubule dissociators. It indicates integrity of microtubule function is needed for XPAT-GFP localisation.

Table 4.1 summarises that 35.1% of XPAT-GFP–expressing oocytes incubated in taxol showed vegetal fluorescence 66 hours after injection. 45.6% of oocytes showed general fluorescence and the remaining 19.3% were negative. In all positive oocytes, diffuse fluorescence was visible as well as particles of XPAT-GFP, 2.5μm in diameter. These particles formed a visible network of fluorescence, throughout the oocyte, but especially obvious in the vegetal pole. An oocyte expressing such a pattern of XPAT-GFP localisation is shown in Figure 4.3E.

4.3.5 Localisation of XPAT-GFP in oocytes treated with both cytochalasin D and colcemid

Table 4.1 shows that, 18 hours after injection of *Xpat-GFP*, 66.7% of oocytes incubated in the presence of both cytochalasin D and colcemid expressed XPAT-GFP ubiquitously. The remaining 33.3% of oocytes were scored as negative. Thus, none of these oocytes showed any localisation of XPAT-GFP around the injection site or at the vegetal pole. The fluorescence seen in these oocytes was almost entirely diffuse (as illustrated by the oocyte shown in Figure 4.2K). There were a small number of 1μm particles visible in these oocytes, but as shown in Figure 4.2L, these particles were difficult to distinguish and certainly not as abundant as those seen in control XPAT-GFP expressing oocytes.

66 hours after injection of *Xpat-GFP*, 50% of those oocytes incubated in both cytochalasin D and colcemid showed a general and diffuse fluorescence, the other 50% were negative. A photograph of one generally positive oocyte is shown in Figure 4.3F.

Figure 4.3 (Opposite): Localisation of XPAT-GFP in oocytes treated with cytoskeletal inhibitors
Stage VI *Xenopus* oocytes were injected equatorially with 2 ng of *Xpat-GFP* mRNA and cultured *in vitro* in OCM at 18°C in the presence of anti-cytoskeletal drugs. After 72 hours in culture, XPAT-GFP localisation was visualised using a fluorescent microscope.

(A) Three oocytes cultured with no drugs expressing large granules of XPAT-GFP at their vegetal poles (arrowed).

(B) Three oocytes, which have been cultured in the presence of cytochalasin D, express XPAT-GFP in an even and general distribution. Fluorescence is diffuse in all these oocytes.

(C) Four oocytes treated with colcemid express XPAT-GFP generally. Fluorescence is diffuse and nuclei are visibly fluorescent under surface of all oocytes.

(D) Six oocytes injected with *Xpat-GFP* and cultured in the presence of colcemid. The nuclei of all six oocytes are fluorescent and visible under surface.

(E) An oocyte treated with taxol after injection of *Xpat-GFP*. A network of small granules of XPAT-GFP is visible all over this oocyte's surface.

(F) An oocyte treated with both colcemid and cytochalasin D expressing XPAT-GFP. The XPAT-GFP is non-localised; the nucleus is fluorescent and visible under surface of the animal pole (arrowed), and the pigment is disrupted.

Each oocyte is ~1.2 mm in diameter.

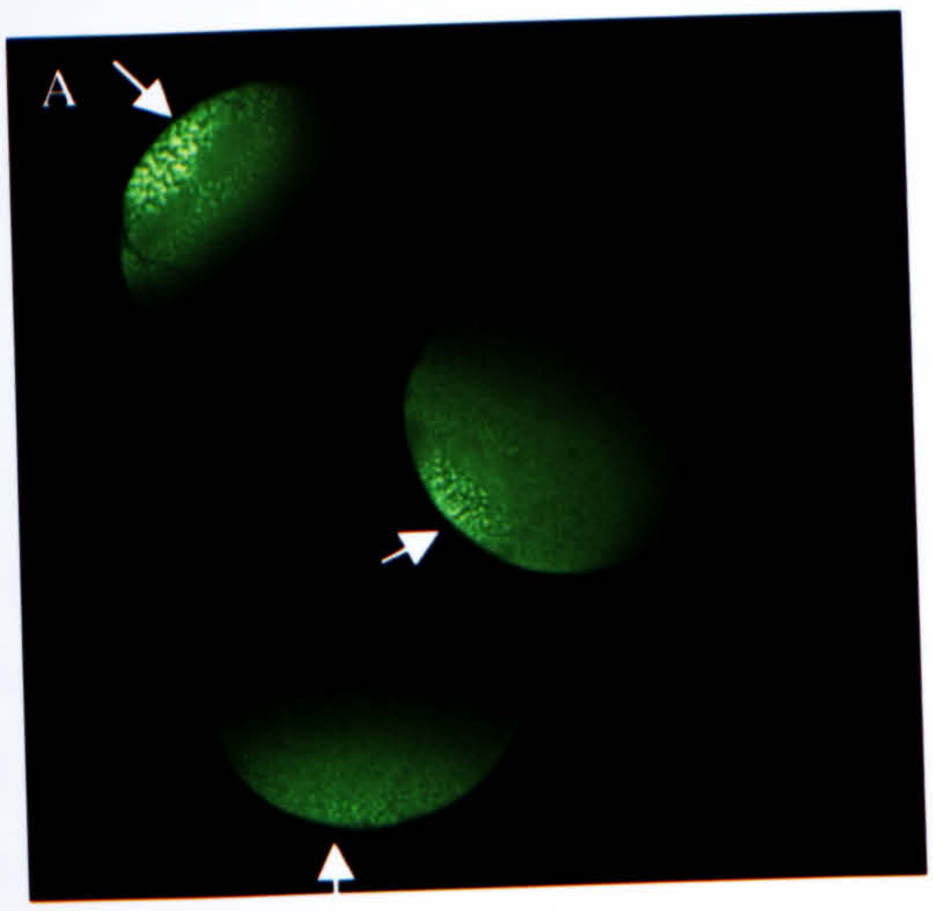
A

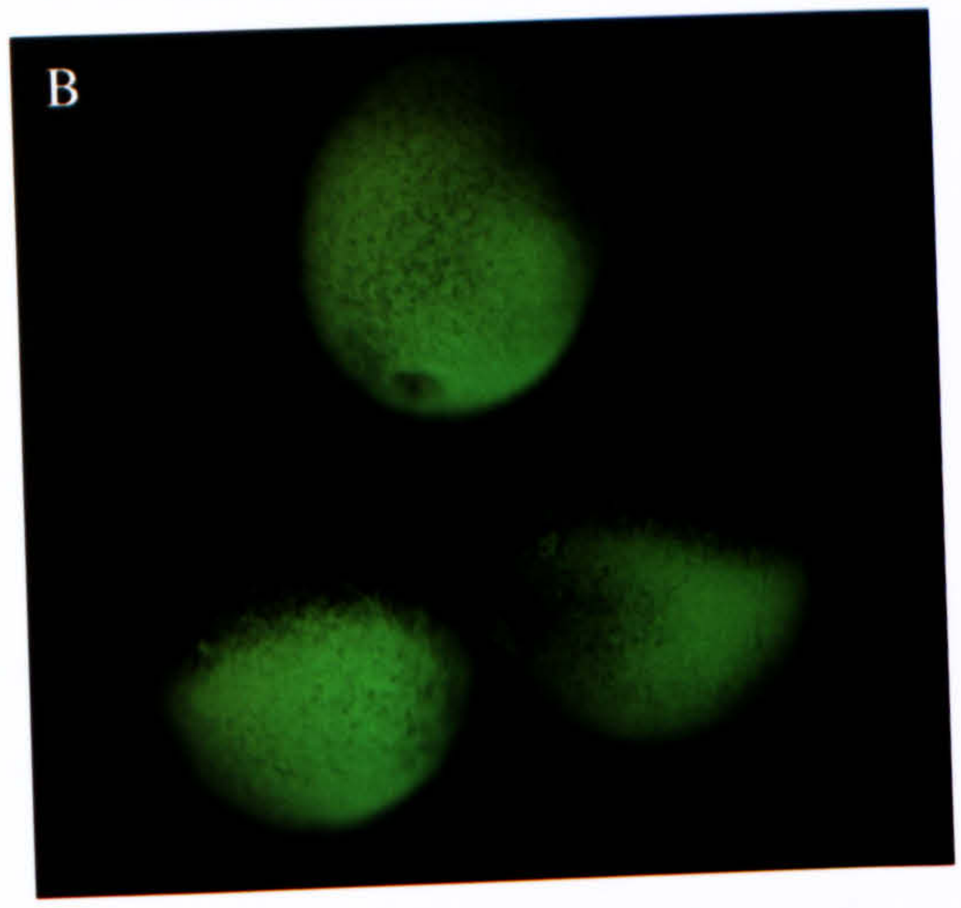
B

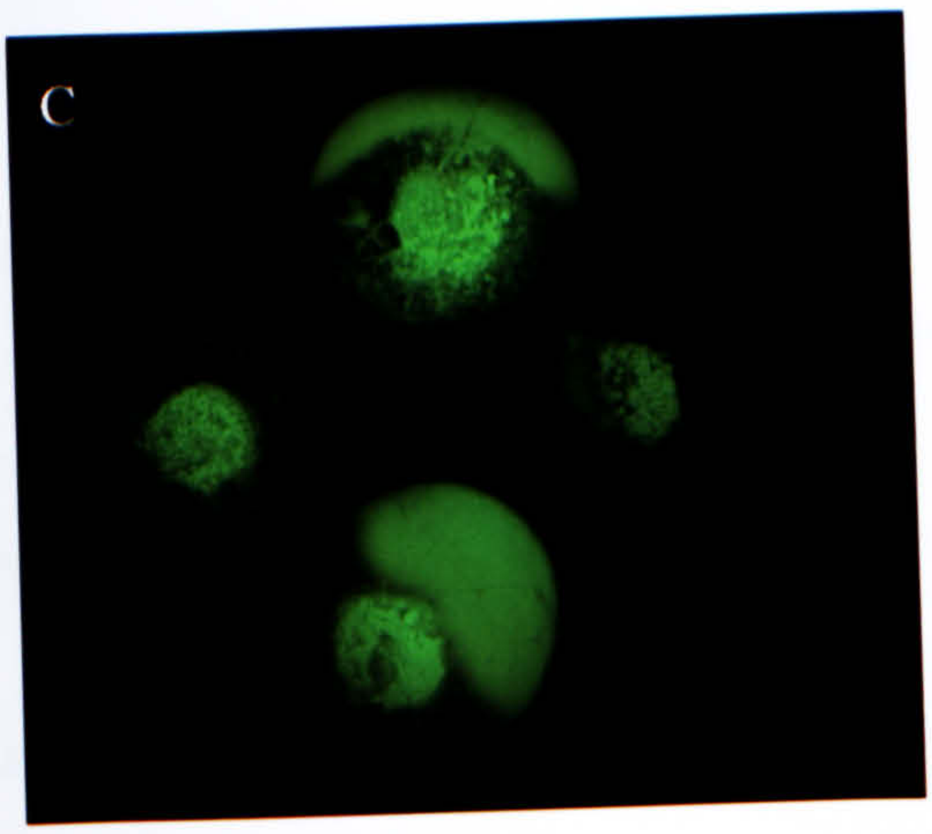
C

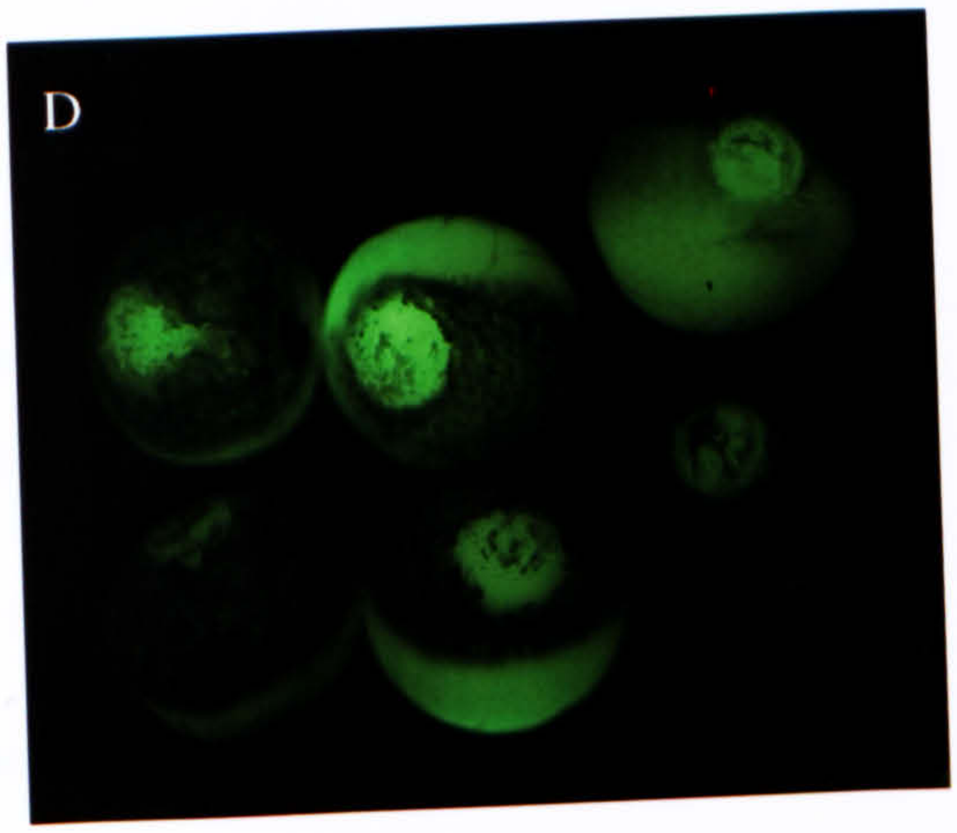
D

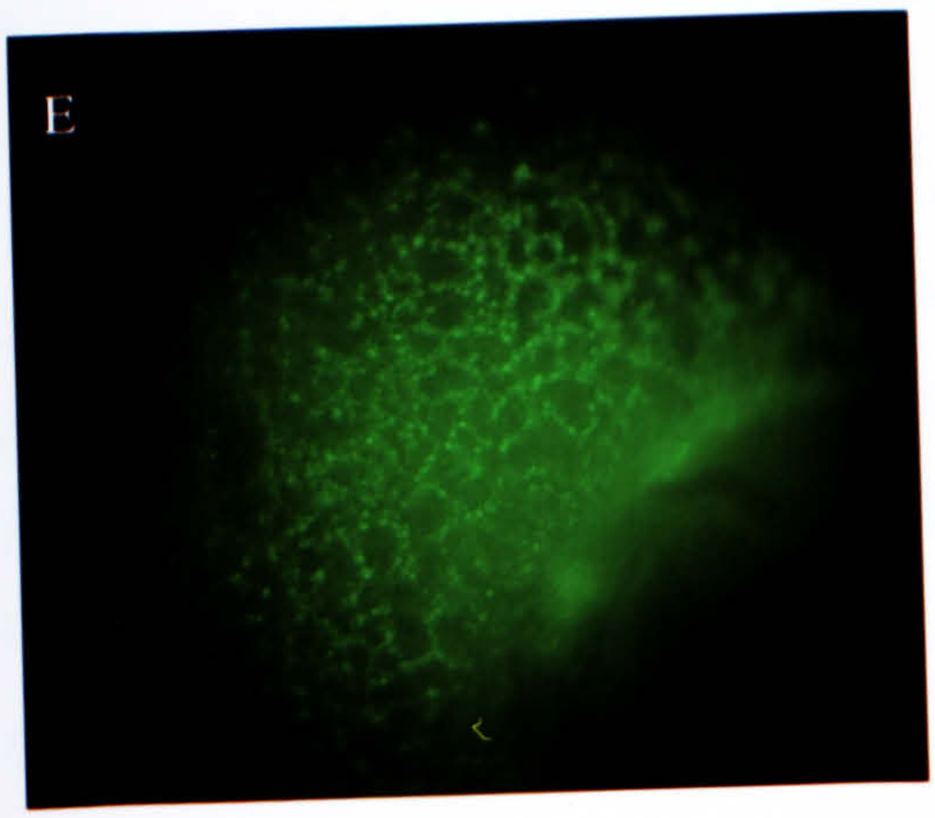
E

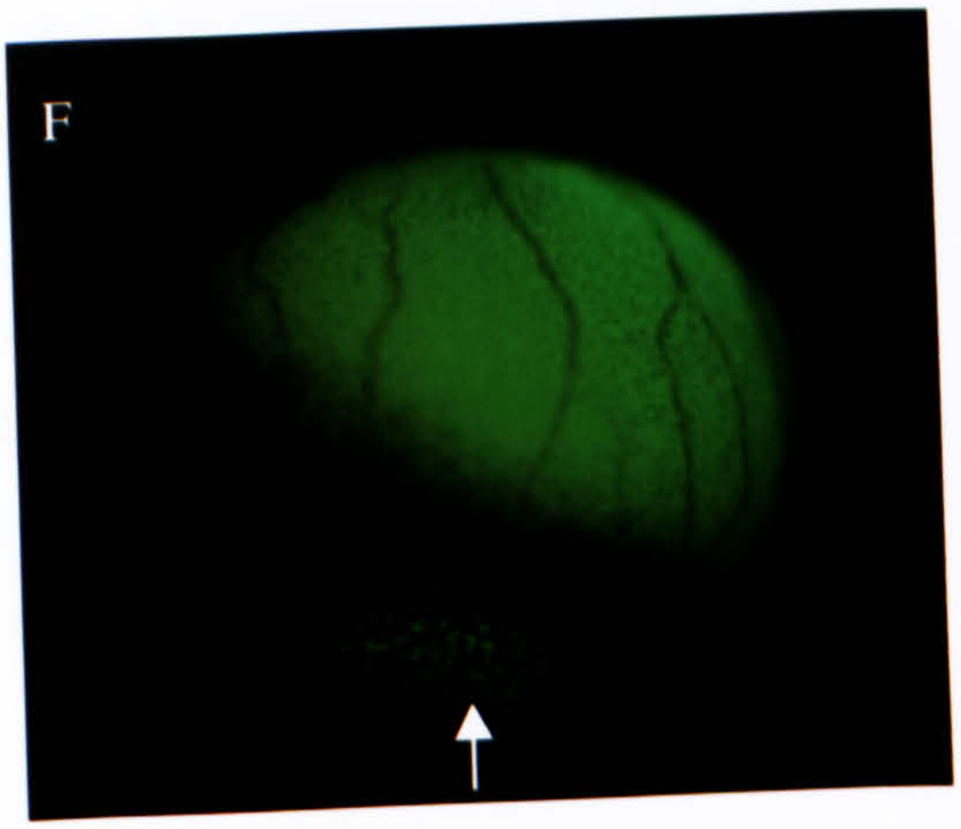
F

Thus, both particle formation and vegetal localisation are affected when both microtubules and microfilaments are disrupted. Thus, either microtubules and microfilaments are both necessary for translocation, or one of them only is involved but one of the anti-cytoskeletal drugs used is only partially effective at disrupting its respective polymers.

The results described above (all summarised in Table 4.1) indicate that oocytes incubated in inhibitors became sicker than control oocytes. Consequently, substantial numbers of oocytes began to lose fluorescence and thus be scored as negative. By day 2, the numbers of negative oocytes decreased when compared with day 1 scores. This was because oocytes scored as negative on day 1 typically became sick and died, thus were removed and not scored on day 2. During the course of days 2 and 3, more oocytes became sick and lost fluorescence, thus on day 3 high numbers of oocytes were scored as negative.

None of the *Xpat-GFP*-injected oocytes incubated in the presence of cytoskeletal inhibitors displayed any large granules; only small (1 to 2.5 μm) particles were seen in these oocytes. This was in contrast to control oocytes that expressed large (up to 50 μm across) granules of XPAT-GFP protein.

4.3.6 To confirm that anticytoskeletal drugs affect the size of XPAT-GFP particles in oocytes

In order to gain a better perception of exactly what was happening to the particles and granules of XPAT-GFP in oocytes, a higher magnification microscope was used (Figure 4.4). Figure 4.4A shows a higher magnification view (x200) of large granules of XPAT-GFP protein in control oocytes formed 42 hours after injection. These granules are up to 50 μm in size and seem to be large aggregates of smaller particles (of ~5 μm diameter). Figure 4.5B is a high power view (x200) of particles of XPAT-GFP protein in control oocytes, formed 16 hours after mRNA injection. These particles are 1-2 μm in diameter.

Figure 4.4C is a high power picture (200x magnification) of the vegetal region localisation of XPAT-GFP in oocytes treated with cytochalasin D, 42 hours after

injection. The largest of the particles were 7 μm in size. The oocyte shown in this figure is a typical example of a cytochalasin D-treated oocyte and its largest granules are much smaller than the largest granules seen in control oocytes.

Figure 4.4D is a high magnification view (x200) of the vegetal region of an oocyte expressing XPAT-GFP that had been treated with colcemid. This photograph was taken 42 hours after injection. The particles in this oocyte were 1 μm in diameter, and these were the largest seen in any *Xpat-GFP*-injected oocyte cultured in colcemid.

Figure 4.4E shows a high magnification view (x200) of the particles seen at the vegetal pole of an oocyte treated with nocodazole. The particles were mostly 1 μm in diameter, but a few were up to 4 μm. The photograph was taken 42 hours post *Xpat-GFP* injection, and this oocyte was typical of all such nocodazole-treated oocytes.

Figure 4.4F is a high magnification view (x200) of the vegetal pole of an oocyte cultured in the presence of both cytochalasin D and colcemid. Very few particles were seen in this oocyte, the vast majority of fluorescence was diffuse and non-granular. The oocyte shown in 4.4F had been injected with *Xpat-GFP* 42 hours previously and was a typical example of an oocyte treated with both inhibitors.

Figure 4.4H is a high power picture (200x magnification) of the particles seen in *Xpat-GFP*-injected oocytes treated with taxol. The particles were between 1 and 3 μm in diameter and appeared to be forming tracks of fluorescence in a tubule-like pattern. The tracks were long and stretched for lengths of greater than 300 μm.

Figure 4.4 (Opposite): Anti-cytoskeletal drugs prevent the formation of large aggregates of XPAT-GFP in oocytes

Oocytes were injected with 2 ng of *Xpat-GFP* mRNA equatorially and cultured *in vitro* in OCM in the presence of anti-cytoskeletal drugs. After 42 hours, the vegetal localisation of XPAT-GFP was examined using high magnification fluorescent microscopy. In (A) – (F) the scale bar represents 50 μm, in (G) it represents 250 μm and in (H) it represents 30μm.

(A) Vegetal view of a control oocyte expressing large granules of XPAT-GFP up to 50 μm in size.

(B) Vegetal view of a control oocyte expressing XPAT-GFP in particles of between 1-2 μm diameter. This photograph was taken 16 hours after mRNA injection and is shown for comparison with the particles seen in oocytes treated with anti-cytoskeletal drugs.

(C) Oocyte treated with cytochalasin D expressing granules of XPAT-GFP at the vegetal pole, up to 7 μm in diameter.

(D) Vegetal view of an oocyte, cultured in the presence of colcemid, expressing particles of XPAT-GFP ~1 μm in diameter.

(E) Oocyte treated with nocodazole expressing small granules of XPAT-GFP at the vegetal pole, these granules were up to 4 μm in diameter.

(F) Vegetal view of an oocyte cultured in the presence of both cytochalasin D and colcemid. Very few particles of XPAT-GFP are visible in this oocyte, the fluorescence is diffuse.

(G) An oocyte treated with taxol after injection of *Xpat-GFP*. A network of small granules of XPAT-GFP is visible all over this oocyte's surface.

(H) High magnification view of the boxed region of (G). Granules of XPAT-GFP visible at the vegetal pole in an oocyte treated with taxol. These granules were between 1 and 3 μm in diameter and appear to be localised in tracks of fluorescence.

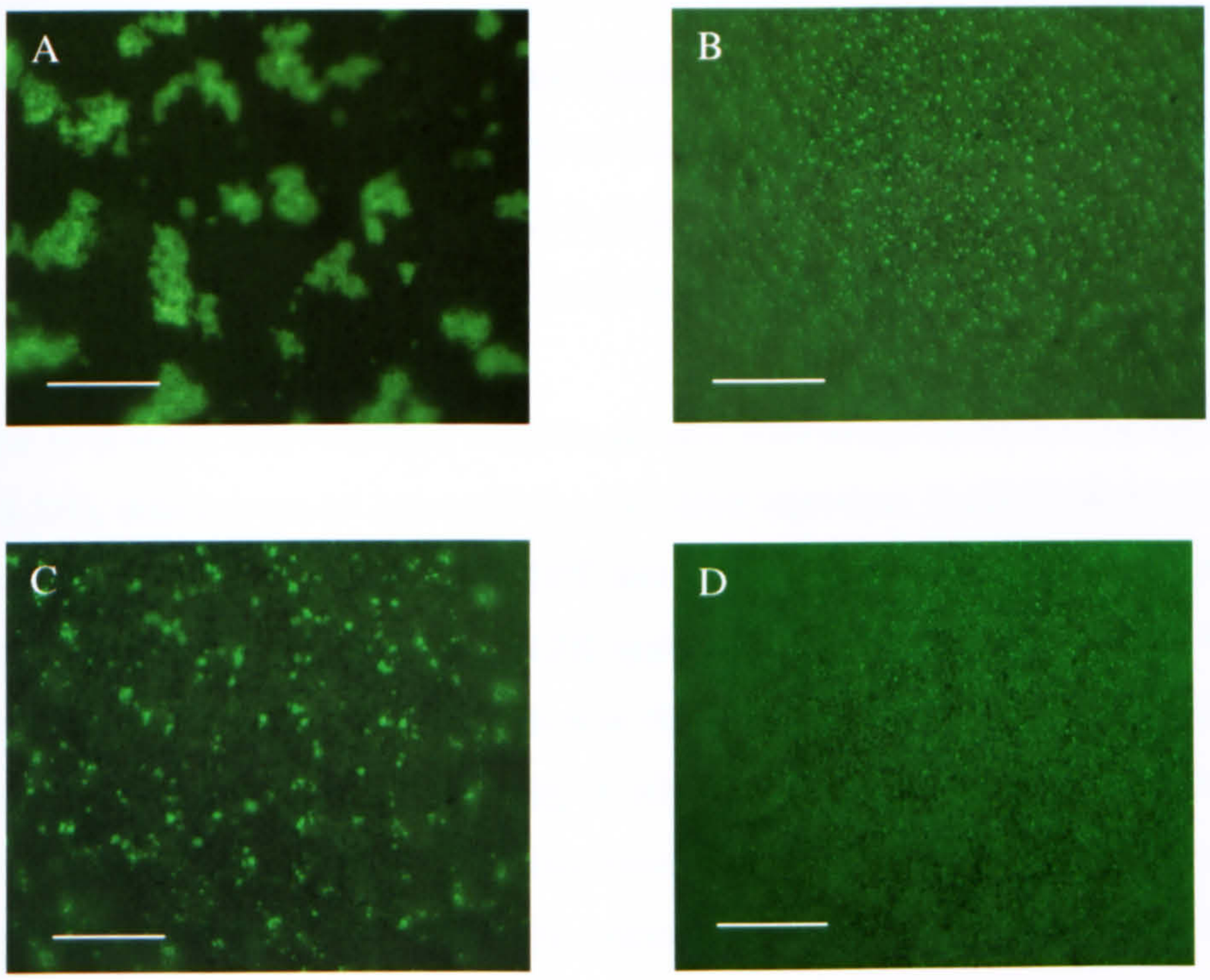
A
B
C
D
E
F
G
H

4.4 The internal and nuclear localisation of XPAT-GFP in oocytes treated with cytoskeletal inhibitors

To determine whether granules and particles of XPAT-GFP were purely superficial or not and to see whether nuclei were fluorescent, *Xpat-GFP*-injected oocytes that had been cultured in the presence of cytoskeletal inhibitors were viewed internally. Oocytes were fixed by heating to 75-85°C in Barth's saline for 30 seconds and then cut open using a scalpel. Figure 4.5 shows oocytes dissected this way.

Figure 4.5B to E show *GFP*-injected oocytes, treated with drugs (controls are shown in Figure 4.5A), which were all bisected 48 hours after injection. In all these oocytes, fluorescence was diffuse, no particles of GFP were seen and the nuclei in all oocytes were fluorescent. The oocyte in Figure 4.5B appears to have a negative nucleus but this was not the case however, the nucleus was in the other (unphotographed) half of the oocyte. Fluorescence was quite strong in all oocytes except taxol-treated ones (Figure 4.5E) that were quite weakly fluorescent, because the fluorescence was mostly superficial and not present inside the oocytes.

Figure 4.5F to J show *Xpat-GFP* injected oocytes that had been treated with inhibitors and bisected after 48 hours in culture. Figure 4.5F is a control (untreated) oocyte, expressing particles of XPAT-GFP in a domain stretching from the equator to just lateral to the vegetal pole. These granules were not purely superficial, they were present inside the oocyte in the cytoplasm and the nucleus also contained non-particulate XPAT-GFP.

Figure 4.5G is a photograph of an XPAT-GFP expressing oocyte that had been treated with cytochalasin D and bisected 48 hours post-injection. Again, it is obvious that the particles of XPAT-GFP protein were not purely superficial, they were present in the cytoplasm inside the oocyte and were spread out over quite a large area. Unlike control oocytes, the particles appeared irregular in arrangement and were present in patches. The majority of particles were present just under the surface near the equator, but there were other particles present throughout cytoplasm even near the nucleus. The nucleus of this oocyte was also fluorescent and there was a lot of general diffuse fluorescence throughout the oocyte.

Figure 4.5H shows an XPAT-GFP-expressing oocyte that had been treated with colcemid and bisected after 48 hours in culture. The fluorescence in this oocyte was quite patchy and mainly present equatorially and in the deeper cytoplasm. The small particles of XPAT-GFP were not purely superficial; where they were visible on the oocyte surface at the equator, they were also present inside the oocyte in a cluster in the same region. The particles were similar in arrangement to those seen in control oocytes.

Figure 4.5I shows a bisected XPAT-GFP expressing oocyte that had been cultured for 48 hours *in vitro* in the presence of nocodazole. The fluorescence in this oocyte was in the vegetal region, and the small particles visible at the vegetal pole surface were not purely superficial. There was a patch of particles present in the cytoplasm reaching from the vegetal pole towards the nucleus. The particles extended further towards the nucleus than those seen in control oocytes.

Figure 4.5J shows a high magnification photograph of a bisected XPAT-GFP expressing oocyte that had been treated with taxol and cultured *in vitro* for 48 hours. The particles visible at the surface of this oocyte were not totally superficial but much more so than with other treatments. They were present inside the cytoplasm and appeared to form linear rows of particles under the oocyte's surface, extending for lengths of ~250 μm. The particles also extended inside the oocyte towards the nucleus.

The oocytes that had been treated with anti-cytoskeletal drugs were generally less healthy than control oocytes. Thus, dissections were more difficult to perform and generally looked less neat, regular and sharp than controls, as the photographs in Figure 4.5 illustrate.

Figure 4.5 (opposite): Internal and nuclear localisation of XPAT-GFP and GFP in oocytes treated with cytoskeletal inhibitors
Stage VI *Xenopus* oocytes were injected with 2 ng of *Xpat-GFP* or *GFP* mRNA and cultured *in vitro* in OCM in the presence of anti-cytoskeletal drugs -3 μM nocodazole, 10 μM colcemid, 2 μM cytochalasin D or 5 μM taxol. After 48 hours in culture, oocytes were fixed by heating to 75 to 85 °C in Barth's saline for 30 seconds and then cut open using a scalpel. The internal localisation of XPAT-GFP (or GFP) was then examined by fluorescent microscopy.

(A) A control *GFP*-injected oocyte expressing GFP throughout nucleus and cytoplasm.

(B) An oocyte treated with cytochalasin D expressing GFP throughout the cytoplasm. The nucleus of this oocyte was also fluorescent but is not shown in this photograph.

(C) An oocyte treated with colcemid expressing GFP throughout its cytoplasm and nucleus.

(D) Oocyte cultured in the presence of nocodazole expressing GFP throughout the nucleus and cytoplasm.

(E) Oocyte cultured in presence of taxol expresses GFP weakly throughout cytoplasm and nucleus.

(F) An untreated oocyte which had been injected with *Xpat-GFP* expressed particles of XPAT-GFP on surface in a domain stretching from the equator to just lateral to the vegetal pole. XPAT-GFP granules are present inside the oocyte and the nucleus also contains fusion protein.

(G) An XPAT-GFP expressing oocyte that has been treated with cytochalasin D. Particles of XPAT-GFP are present in cytoplasm over a large domain but are irregular in arrangement. The nucleus also contains XPAT-GFP.

(H) An oocyte treated with colcemid expressing XPAT-GFP equatorially in patches throughout the cytoplasm (arrowed).

(I) An oocyte cultured in presence of nocodazole. Particles of XPAT-GFP are present at the vegetal pole surface and throughout cytoplasm towards the nucleus (arrowed).

(J) An oocyte treated with taxol, expressing XPAT-GFP in granules at the oocyte surface and inside the cytoplasm. The particles appear to form linear rows in the cytoplasm and towards the nucleus (arrowed).

Each oocyte shown is ~1.2 mm in diameter.

GFP **XPAT-GFP**

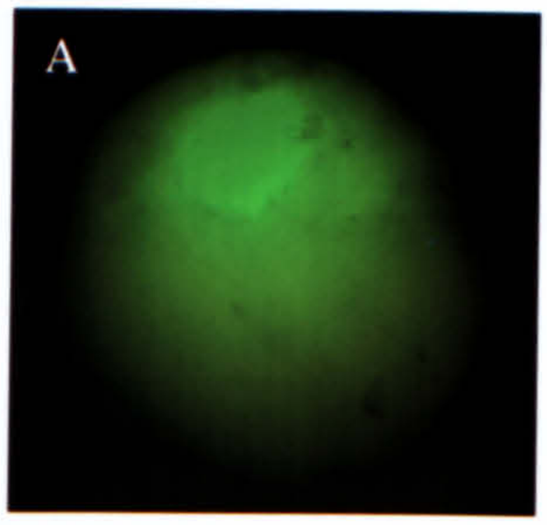

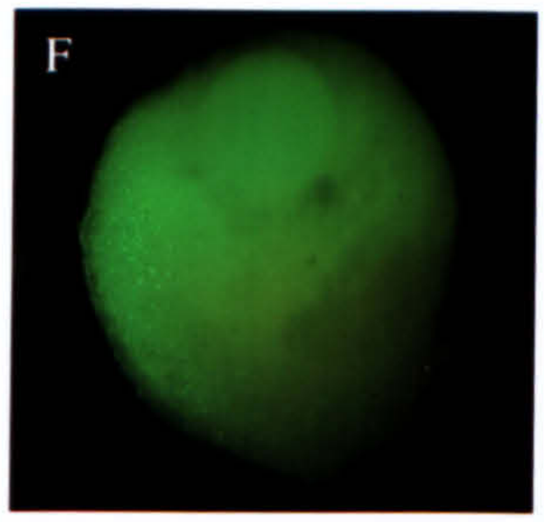

Control

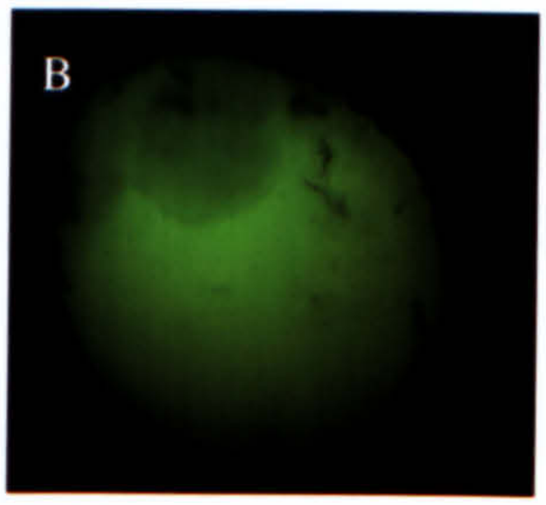

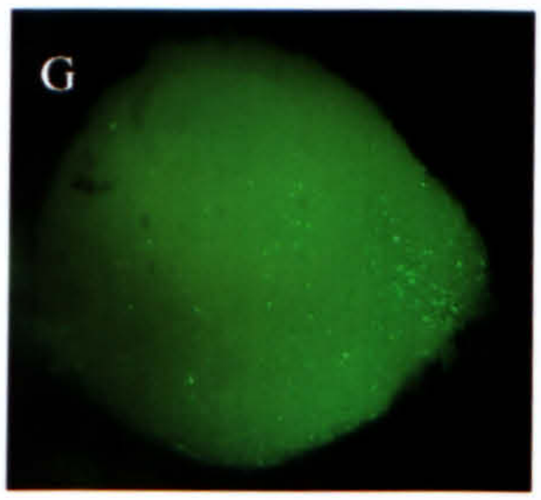

Cytochalasin D

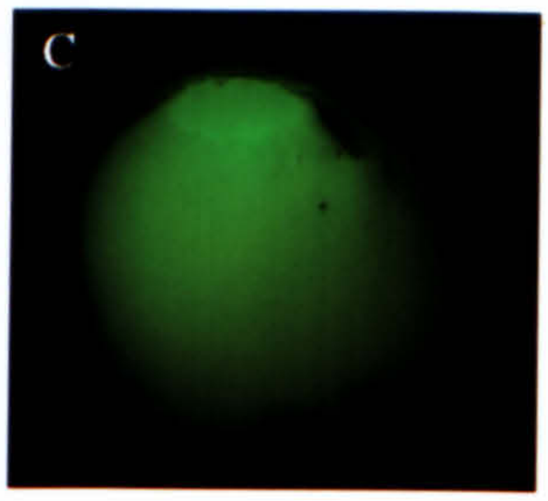

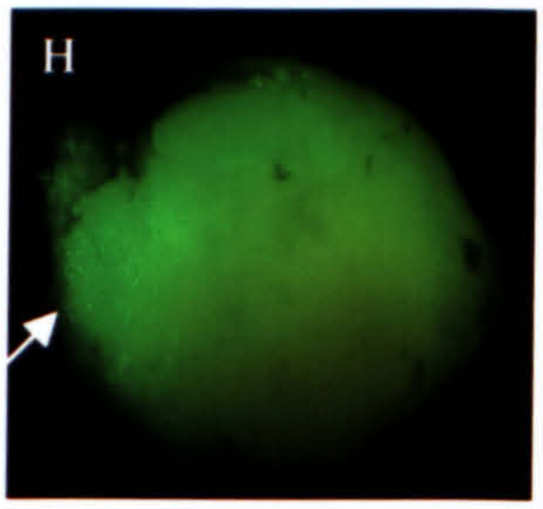

Colcemid

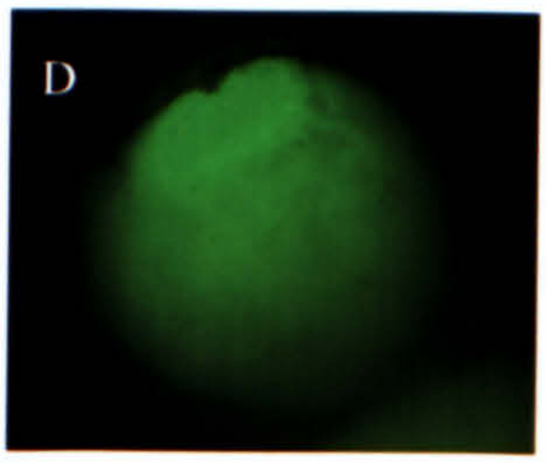

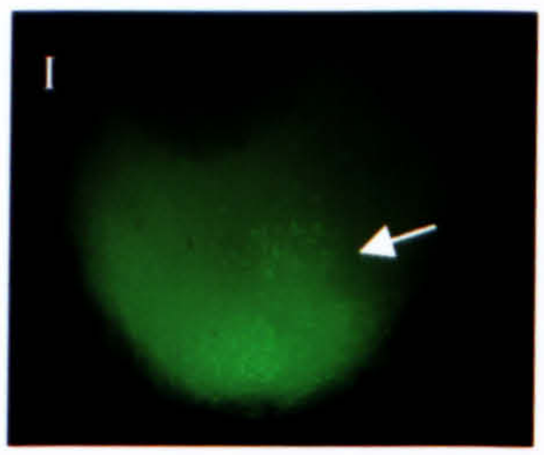

Nocodazole

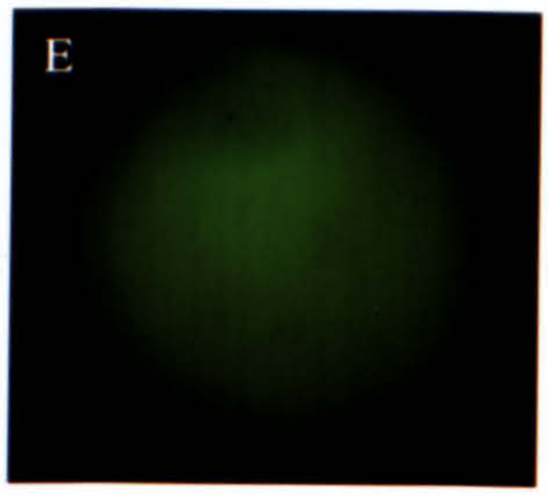

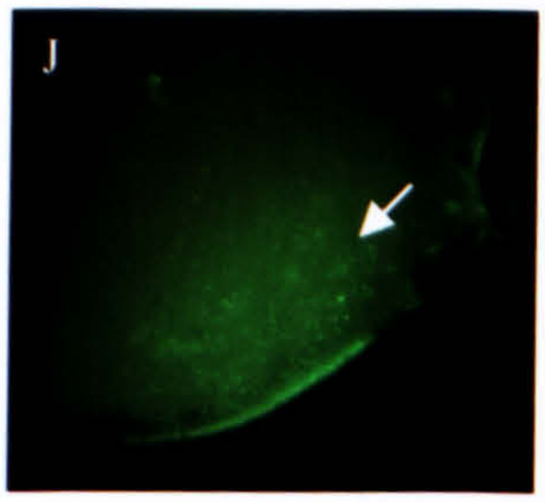

Taxol

4.5 Do inhibitors of the cytoskeleton affect localisation of endogenous *Xpat* mRNA?

Stage VI *Xenopus* oocytes were treated with cytochalasin D, colcemid, nocodazole or taxol as previously described (Section 4.2). These oocytes were cultured *in vitro* in OCM for 42 hours at 18°C and then fixed. *In situ* hybridisation showed that, in all cases, the distribution of endogenous *Xpat* mRNA was the same as in control oocytes and was thus unaffected by these treatments (results not shown). This experiment focused on the steady state distribution of endogenous mRNA in fixed cells. This in an equilibrium condition and as such may not be directly relevant to understanding the mechanism of RNA (or indeed protein) localisation, since RNA localisation is a dynamic process (Ainger *et al.*, 1993). However, what could be determined from this experiment was that endogenous *Xpat* mRNA localisation had not been altered by drug treatment. By stage VI, *Xpat* mRNA had already localised and thus, from these results, once *Xpat* mRNA has localised in oocytes none of the anti-cytoskeletal drugs can disrupt it. Experiments have not yet been done to determine whether injected *Xpat* or *Xpat-GFP* mRNA localisation is affected by the use of cytoskeletal inhibitors.

4.6 Discussion

Preliminary experiments on the mode of localisation of XPAT-GFP have been conducted, using cytoskeletal inhibitors. These indicate that microtubules, but not microfilaments, are essential for transport from the equator to the vegetal pole; neither are needed for the small punctate particles to form. Larger aggregates of XPAT-GFP do not form when either microtubules or microfilaments are disrupted. This is obvious since equivalent levels of vegetal localisation of XPAT-GFP are seen in cytochalasin D-treated oocytes when compared with control oocytes. However, the result from oocytes treated with both cytochalasin D and colcemid is most convincing. This implies that to completely prevent vegetal localisation or any localisation around the injection site, both microtubule and microfilament destruction is necessary. Also, when both are destroyed, not even small particles of XPAT-GFP can form. Although intermediate filaments as a class cannot be targeted with inhibitors, they are disrupted by depolymerising microtubules. It is unlikely though that intermediate filaments can direct transport of XPAT-GFP, indeed no motor

proteins are known for intermediate filaments and they have not been shown to transport mRNAs. However, intermediate filaments are required for the cortical anchoring of *Vg1* RNA (Yisraeli *et al.*, 1990; Kloc and Etkin, 1995), and could likewise be involved in the anchoring of *Xpat-GFP* mRNA or the protein it encodes.

Colcemid- and nocodazole-treated oocytes exhibited a reduced frequency of XPAT-GFP localisation, but these inhibitors did not totally prevent localisation. This could be because total disruption of all oocyte microtubules would not be possible in 24 hours, or could indicate that these drugs were not totally effective in disrupting all oocyte microtubules at the concentrations used in these experiments. Thus, microtubules may be required for vegetal localisation of XPAT-GFP - it depends how many remain intact in colcemid- and nocodazole-treated oocytes; in fact, γ-tubulin is not disrupted by nocodazole. A second possibility is that the inhibitors are working efficiently but microfilaments, in addition to microtubules, are functional in vegetal localisation of XPAT-GFP.

High magnification photographs (x200) indicate that fluorescent granules of XPAT-GFP appear to be closely associated with microtubules when they had been stabilised by taxol. It is possible that they are transported along microtubule bundles but there is no direct evidence of this. γ-tubulin is asymmetrically distributed along the A-V axis, with foci of γ-tubulin concentrated at the vegetal cortex of *Xenopus* oocytes (Gard, 1994; Gard *et al.*, 1995). The majority of microtubules have their minus ends directed towards the oocyte cortex (Pfeiffer and Gard, 1999). Thus, there might be a population of microtubules nucleated by γ-tubulin at the vegetal pole, with their minus ends at the vegetal cortex in stage VI oocytes; any transport of XPAT-GFP along these tubules would probably involve dynein, a minus end-directed motor (Fox and Sale, 1987; Paschal and Vallee, 1987; Paschal *et al.*, 1987; Schroer *et al.*, 1989; Schnapp and Reese, 1989). In order to gain more information on possible microtubular transport of XPAT-GFP, rhodamine-labelled tubulin monomers could be used to determine whether XPAT-GFP can colocalise with the rhodamine labelled tubulin. This was attempted, but the method was not optimised due to time restrictions.

The velocity of movement of XPAT-GFP protein (600 μm over 24 hours) is slower than microtubule-based, kinesin-driven transport (Okabe & Hirokawa, 1989; Vallee & Bloom, 1991; Ainger *et al.*, 1993). Ainger and colleagues found that granules in such processes underwent sustained directional movement with a velocity of ~0.2μm/s along microtubules. This is equivalent to 720 μm per hour (Ainger *et al.*, 1993). Similarly, most organelles move toward the minus ends of centrosome microtubules (dynein-driven transport) at an average velocity of 0.5±0.2 μm/s (Schroer *et al.*, 1989), again faster than the observed movement of XPAT-GFP towards the vegetal pole.

There are three possible mechanisms of intracellular localisation:

1) Diffusion plus local binding
2) Diffusion plus degradation (P-granules localise this way in *C. elegans;* Strome and Wood, 1982, 1983)
3) Active transport.

However, the results presented in this study indicate that XPAT-GFP is transported and the protein is not degraded. This is evident because XPAT-GFP fluorescence is visible at the injection site even when mRNA is injected at the animal pole, and oocytes remain fluorescent for at least 3-4 days post-injection.

XPAT-GFP could bind to an RNA that, in turn, binds to the cytoskeleton. This is unlikely to be an endogenous mRNA since such large quantities of XPAT-GFP protein, as are present in these injected oocytes, would be expected to saturate such an endogenous pathway. However, it is possible that it could bind to *Xpat-GFP* mRNA that could then be localised by microtubules. However, proteins usually bind to 3′UTR sequence and *Xpat-GFP* mRNA does not contain any of *Xpat*'s UTR. Most germ plasm localised molecules have been discovered to be RNA-binding proteins (such as Xdazl; Houston *et al.*, 1998). Chapter 6 looks at the RNA-binding properties of XPAT.

Chapter 5: The localisation of XPAT-GFP deletion proteins in *Xenopus* oocytes

5.1 Introduction

XPAT-GFP localises to the vegetal pole of stage VI *Xenopus* oocytes, and forms small particles that aggregate over time to form larger granules (20-50μm in diameter) reminiscent of the germ plasm (see Chapter 3). It also enters the nucleus. It was decided that it would be useful to produce several protein isoforms in order to establish what regions of XPAT are involved in these processes. These proteins were deletion variants of XPAT that were fused in frame with GFP at their C-termini. Three variants lacking amino acids at the amino-terminus of XPAT - ΔN1 lacking the first 61 amino acids, ΔN2 lacking the first 92 amino acids and ΔN3 lacking N-terminal 159 amino acids, were produced. Also, a C-terminal deletion protein, lacking the last 128 amino acids of XPAT, was generated and tagged in frame with GFP at its carboxy-terminus. These proteins were all expressed in stage VI *Xenopus* oocytes and examined for their localisation in the oocyte. This was done in order to try to determine which domains in XPAT are responsible for its vegetal localisation and if the same amino acids also cause it to form granules. It was also thought that these proteins would serve as a useful control to show that all proteins do not localise in the same manner as full-length XPAT when C-terminally tagged with GFP.

5.2 Production of ΔN1, ΔN2, ΔN3 and ΔC1 deletion proteins

Fluorescently tagged deletion variants of XPAT were prepared using pSPJC2L-cGFP as a vector (see 3.2.2 for details of construction). This vector contained restriction sites that could be used to create cDNAs encoding proteins tagged with GFP at their C-termini. The DNA containing the required region of the Xpat ORF was amplified from a cDNA library clone with primers designed to create 5′ and 3′ *Bgl*II sites. In each case, the resulting fragment was cloned into the *Bgl*II site of pSPJC2L-cGFP, generating N-terminal deletion variants ΔN1, ΔN2, ΔN3 and a C-terminal deletion ΔC1. The proteins encoded by these constructs are shown schematically in Figure 5.1A. This figure indicates which amino acids of XPAT are included in each variant protein and also shows full-length XPAT-GFP. Each of the ΔN deletions was designed to start at a genuine methionine in XPAT (see appendix 2) and ΔC1 and ΔN1 have 6 amino acids in common.

A

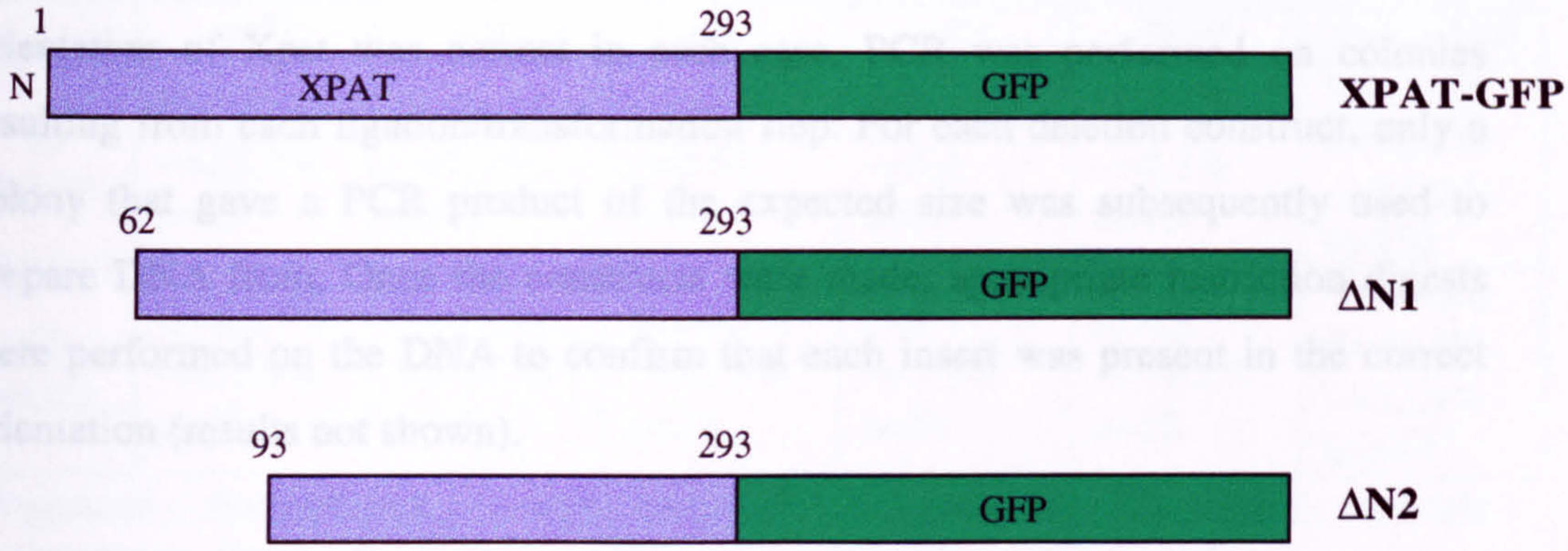

B

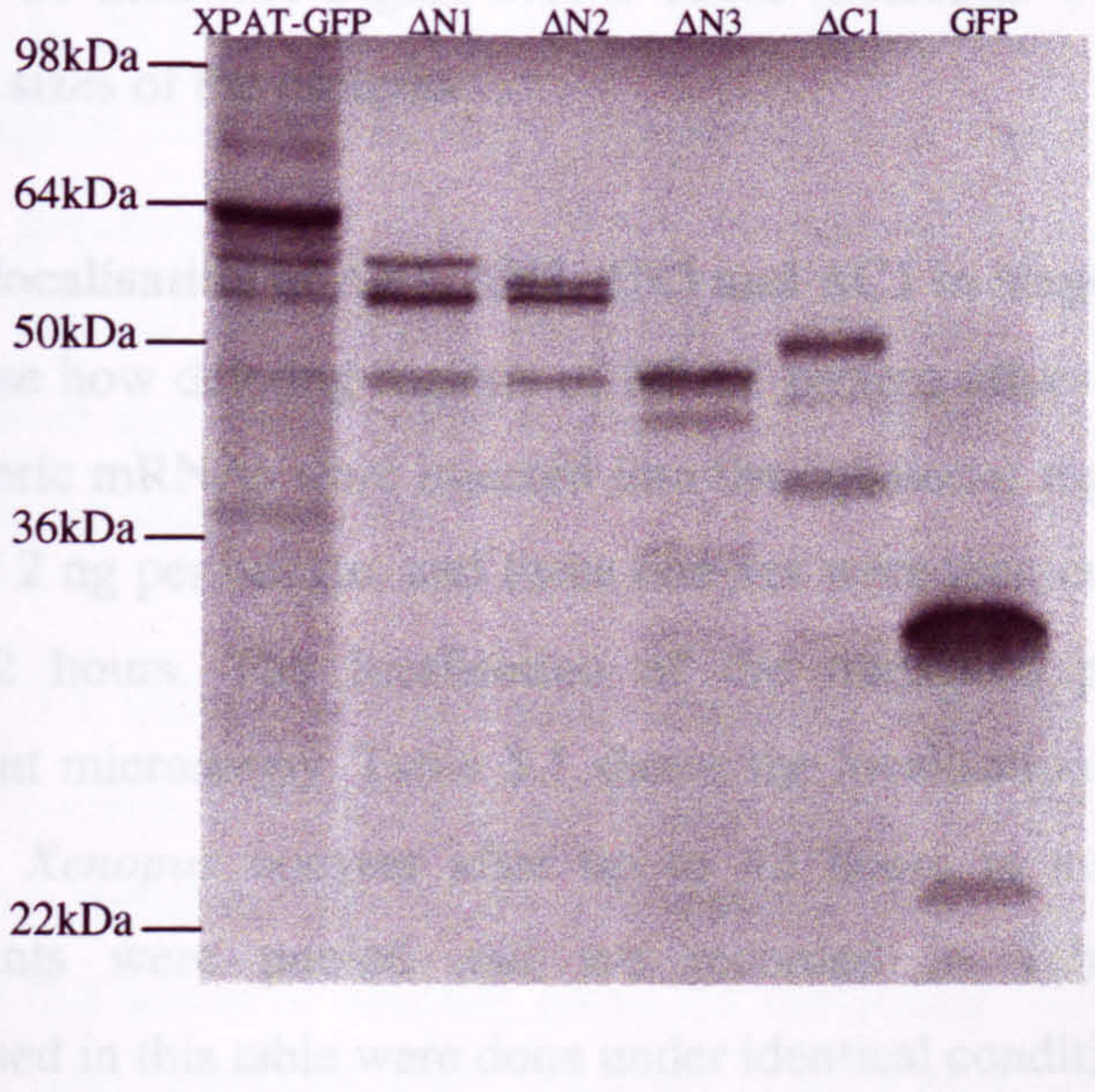

Figure 5.1

(A) Constructs used in this study. In each protein illustrated GFP is shown in green and parts of XPAT are shown in blue. To make XPAT-GFP deletions, XPAT was truncated and GFP fused in-frame. The numbers indicate amino acid residues of XPAT included in each fusion protein.

(B)An autoradiograph of *in vitro* transcription and translation reactions. Coupled *in vitro* transcription and translation reactions were performed using Xpat-GFP, ΔN1, ΔN2, ΔN3, ΔC1 or GFP cDNA as a template in rabbit reticulocyte lysate. 1/10 of each reaction was then resolved by SDS-PAGE and autoradiographed. The size markers are indicated (on left).

In order to check that each deletion construct contained an insert and that the orientation of Xpat was correct in each case, PCR was performed on colonies resulting from each ligation/transformation step. For each deletion construct, only a colony that gave a PCR product of the expected size was subsequently used to prepare DNA from. Once the constructs were made, appropriate restriction digests were performed on the DNA to confirm that each insert was present in the correct orientation (results not shown).

Following restriction digestion, *in vitro* coupled transcription and translation reactions were performed using ΔN1, ΔN2, ΔN3 or ΔC1 DNA as a template. A fraction of each reaction was resolved on a protein gel, alongside translations of both Xpat-GFP and GFP. An autoradiograph of this gel is shown in Figure 5.1B, and indicates that the ΔN deletion constructs have increasingly smaller molecular weights. All are, as expected, smaller in molecular weight than XPAT-GFP (which has an apparent molecular weight of 65 kDa), but larger than GFP (which is 30kDa). ΔN1 has an apparent molecular weight of 59 kDa, ΔN2 of 56 kDa, ΔN3 47.5 kDa and ΔC1 50 kDa (see Figure 5.1B). These molecular weights correspond with the expected sizes of the proteins.

5.3 The localisation of ΔN1, ΔN2, ΔN3 and ΔC1 in stage VI *Xenopus* oocytes

To analyse how deleting regions of XPAT protein affect its subcellular localisation, the chimeric mRNAs were injected into the equatorial region of *Xenopus* oocytes, at a dose of 2 ng per oocyte, and these oocytes were then cultured *in vitro* in OCM for up to 72 hours. The localisation of the translated product was examined by fluorescent microscopy. Table 5.1 shows the localisation of these fusion proteins in stage VI *Xenopus* oocytes after up to 42 hours in culture. The results from 2 experiments were pooled and are recorded in Table 5.1. The experiments summarised in this table were done under identical conditions.

Table 5.1: The expression of deletion variants of XPAT-GFP in *Xenopus* oocytes

	ΔN1	ΔN2	ΔN3	ΔC1	GFP	Xpat-GFP
18 hours	G: 74.4% –=25.3% n=83	G=94.1% –=5.9% n=85	G=90.1% –=9.9% n=91	G=94.6% –=5.4 n=93	G=91.7% –=8.3% n=48	V=13.0% E=60.1% –=26.9% n=238
42 hours	G=66.7% –=33.3% n=43	G=85.3% –=14.7% n=45	G=48.7% –=51.3% n=39	G=94.7% –=5.3% n=38	G=85.7% –=14.3% n=28	V=20.3% E=46.8% –=32.9% n=143

G=general fluorescence, –=no external fluorescence, V=vegetal specific fluorescence, E=equatorial fluorescence, n= number of oocytes scored.

As previously shown, XPAT-GFP protein localised in stage VI *Xenopus* oocytes. On day 1 (18 hours after injection), the fusion protein was expressed principally in an equatorial domain around the point of injection (60.1% of oocytes- Table 5.1). There was diffuse fluorescence in most oocytes (as illustrated in Figure 5.2A) but also some small particles of ~2.5 μm in diameter. 13.0% of oocytes expressed XPAT-GFP in small particles at the vegetal pole and 26.9% of oocytes showed no external fluorescence and were thus scored as negative (Table 5.1). By 42 hours after injection, in 20.3% of oocytes most of the fluorescence was found at, or just lateral to, the vegetal pole. At this stage the fluorescence was mostly particulate, but at the pole the granules were larger. 46.8% of oocytes expressed XPAT-GFP in small particles equatorially around the point of injection and the remaining 32.9% of oocytes were apparently negative. Figure 5.2B shows five oocytes expressing XPAT-GFP 42 hours after injection.

As Table 5.1 shows, 18 hours after equatorial injection of *GFP*, used as a control, 91.7% of oocytes showed a general fluorescence throughout the oocyte. By day 2 (42 hours after injection) this figure had reduced to 85.7%. This reduction is probably related to the health of oocytes, since the remaining 14.3% are apparently negative. As can be seen in Figures 5.2C and 5.2D, control *GFP* mRNA injection into *Xenopus* oocytes resulted in an even and non-localised distribution of GFP fluorescence within the oocyte, and homogeneous signals in the cytoplasm.

As Table 5.1 summarises, stage VI *Xenopus* oocytes appeared generally fluorescent when injected with *ΔN1* (74.7% general after 18 hours in culture). Numbers of oocytes showing general fluorescence reduced slightly to 66.7% after 42 hours in culture but this was again due to oocyte health as the remaining 33.3% were negative, showing no external fluorescence. As a general rule, sick oocytes lose fluorescence, thus appearing negative and then die. Figure 5.2E shows oocytes expressing ΔN1 after 18 hours in culture, the very strong patches of fluorescence visible in the animal pole are likely to be the nuclei inside the oocytes, as they are highly fluorescent (see Section 5.4). By day 2 (42 hours after injection) the fluorescence was very strong, as shown in Figure 5.2F. In some oocytes (~20% of those showing external fluorescence), the fluorescence appeared slightly stronger on the side of the oocyte that had been injected. This was only apparent on day 1, and only obvious in oocytes that expressed ΔN1 less strongly than others, by day 2 when the fluorescence was generally stronger, this was not seen. This is not obvious in the photographs shown in Figure 5.2, as it was quite a difficult phenomenon to capture.

As Table 5.1 shows, 18 hours after equatorial injection of *ΔN2*, 94.1% of oocytes showed general fluorescence, by day 2 this had decreased to 85.3% (due to health of oocytes). The remaining 14.7% were scored as negative on day 2. This fluorescence was evenly distributed throughout the oocyte, like GFP, as shown in Figure 5.2G and Figure 5.2H. Likewise, ΔN3 (Figures 5.2I and J) and ΔC1 (Figures 5.2K and L) were expressed ubiquitously in oocytes. They showed an even and non-localised distribution of fluorescence, which looked identical to GFP expression. As a general rule, oocytes that expressed ΔN3 were less fluorescent than those expressing ΔN1 and ΔN2.

Thus, by external appearance, deletion of between 61 and 159 N-terminal amino acids or 128 C-terminal amino acids of XPAT causes its localisation in *Xenopus* oocytes to be disrupted.

Figure 5.2 (Opposite): Expression of deletion variants of XPAT-GFP and GFP in stage VI *Xenopus* oocytes
Oocytes were each injected with 2 ng of mRNA and were then cultured *in vitro* in OCM at 18°C. 18 hours after injection (day 1) and 42 hours post-injection (day 2), photographs were taken under a fluorescent microscope using a digital camera.

(A) Equatorial localisation of XPAT-GFP in four oocytes 18 hours after injection.

(B) Five oocytes demonstrating localisation of XPAT-GFP after 42 hours in culture. Oocytes arrowed show vegetal expression, whereas other oocytes show equatorial/lateral expression.

(C) General diffuse fluorescence in five oocytes expressing GFP.

(D) Non-localised distribution of fluorescence in oocytes 42 hours after GFP injection.

(E) Five oocytes expressing ΔN1 18 hours after mRNA injection.

(F) 42 hours after injection of *ΔN1* mRNA, five oocytes express ΔN1 in a non-localised distribution.

(G) Five oocytes expressing ΔN2 18 hours after mRNA injection.

(H) 42 hours after injection with *ΔN2* mRNA, four oocytes express ΔN2 in a general, non-localised manner.

(I) Six oocytes express ΔN3 18 hours after mRNA injection.

(J) Four oocytes show fluorescent expression of ΔN3 42 hours after mRNA injection. Some oocytes (such as the one arrowed) were scored as negative since they exhibited no external fluorescence.

(K) Six oocytes 18 hours after *ΔC1* mRNA injection exhibit general distribution of ΔC1.

(L) Six oocytes expressing ΔC1 after 42 hours *in vitro*.

Each oocyte shown is ~1.2 mm in diameter.

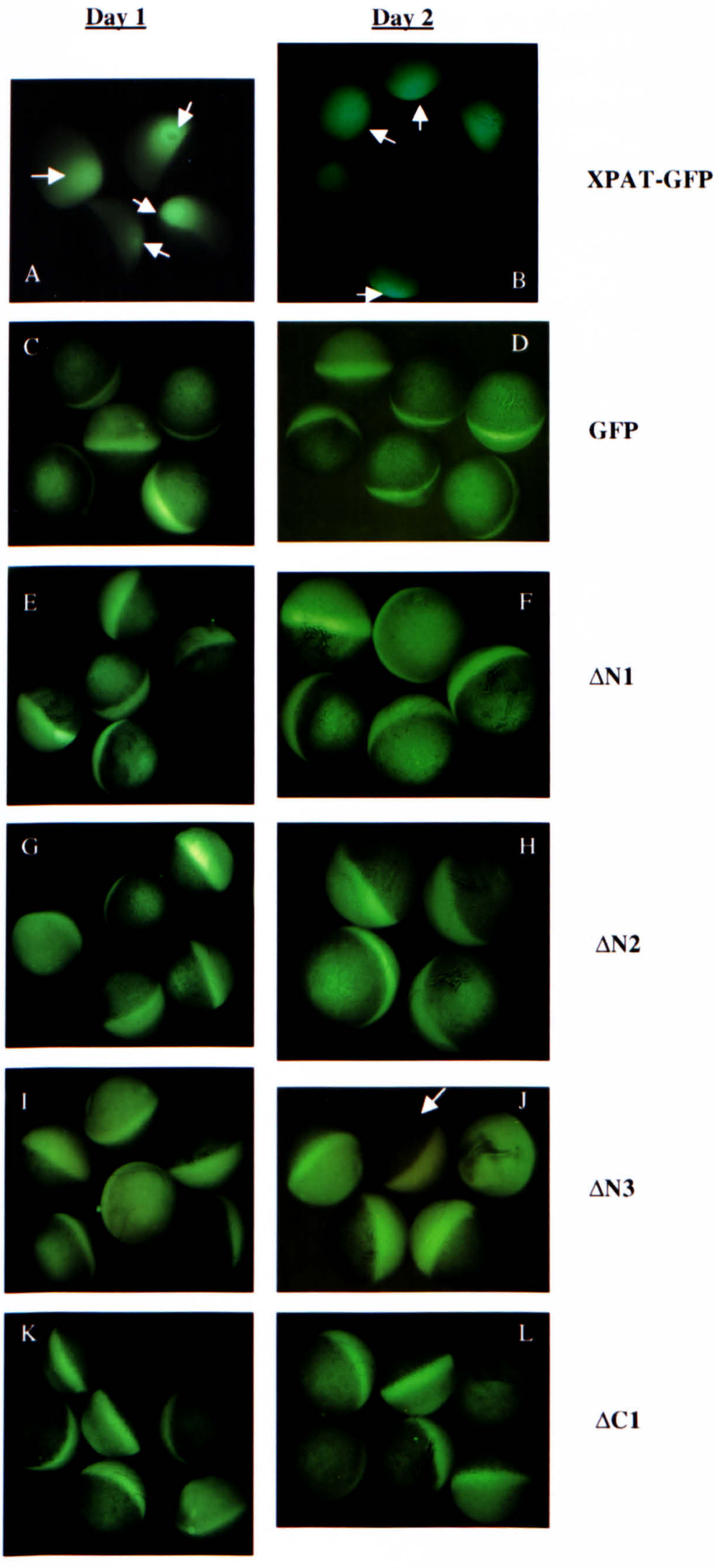
Day 1
Day 2
A
B
XPAT-GFP
C
D
GFP
E
F
ΔN1
G
H
ΔN2
I
J
ΔN3
K
L
ΔC1

In order to gain a better perception as to whether ΔN1, ΔN2, ΔN3 or ΔC1 proteins formed particles which were not easily visible under low magnifications, a higher magnification was used to view oocytes after 42 hours in culture (Figure 5.3). Figure 5.3F shows a higher magnification view of the vegetal region localisation of XPAT-GFP protein after 42 hours in culture. This photograph clearly shows small punctate spots of XPAT-GFP protein aggregating into larger granular structures.

Figure 5.3A shows a high power view of the fluorescence seen in an oocyte expressing ΔN1. This figure clearly shows that ΔN1 is not expressed in granules in this oocyte, and this is true of 95.2% of those oocytes fluorescing, it is expressed in a diffuse manner. However, in a small number of oocytes expressing ΔN1 (4.8% of those with external fluorescence) a small projection of cytoplasm could be seen at the injection site on the equator. In this small protrusion, small punctate fluorescent particles of ΔN1 could be seen (Figure 5.3B shows one such oocyte). Such projections would trap the injected mRNA and prevent movement of its product to the interior of the oocyte. Thus, although not normally apparent on the surface of the majority of oocytes, ΔN1 was expressed in tiny particles (of ~1 μm diameter). At no time were any larger granules seen, certainly none of the same size (10-50 μm diameter) as XPAT-GFP granules. Thus, ΔN1 can form particles, but these do not seem to show cortical anchoring.

Figure 5.3C shows a high power view of an oocyte expressing ΔN2. This figure shows that ΔN2 is not expressed in particles or granules and its fluorescence is evenly distributed throughout the oocyte.

Figure 5.3D is a high magnification view of an oocyte expressing ΔN3. This photograph clearly shows that ΔN3 fluorescence is diffuse, even and non-localised. Thus, ΔN3 does not localise or form particles in stage VI *Xenopus* oocytes. The same is true of ΔC1 (Figure 5.3E).

Figure 5.3 (Opposite): To illustrate the diffuse nature of ΔN1, ΔN2, ΔN3 and ΔC1 fluorescence in stage VI *Xenopus* oocytes
Stage VI *Xenopus* oocytes were each injected with 2 ng of mRNA and cultured *in vitro* in OCM at 18°C. 42 hours after injection, oocytes were viewed under a fluorescent microscope at high magnification. These photographs illustrate the diffuse nature of the fluorescent expression. In each photograph the original magnification was x10 and the scale bar represents 100 μm.

(A) A typical ΔN1 oocyte expressing ΔN1 in a diffuse, non-granular pattern.

(B) An example of one of the 4.8% of fluorescent oocytes expressing ΔN1 that had small protrusions of cytoplasm visible near to the equator at the site of injection. In this projection small particles of ΔN1 can be clearly seen.

(C) An oocyte expressing ΔN2, no particles are visible in the cytoplasm as the fluorescence is totally diffuse.

(D) An oocyte injected with ΔN3. The fluorescence is diffuse and no particles are visible in the oocyte's cytoplasm.

(E) View of an oocyte expressing ΔC1. ΔC1 does not form granules and thus the fluorescence is diffuse.

(F) An oocyte expressing particles and small granules of XPAT-GFP in a localised domain at the vegetal pole.

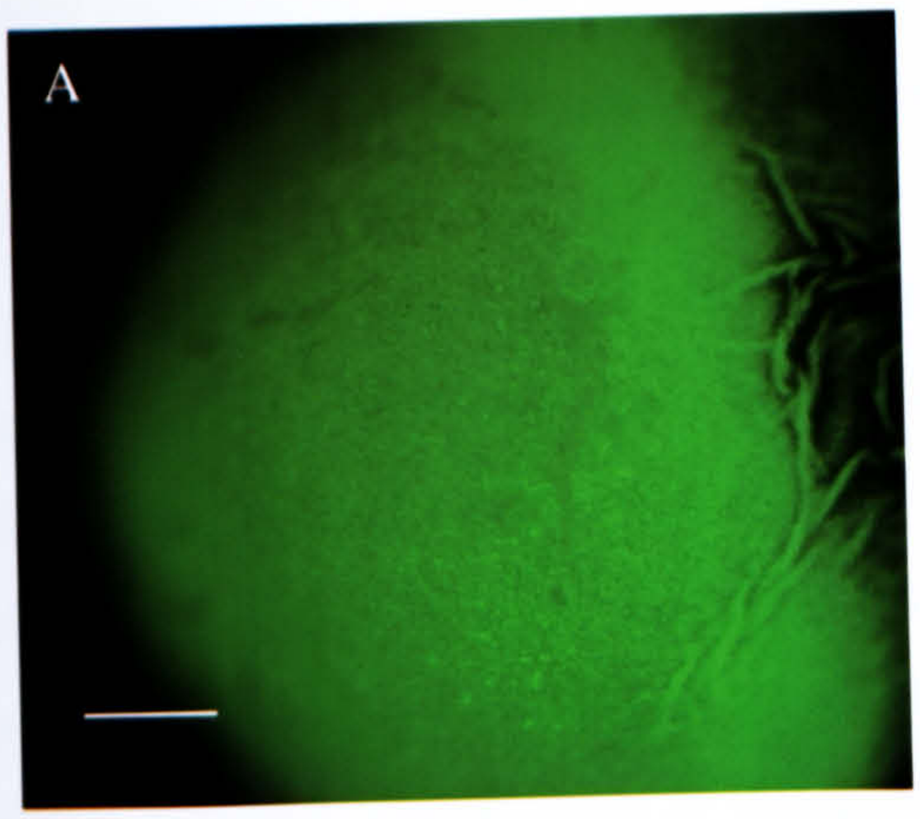
A

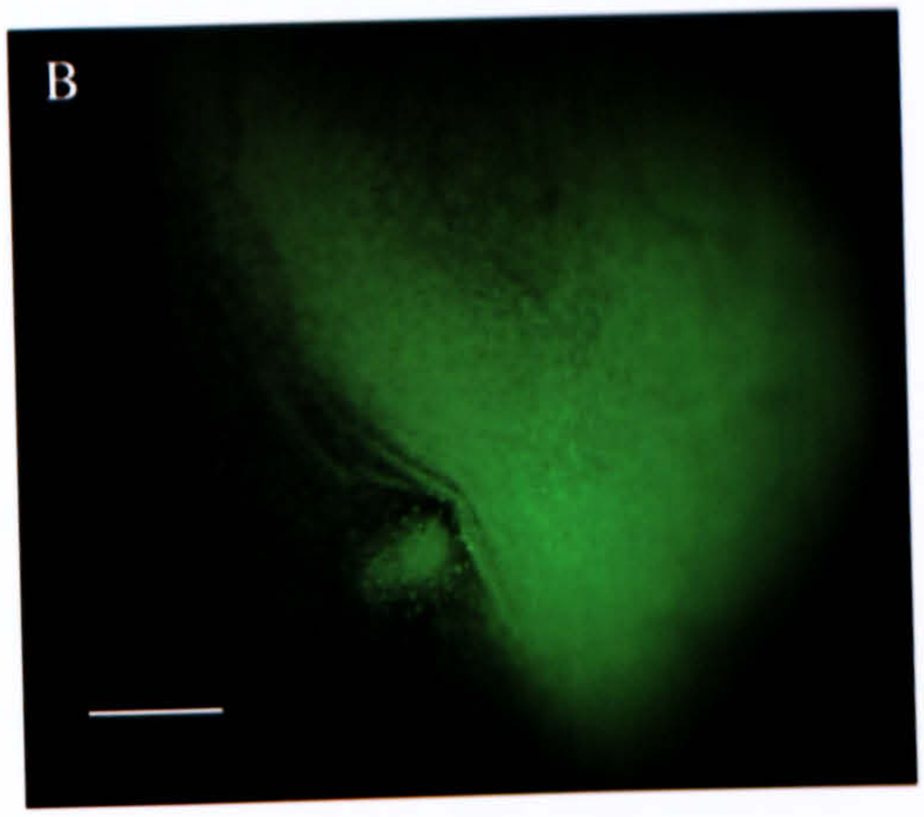
B

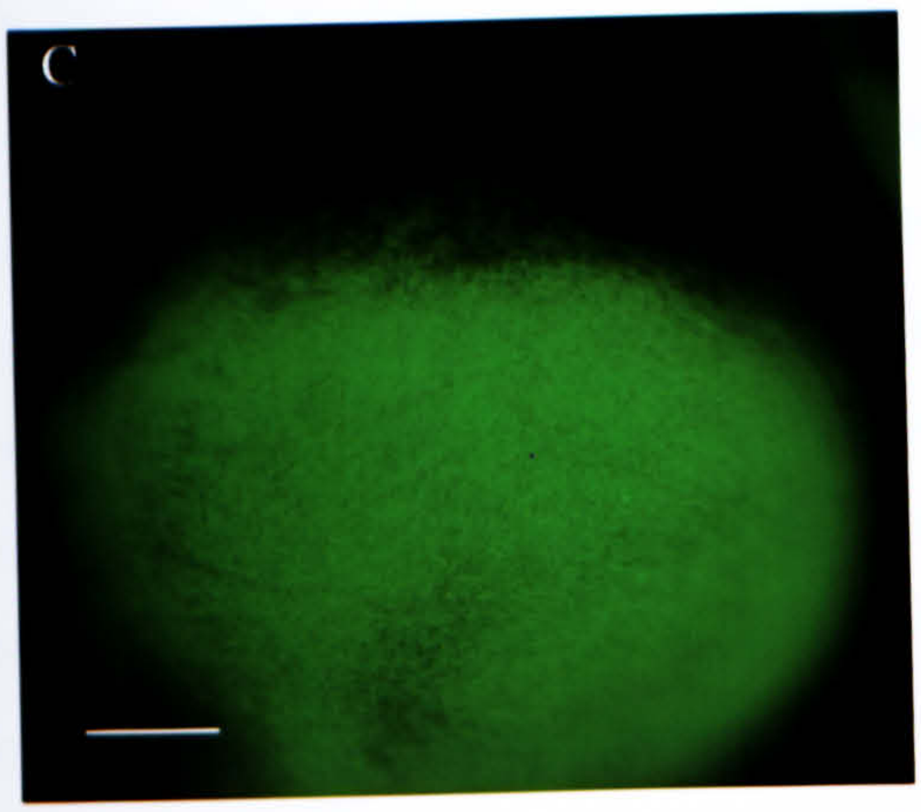
C

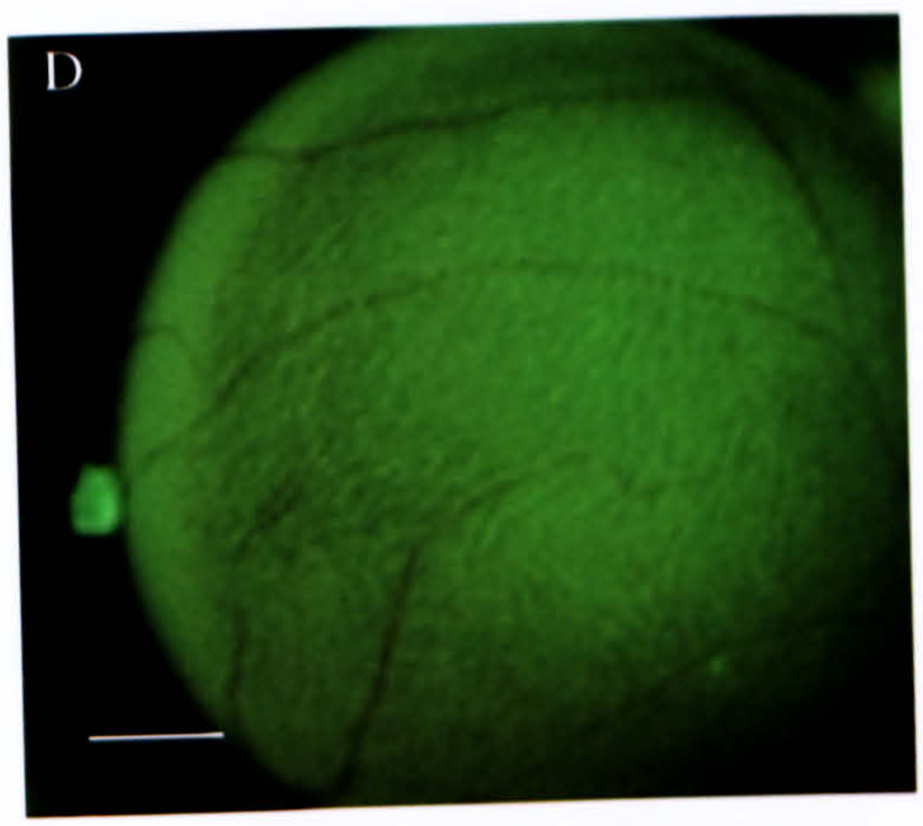
D

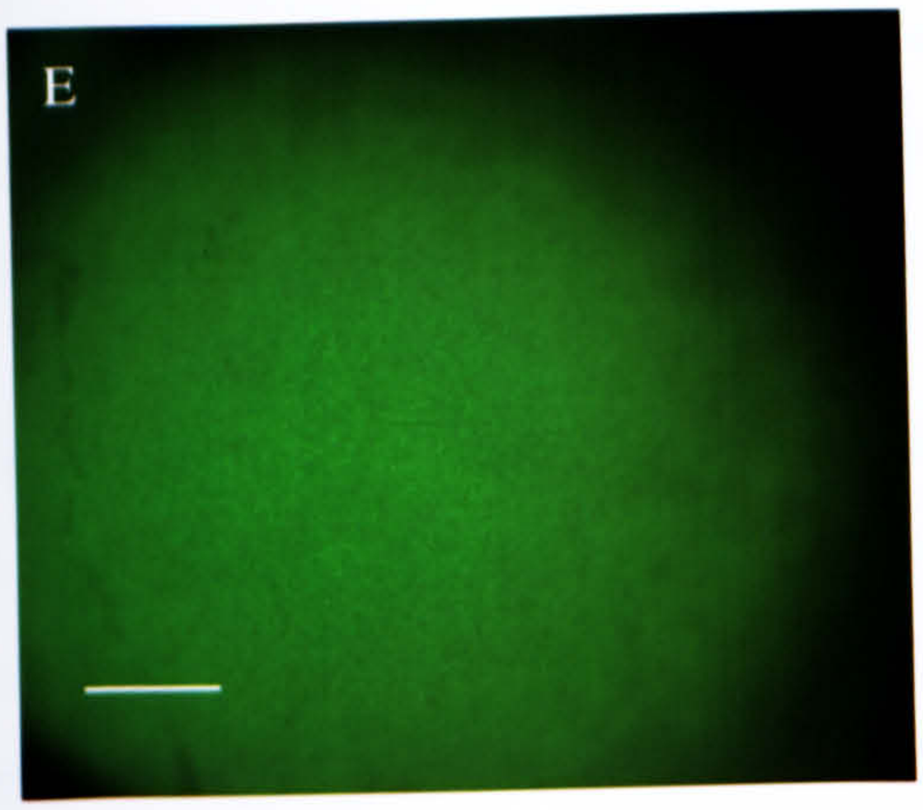
E

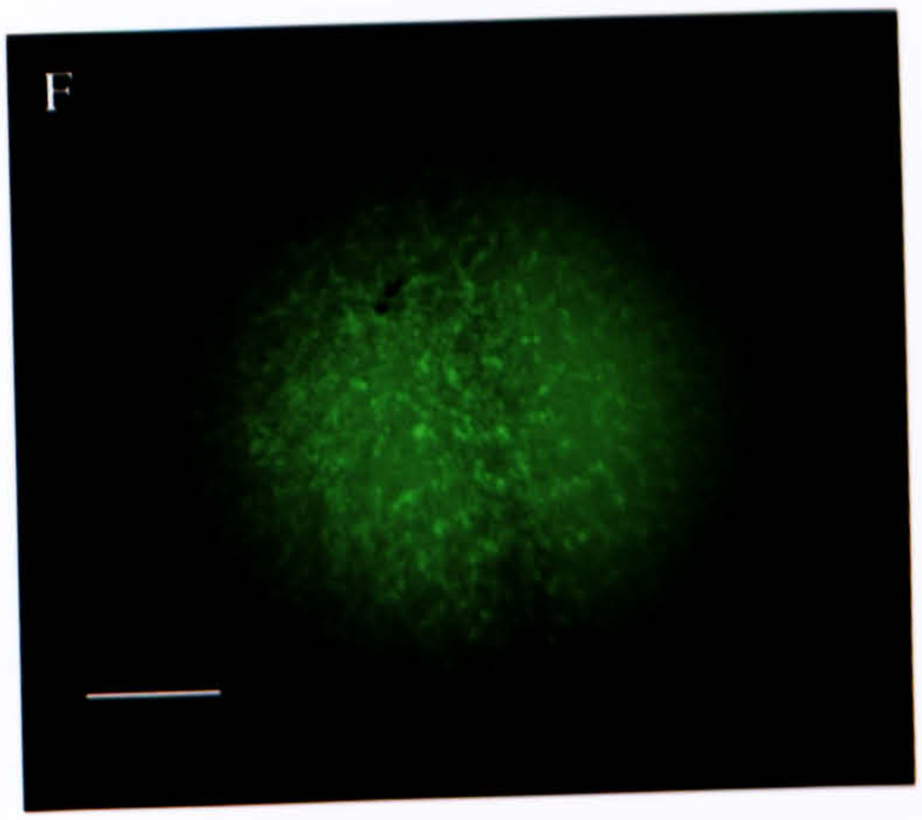
F

5.4 The nuclear localisation of ΔN1, ΔN2, ΔN3 and ΔC1

To determine whether *ΔN1*, *ΔN2*, *ΔN3* or *ΔC1*-injected oocytes contained any internal particles or granules and to see if their nuclei were fluorescent, oocytes that had been cultured for 42 hours *in vitro* were fixed by heating to 75-85°C in Barth's saline for 30 seconds and then cut open using a scalpel. Figure 5.4A depicts an oocyte that expressed ΔN1 and was bisected, the nucleus was fluorescent, as was the area immediately surrounding it. However, the rest of the oocyte was not. Figure 5.4B shows an oocyte that expressed ΔN2 and was bisected. It can be seen that the nucleus was highly fluorescent but the rest of the oocyte was not, thus the nucleus contained the majority of ΔN2. Figure 5.4C illustrates an oocyte that expressed ΔN3 and was bisected. The nucleus of this oocyte is highly fluorescent and thus contains ΔN3, but the rest of the oocyte is negative. Figure 5.4D is a photograph of a bisected oocyte expressing ΔC1. This oocyte is highly fluorescent throughout its cytoplasm and also in the nucleus. Thus, the entire oocyte is expressing ΔC at high levels, and the nucleus also contains high levels of fusion protein. None of the deletion proteins formed granules inside oocytes. The yolk concentration has an effect on the distribution of proteins in oocytes. There is a gradient of yolk from the vegetal to the animal pole in oocytes, the highest concentration being present in the vegetal hemisphere. Yolk excludes soluble proteins, thus GFP (see Figure 3.5) and ΔC1 (Figure 5.4D) fluorescence appears slightly more concentrated at the animal pole than at the vegetal pole when oocytes are cut open. Similarly, there is no yolk in the nucleus, thus ΔC1 appears to be expressed slightly more strongly there than in the rest of the animal pole.

After three days in culture, the majority of oocytes that had been injected with *ΔN1*, *ΔN2* or *ΔN3* showed no external fluorescence (that is would be scored as negative). It was thus decided to determine whether the GFP fusion proteins were still present or were no longer being translated. One possible explanation for the large numbers of apparently negative oocytes was that all of the fluorescence was actually present in the nucleus. The results shown in Figures 5.4 A to C (bisection of oocytes expressing ΔN1, ΔN2 or ΔN3) indicate this is true. To quantify what was occurring, nuclei were removed from several oocytes that had been injected with *ΔN1*, *ΔN2* or *ΔN3* and yet appeared negative. All nuclei removed were positive for fluorescence and thus

Figure 5.4 (Opposite): To determine where deletion variants of XPAT-GFP localise within *Xenopus* oocytes following microinjection of mRNA
Stage VI *Xenopus* oocytes were injected with *ΔN1*, *ΔN2*, *ΔN3* or *ΔC1* mRNA and cultured *in vitro* in OCM for 42 hours. Some oocytes were fixed and bisected in order to determine whether any fluorescence was visible inside the oocyte (A, B, C and D). The nuclei from other oocytes were removed (E, F, G and H) to ascertain whether the nuclei contained fusion protein.

(A) An oocyte with no visible external fluorescence that had been injected with *ΔN1*. After bisection, fluorescence is clearly visible in and around the nucleus.

(B) ΔN2 is expressed in the nucleus of an oocyte that appeared negative prior to dissection.

(C) An oocyte injected with *ΔN3* contains fusion protein in its nucleus.

(D) An oocyte injected with *ΔC1* mRNA expressed ΔC1 throughout its cytoplasm and also contains fusion protein in its nucleus.

(E) An oocyte expressing ΔN1 that has had its nucleus removed. This photograph is a dual exposure of white light and UV and shows that the nucleus is highly fluorescent.

(F) An oocyte injected with ΔN2 that has had its nucleus removed. The nucleus is highly fluorescent (photograph is a dual exposure of UV and white light).

(G) An oocyte expressing ΔN3 that has had its nucleus removed. Again, the nucleus contains fusion protein.

(H) An oocyte expressing ΔC1 that appears generally fluorescent externally. Nuclear removal shows that the nucleus also contains ΔC1.

Each oocyte shown is ~1.2 mm in diameter.

ΔN1

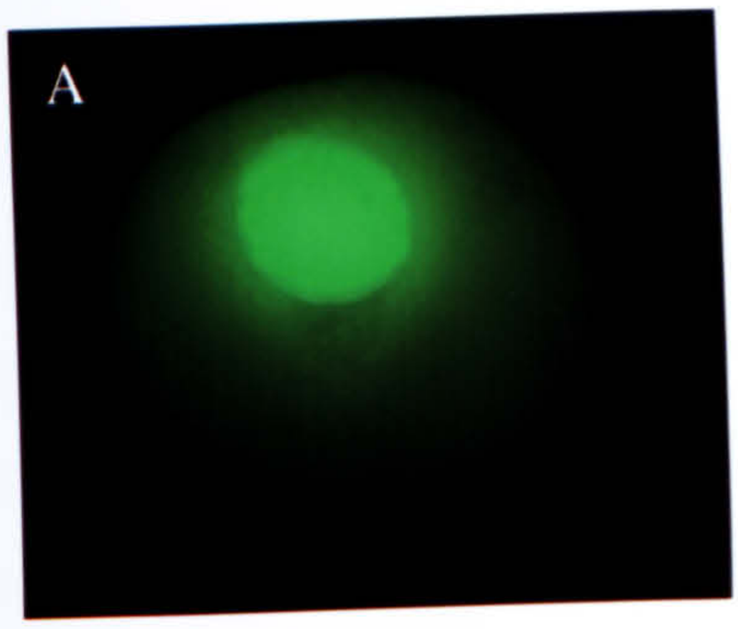

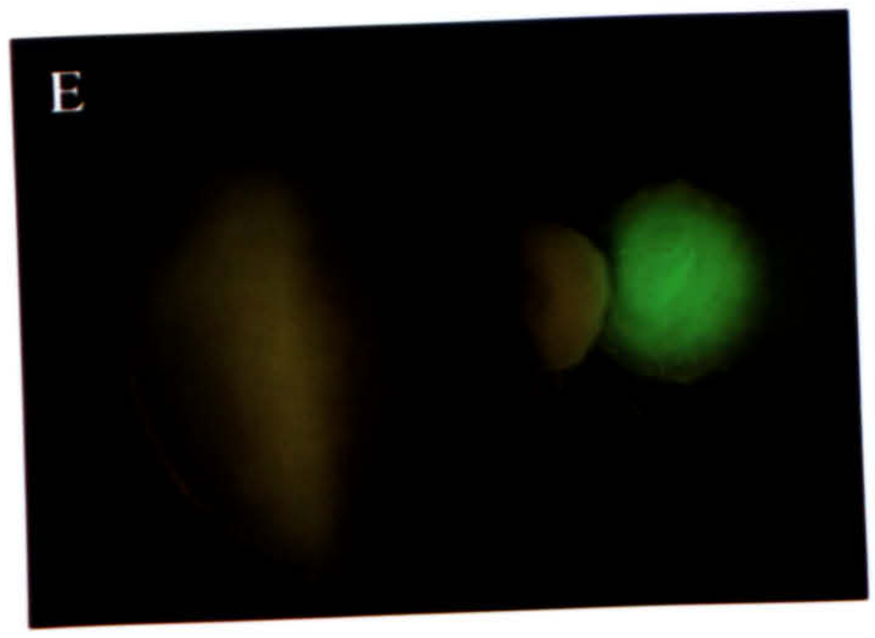

ΔN2

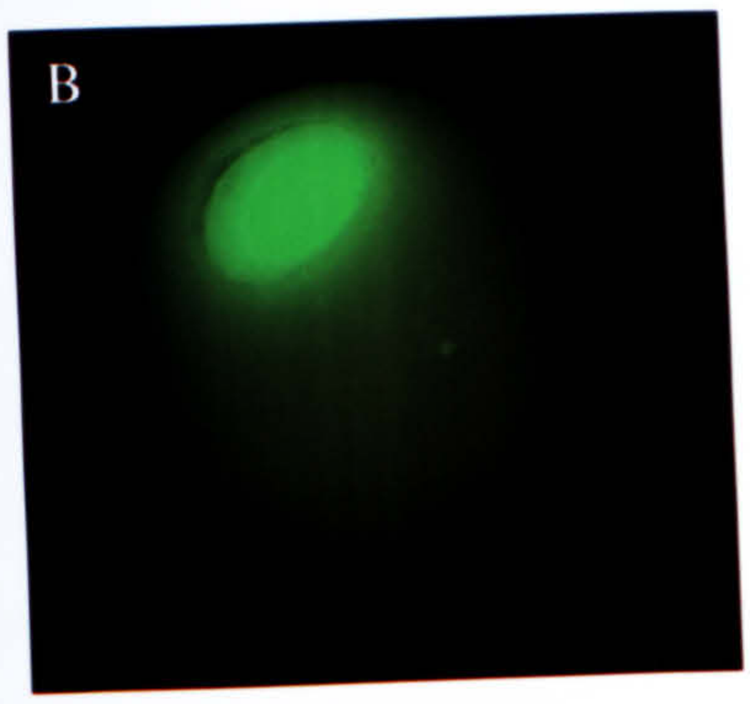

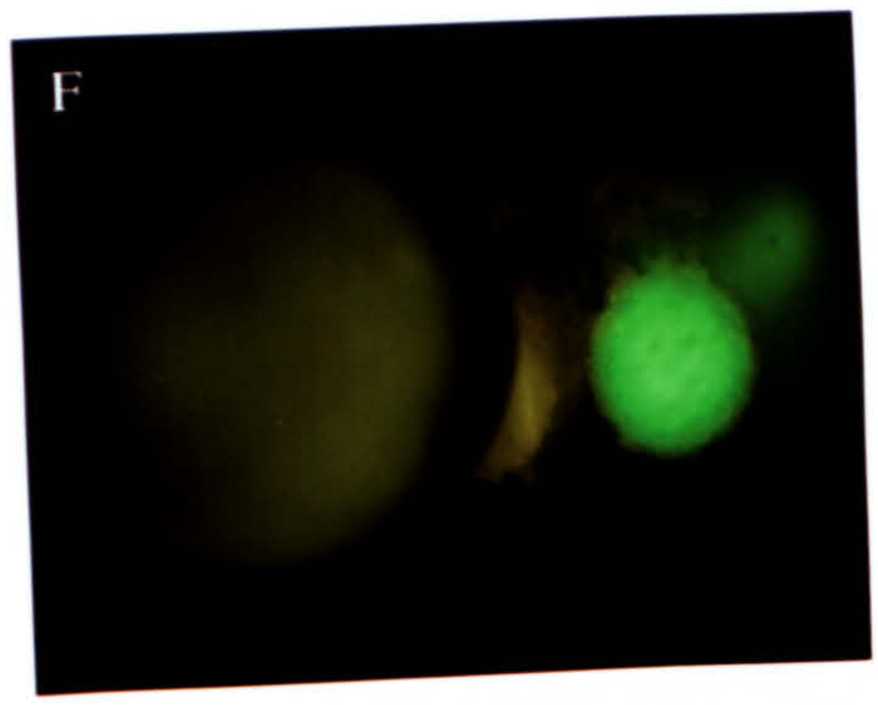

ΔN3

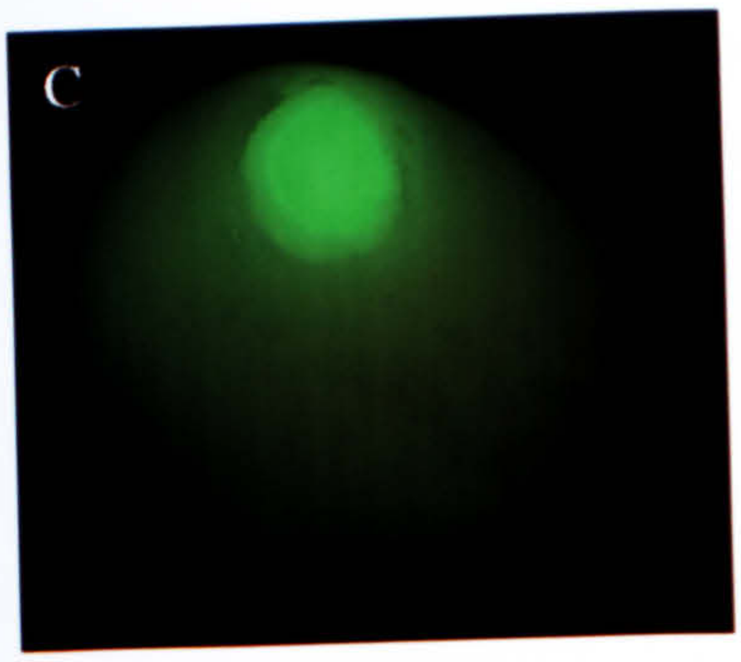

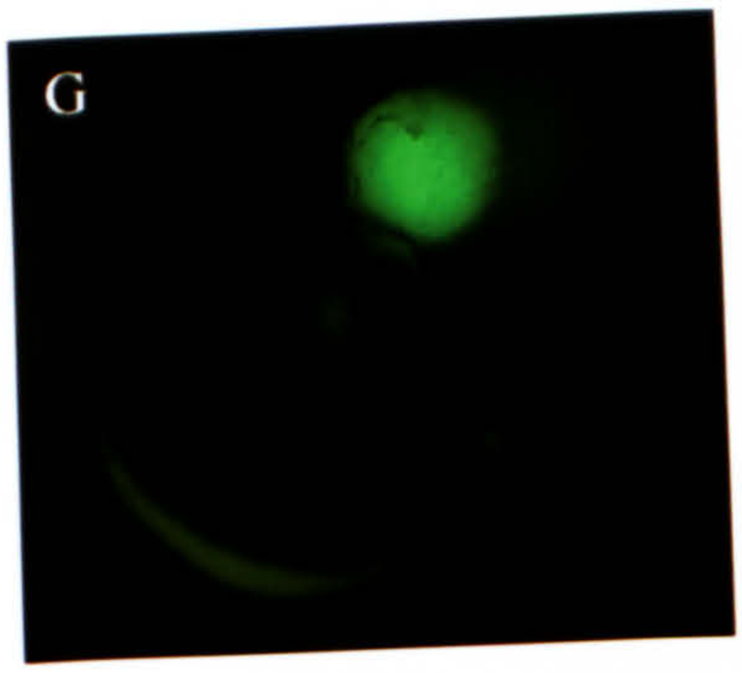

ΔC1

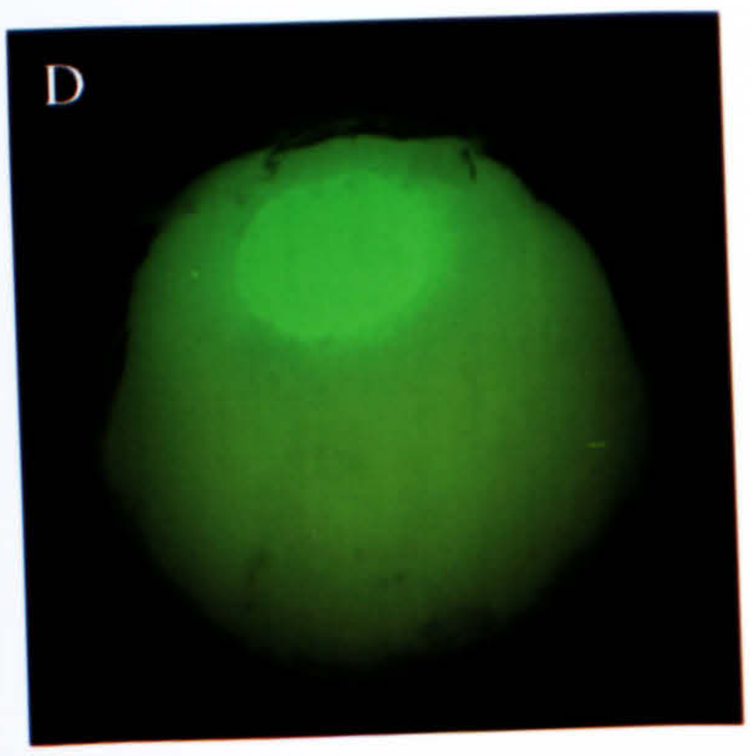

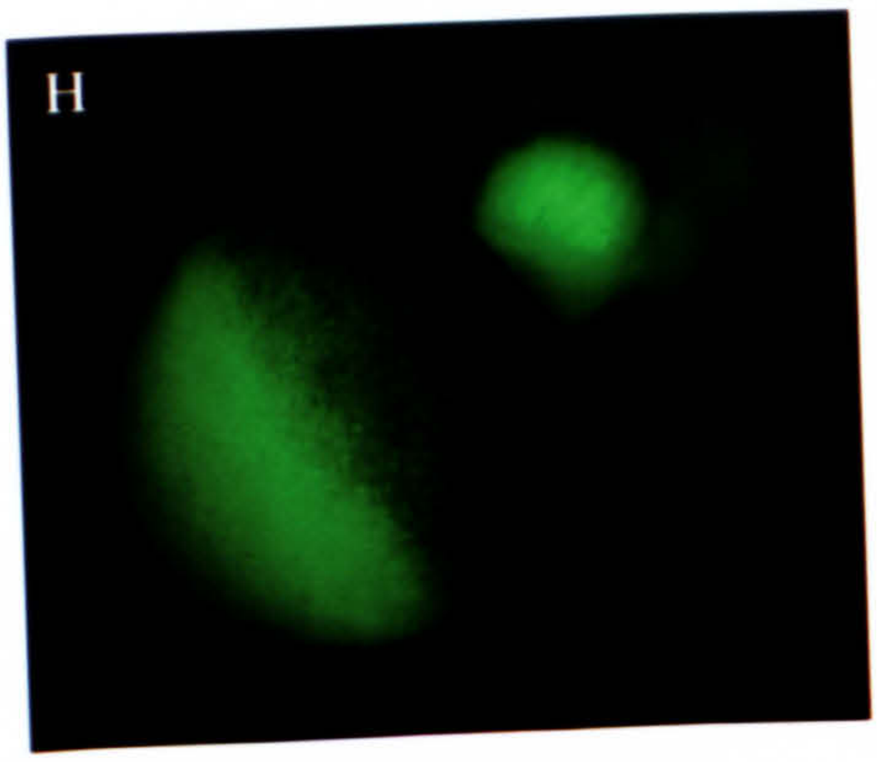

contained GFP fusion protein (as shown in Figures 5.4E to G). In total, 5/5 nuclei from superficially negative *ΔN1*-, 5/5 nuclei from superficially negative *ΔN2*- and 5/5 nuclei from superficially negative *ΔN3*-injected oocytes were fluorescent. After 3 days in culture, the majority of oocytes that had been injected with *ΔC1* still appeared externally generally fluorescent. The nuclei were removed from five oocytes that expressed ΔC1 and all five were fluorescent. Figure 5.4H shows the nucleus from one of these oocytes. By observation, it appeared that the nuclei removed from ΔC1-expressing oocytes were less strongly fluorescent than the nuclei of oocytes injected with *ΔN1*.

5.5 To show the subcellular localisation of ΔN3 and ΔC1 by *in vivo* radiolabelling

It was decided to use a more quantitative approach to investigate the localisation of ΔN3 and ΔC1 within *Xenopus* oocytes. ΔN3 and ΔC1 were chosen since they are deletions of opposite ends of XPAT protein and have only a six amino acid region in common. To this end, stage VI *Xenopus* oocytes were injected with 20 ng of *ΔC1, ΔN3, Xpat-GFP* or *Xpat* mRNA. The oocytes were then cultured overnight at 18°C in the presence of ^{35}S-methionine. This is taken up by oocytes and radiolabels all newly translated proteins. The following day, nuclei were removed from some of these oocytes and homogenised (N fraction) and the remaining cytoplasm and membranes were homogenised and centrifuged to give a cytosol (soluble, Cs) fraction and a cytoplasm insoluble (pellet, Ci) fraction. Particles would be expected to enter the Ci fraction. Some oocytes were homogenised whole to give an oocyte total protein (T) sample.

These fractions were then resolved on an acrylamide gel, alongside control (uninjected) oocyte fractions that were prepared in the same way. The gels were then autoradiographed. An extra protein band (of expected size) was seen in fractions from each of the injected oocyte samples when compared with control oocyte fractions. Figure 5.5 shows autoradiographs of these protein gels.

Figure 5.5: To determine the subcellular localisation of ΔN3 and ΔC1 by *in vivo* radiolabelling.

Stage VI *Xenopus* oocytes were injected with 20ng of *Xpat-GFP, ΔN3, ΔC1* or *Xpat* mRNA, or left uninjected. They were cultured over-night in the presence of ^{35}S-methionine. The following day, oocytes were homogenised to give a Total protein sample (T), nuclei were removed from oocytes to give a nuclei (N) fraction. The remaining membranes and cytoplasm were homogenised and centrifuged (13K rpm, 5 minutes) to give a cytosol soluble fraction (Cs) and a pellet of insoluble cytoplasm (Ci). These fractions were resolved by SDS-PAGE. On each gel all 4 control (uninjected) oocyte samples were run alongside 4 fractions from one of the injected oocytes. Gels were then autoradiographed and these autoradiographs are shown: (A) XPAT-GFP, (B) ΔN3, (C) ΔC1 (D) XPAT. Size markers are shown on the left hand side (sizes in kDa). The letters above each gel indicate which sample was loaded.

As previously shown (Section 3.4) XPAT-GFP (65 kDa) is seen in all fractions, but it is a faint band in the nucleus and the soluble fraction of the cytosol, whereas the majority of the protein is seen in the cytoplasm insoluble fraction (Figure 5.5A). As Figure 5.5B shows, ΔN3 (47.5 kDa) is found in the nuclear and cytosolic soluble fractions of the oocyte but is not seen in the cytoplasmic insoluble fraction thus it does not form granules. The ΔN3 band is strongest in the nuclear fraction, which corresponds to its fluorescent localisation (Figure 5.4C). ΔC1 (50 kDa) is present mainly in the cytosolic soluble and nuclear fractions, but is stronger in cytosolic fraction (Figure 5.5C), which indicates that ΔC1 is not localised or forming (insoluble) granules – again similar to the fluorescence data. Thus, ΔN3 is present in the nucleus to a greater extent than ΔC1, XPAT-GFP or XPAT. This closely resembles fluorescence data (Figure 5.4) and indicates that the C-terminus of XPAT contains a nuclear localisation domain. The localisation of ΔC1 resembles the expression pattern shown, using this method, by XPAT (although not XPAT-GFP, see Section 3.4), which is presented again in Figure 5.5D. These results suggest that nuclear entry is opposed by particle formation and/or anchoring. The domains of XPAT that cause particle formation, but not particle anchoring, are likely to be found in the N-terminal portion of XPAT protein. However, this is not true of the vegetal localisation domains since ΔC1 does not localise to the vegetal pole, unlike XPAT-GFP.

5.6 XPAT contains a putative NLS

Xpat is a novel gene that encodes a 35 kDa protein with no known homologies. Although XPAT has no homology to any proteins, particular domains are of note. Figure 5.6 shows the amino acid sequence of XPAT; in this figure, basic and acidic residues are highlighted. The carboxyl terminal region of XPAT protein is rich in basic residues; indeed 15/53 amino acids at the C-terminus are basic. A basic region is a common characteristic of nuclear proteins such as transcription factors and histones, which bind to DNA. In the amino terminal half, XPAT contains a high number of acidic residues (aspartic acid and glutamic acid).

Figure 5.6: XPAT contains a putative NLS

```
MALKAEDSFD  IYSQLIQSFC  RYAENTTVSE  SQSPAFNAQK  EFQTCQDHAC  CTHSEAHTHI  60
LMQQWQLLEE  QWEYIDHLKT  DVAALKQLLH  GFMNSLSGTD  SGMEGTNHFL  PPHQNPTLLK  120
DEEIVASALN  RPSVDINGFE  ENITTGAQIH  AAFTKSPKKM  PATSTPRKSE  VLWSCSPTLA  180
TDGYFMLPDI  ILNPLDGKKL  VSMLRSSNYE  PHRFAELLFQ  HHVPHSLFQL  WANKVNFDGS  240
RGKLGLPRNL  MIDILHQTSK  RFVLGPKEKR  KIKTRLNLLL  RTRQDRAWWD  VGL
```

The amino acid sequence of XPAT. XPAT contains a predicted putative bipartite NLS (blocked). Basic residues are highlighted in green, acidic residues in red, and leucine residues in blue. The C-terminal portion of XPAT is particularly rich in basic residues, which is a common feature of nuclear proteins. In contrast, the N-terminal region contains multiple acidic residues.

Experiments with GFP-tagged XPAT indicate that XPAT protein could naturally be a nuclear protein. In particular, the ΔN proteins, which all lack the N-terminal region of XPAT protein, are localised specifically to the nucleus suggesting that XPAT contains a NLS in its carboxy-terminal portion. This is supported by sequence data (Figure 5.6), as XPAT contains a putative bipartite NLS in its C-terminal half. XPAT's putative NLS has features common to proven nuclear targeting sequences; these are typically short, generally less than 12 amino acids long, and contain one or two essential clusters of basic amino acids (Dingwall *et al.*, 1982; Robbins *et al.*, 1991; Dingwall and Laskey, 1991). These structural and localisation features suggest that XPAT is a nuclear component, possibly functioning in germ plasm-specific transcriptional regulation. This hypothesis is further supported by *in vitro* binding assays (Chapter 6), which indicate that both XPAT and XPAT-GFP bind dsDNA.

In contrast to the ΔN proteins, ΔC1 protein, which lacks the carboxy-terminal region of XPAT protein, is present in both the cytoplasm and the nucleus of *Xenopus* oocytes. This suggests that XPAT might contain a Nuclear Export Sequence (NES) in its amino-terminal half, in addition to an NLS in its carboxy-terminal half. NES motifs are typically leucine-rich and have a consensus sequence of LXLX(X)LXXLXL/I (Nakielny and Dreyfuss, 1997; Feng *et al.*, 1999). Whilst XPAT protein is very leucine-rich (35 out of its 293 amino acids are leucines - highlighted in blue in Figure 5.6), there is no obvious NES consensus sequence in its amino terminal half, or indeed anywhere in the protein.

5.7 Discussion

XPAT contains a putative bipartite NLS sequence in its carboxyl terminal half. It is also rich in basic residues, particularly in its carboxyl terminus, which is a common feature of nuclear proteins. Several large N-terminal deletions and one C-terminal deletion of XPAT protein were made to investigate possible XPAT domain structure. The C-terminal deletion protein, which lacked the putative NLS, was evenly distributed throughout the nucleus and cytoplasm. The N-terminal deletions became predominantly localised to the nucleus. None showed vegetal transport or granule formation, but 4.8 % of ΔN1 expressing oocytes, which had a small protrusion of cytoplasm at the injection site, contained small particles (1-2 μm). Thus, particles can form with a small N-terminal deletion, but ΔN1 cannot form larger granules or be transported to the vegetal pole. These two processes might therefore be coupled. One hypothesis is that ΔN1 forms particles in protrusions because they cannot enter the nucleus. In the cytoplasm, particulate material gradually enters the nucleus (XPAT-GFP; see Section 3.3.3), but nuclei only contain soluble proteins. These observations suggest that nuclear entry is opposed by particle formation and/or anchoring, i.e.:

Particle ↔ soluble protein → nucleus

If ΔN1 particles were less stable than those of wild-type XPAT this might account for the progressive movement of fluorescence to the nucleus. It will be interesting to perform oocyte enucleation experiments with ΔN1 to assess where ΔN1 protein will localise if nuclear entry is abrogated.

These results indicate that XPAT is not composed of totally independent domains and suggest that both the N-terminal and C-terminal regions of XPAT are required for its stable localisation to the vegetal pole. These data emphasise that nuclear entry is opposed by binding to cytoplasmic components, most likely microtubules, and possibly microfilaments. The ΔN deletion proteins presumably have enhanced nuclear localisation due to less cytoplasmic binding activity. These structural features, when taken in context with the localisation of wild-type XPAT, which also enters the nucleus, suggest that XPAT may be a nuclear component of *Xenopus* oocytes or PGCs.

It is possible that the N-terminus and the C-terminus of XPAT are located spatially close to each other and form a microtubule- or microtubule-associated protein-binding surface. The finding that the deletion of either the N-terminus or the C-terminus affects localisation to the vegetal pole may also suggest that the stable localisation of XPAT to the vegetal pole requires optimal binding activity to microtubules or multiple interactions with cytoskeletal structures. Possibly there could be a microtubule and also a microfilament binding sequence in different parts of the protein. It could be that the overall conformation is affected. Particle formation may involve intermediate filaments or non-cytoskeleton protein(s).

ΔC1 protein is less concentrated in the nuclei of oocytes than any of the ΔN proteins. Cytoplasmic fluorescence and localisation as determined by *in vivo* radiolabelling experiments indicate that ΔC1 is very strongly localised in the cytoplasm, much more so than any of the ΔN proteins. This implies that ΔC1 may enter the nucleus passively, whereas the ΔNs could be directed into the nuclei of *Xenopus* oocytes using XPAT's putative nuclear localisation signal. Another possibility is that ΔC1 could contain a nuclear export signal so it is pushed back out into the cytosol, although no consensus NES has been found anywhere in XPAT.

Chapter 6: Functional studies with XPAT Part 1: RNA binding assays

6.1 Introduction

The common theme amongst germ plasm proteins and those encoded by germ plasm mRNAs is actual or postulated RNA-binding properties. For example, Xdazl contains an RNP domain implying an RNA-binding function and has subsequently been shown to function as an RNA-binding protein *in vitro* (Houston *et al.*, 1998). Despite lack of homology to other RNA binding proteins, it was decided to do some preliminary experiments to determine whether XPAT could bind RNAs.

Since potential *in vivo* RNA targets of XPAT are unknown, it was decided to test whether XPAT could function as an RNA-binding protein *in vitro* by using homopolymeric RNAs bound to beads. This assay has been used to characterise the RNA-binding properties of a variety of proteins (Swanson and Dreyfuss, 1988; Siomi *et al.*, 1993). In order to do this, it was first necessary to clone the Xpat ORF into a vector which could be used to generate *Xpat* mRNA for use in *in vitro* translation reactions and also further experiments described in Chapter 7.

6.2 The cloning of Xpat into a transcription vector

In order to clone Xpat into a vector to enable its transcription, the ORF of Xpat was amplified from a cDNA library clone by PCR using primers that created 5′ and 3′ *Hind*III sites. The resulting PCR fragment was cloned into the *Hind*III site of pSPJC2L. Following ligation and transformation into DH5α cells, colony PCR was performed using a vector-specific upstream primer (SP6) and an insert-specific downstream primer. This was in order to determine whether Xpat had inserted into the vector and check its orientation in the vector was correct. Once the construct was made, restriction digests were performed on the DNA to confirm the orientation of the insert. The miniprep DNA was then sequenced on both strands to check whether any PCR-induced mutations had occurred. The sequence of this clone matched that of the cDNA library clone. Thus, *in vitro* coupled transcription and translation reactions were performed using Xpat DNA as a template. A fraction of this reaction was then resolved on a protein gel; this showed that XPAT had an apparent molecular weight of 35kDa, as expected (results not shown).

6.3 RNA binding properties of XPAT

In order to test whether XPAT could function as an RNA-binding protein *in vitro*, an assay using homopolymeric RNAs bound to beads was used. This is the conventional approach to test RNA binding proteins (Swanson and Dreyfuss, 1988). To test the specificity of the assay, Xdazl was included as a positive control. Xdazl was previously shown to bind primarily to poly(G) and poly(U) at 100 mM NaCl and also weakly bind to poly(A) RNA sequences in the homopolymer assay (Houston *et al.*, 1998). Xdazl behaved accordingly in experiments conducted at the same time as XPAT (Figure 6.1A), which were all performed in binding buffer at moderately high salt concentration (1 M NaCl). Xdazl was also seen to bind dsDNA in this assay. β-galactosidase was included as a negative control for the assay (Figure 6.1B), and bound none of the homopolymeric RNAs or dsDNA. These assays were originally attempted using binding buffer containing a lower salt concentration (100 mM NaCl), however, non-specific binding to Sepharose 4B control beads was observed for both Xdazl and XPAT (data not shown). Thus, more stringent conditions were used (1 M NaCl) and these results are presented here.

XPAT bound primarily to poly(C), poly(A) and poly(U) RNAs in 1M NaCl, and bound poly(G) RNA sequences and dsDNA at a level ~3 times less than poly(C). XPAT did not bind to Sepharose 4B control beads (Figure 6.1C). XPAT was also able to bind poly(C) sequences in higher salt conditions (2M NaCl, data not shown) suggesting that the binding is mediated partially through base-specific hydrophobic interactions. From these experiments it is concluded that XPAT can function as an RNA-binding protein and may bind to C-, U- or A-rich RNAs *in vivo*.

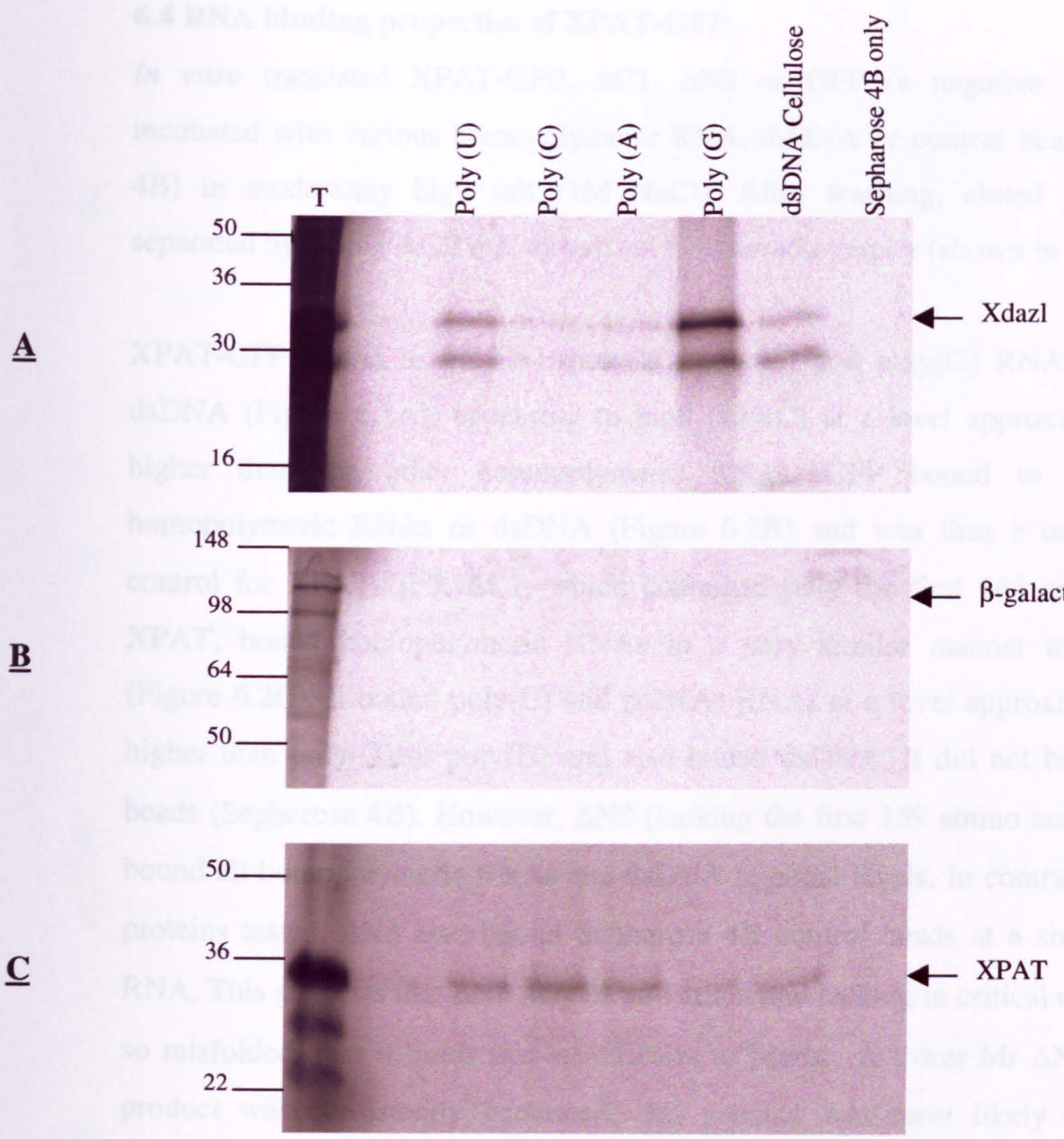

Figure 6.1 XPAT protein can bind RNA.

In vitro translated Xdazl, a previously characterised RNA-binding protein (A), β-galactosidase, a negative control (B), or XPAT (C) were incubated with various homopolymeric RNA, dsDNA or control beads (Sepharose 4B) in binding buffer containing 1M NaCl. After washing, eluted proteins were separated by SDS-PAGE and visualised by autoradiography. Mr (in kDa) is shown at the left of each autoradiograph. (T), aliquot of the initial translation corresponding to 20% of the input per binding reaction. A lower Mr Xdazl translation product was consistently generated- this product was most likely the result of translation initiation at an alternative methionine and bound homopolymeric RNAs with the same specificity as the full-length protein.

6.4 RNA binding properties of XPAT-GFP

In vitro translated XPAT-GFP, ΔC1, ΔN3 or GFP (a negative control) were incubated with various homopolymeric RNA, dsDNA or control beads (Sepharose 4B) in moderately high salt (1M NaCl). After washing, eluted proteins were separated by SDS-PAGE and visualised by autoradiography (shown in Figure 6.2).

XPAT-GFP bound to poly(A), poly(U), poly(C) and poly(G) RNAs and also to dsDNA (Figure 6.2A); appearing to bind poly(C) at a level approximately 2-fold higher than the other homopolymeric RNAs. GFP bound to none of the homopolymeric RNAs or dsDNA (Figure 6.2B) and was thus a useful negative control for XPAT-GFP. ΔC1, which contained only the first 165 amino acids of XPAT, bound homopolymeric RNAs in a very similar manner to XPAT-GFP (Figure 6.2C). It bound poly(C) and poly(A) RNAs at a level approximately 2-fold higher than poly(G) or poly(U) and also bound dsDNA. It did not bind to control beads (Sepharose 4B). However, ΔN3 (lacking the first 159 amino acids of XPAT) bound all homopolymeric RNAs and dsDNA to equal levels. In contrast to all other proteins tested, ΔN3 also bound Sepharose 4B control beads at a similar level to RNA. This suggests that ΔN3 may be so variant and lacking in critical domains, or is so misfolded, that it binds non-specifically to beads. A lower Mr ΔN3 translation product was consistently generated; this product was most likely the result of translation initiation at an alternative methionine. Intriguingly, this lower Mr product bound homopolymeric RNAs, but not Sepharose 4B beads, with the same specificity as the full length ΔN3. Quite what can be concluded from this observation is not yet apparent.

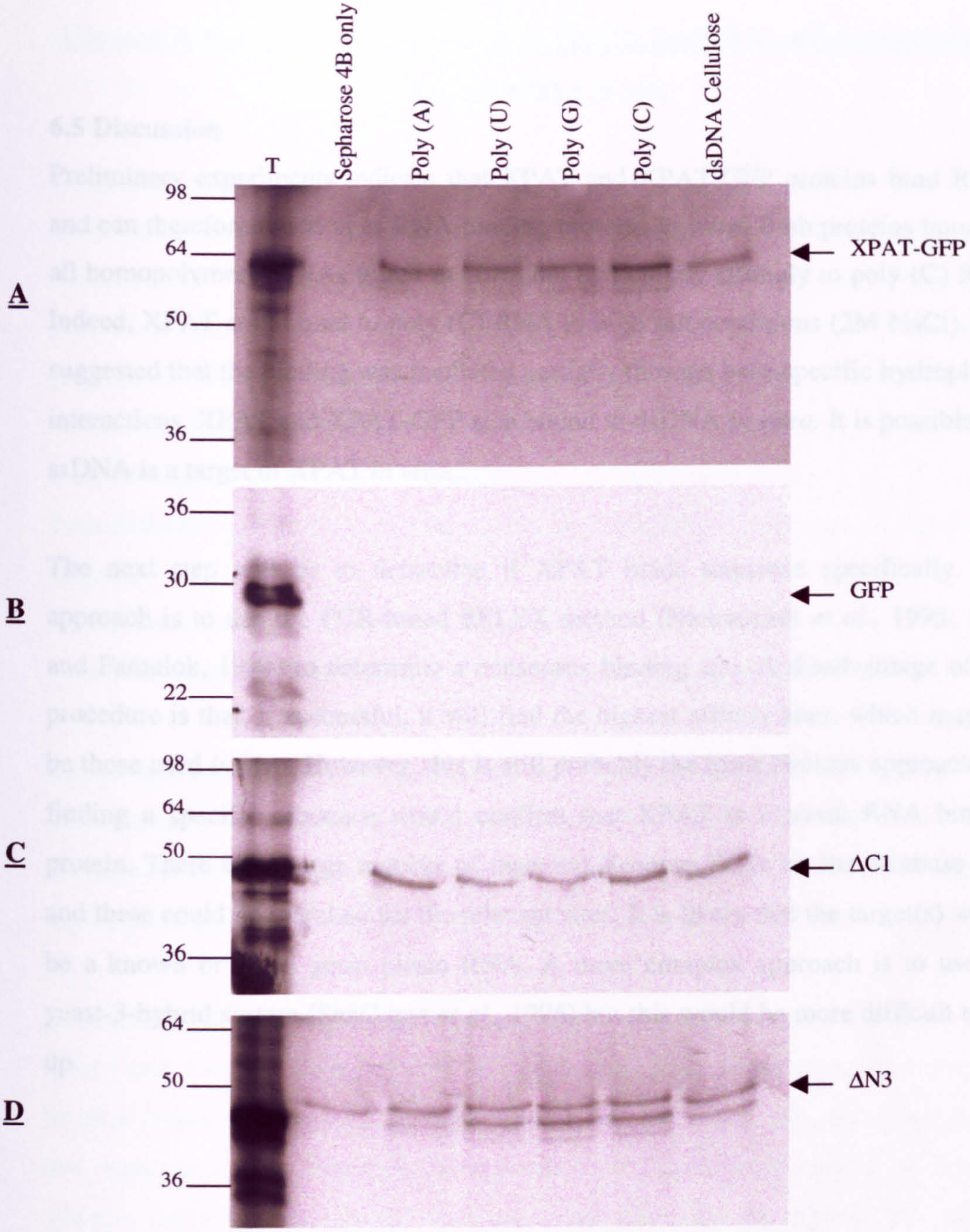

Figure 6.2: XPAT-GFP, ΔC1 and ΔN3 proteins can bind RNA.

In vitro translated XPAT-GFP (A), GFP- a negative control (B), ΔC1 (C), or ΔN3 (D) were incubated with various homopolymeric RNA, dsDNA or control beads (Sepharose 4B). After washing in buffer containing 1M NaCl, eluted proteins were separated by SDS-PAGE and visualised by autoradiography. Mr (in kDa) is shown at the left. (T), aliquot of the initial translation corresponding to 20% of the input per binding reaction. A lower Mr ΔN3 translation product was consistently generated - this product was most likely the result of translation initiation at an alternative methionine and bound homopolymeric RNAs (though not Sepharose 4B control beads) with the same specificity as the full-length protein.

6.5 Discussion

Preliminary experiments indicate that XPAT and XPAT-GFP proteins bind RNAs and can therefore function as RNA-binding proteins *in vitro*. Both proteins bound to all homopolymeric RNAs tested *in vitro*, but particularly strongly to poly (C) RNA. Indeed, XPAT could bind to poly (C) RNA in high salt conditions (2M NaCl). This suggested that the binding was mediated partially through base-specific hydrophobic interactions. XPAT and XPAT-GFP also bound to dsDNA *in vitro*. It is possible that ssDNA is a target of XPAT *in vivo*.

The next step will be to determine if XPAT binds sequence specifically. One approach is to use the PCR-based SELEX method (Nieuwlandt *et al.*, 1995; Klug and Famulok, 1994) to determine a consensus binding site. A disadvantage of this procedure is that, if successful, it will find the highest affinity sites, which may not be those used *in vivo*. However, this is still probably the most obvious approach and finding a specific sequence would confirm that XPAT is a novel RNA binding protein. There are a large number of maternal *Xenopus* ESTs on the database now and these could be searched for the relevant sites. It is likely that the target(s) would be a known or novel germ plasm RNA. A more complex approach is to use the yeast-3-hybrid system (SenGupta *et al.*, 1996) but this would be more difficult to set up.

Chapter 7: Functional studies with *Xpat* Part II: Depletion and overexpression of *Xpat* mRNA *in vivo*

7.1 Introduction

Maternal *Xpat* mRNA is localised in the germ plasm of the full-grown oocyte (Hudson and Woodland, 1998). To address the function of maternal *Xpat* it was decided to attempt to use depletion analysis. This is frequently used to study the function of mRNAs *in vivo*, since one limitation of the *Xenopus* system is the inability to disrupt the function of a gene based on sequence alone, as is possible in mice through homologous recombination in embryonic stem cells.

Two different methods were undertaken to attempt the depletion of *Xpat* from oocytes:

(a) Depletion by antisense oligodeoxynucleotides (oligos).

(b) The use of double-stranded RNA to silence gene expression.

7.1.1 Depletion of *Xpat* mRNA by antisense oligodeoxynucleotide injection

This method is frequently used to cause the specific depletion of mRNAs *in vivo*. For example, the elimination of maternal *VegT* mRNA was achieved by injection of antisense oligos into the vegetal poles of defolliculated oocytes (Zhang *et al.*, 1998).

In total, 12 antisense oligos were designed that were complementary to regions of the *Xpat* Open Reading Frame (ORF). It was necessary to design a number of oligos because it was not possible to predict which would work. It is not uncommon to find that many do not; for example, Zhang *et al.* (1998) designed a total of 12 oligos to attempt degradation of *VegT*, and only one was able to deplete this mRNA substantially. The oligos were all 18-mers, and were synthesized in a more stable modified form in which the 5′ and 3′ terminal four bases were linked by phosphorothioate linkages instead of the conventional phosphodiester bonds.

Each oligo was injected into stage VI oocytes, which were then cultured in 50% Leibowitz medium for 42 hours to allow formation and consequent degradation of the oligo:RNA hybrid. Total RNA was then extracted and RT-PCR analysis was used

to determine whether any of the oligos reduced *Xpat* mRNA levels significantly, compared to control oocyte levels.

Firstly, 5 oligos were tested (*asXpat 1-5*) to determine whether they could inhibit *Xpat* expression. Duplex PCR was performed using primers for *ornithine decarboxylase (ODC)* as a loading control and *Xpat* PCR primers in the same reaction. None of these oligos caused any obvious reduction in *Xpat* mRNA levels (Figure 7.1A). Thus, another 6 oligos were tested. None of these oligos caused a reduction in the amount of endogenous *Xpat* mRNA assayed by RT-PCR (Figure 7.1.B). In this next set of duplex PCRs, EF1α was used as a loading control, because a greater size difference between the Xpat and EF1α PCR products was discernible compared to Xpat and ODC PCR products.

A twelfth oligo (designed by A. Chan) was shown by triplex quantitative RT-PCR analysis (Figure 7.1.C) to noticeably reduce the amount of endogenous *Xpat* mRNA, when injected into oocytes. As a control to show that the injection procedure was working, an antisense oligo to *VegT* was used. This oligo had previously been shown by Zhang and co-workers (Zhang *et al.*, 1998) to deplete *VegT* from *Xenopus* oocytes. And, in this experiment, the same effect was seen when assayed by RT-PCR (Figure 7.1.C). EF1α was again used as a loading control in this triplex PCR reaction.

7.1.2 The use of dsRNA to attempt to deplete *Xpat* mRNA from oocytes

A second way to deplete mRNAs *in vivo* is to introduce double-stranded RNA into organisms to interfere with gene function. The term RNA interference (or "RNAi", Reviewed by Sharp, 1999) was initially coined by Fire and co-workers to describe the observation that dsRNA can potently and specifically inhibit gene activity when introduced into the nematode *Caenorhabditis elegans* (Fire *et al.*, 1998). Their discovery was built upon the previous observation that sense and antisense RNAs were equally effective in suppressing specific gene expression (Guo and Kemphues, 1995), a paradox resolved by the discovery that small amounts of dsRNA contaminate sense and antisense preparations (Fire *et al.*, 1998). RNAi has since been discovered in a wide variety of organisms including *Drosophila* (Kennerdell

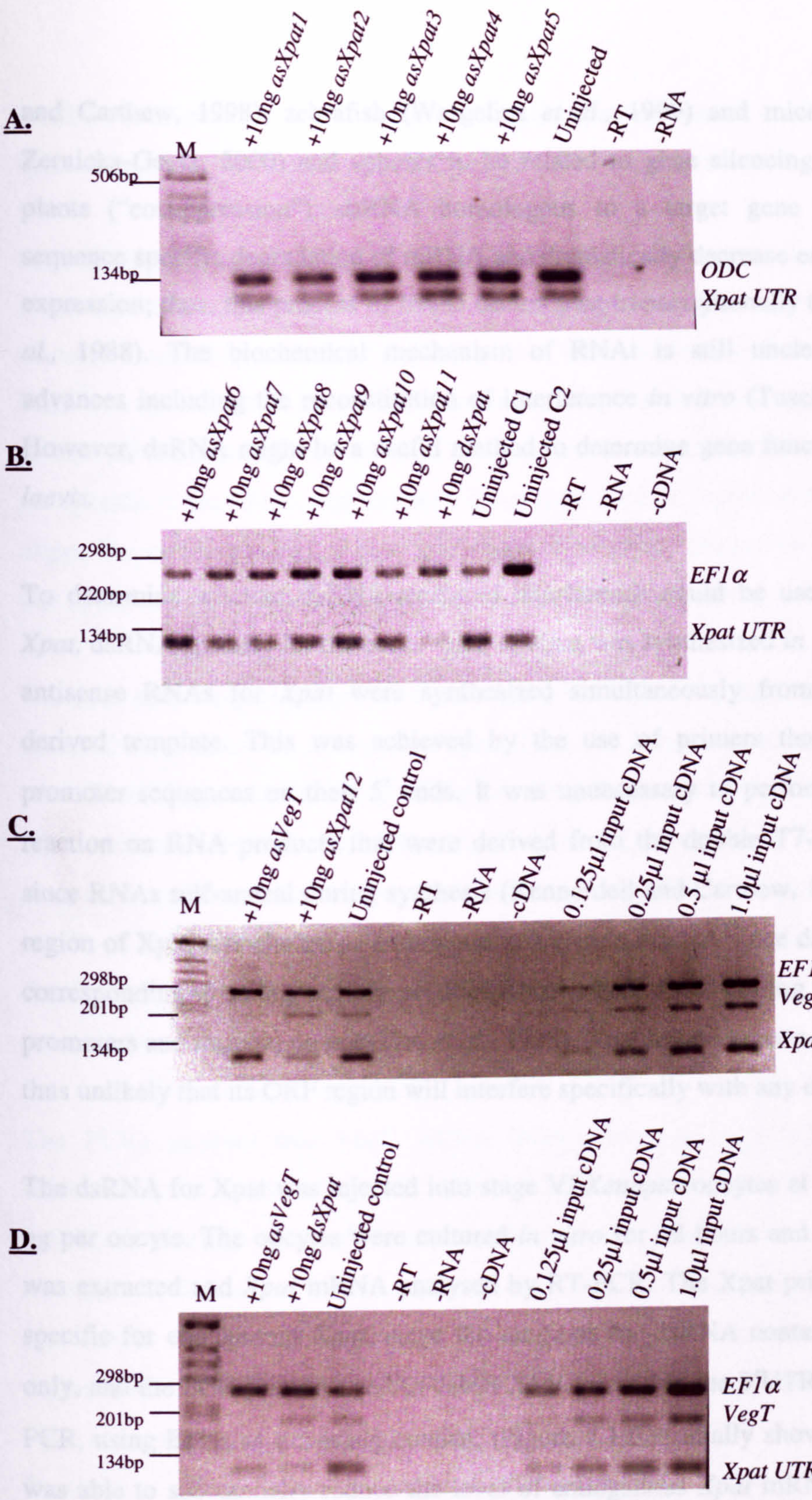

Figure 7.1: Attempts to deplete *Xpat* mRNA by antisense oligodeoxynucleotide injection.
(**A**) 5 oligos designed to Xpat (*asXpat1-5*) were injected into stage VI *Xenopus* oocytes each at 10ng per oocyte. After 42 hours in culture, RNA extraction, cDNA synthesis and duplex PCR (using primers to Xpat and ODC) were performed. PCRs were run on 2% agarose gels. (**B**) 6 further oligos (*asXpat 6-11*)and *dsXpat* RNA were all injected into oocytes at 10ng per oocyte and PCRs performed as in (a) using primers to EF1α and Xpat. (**C**) *asVegT* and *asXpat12* oligos were injected into oocytes at 10ng per oocyte. Triplex RT-PCRs were done as in (a) using primers to EF1α, VegT and Xpat. (**D**) *asVegT* and *dsXpat* were injected into oocytes at 10ng per oocyte. Oocytes were cultured and triplex RT-PCR done as in (a), using primers to EF1α, VegT and Xpat.

and Carthew, 1998), zebrafish (Wargelius *et al.*, 1999) and mice (Wianny and Zernicka-Goetz, 2000) and appears to be related to gene silencing phenomena in plants ("cosuppression"). dsRNA homologous to a target gene can direct the sequence specific degradation of mRNA and dramatically decrease endogenous gene expression; thus, this process of RNAi occurs post-transcriptionally (Montgomery *et al.*, 1988). The biochemical mechanism of RNAi is still unclear, with recent advances including the reconstitution of interference *in vitro* (Tuschl *et al.*, 1999). However, dsRNA might be a useful method to determine gene function in *Xenopus laevis.*

To determine whether dsRNA-mediated interference could be used to knock-out *Xpat,* dsRNA specific for the entire ORF of Xpat was synthesized *in vitro.* Sense and antisense RNAs for *Xpat* were synthesized simultaneously from a single PCR derived template. This was achieved by the use of primers that contained T7 promoter sequences on their 5′ ends. It was unnecessary to perform an annealing reaction on RNA products that were derived from the double T7-PCR templates, since RNAs self-anneal during synthesis (Kennerdell and Carthew, 1998). The ORF region of Xpat was chosen as a template to generate dsRNA since dsRNA segments corresponding to coding regions produce RNAi whereas non-coding regions (such as promoters and introns) do not (Fire *et al.*, 1998). Xpat has no known homologies it is thus unlikely that its ORF region will interfere specifically with any other DNA.

The dsRNA for Xpat was injected into stage VI *Xenopus* oocytes at a dose of 10-50 ng per oocyte. The oocytes were cultured *in vitro* for 42 hours and then total RNA was extracted and *Xpat* mRNA analysed by RT-PCR. The Xpat primers used were specific for endogenous *Xpat*, since the template for dsRNA contains Xpat's ORF only, and the PCR primers used to detect *Xpat* are within the 3′UTR region. Duplex PCR, using EF1α as a loading control, (Figure 7.1.B) initially showed that dsRNA was able to substantially reduce the level of endogenous *Xpat* mRNA compared to control levels. Quantitative triplex RT-PCR was then performed using primers to *VegT, EF1α* and *Xpat* (Figure 7.1.D). RNA extracted from oocytes depleted of *VegT* was also used in one of these triplex PCR reactions as a control. These triplex PCRs

confirm that dsRNA can substantially reduce endogenous levels of *Xpat*, to approximately 25% of the level seen in uninjected (control) oocytes.

7.1.3 RT-PCR analysis of other germ plasm mRNAs in oocytes depleted of *Xpat*

Since antisense oligo *asXpat12* gave the best reduction in *Xpat* mRNA levels, it was decided to use this method of depleting *Xpat* from oocytes in further experiments. This was also the best method to use as the *VegT* antisense oligo gives a useful control for the experiment. The *VegT* results show that the effects of the *asXpat* oligo are specific to that oligo, and are not a consequence of the injection or toxicity of the oligo. The results obtained when *dsXpat* was injected are shown for comparison, but this approach was not pursued because it appeared less effective.

The next set of experiments was to determine the effect that *Xpat* depletion had on other RNAs within the *Xenopus* oocyte. Stage VI *Xenopus* oocytes were injected with either 10ng *asXpat12*, 10ng *asVegT* or 10ng *dsXpat* and then cultured *in vitro* in 50% Leibowitz medium for 42hours. RNA was extracted and RT-PCR used to analyse the effect of the depletion on other localised RNAs. Figure 7.2 shows the results of these quantitative RT-PCRs. ODC was used as a loading control and it should be noted that slightly less cDNA was added to each of the *asXpat* PCRs compared to the control samples.

The PCRs indicate that *VegT* mRNA levels have, as expected, been reduced substantially in oocytes injected with *asVegT* (to less than 10% compared to uninjected control). None of the other mRNA levels (*Xpat, β-catenin, fatvg, Xcat-2, DEADsouth, Xdazl* or *XVLG1*) seem affected, with the exception of *Vg1*. Levels of *Vg1* mRNA are increased to 4 times their control level, in oocytes that have been depleted of *VegT*. The implication of this result is not known, although *VegT*, like *Vg1*, is localised by the late pathway (Kloc and Etkin, 1995; Lustig *et al.*, 1996; Stennard *et al.*, 1996; Zhang and King, 1996; Horb and Thomsen, 1997). It has also been reported recently that *VegT* mRNA has been detected in the germ plasm in cleavage stage embryos (unpublished, cited in Chan *et al.*, 2001).

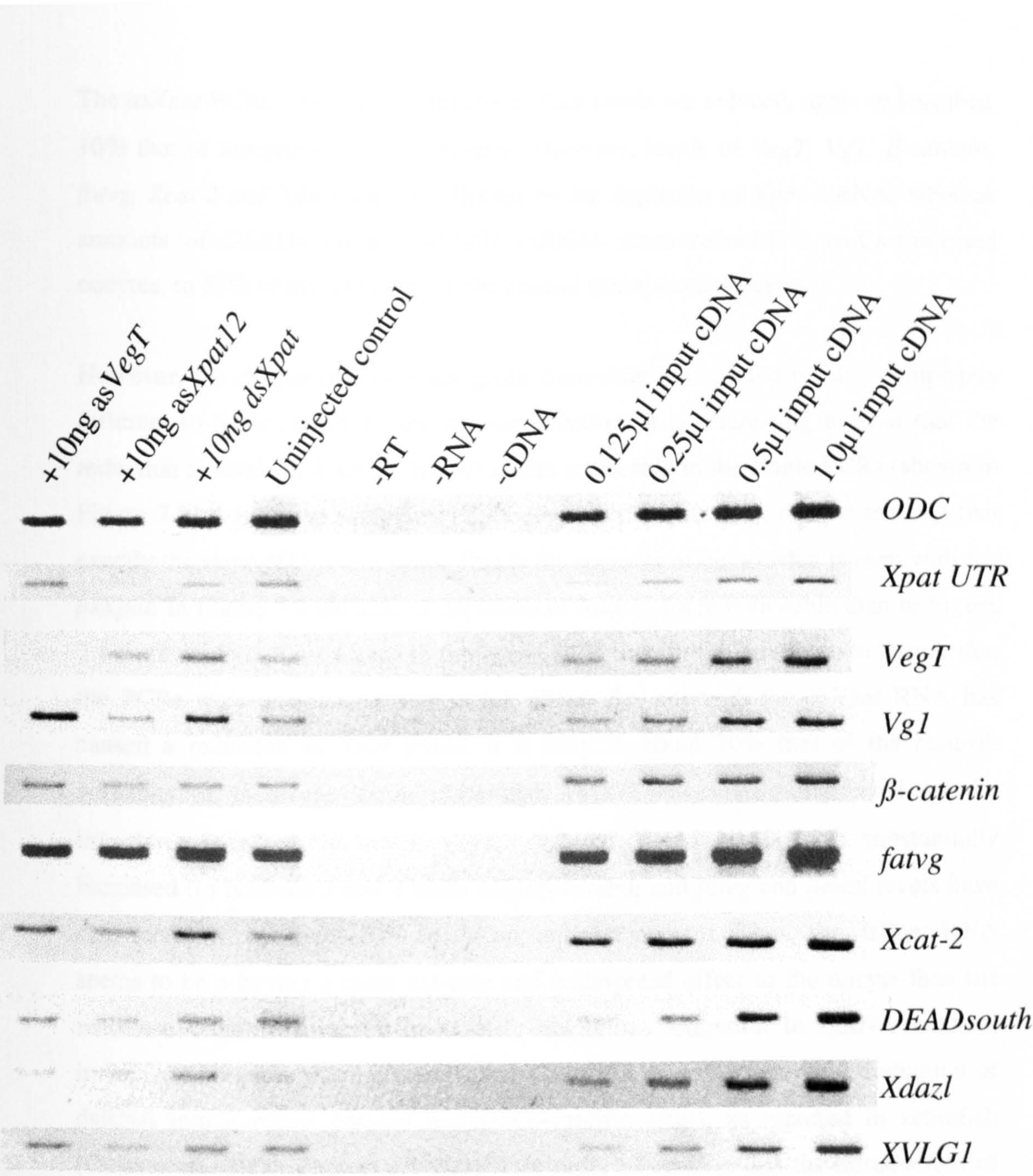

Figure 7.2: RT-PCR analysis to determine the effects of depleting *Xpat* mRNA from oocytes.

Xenopus oocytes were injected with either 10ng of *asVegT* oligo, 10ng of *asXpat12* oligo, 10ng of *dsXpat* RNA or left uninjected. The oocytes were cultured *in vitro* in 50% Leibowitz medium at 18° for 42 hours and then RNA was extracted, cDNA synthesised and PCRs performed and resolved on 2% agarose gels. Each PCR set included 3 negative controls to show there was no contamination (-RT, -cDNA and -RNA) and 4 linearities to show PCRs were in the exponential phase and thus quantitative.

The *asXpat* PCRs show that, as expected, *Xpat* levels are reduced, again to less then 10% that of uninjected control amounts. However, levels of *VegT, Vg1, β-catenin, fatvg, Xcat-2 and Xdazl* seem unaffected by the depletion of *Xpat* mRNA, whereas amounts of *DEADsouth* and *XVLG1* mRNAs seem reduced in *asXpat*-injected oocytes, to 50% of the level seen in the control (uninjected) oocytes.

However, the *dsXpat* injection has given somewhat unexpected results, completely different to those shown by the *asXpat* injection. It is interesting to note that the reduction in levels of *Xpat* by dsRNA is less noticeable in the single PCRs (shown in Figure 7.2) than in the multiplex PCRs (shown in Figure 7.1), despite the fact that exactly the same cDNA was used. This is the opposite effect to what is seen with the *asXpat.* In Figure 7.2 the *asXpat* depletion of *Xpat* is more noticeable than in Figure 7.1 as fewer cycles were used in the single PCR than in the multiplex to ensure that the PCRs were quantitative and in log phase. So, although the *dsXpat* RNA has caused a reduction in *Xpat* levels, it is only to about 70% that of the control. Amounts of *β-catenin, DEADsouth* and *XVLG1* have been unaffected by the injection of *dsXpat.* However, *VegT, Vg1* and *Xcat-2* levels have substantially increased (to between 2 and 4 times control levels); and *fatvg* and *Xdazl* levels have also increased by about 50% in *dsXpat*-injected oocytes. Thus, the *dsXpat* RNA seems to be a having a more extreme and widespread effect in the oocyte than the antisense oligo, and results in a fairly ubiquitous alteration in mRNA content, including non-germ plasm determinants. These results imply that the introduction of dsRNA into *Xenopus* oocytes has a non-specific effect, as reported in zebrafish (Oates *et al.,* 2000; Zhao *et al.,* 2001b). In order to confirm that the introduction of any dsRNA (and not simply *dsXpat*) has this effect, a control dsRNA would need to be made and introduced into oocytes and assayed in the same way. However, the dsRNA approach was not followed further. In contrast, the antisense method has been shown to give good depletion of *Xpat* and causes specific reduction in levels of two germ plasm-specific mRNAs (*XVLG1* and *DEADsouth*), thus the antisense oligo (*asXpat12*) was used in *in situ* hybridisation experiments.

7.1.4 *In situ* hybridisation analysis of germ plasm mRNAs in oocytes depleted of *Xpat*

Stage VI *Xenopus* oocytes were each injected with 10 ng of *asXpat12* to deplete *Xpat* mRNA. These oocytes, and some uninjected controls, were then cultured in OCM for 42 hours at 18°C and fixed. *In situ* hybridisation to germ plasm-specific molecules was then performed to analyse the effects of this depletion on other localised mRNAs. Figure 7.3 shows results of these *in situ* hybridisations.

In situ hybridisation to *Xpat* mRNA was performed using an antisense riboprobe containing the ORF of *Xpat.* Control oocytes show a disc of fine particles of *Xpat* expression in the vegetal pole, as expected. Oocytes injected with *asXpat12* show no expression of *Xpat* mRNA in the oocyte at all. Thus, *Xpat* mRNA has been depleted (Figure 7.3). This result agrees with the RT-PCR result shown in Figure 7.2.

Xcat-2 mRNA is localised in a very similar disc on the vegetal pole in control oocytes. This is smaller than that of *Xpat* expression (see Tables 7.1 and 7.2 in Section 7.2.4). In *Xpat*-depleted oocytes, *Xcat-2* expression looks the same as in control oocytes; that is, the disc of expression appears to be the same size, as do the particles themselves.

Likewise, *Xdazl* mRNA is expressed in a disc of particles on the vegetal pole of uninjected oocytes. In *Xpat*-depleted oocytes, *Xdazl* mRNA is expressed in the same pattern, and the domain of expression is the same size.

DEADsouth is expressed in the vegetal pole of control oocytes in fine particles that form a disc. In *Xpat*-depleted oocytes, *DEADsouth* expression is not detectable by *in situ* hybridisation. This confirms the RT-PCR result (Section 7.1.4), that removal of *Xpat* mRNA also reduces *DEADsouth* mRNA levels.

mtlrRNA is expressed in the vegetal pole of oocytes in fine particles. These do not always appear in a disc shape and in the photograph shown in Figure 7.3, the expression domain is shaped like a tear-drop. In *Xpat*-depleted oocytes, *mtlrRNA* is still expressed in fine particles in the vegetal region, again in a pattern that is not

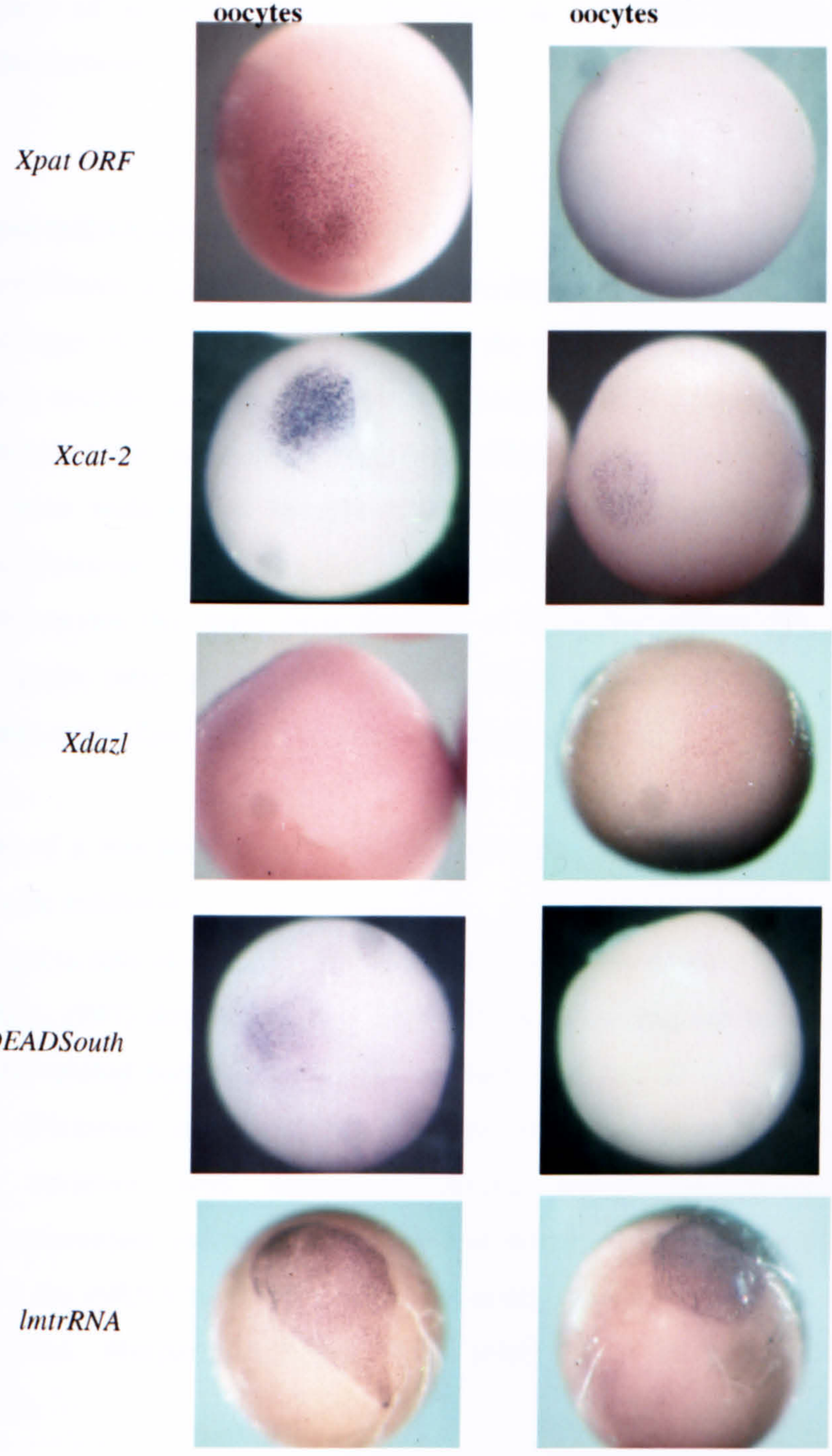

Figure 7.3 *In situ* hybridisation analysis of various germ plasm mRNAs in oocytes depleted of *Xpat* mRNA.

Stage VI *Xenopus* oocytes were each injected equatorially with 10 ng of *asXpat-12* oligo and cultured *in vitro* at 18°C for 42 hours in 50 % Leibowitz medium. Oocytes were then fixed and *in situ* hybridisation was performed using a riboprobe specific for *Xpat, Xcat-2, Xdazl, DEADSouth* or *mtlrRNA* (as indicated at the left hand side of photographs). Each oocyte is ~1.2 mm in diameter.

always disc-like in shape. In the photograph in Figure 7.3 the domain is lateral to the vegetal pole, in a disc shape. It is not likely that *Xpat* depletion has affected the localisation of *mtlrRNA*, simply that there is a natural variation of *mtlrRNA* expression between oocytes.

7.1.5 *Xpat* mRNA elimination in embryos

Phosphorothioate oligos used in depletion studies in oocytes are toxic and unstable in fertilised eggs (Kofron *et al.*, 1997) and so the experiments involved injecting such oligos into oocytes. Injected defolliculated oocytes can be cultured *in vitro* and then fertilised using the host-transfer technique (Heasman *et al.*, 1991). This technique has not been widely used because it is difficult and is not applicable to zygotic mRNAs. However, A. Chan and L. Etkin have attempted this technique and have fertilised oocytes that have been depleted of *Xpat* (by *asXpat 12*). They saw no obvious germ cells in embryos resulting from such fertilisations and a rescue experiment using *Xpat* mRNA is currently being attempted.

7.1.6 Use of a morpholino oligo- an *in vitro* assay to determine if translation of *Xpat* can be inhibited

An alternative loss-of-function approach is to use a "morpholino" oligo (Summerton and Weller, 1997) directed against *Xpat* mRNA. This acts, not by degrading RNA, but by preventing translation of protein. Such morpholino oligos are not toxic to embryos (Heasman *et al.*, 2000). Morpholino oligos have substitutions of the riboside moieties with nitrogen-containing morpholine moieties and are phosphorodiamidate linked (Summerton and Weller, 1997). These oligos are very stable and the mRNA/morpholine complex is not recognised by RNAse H and thus not degraded. Morpholino oligos work solely by a steric translational block mechanism.

An *in vitro* assay was designed which was a variation on the standard rabbit reticulocyte lysate (RRL) *in vitro* translation system. The rationale was to assay whether the presence of a morpholino oligo designed to prevent translation from a particular mRNA could do so directly and specifically in this system. Each mRNA and morpholino was allowed to interact directly for 15 minutes at 30°C, then the

standard RRL *in vitro* reaction mix (including ^{35}S-methionine) was added and the translation allowed to continue for a further 90 minutes. The translation products were then resolved on a standard 12% acrylamide gel and autoradiographed.

Firstly, it was necessary to determine whether this system actually worked. Therefore, a morpholino oligo designed to a region of the 5′ UTR of *Xsox17β*, and mRNA to Myc-tagged Xsox17β (*Xsox17β-myc*) that contained its 5′UTR region, were annealed *in vitro* (this construct was provided by D. Clements). Xsox17β was chosen as it had previously been shown, by immunoprecipitation using an anti-myc-antibody, that the Xsox17β morpholino had inhibited translation of the *Xsox17β-myc* mRNA in *Xenopus* embryos (D. Clements, unpublished data).

3 different morpholino oligos were separately reacted with each mRNA used in this system. These morpholino oligos were:

(a) Xsox17 β morpholino,

(b) Xpat morpholino,

(c) Standard control morpholino (designed by Gene Tools LLC).

These were used so that it could be determined whether inhibition of translation was specific or simply due to the presence of the morpholino side chain. For each mRNA used, two different ratios of mRNA: morpholino were used:

0.02 μg mRNA: 0.25 μg morpholino (a 10 excess of morpholino) and,

0.02 μg mRNA: 2.5 μg morpholino (a 100-fold excess of morpholino oligo).

Figure 7.4A shows an *in vitro* translation assay using *Xsox17β* mRNA as a template. 0.25 μg and 2.5 μg of control morpholino and 0.25 μg and 2.5 μg of Xpat morpholino have no effect on translation of Xsox17β compared with control translation levels (with no morpholino). However, 0.25μg Xsox17β morpholino reduces translation to 10% of control and 2.5 μg of Xsox17β morpholino reduces translation to 1% of control levels. This mimics the *in vivo* results, namely that in the presence of Xsox17β morpholino translation of *Xsox17β* mRNA is specifically reduced.

Thus, this assay appears to be a useful tool in determining whether a morpholino oligo has a specific effect *in vitro* and is thus likely to be useful to specifically inhibit translation *in vivo.*

Figure 7.4B shows an *in vitro* translation assay using *Xpat* mRNA as a template. The mRNA generated contained the 5′ UTR and ORF of *Xpat* since the Xpat morpholino is complementary to 25 nucleotides in the 5′ UTR region. 0.25 μg and 2.5 μg of both control and Xsox17β morpholinos have no effect on translation compared to control translation levels (no morpholino). However, 0.25 μg Xpat morpholino reduces translation to 50% of control levels and 2.5 μg Xpat morpholino only reduces translation to ~ 30% of control levels (Figure 7.4B)

Thus, it does not seem that this morpholino, designed to inhibit translation of *Xpat* mRNA, is having any great effect. This assay was repeated several times *in vitro*, and each time, the same results were seen. Since the morpholino has no real effect in an assay where mRNA and morpholino interact directly, there seems little likelihood of the morpholino having an effect in a much more complex system *in vivo* in a *Xenopus* oocyte. Indeed, on injection of this morpholino oligo into both cells of a 2-cell stage embryo and subsequent *in situ* hybridisation for *Xpat* in stage 36 and stage 44 embryos (as *Xpat* is the only useful known marker for PGCs at these stages) no change in phenotype was seen. PGC numbers were unaffected and PGCs localised correctly. Thus, it appears this morpholino is not a useful tool to aid elucidation of a role for XPAT protein specifically in germ plasm or PGCs of *Xenopus.* It is important to note that correspondance between cell free and in-cell activities of morpholinos has been previously reported (Taylor *et al.*, 1996).

A.

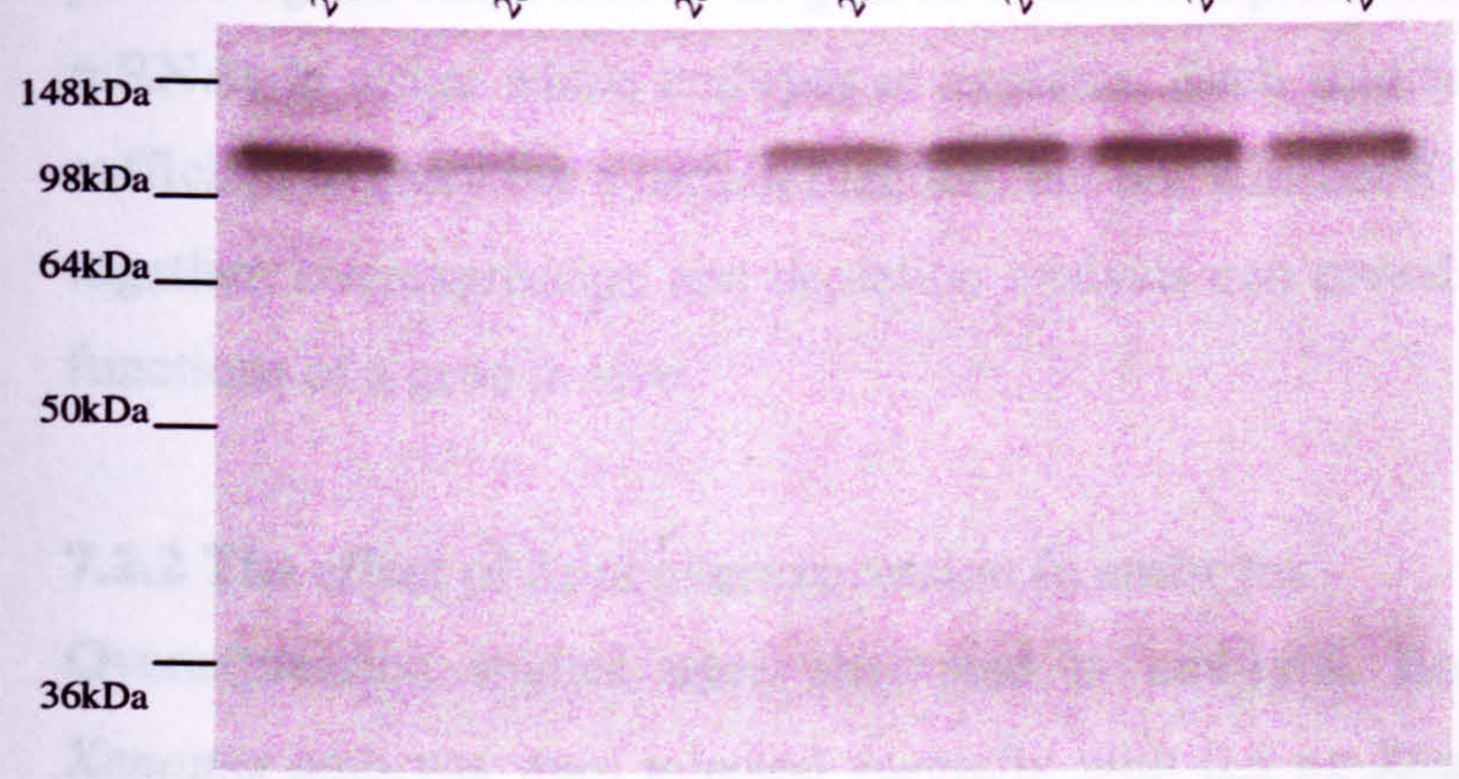

B.

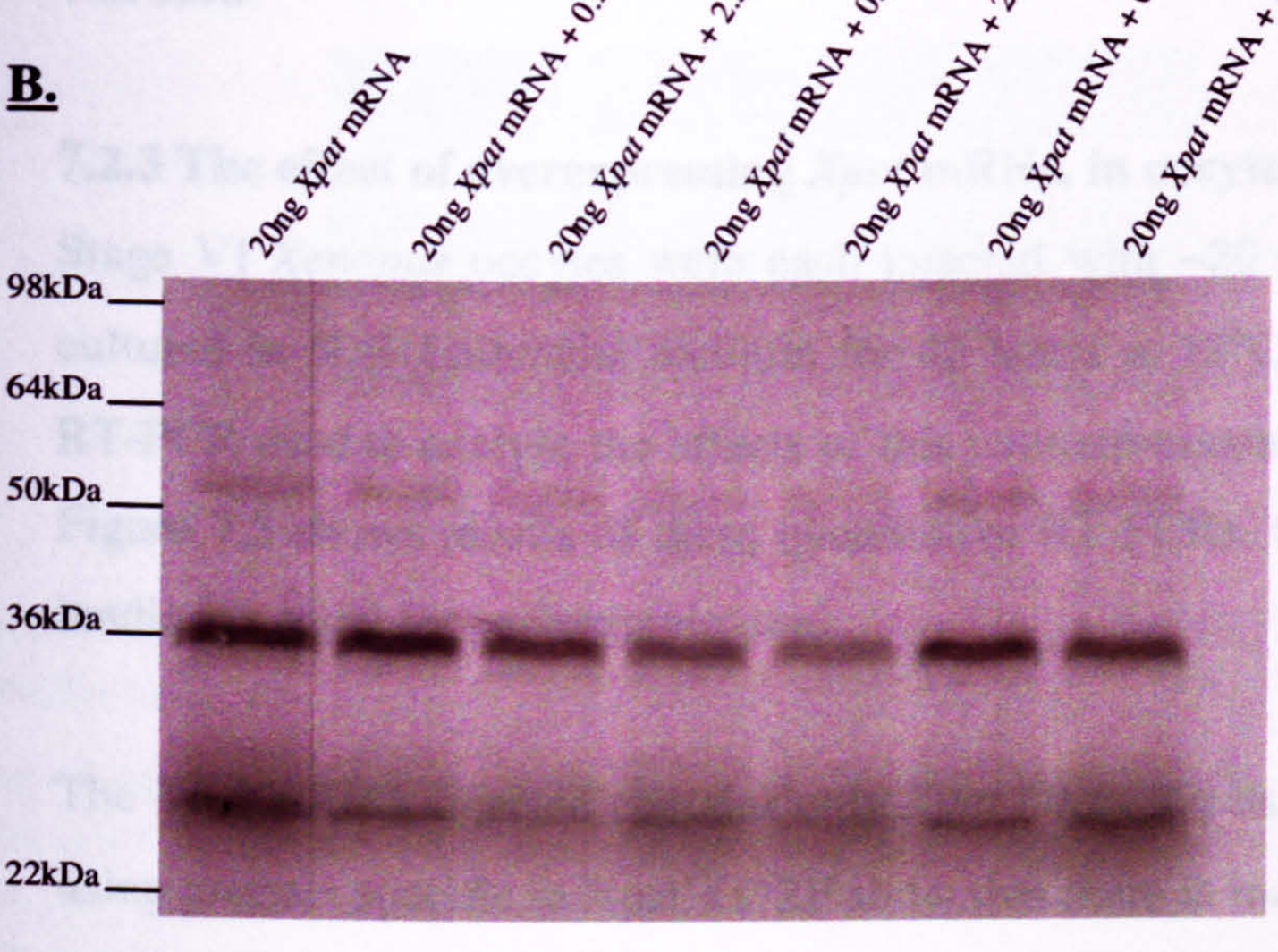

Figure 7.4: *In vitro* translation reactions using (A) *Xsox17β* (B) *Xpat* mRNA as a template. Prior to addition of translation reagents (rabbit reticulocyte lysate plus ^{35}S-methionine), 0.02µg of mRNA was allowed to react with 0.25µg or 2.5µg of morpholino oligo (as indicated) for 15 minutes. Three different morpholinos were used, one specific for the 5' UTR of Xpat (Xpat morpho), one for XSox17β (Sox morpho) and a Control morpholino. The reactions were resolved by 12% SDS-PAGE and autoradiographed.

7.2 Overexpression of *Xpat* mRNA in *Xenopus*

7.2.1 The use of overexpression studies

Overexpression studies are another useful tool for determining the role of mRNAs in development. In *Xenopus* embryos, studies of the genes and activities responsible for patterning are based mainly on gain-of-function experiments by injection of synthetic mRNAs in either whole embryos or explants. Such studies can show that a gene is sufficient to carry out a certain function, but not whether it is required *in vivo*. Taken together, overexpression and depletion analysis can reveal a lot about the potential functions of a gene *in vivo*.

7.2.2 The effect of *Xpat* overexpression in embryos

Overexpression studies were attempted in embryos. Both cells of 2-cell stage *Xenopus* embryos were injected vegetally with 0.5 ng *Xpat ORF* mRNA. Embryos were then fixed and assayed at subsequent stages of development (stages 36 and 44). *In situ* hybridisation analysis was performed, using antisense *Xpat UTR* as a riboprobe. No alteration in PGC numbers or migration was detected when compared with control embryos of the same developmental stage; in fact, no obvious phenotype was seen.

7.2.3 The effect of overexpressing *Xpat* mRNA in oocytes

Stage VI *Xenopus* oocytes were each injected with ~20 ng *Xpat* mRNA and then cultured in 50% Leibowitz medium for 42 hours at 18°C. RNA was extracted and RT-PCR used to analyse the effects of this overexpression on other localised RNAs. Figure 7.5 shows results of these quantitative RT-PCRs. ODC is used to show that loading is equal for each sample used.

The *Xpat* mRNA injected contains only *Xpat ORF*- not its 5′ or 3′ UTR. Thus, PCR using primers specific to Xpat's ORF show that there is much more *Xpat ORF* in the injected than in uninjected oocytes. Similarly, PCR using primers specific to Xpat's 3′UTR show that there are equal amounts of *Xpat UTR* in both control (uninjected) oocytes and in the sample containing over-expressed *Xpat ORF* mRNA. *VegT* levels are equal in both samples as are *Vg1*, *β-catenin* and *fatvg*. Of the germ plasm-

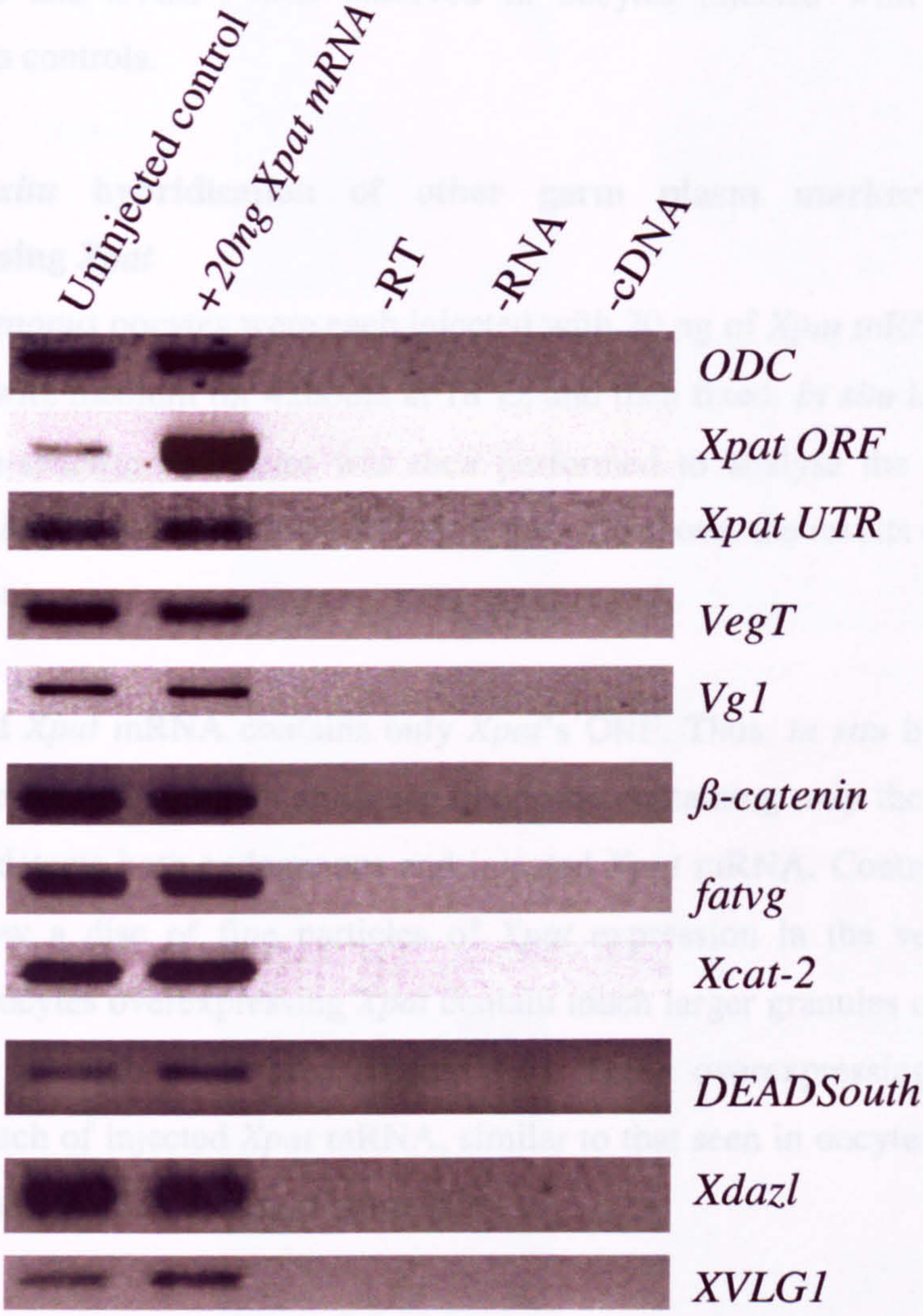

Figure 7.5: RT-PCR analysis to determine the effect of over-expressing *Xpat* mRNA in *Xenopus* oocytes.

20ng of *Xpat* mRNA was injected per oocyte, oocytes were cultured *in vitro* in 50% Leibowitz medium at 18°C for 42 hours and then RNA was extracted, cDNA synthesised and PCRs performed and run on 2% agarose gels. Negative controls were included in each set of PCRs (-RT, -RNA and -cDNA). Linearity curves were run for each marker used (as shown in figure 7.2) to show that RT-PCRs were all in exponential phase and thus quantitative.

specific clones sampled, *Xcat-2* and *Xdazl* had the same levels in control oocytes as in oocytes overexpressing *Xpat*. However, a two-fold increase in the level of both *DEADsouth* and *XVLG-1* was observed in oocytes injected with *Xpat* mRNA, compared to controls.

7.2.4 *In situ* hybridisation of other germ plasm markers in oocytes overexpressing *Xpat*

Stage VI *Xenopus* oocytes were each injected with 20 ng of *Xpat* mRNA, cultured in 50% Leibowitz medium for 42hours at 18°C, and then fixed. *In situ* hybridisation to germ plasm-specific molecules was then performed to analyse the effects of this overexpression on other localised RNAs. Figure 7.6 shows the results of these *in situ* hybridisations.

The injected *Xpat* mRNA contains only *Xpat*'s ORF. Thus, *in situ* hybridisation to *Xpat* was performed using an antisense riboprobe containing only the ORF of *Xpat*. This probe detects both endogenous and injected *Xpat* mRNA. Control (uninjected) oocytes show a disc of fine particles of *Xpat* expression in the vegetal pole, as expected. Oocytes overexpressing *Xpat* contain much larger granules of *Xpat* mRNA spread over a much wider area (Figure 7.6). These overexpressing oocytes also contain a patch of injected *Xpat* mRNA, similar to that seen in oocytes injected with *Xpat-GFP* (see Section 3.5 and Figure 3.7).

Xcat-2 expression is again found in a very similar disc on the vegetal pole in control oocytes. However, it does appear to be more compact than *Xpat* expression. The expression pattern of *Xcat-2* in oocytes overexpressing *Xpat* appears very similar to that of control *Xcat-2* expression. However, the particles of *Xcat-2* expression do appear slightly larger in oocytes overexpressing *Xpat* than in control ones (Figure 7.6).

Expression of *Xdazl* mRNA in uninjected oocytes was again seen in a disc of particles at the vegetal pole, similar in area to *Xpat*. *Xdazl* mRNA expression in oocytes overexpressing *Xpat* is again across the vegetal pole, but in many oocytes

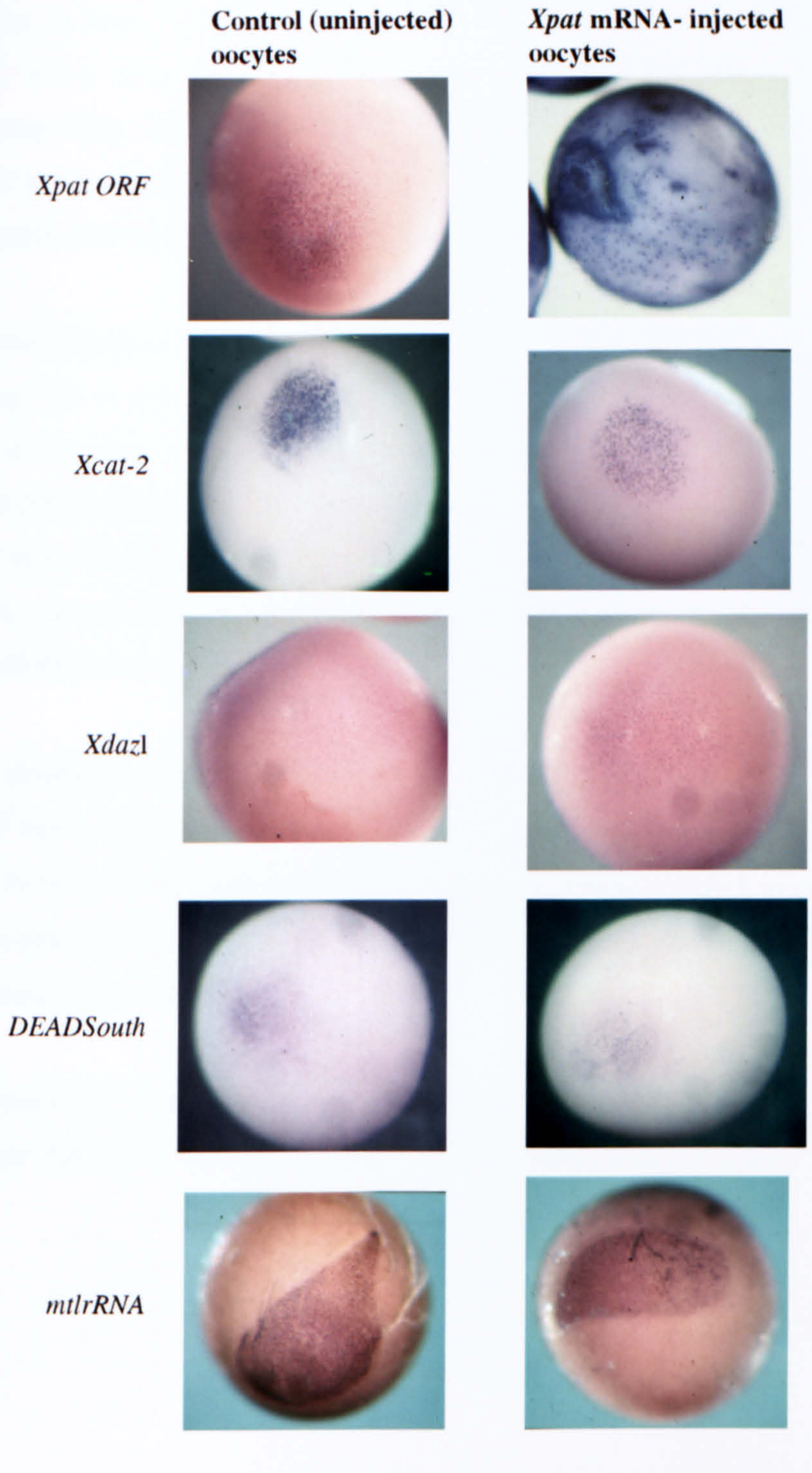

Figure 7.6 *In situ* hybridisation analysis of various germ plasm mRNAs in oocytes overexpressing *Xpat*.

Stage VI *Xenopus* oocytes were each injected equatorially with 20ng of *Xpat* mRNA and cultured *in vitro* in 50 % Leibowitz medium for 42 hours at 18°C. Oocytes were then fixed and *in situ* hybridisation was performed using a riboprobe specific for *Xpat ORF*, *Xcat-2*, *Xdazl*, *DEADSouth* or *mtlrRNA* (as indicated at the left hand side of photograph). *Xpat ORF* riboprobe was designed to hybridise to both endogenous *Xpat* and injected *Xpat* mRNA. When oocytes overexpressing *Xpat* were hybridised *in situ* with *Xpat ORF* riboprobe, background staining was very dark and no particular expression pattern was obvious.These oocytes were all cleared in Murray's and no internal *Xpat* expression was seen. On subsequently placing oocytes into 100% methanol, granules of *Xpat* mRNA were visible, but staining became purple in colour and thus appeared different to other oocytes hybridised *in situ* with other riboprobes. Each oocyte is ~1.2 mm in diameter.

this region appeared wider spread than control *Xdazl* expression. The particles were similar in size in both cases. *DEADsouth* mRNA forms a disc in control oocytes of around the same area as *Xdazl* and *Xpat* expression. However, in oocytes overexpressing *Xpat, DEADsouth* expression seems to be over a smaller area and there appear to be more particles of *DEADsouth* mRNA but they are smaller in size than those particles seen in control oocytes (Figure 7.6).

mtlrRNA (mitochondrial RNA) expression was also studied. *mtlrRNA* expression is not in a disc, but is seen in different shapes on the vegetal pole. For example, in Figure 7.6, a tear-drop shaped pattern of expression is seen in the control oocyte. Likewise, in *Xpat*-overexpressing oocytes, the expression pattern is not in a disc, but in a kind of elongated oval. It does not seem that overexpressing *Xpat* has any effect on *mtlrRNA*, the particles are the same size and density it is more likely that the pattern of *mtlrRNA* expression is naturally variable.

In order to determine whether the differences that were seen in expression pattern diameter of these molecules is statistically significant, the student's T-test was performed. Firstly, the diameter of the disc of expression in oocytes was measured using an eye-piece graticule on a dissecting microscope. The eye-piece graticule was calibrated using a micrometer slide.

Table 7.1 shows the mean diameter of expression of *Xcat-2, Xdazl* and *DEADsouth* in control and *Xpat*-overexpressing oocytes. The raw data is presented in Appendix 1.

Table 7.1: Means and variance for germ plasm diameter in *Xenopus* oocytes injected with *Xpat* mRNA

This was determined by *in situ* hybridisation to various germ plasm components.

OOCYTE: *ISH probe*	Mean (epu)	Mean (μm)	Variance	Number of oocytes (n)
CONT: *Xcat-2*	20.9	522.5	11.5	14
XPAT: *Xcat2*	18.6	465.0	7.44	15
CONT: *Xdazl*	26.9	672.5	11.57	8
XPAT: *Xdazl*	29.0	725.0	9.43	21
CONT: *DEADsouth*	26.5	662.5	12.25	2
XPAT: *DEADsouth*	20.4	510.0	2.44	10
CONT: *Xpat ORF*	27.0	675.0	15.2	20

Control (uninjected) oocytes or oocytes injected with 2 ng of *Xpat* mRNA were cultured *in vitro* for 42 hours and then *in situ* hybridisation was performed. CONT= control (uninjected) oocytes, XPAT= oocytes overexpressing *Xpat* mRNA. ISH probe= riboprobe used in *in situ* hybridistion, *Xcat-2=Xcat-2* riboprobe, *Xdazl=Xdazl* riboprobe, *DEADsouth=DEADsouth* riboprobe, *Xpat ORF*= riboprobe specific for *Xpat's* ORF. The diameter of the expression domain of each germ plasm RNA was measured using an eye-piece graticule in a dissecting stereomicroscope. The first column shows mean (Σdiameters / n) in epu (eye piece graticule units), where n is the total number of oocytes measured. This was converted into μm (after the graticule had been calibrated). Variance is $(\Sigma\text{diameters})^2/n - \text{mean}^2$ and is a measure of the differences in the means. Raw data is shown in Appendix 1.

The means and variance were then converted into T-values for use in the student's T-test. This test compares 2 sets of data. Table 7.2 shows which sets of data were compared and also T-values and critical T values. The critical T value is taken at the 95% level of significance for the appropriate degrees of freedom from statistical tables, (degrees of freedom = total number of oocytes (for both sets of data) –2).

Table 7.2: T values for student's T-test, comparing germ plasm diameter

OOCYTE/ *ISH probe*	**T-value**	**Critical T-value**	**Significant?**
CONT: *Xdazl + Xpat*	0.067	2.056	X
CONT: *Xcat-2 + Xpat*	4.88	2.042	√
CONT: *Xdazl + Xcat-2*	3.984	2.086	√
CONT: *Xdazl + Dsouth*	0.145	2.306	X
CONT: *Dsouth + Xpat*	0.191	2.086	X
CONT: *Dsouth + Xcat-2*	2.125	2.145	X
XPAT+ CONT: *Xcat-2*	2.00	2.052	X
XPAT+CONT: *Dsouth*	2.417	2.228	√
XPAT+CONT: *Xdazl*	1.525	2.052	X

CONT= control (uninjected) oocytes, XPAT= oocytes overexpressing *Xpat* mRNA.
ISH probe=riboprobe used in *in situ* hybridisation, *Xdazl*= *Xdazl* riboprobe, *Xpat*= riboprobe specific for *Xpat*'s 3'UTR, *Xcat-2=Xcat-2* riboprobe, *Dsouth*= riboprobe specific for *DEADsouth*.
√= statistically significant, X=NOT statistically significant.

Thus, there is no significant difference between the diameter of expression of *Xdazl* and *Xpat* in control oocytes; likewise, comparing diameter of expression domains of

Xdazl + *DEADsouth*, *Xpat* + *DEADsouth* and *Xcat-2* + *DEADsouth* in control oocytes shows no significant difference in diameter (Table 7.2).

However, comparing *Xcat-2* and *Xpat* diameters in control oocytes shows there is a significant difference. That is, the *Xcat-2* expression domain is significantly smaller then *Xpat*'s. Also, comparing *Xcat-2* and *Xdazl* diameter in control oocytes, a similar result is obtained. That is, *Xcat-2*'s expression domain is significantly smaller than *Xdazl*'s.

The same is NOT seen for *DEADsouth* and *Xcat-2*, but this could be due to the fact that only two oocytes were scored for *DEADsouth* control diameter. Thus, the variance is quite large and degrees of freedom smaller than might otherwise be seen. A greater number of control oocytes that have been *in situ* hybridised for *DEADsouth* mRNA expression need to be scored to be confident of a significant result.

These findings are likely to be important. This is because it seems that *Xcat-2* is expressed in only a subset of the granules that express *Xpat* and *Xdazl* and this has not been noted before. It is not self evident from the results presented here, or indeed any published, that any germ plasm RNAs are localised in the same granules. Double *in situ* hybridisation will be necessary to clarify this point.

Comparing *Xcat-2* expression domains in control oocytes and those overexpressing *Xpat* shows no significant size difference (Table 7.2). Likewise, for *Xdazl* there is no significant difference between control and *Xpat* overexpressing oocytes. However, when comparing *DEADsouth* in control oocytes and those overexpressing *Xpat*, a significant difference in diameter is seen. Thus, the diameter of *DEADsouth* expression is less in *Xpat* overexpressing oocytes than in control oocytes. Since *DEADsouth* expression diameter is not different from *Xcat-2*, *Xpat* or *Xdazl* domains in control oocytes, this result does appear to be a significant one.

These results are different from those seen in oocytes injected with *Xpat-GFP* mRNA (see Table 3.5), where overexpression of XPAT-GFP has a significant effect on *Xcat-2* expression 72 hours after injection. This difference could be due to the fact that the *Xpat-GFP* injected oocytes were fixed 72 hours after injection, not 42 hours.

Also, 10 times more mRNA was injected into oocytes in the experiments described here than in those in Section 3.6 and *Xpat*-injected oocytes were not cultured in the presence of serum, unlike *Xpat-GFP*-injected oocytes.

7.3 Discussion

Two different methods were attempted to deplete *Xpat* mRNA from *Xenopus* oocytes- the use of antisense oligodeoxynucleotides and dsRNA. *asXpat12* was more effective than *dsXpat* at this depletion and *dsXpat* caused nonspecific changes to levels of mRNA. Since the gene dosage is too small in an oocyte to have a significant impact on maternal mRNAs (Woodland, 1982), it is possible that levels of mRNAs in oocytes decrease naturally with increasing time in culture; although actual levels of mRNAs after various times in culture were never directly compared. Thus, possibly *dsXpat* has a general stabilisation effect in cultured oocytes and prevents mRNA degradation, whereas *Xpat* mRNA, or the protein it encodes, could have a specific stabilising effect on *DEADSouth* and *XVLG1* mRNAs. *Xpat* (or XPAT protein) could therefore stabilise *DEADSouth* and *XVLG1* and prevent their normal degradation by nucleases in the oocyte. Since injection of *asXpat12* has the opposite effect to injection of *Xpat* mRNA on *DEADSouth* and *XVLG1*, it is hypothesised that removal of *Xpat* mRNA from the oocyte (by *asXpat12*-induced degradation) causes the stabilising effect of *Xpat* on *DEADSouth* and *XVLG1* to be removed. These mRNAs thus become subject to attack by nucleases.

In situ hybridisation and RT-PCR analysis gave the same result for *DEADSouth*. It would be interesting to determine whether *in situ* hybridisation to *XVLG1* in *Xpat*-depleted oocytes would confirm the RT-PCR result. When *Xpat* mRNA was overexpressed in oocytes, more particles of *DEADSouth* were detected by *in situ* hybridisation than in controls. Similarly, RT-PCR indicated that increased levels of *DEADSouth* mRNA were present in oocytes overexpressing *Xpat*. RT-PCR revealed increased levels of *XVLG1* mRNA in oocytes injected with *Xpat* mRNA; *in situ* hybridisation analysis has not yet been performed.

The *in situ* hybridisation results presented in this chapter suggest that there are distinct sets of granules within the germ plasm. Where endogenous granules behave differently (i.e. the distribution of *Xcat-2* looks different to that of *Xpat* and *Xdazl*),

the only reasonable interpretation is that there are different sorts of granules. This model fits the distribution of some of the granules discussed here, although it will be necessary to perform double *in situ* hybridisation analysis to confirm this hypothesis. Conversely, where an effect is seen after injection of *Xpat* mRNA into oocytes (e.g. greater numbers of *DEADSouth* granules and larger granules of *Xpat* mRNA) this implies that either the injected *Xpat* mRNA, or the protein it encodes, is interacting with some component that influences the distribution of that RNA. Interestingly, *DEADSouth* has recently been stated not to be present on the germ granules (M.L. King, unpublished; cited in Houston and King, 2000a). L. Etkin has reported that *Xpat* mRNA is peripheral on granules, whereas *Xcat-2* is central (Etkin, 2000). There is no evidence that injected *Xpat* mRNA colocalises with endogenous granules of *Xpat* mRNA, as double *in situ* hybridisation analysis has not been performed.

It is worth noting that the culture conditions used in these experiments were different from those used for XPAT-GFP localisation experiments (in Chapters 3 and 4). All oocytes injected with *asXpat12, dsXpat* or *Xpat* mRNA were cultured in 50% Leibowitz medium (with no added serum), and these conditions were found to be suboptimal for XPAT-GFP localisation (see Section 3.3.2). Since lack of serum in culture medium affects XPAT-GFP protein localisation, it is likely that it can also affect the distribution of endogenous and overexpressed mRNA components.

A morpholino oligo specific for the 5′ UTR region of *Xpat* does not appear to reduce the translation of *Xpat* mRNA substantially when assessed by *in vitro* assay. Whilst injection of the morpholino into 2-cell embryos and subsequent *in situ* hybridisation at stages 36 and 44 of development shows no reduction in PGC numbers or affect on migration, this could be the correct result that inhibition of *Xpat* translation has on development after fertilisation. Until an antibody that is able to detect endogenous levels of XPAT is produced this result cannot be confirmed. However, it is important to note that correlation between in-cell and cell-free behaviour of morpholinos has previously been reported (Taylor *et al.*, 1996). This suggests that since the Xpat morpholino is incapable of substantially inhibiting *Xpat* translation *in vitro* it will be unable to do so in oocytes either.

Chapter 8: Raising anti-XPAT peptide antisera to determine endogenous XPAT protein expression

8.1 Introduction

In order to determine at which stages of development and in which region of the *Xenopus* oocyte and/or embryo XPAT protein is expressed it is necessary to raise antisera against XPAT. Clare Hudson had previously attempted to generate antisera against an XPAT peptide and a GST-XPAT fusion protein in rabbits. However, these antibodies could not detect endogenous levels of XPAT protein. To determine whether the localisation of injected XPAT-GFP is identical to the expression pattern of endogenous XPAT in *Xenopus* oocytes, two more peptides were manufactured and used to raise antisera in both rabbits and mice.

8.2 Design of peptides for XPAT antisera production

Two different regions of XPAT sequence were chosen which were proline-rich and had low hydrophobicity (and were therefore likely to be present on the outside of the protein and not facing inside), had a high antigenic index and high surface probability. These two chosen regions are highlighted in Figure 8.1: peptide A in red and peptide B in green. The sequences chosen were, peptide A: PPHQNPTLLKDEE and peptide B: PKKMPATSTPRK. Also highlighted in blue in Figure 8.1 is the sequence of the peptide Clare Hudson used to generate antisera previously. These sequences were manufactured as multi antigenic peptides (MAPs). These peptides were purified and used to immunise rabbits and mice every four weeks.

Figure 8.1: Sequences of XPAT peptides used to raise antisera

```
MALKAEDSFD IYSQLIQSFC RYAENTTVSE SQSPAFNAQK EFQTCQDHAC CTHSEAHTHI  60

LMQQWQLLEE QWEYIDHLKT DVAALKQLLH GFMNSLSGTD SGMEGTNHFL PPHQNPTLLK 120

DEEIVASALN RPSVDINGFE ENITTGAQIH AAFTKSPKKM PATSTPRKSE VLWSCSPTLA 180

TDGYFMLPDI ILNPLDGKKL VSMLRSSNYE PHRFAELLFQ HHVPHSLFQL WANKVNFDGS 240

RGKLGLPRNL MIDILHQTSK RFVLGPKEKR KIKTRLNLLL RTRQDRAWWD VGL
```

The amino acid sequence of XPAT. The sequences of peptides used to immunise rabbits and mice are highlighted: peptide A in red and peptide B in green. The sequence of a peptide previously used by Clare Hudson to immunise rabbits is highlighted in blue. Peptides A and B were chosen as they are proline-rich, have low hydrophobicity, high antigenic index and high surface probability.

8.3 Characterisation of antisera resulting from immunisations of rabbits

8.3.1 ELISA-Enzyme Linked Immunosorbent Assay

Two weeks after each immunisation, a small sample of blood was taken from each rabbit and serum was isolated and characterised, firstly by ELISA. This was to determine whether the rabbit had responded to the injected peptide and generated appropriate antibodies. If antisera showed good responses in ELISA they were then further characterised. Antisera raised against both peptide A and peptide B showed good responses when tested in ELISA. Peptide B showed non-specific binding with antisera raised against both peptides and also pre-immune serum and thus gave high background measurements in all cases.

8.3.2 Dot-blots

Following ELISA, the peptide antisera were tested on dot-blots of the peptide and GST-XPAT on nitrocellulose membranes alongside equal amounts of BSA as a control. (The cloning and expression of GST-XPAT is described in 8.4.2). Pre-immune serum from the rabbit injected with peptide B reacted with peptide B (Figure 8.2A), as shown previously in ELISA. This was because peptide B (when present at concentrations higher than 0.15µg/µl) was 'sticky' and could bind non-specifically to antisera. Pre-immune serum did not detect BSA or GST-XPAT.

The peptide B antiserum was able to detect down to 15ng of peptide and 20ng of GST-XPAT by the final bleed (Figure 8.2B). Antiserum raised against peptide A was able to detect down to 1.5ng of peptide by the final bleed but was not able to detect GST-XPAT (Figure 8.2C). Obviously this was unsatisfactory, as it was unlikely that either antiserum could detect endogenous levels of protein on a western blot or by immunoprecipitation. However, both sera were next tested by immunoprecipitation on over-expressed XPAT.

8.3.3. Immunoprecipitations using over-expressed XPAT in RRL and oocytes

In order to test the translatability of XPAT, oocytes were injected with 20ng *Xpat* mRNA, cultured in Barths' saline over-night in the presence of ^{35}S-methionine and then proteins were extracted. Concomitantly, *Xpat* mRNA was translated *in vitro* using RRL plus ^{35}S-methionine. Proteins were resolved using SDS-PAGE and

(A) Pre-immune serum

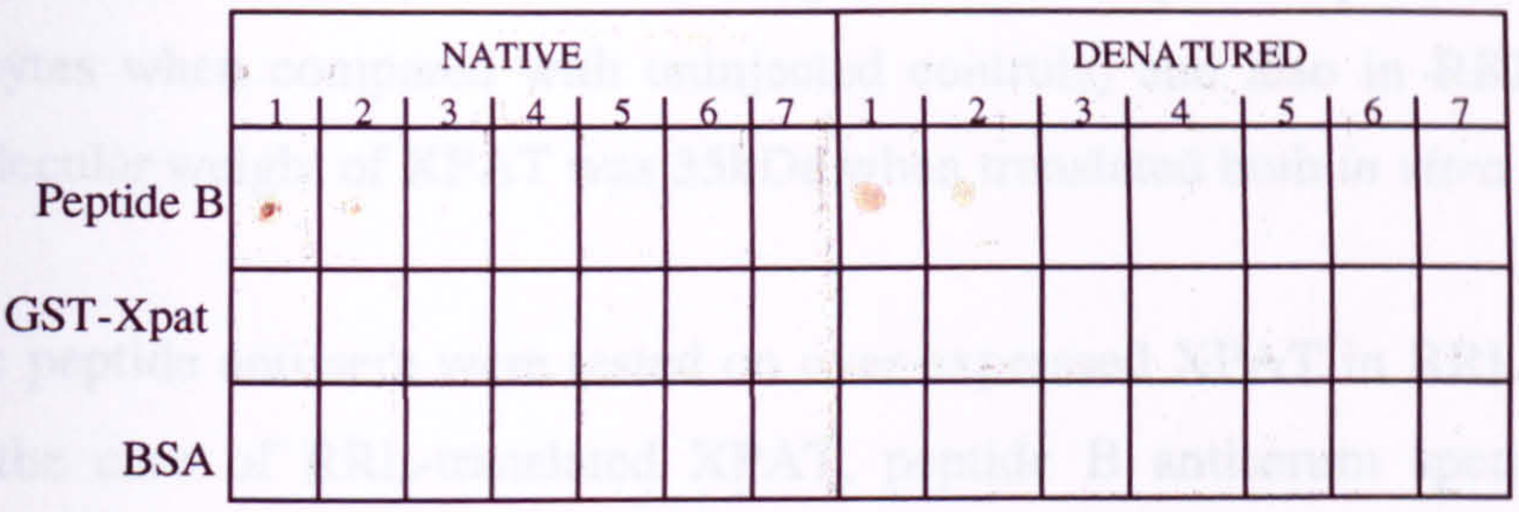

(B) Serum from rabbit immunised with peptide B.

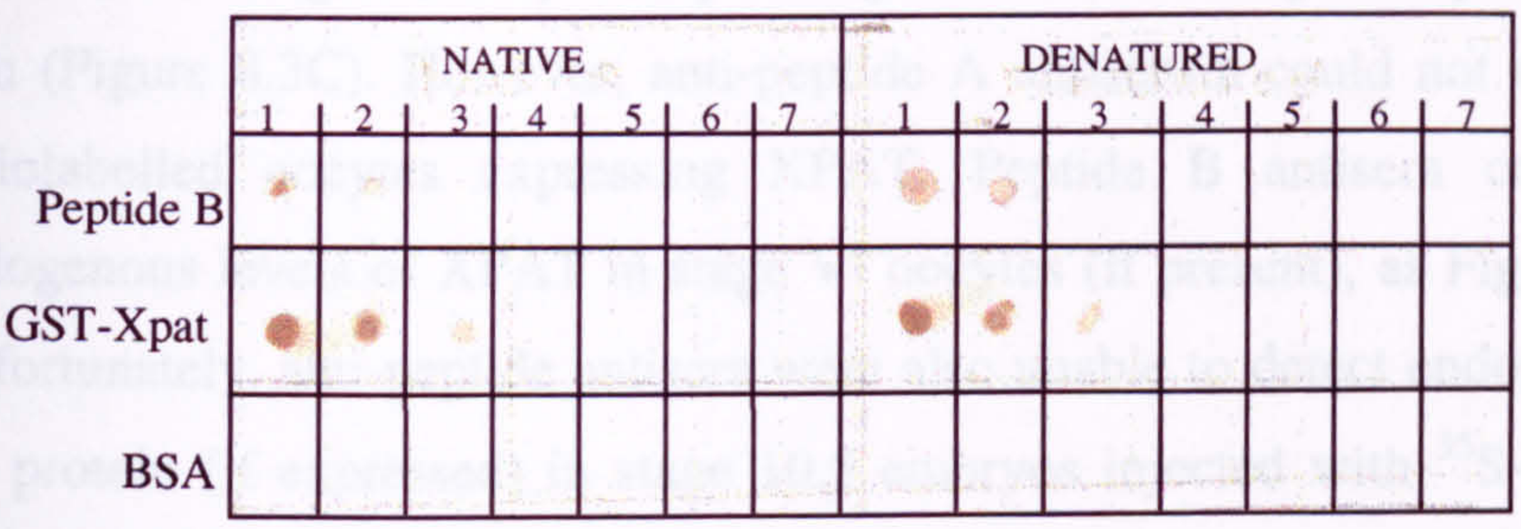

(C) Serum from rabbit immunised with peptide A.

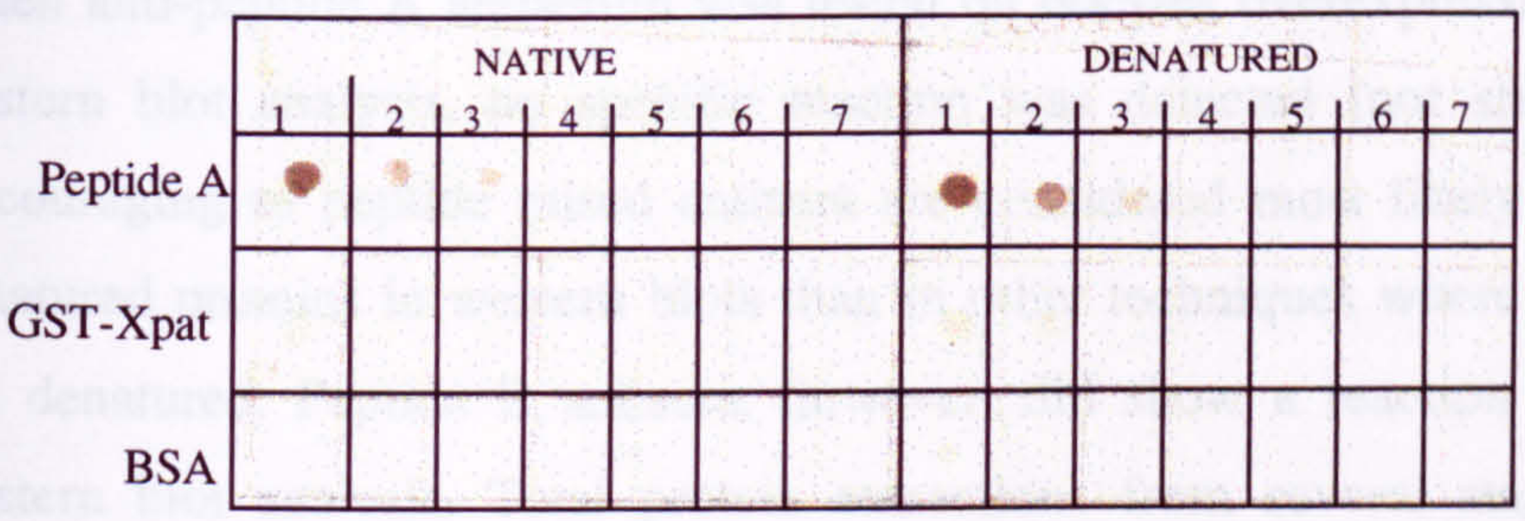

Figure 8.2: Characterisation of antisera raised against XPAT peptides in rabbits using dot blots.
(A). A dotblot of peptide B: (1) 150ng, (2) 15ng, (3) 1.5ng, (4) 0.15ng, (5) 15pg, (6) 1.5pg, (7) 0.15pg.
GST-XPAT and BSA each at: (1) 2µg (2) 0.2µg, (3) 20ng, (4) 2ng, (5) 0.2ng, (6) 20pg, (7) 2pg.
This dot blot was hybridised with pre-immune serum from a rabbit injected with peptide B, diluted 1/100.
(B). A dotblot of peptide B, GST-XPAT and BSA: amounts exactly as described in (A). This nitrocellulose membrane was hybridised with serum from the final bleed of a rabbit immunised with peptide B, diluted 1/100.
(C). A dotblot of peptide A: (1) 150ng, (2) 15ng, (3) 1.5 ng, (4), 0.15ng, (5) 15pg, (6) 1.5pg, (7) 0.15pg.
GST–XPAT and BSA each at: (1) 2µg, (2) 0.2µg, (3) 20ng, (4) 2ng, (5) 0.2ng, (6) 20pg, (7) 2pg.
This dot-blot was hybridised with serum from the final bleed of a rabbit immunised with peptide A, diluted 1/100.

On all of these dot blots, for denatured proteins and peptides, proteins and peptides were heated at 95°C for 3 minutes prior to spotting on nitrocellulose. Native peptides were simply spotted directly onto the membrane prior to hybridisation.

autoradiography. As Figure 8.3A shows, XPAT translated in stage VI *Xenopus* oocytes (indicated by the extra band present in the protein profile of *Xpat*-injected oocytes when compared with uninjected controls) and also in RRL. The apparent molecular weight of XPAT was 35kDa when translated both *in vitro* and *in vivo*.

The peptide anti-sera were tested on over-expressed XPAT in RRL and in oocytes. In the case of RRL-translated XPAT, peptide B antiserum specifically detected XPAT, whilst pre-immune serum from this rabbit did not (Figure 8.3B). However, anti-peptide A antiserum could not detect XPAT. Similarly, immunoprecipitations using anti-peptide B antiserum were able to specifically detect XPAT in radiolabelled stage VI oocytes expressing XPAT after 3 nights exposure of the X-ray film (Figure 8.3C). However, anti-peptide A antiserum could not detect protein in radiolabelled oocytes expressing XPAT. Peptide B antisera could not detect endogenous levels of XPAT in stage VI oocytes (if present), as Figure 8.3C shows. Unfortunately, anti-peptide antisera were also unable to detect endogenous levels of the protein (if expressed) in stage 10.5 embryos injected with ^{35}S-methionine (not shown).

8.3.4 Western blot analysis

When anti-peptide A antiserum was tested on oocytes overexpressing XPAT using western blot analysis, no specific reaction was detected (not shown). This was discouraging as peptide raised antisera are considered most likely to work on the denatured proteins in western blots than in other techniques where the proteins are not denatured. Peptide B antisera, however, did show a reaction when tested by western blot analysis. Total protein extractions from several stages of *Xenopus* oocyte and embryo were resolved by SDS-PAGE and then stained with Coomassie blue to check that the amounts of protein were approximately equal in all samples (results not shown). An identical SDS-PAGE gel was then run and blotted onto nitrocellulose and western blot analysis using anti-peptide B antiserum was performed (Figure 8.3D). In every developmental stage of *Xenopus* tested (stage I, II, V and VI oocytes and stage 3, 9, 13, 26 and 36 embryos) a clear, strong band was seen. The apparent molecular weight of the protein detected was between 30 and 36kDa. Whilst this result appeared encouraging, it was difficult to ascertain whether

Figure 8.3 (Opposite): To test specificity of rabbit antisera using immunoprecipitations and western blot analysis

(A). An autoradiograph of an SDS-PAGE run to determine translatability of *Xpat*.
C and XP lanes contain proteins that were extracted from oocytes incubated in the presence of ^{35}S-methionine. C is the protein profile of control (uninjected) stage VI *Xenopus* oocytes. XP is a protein profile of *Xenopus* oocytes injected with 20ng of *Xpat* mRNA. R represents 1/20 of an *in vitro* RRL translation reaction that contained no added mRNA. RX is 1/20 of an RRL reaction that used *Xpat* mRNA as a template for translation. The arrow indicates XPAT protein, which has an apparent molecular weight of 35kDa after translation *in vivo* and *in vitro*. Protein sizes (on left) are given in kDa.

(B). An autoradiograph of immunoprecipitations carried out with antisera raised against XPAT peptide
In vitro translated XPAT was incubated with serum (all used at 1/100 dilution) and protein A Sepharose. After washing, eluted proteins were separated by SDS-PAGE and visualised by autoradiography. The letters indicate which immunoprecipitation reaction was loaded. Letter designations are as follows: T, aliquot of the initial XPAT RRL translation, corresponding to 20% of the input per immunoprecipitation reaction; P-A, pre-immune serum, taken from rabbit prior to immunisation with peptide A; P-B, pre-immune serum taken from rabbit prior to immunisation with peptide B; A3, antiserum taken from rabbit immmunised with peptide A, it was taken from the final bleed following the 3rd boost; B3, antiserum taken from rabbit immunised with peptide B, it was taken from the final bleed following the 3rd boost; –, no serum. Protein sizes (on left) are given in kDa.

(C). An autoradiograph of immunoprecipitations carried out with antisera raised against XPAT peptides
Stage VI *Xenopus* oocytes were cultured *in vitro* in the presence of ^{35}S-methionine and then proteins were extracted. The oocyte proteins were then incubated with sera (all used at 1/100 dilution) and protein A Sepharose. After washing, eluted proteins were separated by SDS-PAGE and then visualised by autoradiography. In the immunoprecipitations, pre-immune sera were also used on the radioactive oocytes and control immunoprecipitations were carried out on radioactive oocytes that were not overexpressing XPAT (C). The letters indicate which samples were loaded and their designation is as follows: C, control (uninjected) oocyte samples; X, oocytes injected with 20ng *Xpat* mRNA; T, aliquot of the initial sample of proteins extracted from oocytes corresponding to 20% of the input per immunoprecipitation; p, pre-immune serum; A, rabbit antiserum taken from the final bleed after 3rd boost of peptide A; B rabbit antiserum taken from the final bleed following the 3rd boost of peptide B.

(D). Western blot analysis of serum raised against peptide B
Proteins were extracted from various stages of *Xenopus* oocytes and embryos and were separated by SDS-PAGE. The gel was then blotted onto nitrocellulose membrane and the western blot was incubated with serum taken from rabbit immunised with peptide B. The serum was diluted 1/100 and was taken from the final bleed following the 3rd boost. The blot was then incubated with Goat Anti-Rabbit IgG HRP conjugate and visualisation of reactivity was performed by addition of DAB substrate. Protein samples were extracted from: I, stage I oocytes; III (stage III oocytes); V, stage V oocytes; VI, stage VI oocytes; 3, stage 3 embryos; 9, stage 9 embryos; 13, stage 13 embryos; 26, stage 26 embryos; 36, stage 36 embryos. The letters above the blot indicate which samples were loaded.

(E) Control western blot
A gel was loaded exactly as in (D), resolved by SDS-PAGE then transferred onto nitrocellulose membrane. The western blot was incubated with 1/100 pre-immune serum taken from a rabbit prior to immunisation with peptide B. The blot was then incubated with Goat Anti-Rabbit IgG HRP conjugate and visualisation of reactivity was performed by addition of DAB substrate. The letters above the blot indicate which samples were loaded [as indicated in (D)].

A

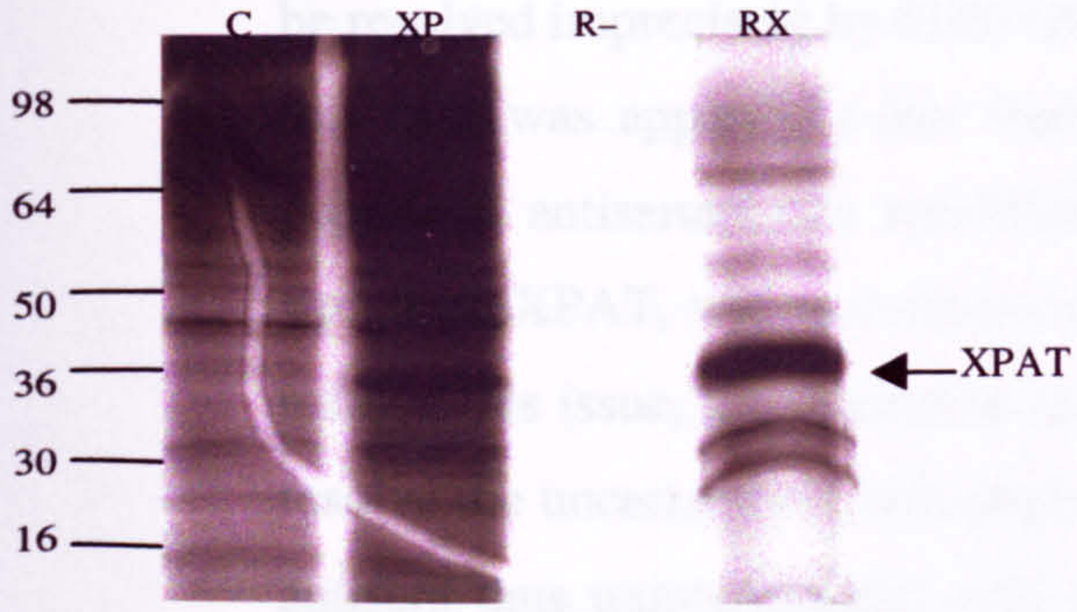
C
XP
R–
RX
98
64
50
36
30
16
XPAT

B

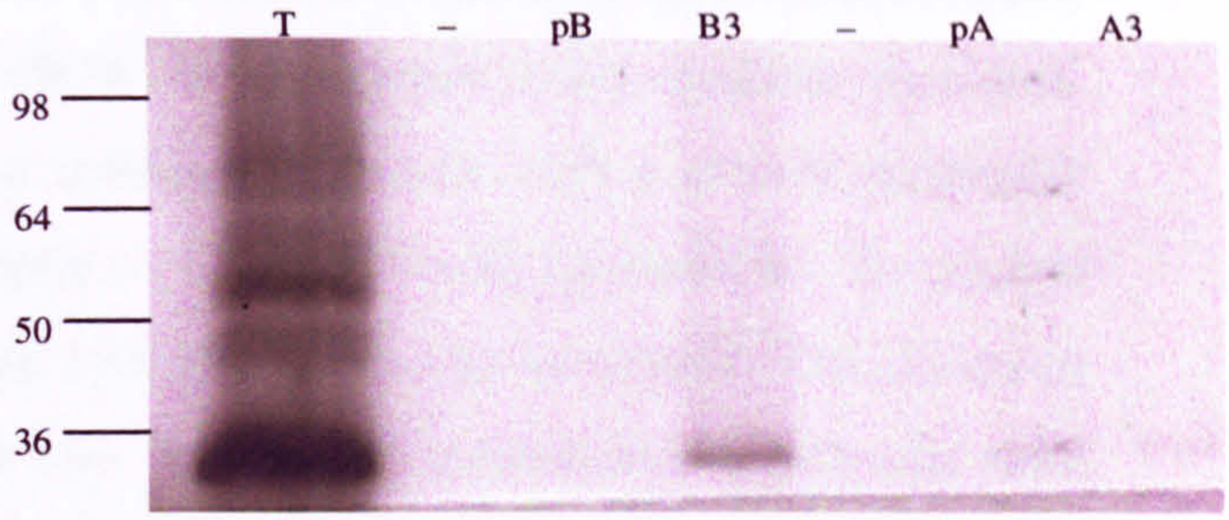
T
–
pB
B3
–
pA
A3
98
64
50
36

C

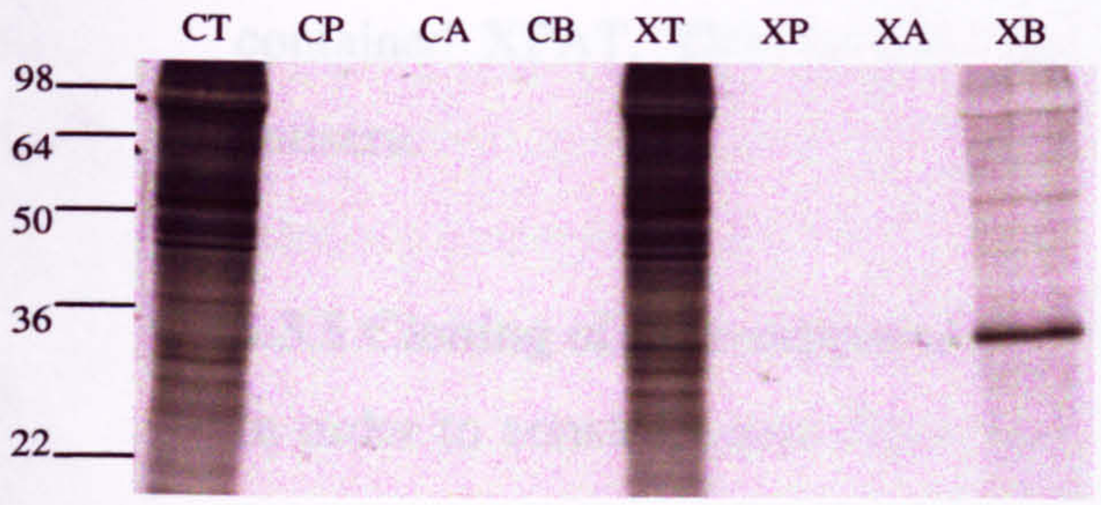
CT
CP
CA
CB
XT
XP
XA
XB
98
64
50
36
22

D

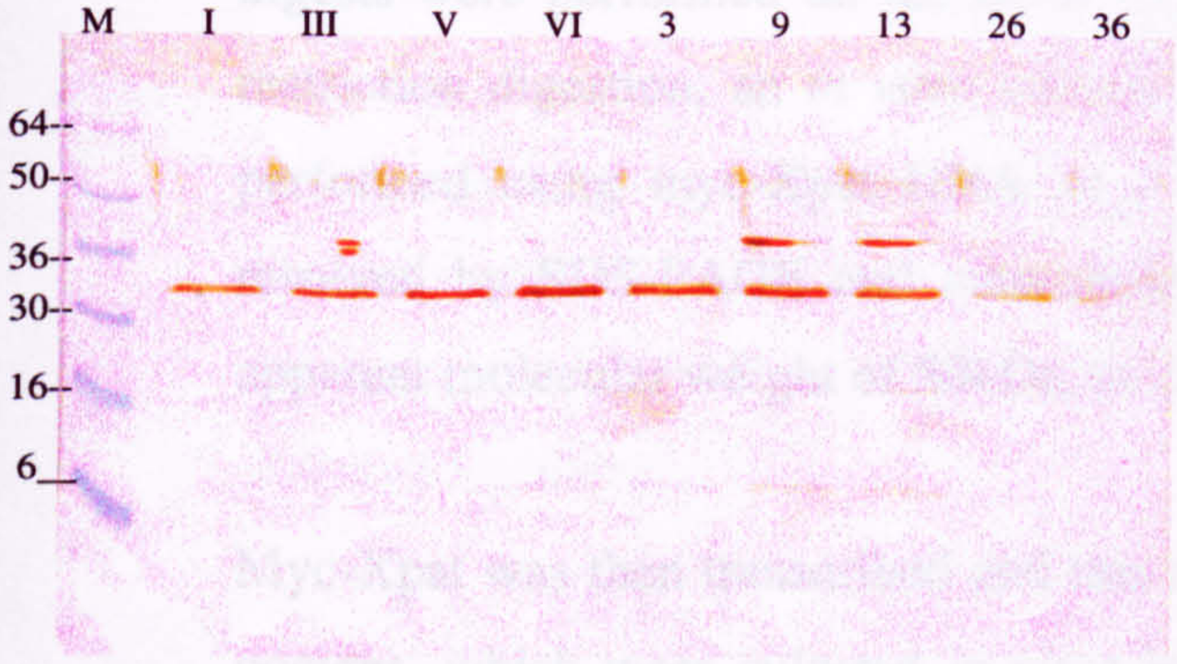
M
I
III
V
VI
3
9
13
26
36
64
50
36
30
16
6

E

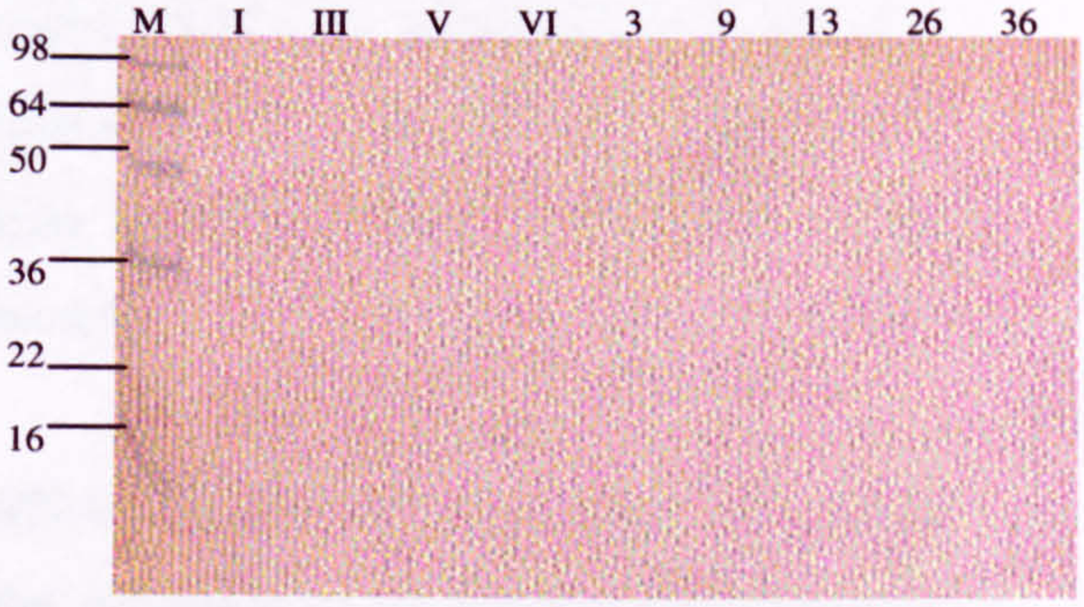
M
I
III
V
VI
3
9
13
26
36
98
64
50
36
22
16

the protein that the antisera detected was indeed XPAT. Whilst protein markers can be resolved imprecisely by SDS-PAGE sometimes, the size of the protein detected in this case was apparently less than 35kDa. It was theoretically possible that anti-peptide B antiserum was specifically detecting a protein with a similar molecular weight to XPAT, with a common region of 13 amino acids (peptide B). To try and resolve this issue, a competition assay with peptide B was attempted. This failed to resolve the uncertainty as this peptide was 'sticky' and reacted non-specifically with antisera thus uninterpretable data (not shown) was obtained. Next, 2-Dimensional gel electrophoresis followed by western blot analysis was attempted. Results were again difficult to interpret (not shown) as high background was seen on the blots. Finally, it was decided to tag XPAT with 6 myc epitopes at its amino terminus thus generating a distinct protein with a greater molecular weight than XPAT but that still contained XPAT. This protein was then used for further characterisation of the antisera.

8.3.5 Cloning of myc-tagged XPAT for use in immunoprecipitations

In order to construct myc-Xpat, the coding region for Xpat was amplified by PCR from a cDNA library clone with primers that created 5′ *Bgl*II and 3′ *Xho*I sites. The resulting PCR fragment was then cloned into the *Bgl*II and *Xho*I sites of pCS3+MT which contained 6 myc epitope tags. This generated myc-Xpat, Xpat tagged with myc at its amino terminus. Once this construct was made, appropriate restriction digests were performed on the DNA to confirm that Xpat was present. Following restriction digestion, an *in vitro* coupled transcription and translation reaction was performed using myc-Xpat DNA as a template. A fraction of the reaction was resolved by SDS-PAGE and autoradiography confirmed that myc-XPAT had an apparent molecular weight of 50kDa, as expected.

Myc-Xpat was then transcribed and this mRNA was injected into stage VI *Xenopus* oocytes, which were cultured *in vitro* in the presence of ^{35}S-methionine. Proteins were extracted from these oocytes and immunoprecipitation using an anti-myc antibody confirmed that this protein could be detected. The immunoprecipitation reactions were resolved by SDS-PAGE and an autoradiograph of the gel is shown in Figure 8.4A. This figure confirms that myc-XPAT is translated in oocytes with an

apparent molecular weight of 50kDa. This is obvious as the protein profile of *myc-Xpat-* injected oocytes has one extra band of 50kDa when compared with the protein profile of uninjected control oocytes (Figure 8.4A). The immunoprecipitation reaction was able to detect protein in radiolabelled oocytes expressing myc-XPAT whereas it was not able to detect protein in radiolabelled uninjected controls. Several break-down proteins were observed in the immunoprecipitation reaction.

Next, immunoprecipitation reactions using anti-peptide B antisera were attempted. Immunoprecipitation was able to detect protein in radiolabelled oocytes expressing myc-XPAT after 1 night exposure of the X-ray film (Figure 8.4B). However, this autoradiograph did not show any detection of XPAT by the peptide antiserum in radiolabelled oocytes expressing XPAT. Thus, the gel was exposed to X-ray film for 3 nights (Figure 8.4C). In this figure, XPAT and myc-XPAT were detected in overexpressing radiolabelled oocytes by anti-peptide B antiserum. However, the pre-immune serum from this rabbit also detected myc-XPAT, indicating that possibly the rabbit had previously encountered myc epitope. The immunoprecipitation reactions indicated that the antiserum worked, but poorly. Unfortunately, myc-XPAT production did not allow any conclusions to be drawn regarding specificity of peptide B antiserum. Further western blot analysis was performed using myc-XPAT expressing oocytes but background staining prevented interpretation (not shown). Western blot analysis of immunoprecipitations did not aid clarification of the problem.

Finally, whole-mount immunostaining of various stages of oocytes and embryos was attempted with both peptide antisera. Whole mount analysis did not give any specific staining pattern (results not shown). Thus, no further experiments were performed with these antisera.

Figure 8.4 (Opposite): The use of myc tagged XPAT to determine the specificity of antipeptide antisera

(A) Autoradiograph of immunoprecipitation reactions that had been resolved by SDS-PAGE. Protein sizes (on left) are given in kDa. The letters above the autoradiograph indicate which samples had been loaded. The letter designation is as follows: CT, control (uninjected) stage VI *Xenopus* oocytes which had been cultured *in vitro* in the presence of ^{35}S-methionine for 18 hours, this aliquot corresponded to 20% of the input per immunoprecipitation reaction; MT, stage VI oocytes which had been injected with 20ng of *myc-Xpat* mRNA and then cultured *in vitro* for 18 hours in the presence of ^{35}S-methionine, this aliquot corresponds to 20% of the input per immunoprecipitation reaction; CαM, immunoprecipitation reaction, proteins extracted from control oocytes were interacted with 1/100 anti-myc antibody and protein A Sepharose, then washed; MαM, immunoprecipitation reaction, proteins extracted from *myc-Xpat*–injected oocytes were interacted with an anti-myc antibody and then washed.

(B) Autoradiograph of immunoprecipitation reactions that had been resolved by SDS-PAGE. This gel was exposed to X-ray film for 18 hours. Stage VI *Xenopus* oocytes were cultured in the presence of ^{35}S-methionine and total protein extractions were performed. The oocyte proteins were then incubated with antisera and protein A Sepharose. After washing, eluted proteins were separated on a 12% acrylamide gel and visualised by autoradiography. Protein sizes (on left) are given in kDa. The letters above the autoradiograph indicate which samples were loaded. Letter designations are as follows: C, control (uninjected) oocytes; X, oocytes injected with 20ng *Xpat* mRNA; M, oocytes injected with 20ng *myc-Xpat* mRNA; T, aliquot of total protein extraction corresponding to 20% of the input per immunoprcipitation reaction; p, immunoprecipitation reaction using 1/100 pre-immune serum; B, immunoprecipitation reaction using 1/100 antiserum taken from final bleed of rabbit immunised with peptide B.

(C) Autoradiograph of immunoprecipitation reactions resolved by SDS-PAGE. This is the same as the gel shown in (B), however, the gel was exposed to X-ray film for 72 hours in this case.

A

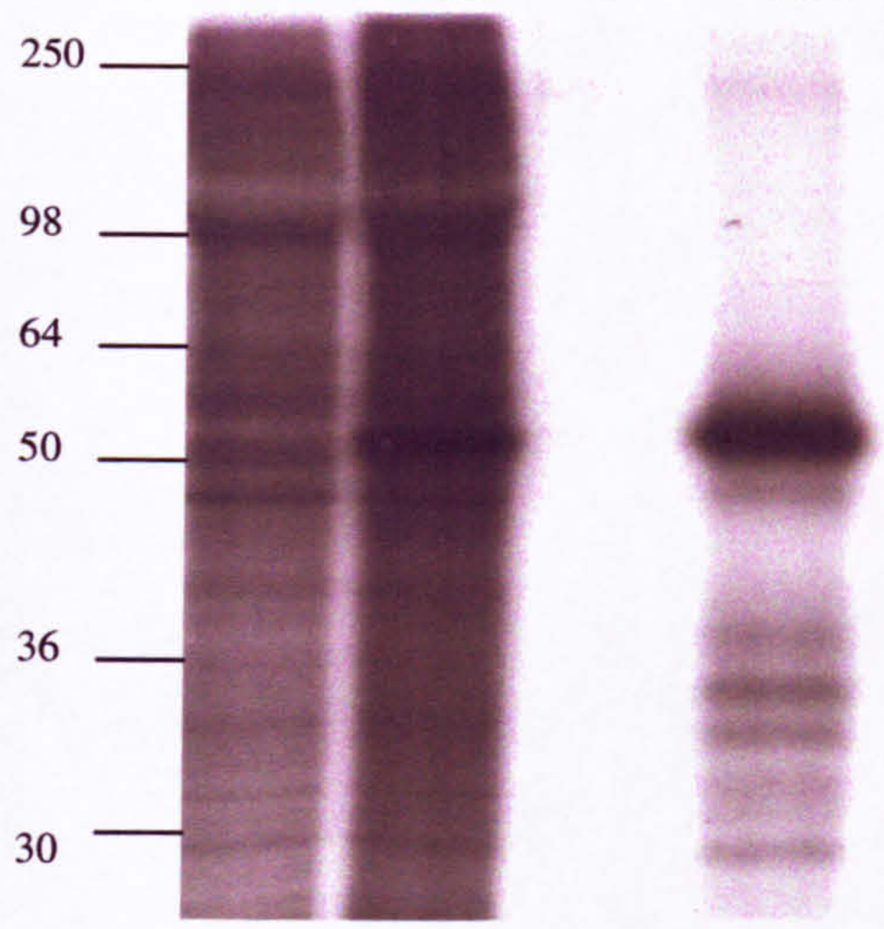
CT
MT
CαM
MαM
250
98
64
50
36
30

B

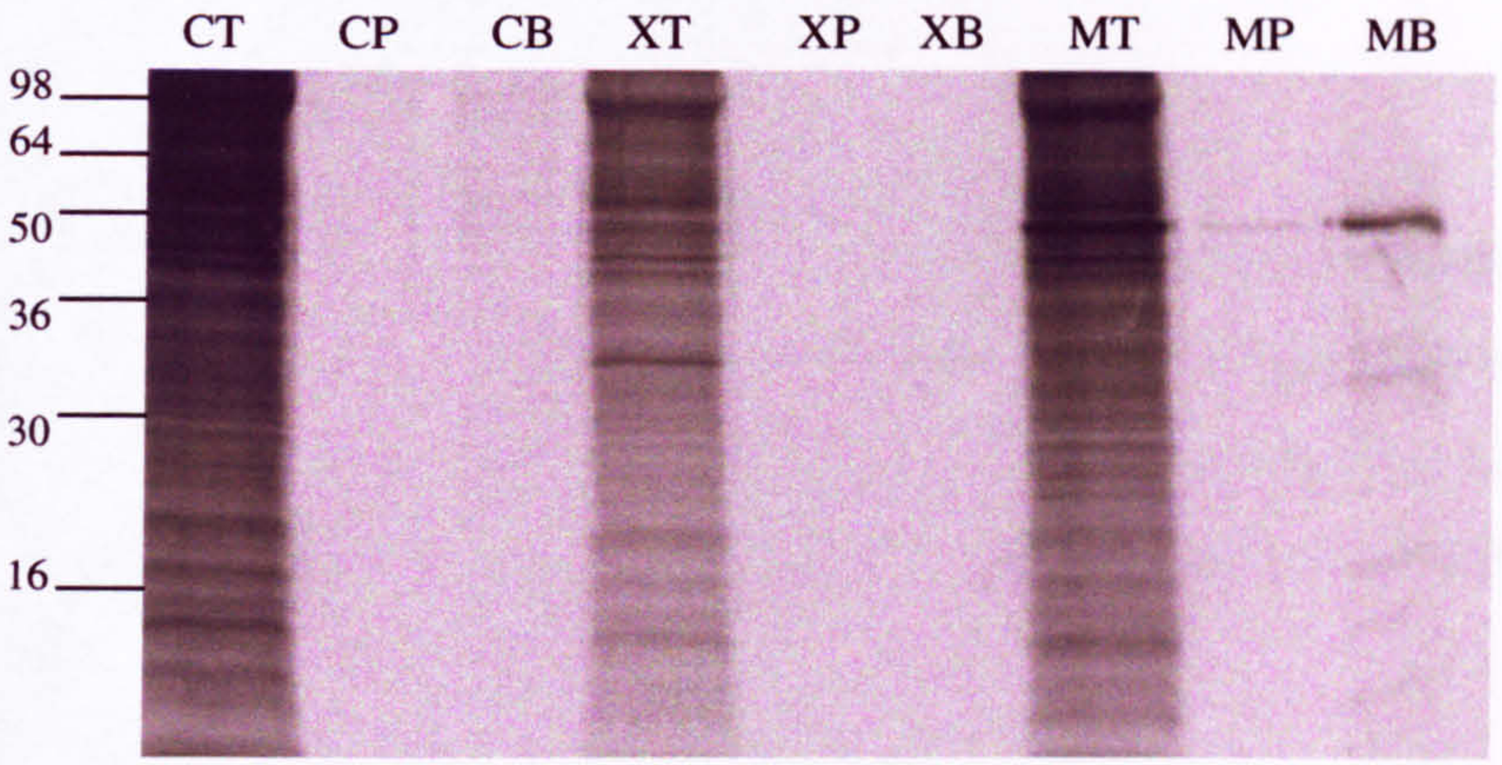
CT
CP
CB
XT
XP
XB
MT
MP
MB
98
64
50
36
30
16

C

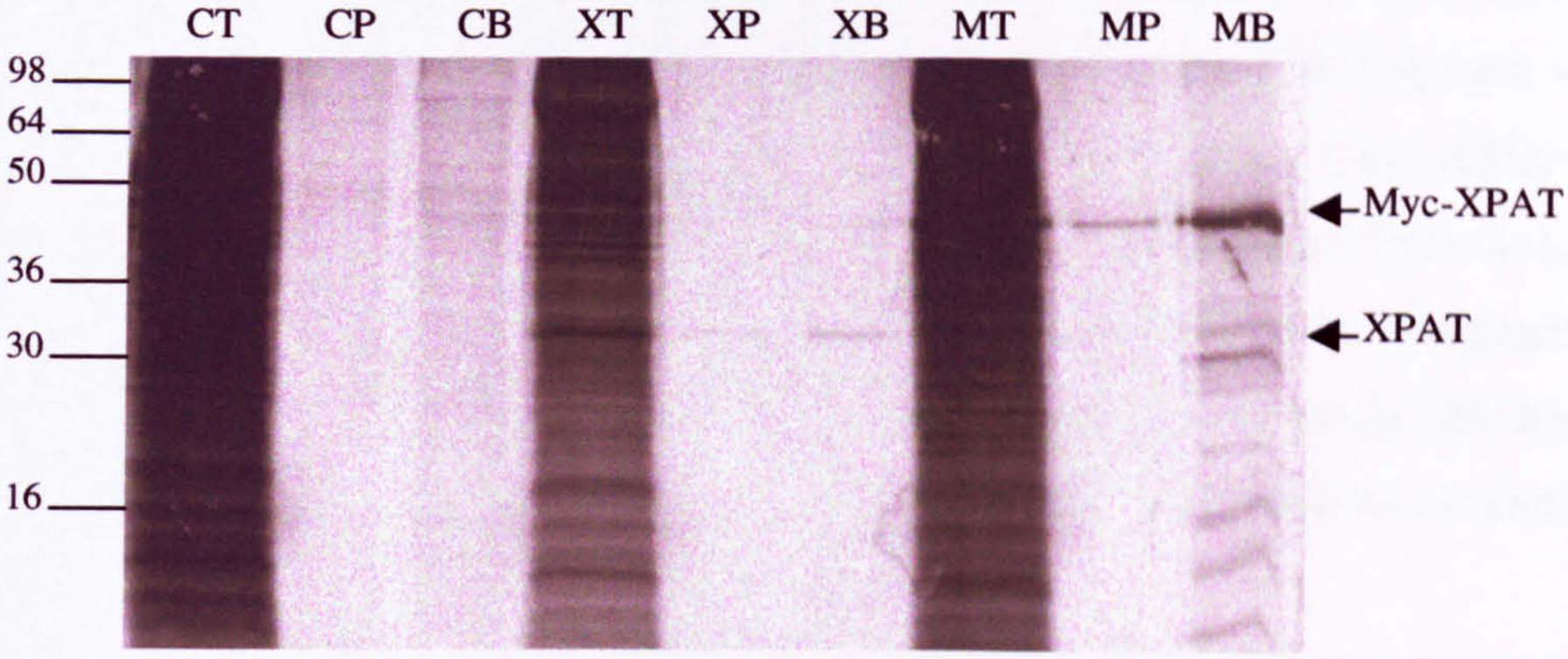
CT
CP
CB
XT
XP
XB
MT
MP
MB
98
64
50
36
30
16
Myc-XPAT
XPAT

8.4 Characterisation of antisera resulting from immunisation of mice

Peptide A and peptide B were each used to immunise 10 mice every four weeks. Small amounts of blood were taken 2 weeks after each immunisation and the resulting sera were characterised.

8.4.1 ELISA

As described for rabbit antisera (in 8.3.1) the serum taken from each mouse was isolated and characterised by ELISA. If antiserum showed a good response to peptide in ELISA they were then further characterised. Only 3/20 antisera showed good responses, all three were from mice immunised with peptide A and were named 1-1, 1-2 and 1-5. It was next determined whether any of these antisera could detect GST-XPAT on western blots.

8.4.2 The production of a GST-XPAT fusion protein

One of the reasons for producing GST-XPAT fusion protein in bacteria was that this could be detected non-radioactively and would not be contaminated with any oocyte proteins. This meant it would be useful for western blot analysis and any antisera which could detect it would be specific for XPAT and not a different *Xenopus* protein of the same molecular weight.

In order to make a GST-XPAT fusion protein, the entire ORF of Xpat was cloned into the expression vector pGEX-2T. The coding region for Xpat was amplified by PCR using primers that created 5′ and 3′ *Bgl*II sites. The resulting PCR fragment was cloned into the *BamH*I site of pGEX-2T, generating GST-Xpat. The pGEX-2T vector allows expression in bacteria, it contains GST downstream from a LacI promoter therefore expression of this fusion protein is IPTG inducible. The plasmid also encodes ampicillin resistance. Once the construct was made, an *EcoR*I digest was performed on the DNA to confirm that the orientation of the insert was correct.

pGEX-Xpat was transformed into three types of cells: DH5α, BL21 and AD202. Induction with IPTG was carried out at 37°C and bacterial samples were taken after 4 hours and assayed for protein production. The protein profiles of bacterial extracts changed only with respect to the induced protein, thus the presence of one extra band

was easily identified. The results of XPAT induction in DH5α cells are shown in Figure 8.5A. Similar results were seen for expression in all other cell types.

The protein gel shows that GST-XPAT is readily expressed in bacteria and runs at a similar size to that predicted - 62.5kDa (35kDa for XPAT plus 27.5kDa for GST). The protein is readily IPTG inducible, expressed to high levels and is stable. However, high levels of GST-XPAT protein were seen in the insoluble fractions but were indetectable in the soluble fractions (Figure 8.5A). Thus, GST-XPAT is insoluble and was found to be so in all bacterial cell types tested. However, GST control had high levels in the soluble fractions and low levels in the insoluble (see Figure 8.5B).

8.4.3 To characterise the antisera using GST-XPAT and western blot analysis

Three anti-peptide antisera from mice (1-1, 1-2 and 1-5) were tested by western blot analysis on bacteria overexpressing GST-XPAT. 1-2 showed a strong specific reaction to GST-XPAT; however, 1-1 and 1-5 did not detect GST-XPAT specifically (not shown).

1-2 antiserum was then used for further western blot analysis. Proteins from *Xenopus* oocytes overexpressing XPAT and myc-XPAT and embryos were resolved by SDS-PAGE alongside expressions of GST-XPAT and GST in DH5α cells. One such gel was stained with Coomassie blue and is shown in Figure 8.5C. The samples were all equalised so that equivalent amounts of protein were present in each lane. A duplicate gel was then run and blotted onto nitrocellulose and tested with 1-2 antiserum. The results of this western blot are shown in Figure 8.5D. Unfortunately, 1-2 could only detect GST-XPAT and was unable to detect protein in overexpressing oocytes or in embryos. Autoclaving the nitrocellulose prior to detection did not increase the sensitivity of detection, nor did increasing the concentration of primary or secondary antibody.

These results were discouraging as peptide raised antisera are considered to be more likely to work on the denatured proteins on western blots than in other techniques where the proteins are not denatured. Despite this, whole mount

Figure 8.5 (Opposite): The use of GST-XPAT to determine specificity of anti-peptide antisera raised in mice

(A) Bacterial expression of GST-XPAT
An SDS-PAGE gel that has been stained with Coomassie blue. 10µl of each sample was loaded onto the gel- thus each lane contains an equivalent amount of protein. M indicates protein size markers; the numbers on the left of the gel are the sizes in kDa of the protein size markers. The letters indicate which sample was loaded, in brackets after each letter designation is the volume of bacterial culture proteins were extracted from. For each sample: U, uninduced culture of DH5α (1ml); I, DH5α culture induced with IPTG (1ml); T, total protein (1ml); P, pellet (equivalent to 1ml); S, soluble fraction (equivalent to 1ml culture). Arrow indicates induced protein.

(B) Expression of GST in DH5α cells
This figure shows an SDS-PAGE gel that has been stained with Coomassie blue. 10µl of each sample was loaded onto the gel and each lane contains an equivalent amount of protein. The DH5α culture was induced with IPTG and 4 hours later samples were taken. M indicates protein size markers, the numbers on the left of the gel are sizes in kDa of the protein markers. The letters indicate which sample was loaded, in brackets after each letter designation is the volume of bacterial culture proteins were extracted from. For each sample: T, total protein (1ml); P, pellet (equivalent to 1ml); S, soluble fraction (equivalent to 1ml culture). Arrow indicates induced protein.

(C) Coomassie blue stained SDS-PAGE gel of *Xenopus* oocyte proteins, GST and GST-XPAT
Proteins were extracted from various stages of *Xenopus* oocytes and proteins from the equivalent of ½ an oocyte were loaded onto a gel. GST (1% of a 1ml DH5α culture) and GST-XPAT (1% of a 1ml DH5α culture) were also resolved on the gel. The numbers above the gel indicate which sample was loaded. The samples were as follows: 1, control stage VI *Xenopus* oocytes; 2, stage VI *Xenopus* oocytes injected with 20ng *Xpat* mRNA; 3, control stage VI *Xenopus* oocytes; 4, stage VI *Xenopus* oocytes injected with 20ng *myc-Xpat* mRNA; 5, DH5α cells expressing GST; 6, DH5α cells expressing GST-XPAT; 7, control stage III *Xenopus* oocytes; 8, control stage IV *Xenopus* oocytes; 9, control stage V *Xenopus* oocytes.

(D) Western blot analysis of serum raised against peptide B
A gel was loaded exactly as in (C) and resolved by SDS-PAGE. The gel was then transferred onto nitrocellulose membrane. The western blot was then incubated with serum (1-2) taken from a mouse immunised with peptide A. The serum was diluted by 1/100 and was taken from the final bleed following the 3rd boost. The blot was then incubated with Rabbit Anti-Mouse IgG HRP conjugate and visualisation of reactivity was performed by addition of DAB substrate. The numbers indicate which sample was loaded onto the original gel, as in (C).

(E) Control western blot
A gel was loaded with protein samples, prepared as described in (C), resolved by SDS-PAGE and then transferred onto nitrocellulose membrane. The western blot was then incubated with 1/100 pre-immune serum taken from a mouse prior to immunisation with peptide A. The blot was then incubated with Rabbit Anti-Mouse IgG HRP conjugate and visualisation of reactivity was performed by addition of DAB substrate. The numbers above the blot indicate which sample was loaded onto the original gel, as follows: 1, DH5α cells expressing GST; 2, DH5α cells expressing GST-XPAT; 3, control stage VI oocytes; 4, stage VI oocytes injected with 20 ng *Xpat* mRNA.

A

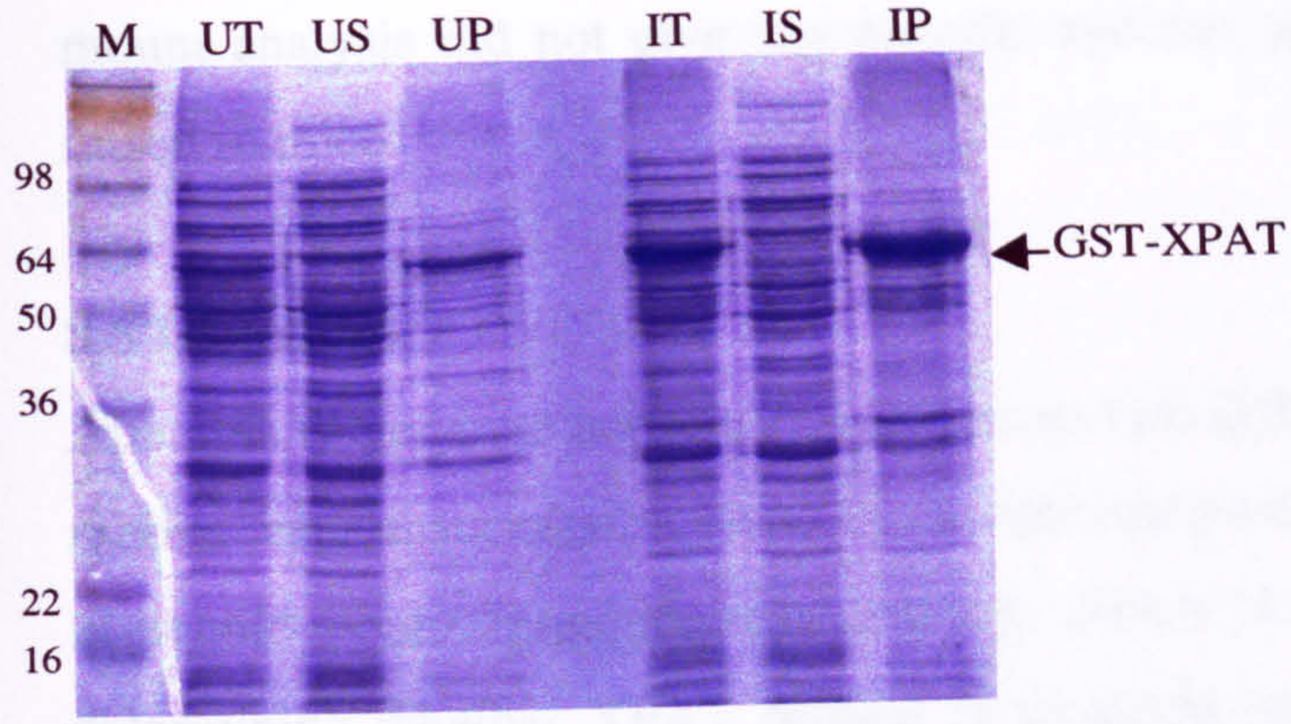
M
UT
US
UP
IT
IS
IP
98
64
50
36
22
16
GST-XPAT

B

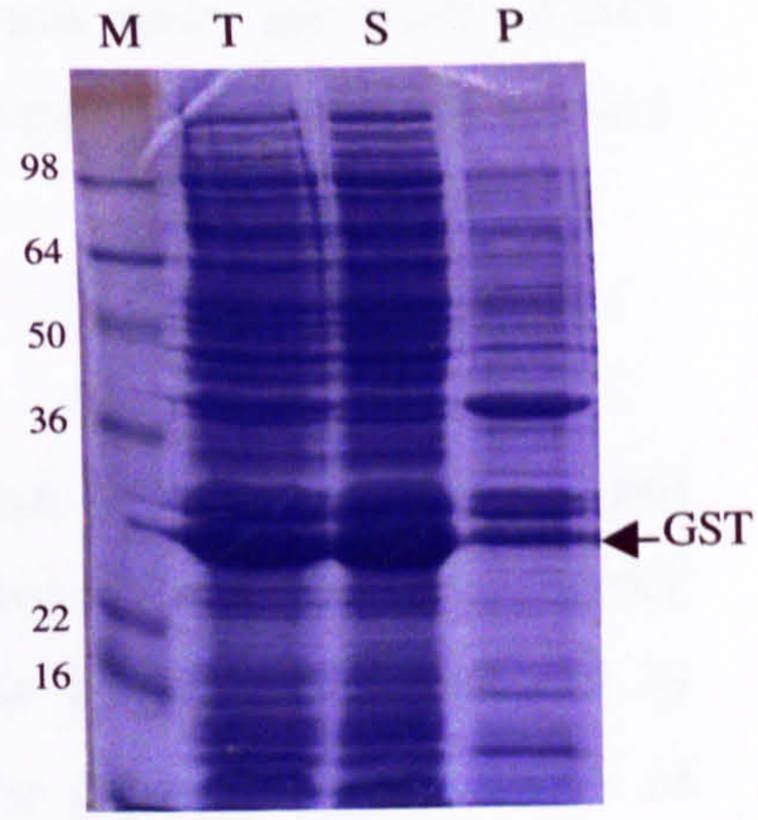
M
T
S
P
98
64
50
36
22
16
GST

C

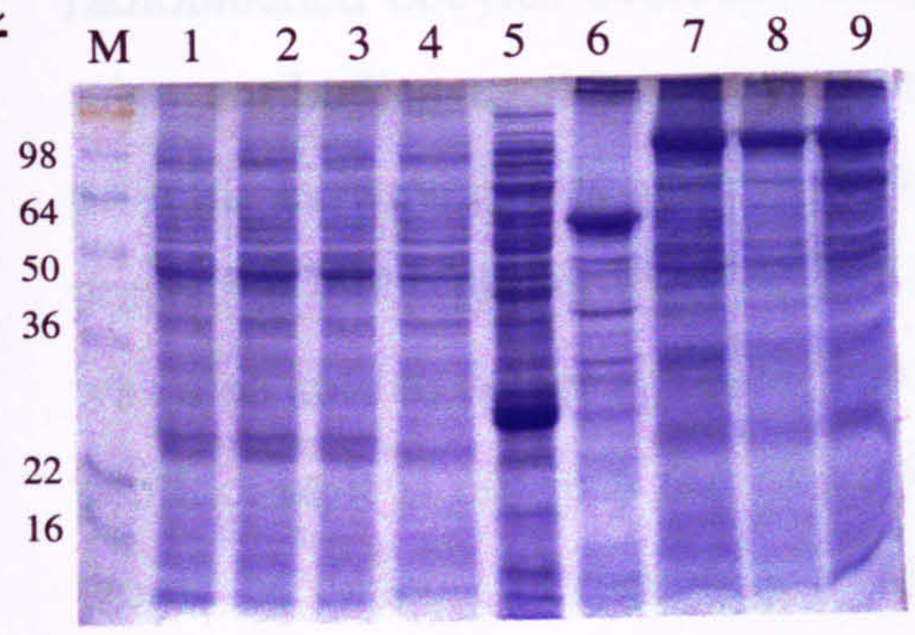
M
1
2
3
4
5
6
7
8
9
98
64
50
36
22
16

D

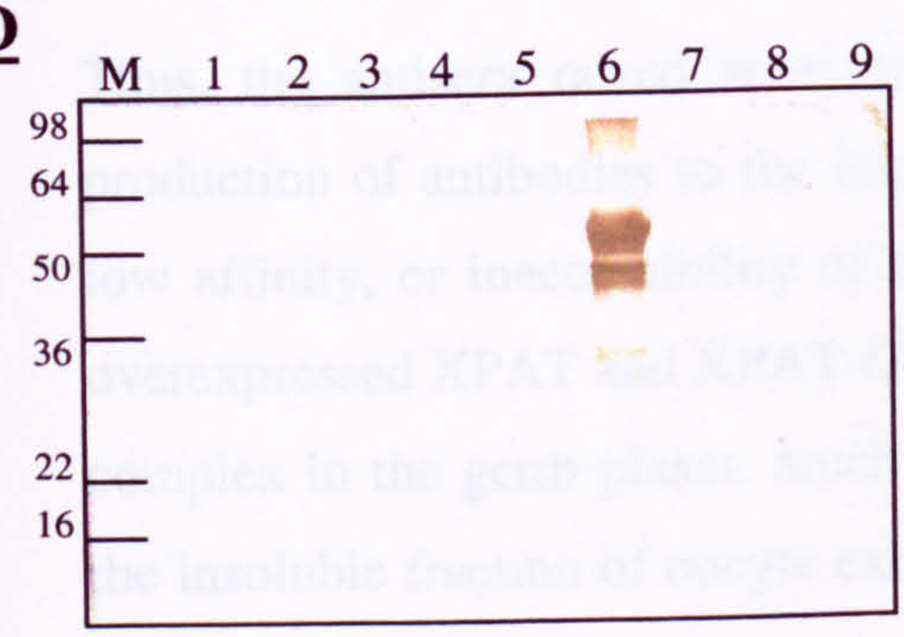
M
1
2
3
4
5
6
7
8
9
98
64
50
36
22
16

E

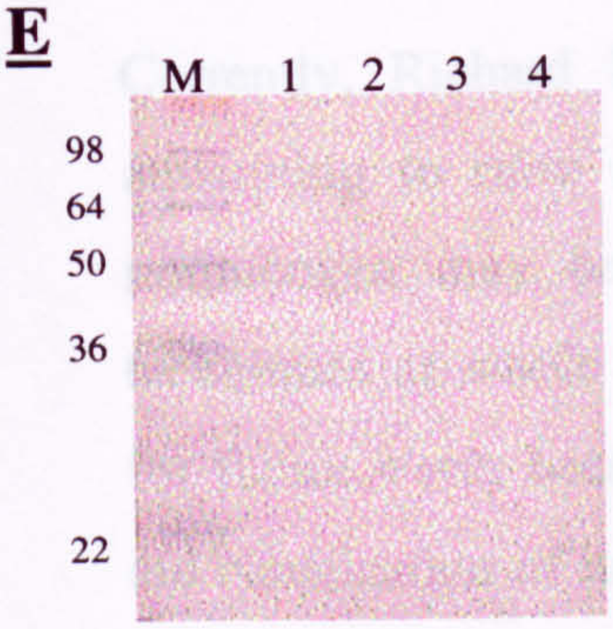
M
1
2
3
4
98
64
50
36
22

immunohistochemistry on *Xenopus* oocytes and embryos were attempted. Whole mount analysis did not give any specific staining pattern with any of the antisera raised in mice.

8.5 Discussion

Attempts to generate antisera raised against two different peptides in both mice and rabbits were unsuccessful. None of the antisera generated were able to detect XPAT in whole-mount immunohistochemistry, which is the technique most useful in determining whether XPAT protein is localised in the germ plasm and PGCs of *Xenopus*. The antisera raised to peptide B in rabbits could detect XPAT only in radiolabelled oocytes overexpressing XPAT. This did show that it was possible to raise antibodies to this peptide and they were capable of binding to the native protein. However, this protein was over-expressed in oocytes and was therefore present at much higher levels than endogenous XPAT would be. The antibody raised was also able to detect a protein by western blot analysis. This is not surprising for a peptide, as it is not in a native conformation and therefore one might expect that it would be capable of detecting a denatured protein rather than the native protein in immunoprecipitation assays.

Thus, the antisera raised were not very useful. This may be due to very low production of antibodies to the immunogen, the antibodies produced having only a low affinity, or inaccessibility of the protein. For example, it is possible that, like overexpressed XPAT and XPAT-GFP proteins, endogenous XPAT is in an insoluble complex in the germ plasm, much as *Xcat-2, Xcat-3* and *Vg1* RNAs are present in the insoluble fraction of oocyte extracts (Elinson *et al.,* 1993). GST-XPAT was also seen to be insoluble when expressed in all bacterial strains tested.

Currently, Richard Hames, a PhD student working with Hugh Woodland, is attempting to raise antisera to His-tagged XPAT. Antisera generated from this immunogen may be more likely to work on non-denatured proteins in such techniques as whole mount immunostaining. An antibody would be very desirable for future work, because knowing where and when the protein is expressed would aid clarification of its function and would allow experiments to be more effectively designed to perturb or increase the function of XPAT during development. An

XPAT antibody could also be used for a direct study of endogenous XPAT to try and determine any possible binding partners. For example, a pull-down assay of oocyte RNA and XPAT protein using an antibody could be performed and the immunoprecipitate could then be assayed for candidiate RNAs that could be bound by XPAT, using PCR analysis. Also, to be totally confident that the localisation of XPAT-GFP is identical to the endogenous XPAT expression pattern in *Xenopus* oocytes, it will be necessary to obtain an antibody that can detect XPAT. However, at present, XPAT's endogenous expression pattern remains unknown.

Chapter 9: Concluding Discussion

9.1 The expression pattern and localisation properties of XPAT

GFP fusion constructs have been thoroughly validated and the live cell imaging of GFP-tagged proteins is now used to generate primary data for determining the cellular localisation of gene products (Matus, 2001). Thus, in order to determine the expression pattern and localisation properties of XPAT protein in *Xenopus* oocytes, Xpat was tagged (at either its carboxy- or amino-terminus) with GFP and the resulting fusion proteins were expressed in *Xenopus* oocytes. GFP-XPAT localised predominantly to the nuclei of stage VI oocytes. However, XPAT-GFP, in addition to being present in the nucleus, formed small (1-2.5μm) particles which aggregated at the vegetal pole into larger (10-50μm) granules over the course of 3 days in culture. XPAT was transported to the vegetal pole of full-grown oocytes, but whether as particles, or as soluble protein existing in equilibrium with particles, cannot be said. The former seems more likely. The XPAT-GFP localisation data suggests that XPAT protein, at least when overexpressed, localises in a manner consistent with it being a component of the germ plasm. The granules of XPAT-GFP are larger than endogenous germ plasm granules seen in stage VI oocytes; they are more consistent with those observed in 2-cell embryos during germ plasm aggregation (Ressom and Dixon, 1988; Savage and Danilchik, 1993).

This is of considerable interest as no other known proteins have been observed to localise in this manner in *Xenopus*. Whilst Denegre *et al.* (1997) generated 3 monoclonal antibodies that recognised antigens localised to the vegetal cortex, which partially overlapped with germ plasm, the identity of the proteins recognised by these antibodies remains to be established.

The pattern of fusion protein distribution can hardly be accidental and, although the distribution of the endogenous protein is not yet known, the implication is that it is a germ granule component at some point. Thus, the data suggest that Xpat is present in germ granules at some stage, both as an RNA (Hudson and Woodland, 1998) and as a protein. The only other known gene whose products do this in any animal is *oskar*, which is a crucial effector of PGC formation in *Drosophila*. *oskar* RNA and the protein it encodes are both essential for germ granule formation and can direct its

ectopic development (Ephrussi *et al.*, 1991; Smith *et al.*, 1992; Ephrussi and Lehmann, 1992). An RNA-binding role has been suggested for Oskar, but is unproven. An intriguing parallel with *Xpat*, for which no homologues exist, is that there are no known *oskar* homologues outside the genus *Drosophila*. As far as germ lineage development is concerned, this is also true of the *C. elegans* protein PIE-1, which associates with the cytoskeleton and is also found in the nucleus (Mello *et al.*, 1996). It is related only to RNA-binding proteins (e.g. MEX-1, which is not nuclear), but is essential for germ line repression of transcription (Seydoux *et al.*, 1996) and it contains a functional transcriptional repressor domain (Batchelder *et al.*, 1999).

Little expression of XPAT-GFP was seen in smaller oocytes even though the injected mRNA contained no Xpat UTRs. Thus, either the Xpat ORF has regulatory sequences, which is most unusual, or XPAT protein is unstable in some embryonic cells, at least when overexpressed. Indeed, the stability of XPAT-GFP in stage VI oocytes was also greatly affected by changes in culture conditions. When XPAT-GFP-expressing oocytes, which had been cultured for three days in OCM, were transferred into Barth's saline for photography, the majority of XPAT-GFP expression disappeared very rapidly.

Since *Xpat-GFP* mRNA is also much more tightly localised than *GFP* mRNA this implies *Xpat* mRNA is anchored at its injection site. *Xpat-GFP* mRNA is translated at the site of its injection and XPAT-GFP protein must be anchored there, otherwise it would diffuse widely, like GFP. Particles would diffuse more slowly than non-particulate material, but this does not account for the fact that even non-particulate XPAT-GFP was tightly localised. It is possible that either *Xpat* mRNA or nascent peptides can bind to the cytoskeleton and thereby anchor XPAT protein at the injection site. This anchoring is likely to involve microfilaments, which anchor *Xlsirts, Xcat-2* and *Xwnt-11* mRNAs (Kloc and Etkin, 1995), and/or intermediate filaments, which are required for cortical anchoring of *Vg1* RNA (Yisraeli *et al.*, 1990; Kloc and Etkin, 1995). Vg1RBP is hypothesised to be involved in both *Vg1* mRNA transport and anchoring and can bind to microfilaments (Havin *et al.*, 1998; Deshler *et al.*, 1998). It is possible that XPAT protein could bind to *Xpat* mRNA (*in vitro* RNA-binding activity of XPAT has been demonstrated) and also to microfilaments and thus anchor *Xpat* mRNA at the vegetal pole. This hypothesis

could be tested by investigating sequence-specific RNA-binding activities of XPAT. The most obvious approach would be to use the PCR-based SELEX method (Klug and Famulok, 1994; Nieuwlandt *et al.*, 1995) to determine a consensus binding site. A more complex approach would be to use the yeast-3-hybrid system (SenGupta *et al.*, 1996), but this would be more difficult to set up.

Preliminary experiments on the mode of XPAT-GFP localisation were conducted using cytoskeletal inhibitors. This study indicated that microtubules, but not microfilaments, are essential for transport of XPAT-GFP from the equator (the site of mRNA injection) to the vegetal pole. When microtubules are disrupted, most XPAT-GFP becomes located in the nucleus. γ-tubulin is asymmetrically distributed along the A-V axis, with foci of γ-tubulin concentrated at the vegetal cortex of *Xenopus* oocytes (Gard, 1994; Gard *et al.*, 1995). The majority of microtubules have their minus ends directed towards the oocyte cortex (Pfeiffer and Gard, 1999). Thus, there could be a population of microtubules nucleated by γ-tubulin at the vegetal pole with their minus ends at the cortex in stage VI oocytes. This microtubule network could localise XPAT-GFP; transport of XPAT-GFP (and hence XPAT) along these tubules would likely involve dynein, a minus end-directed motor (Fox and Sale, 1987; Paschal and Vallee, 1987; Paschal *et al.*, 1987; Schroer *et al.*, 1989).

There are 3 usual mechanisms for intracellular localisation of mRNAs and proteins:

(1) Diffusion plus local binding

(2) Diffusion plus degradation

(3) Active transport

Mechanism (2) seems unlikely for localising XPAT, as it cannot build up a concentration above that seen with diffusion alone. The granules of XPAT-GFP were more intense than the fluorescence seen with GFP or the deletion variants of XPAT-GFP. XPAT-GFP protein is not degraded since oocytes remain fluorescent for at least 3-4 days post-injection, irrespective of injection site. Although the protein is not unstable, it is possible that *Xpat* mRNA is unstable when in the wrong place (i.e. not in germ granules). RNA localisation is an important mechanism by which proteins become spatially restricted in cells (St Johnston, 1995; King, 1996; King *et al.*, 1999), although anchorage of proteins to localised binding sites or directed transport

of proteins are other mechanisms that cells use to localise proteins (St Johnston, 1995). Normally, *Xpat* mRNA is inside the germ granules (Etkin, 2000), and XPAT-GFP data indicates that XPAT protein can similarly form granules in oocytes (unlike unfused GFP). Thus, the localisation of *Xpat* mRNA to the germ plasm could cause restriction of XPAT protein to the same location, but XPAT-GFP data indicate that XPAT protein can itself assist in this process without RNA localisation.

9.2 XPAT can enter the nucleus

XPAT contains a putative bipartite NLS at its carboxy-terminus. Several large N-terminal deletions of XPAT protein were constructed and, like GFP-XPAT, these became predominantly localised to the nucleus. ΔN1, which lacked the first 61 amino acids of XPAT, can form small particles, but these persist only when the mRNA is trapped in small protrusions of cytoplasm. This implies that ΔN1 particles are less stable than those of XPAT and thus a proportion of ΔN1 is non-particulate and progressively moves into the nucleus. Indeed XPAT-GFP that does not bind to the cytoskeleton enters the nucleus, as shown by using cytoskeletal inhibitors. These data imply that XPAT could be a nuclear component of *Xenopus* oocytes or PGCs, and suggest that nuclear entry of the fusion proteins is opposed by particle formation and/or binding to cytoplasmic components. The amino-terminal deletion proteins presumably have enhanced nuclear localisation due to less cytoplasmic binding activity.

At first glance, the localisation of XPAT to both vegetal granules and the nucleus seems hard to reconcile. In the early *C. elegans*, *Drosophila* and amphibian embryos, the germ line granules are found in the cytoplasm. However, at other stages of the life cycle the germ line granules can be associated with nuclei. In *Drosophila*, polar granules become associated with nuclei once the pole cells are formed (Mahowald, 1971; Hay *et al.*, 1988a). In *C. elegans*, P granules remain associated with germ cell nuclei as the gonad forms during larval and adult development, and then detach from the nuclei and become cytoplasmic once again in oocytes (Strome and Wood, 1982, 1983). The ultrastructure of the nuclear-associated P granules has been examined in gonads of adult *C. elegans* hermaphrodites (Pitt *et al.*, 2000). In germ nuclei at the pachytene stages of meiosis, each P granule appears to be associated with a cluster of

nuclear pores (Pitt *et al.*, 2000). Since about 75% of all nuclear pores are in these clusters, P granules could potentially have functions related to the RNAs that exit from, or enter through, those pores. In a similar manner, the germ granules of amphibians are associated with nuclei prior to becoming cytoplasmic (Eddy and Ito, 1971; Mahowald and Hennen, 1971). Thus, germ line granules are localised to nuclei through much of development, and so these granules may have nuclear-related functions. Thus, it is quite feasible for XPAT, likewise, to have a nuclear role.

The association of germ plasm with the nuclear transport suggests a role for germ plasm in the PGC-specific regulation of nuclear transport. For example, the *Drosophila* protein Gcl is a nuclear pore component in pole cells (Jongens *et al.*, 1994). Also, P granules have been shown to associate with nuclear pore material in the adult germ cells and retain this material in the cytoplasm after their detachment from the nuclear envelope (Pitt *et al.*, 2000). Whether this interesting observation is also true for *Xenopus* and *Drosophila* remains to be established.

9.3 The effect of XPAT-GFP expression on the endogenous germ plasm

In situ hybridisation revealed that XPAT-GFP expression in oocytes (when compared with GFP) significantly reduced the mean diameter of the disc of *Xcat-2* mRNA expression, which was used as a marker of the germ plasm. Granules of XPAT-GFP at the vegetal pole reduce this domain more than particles of XPAT-GFP expressed equatorially although, perhaps somewhat surprisingly, equatorial particles can affect endogenous germ plasm (at the vegetal cortex). It is possible that XPAT-GFP causes endogenous *Xcat-2* particles to aggregate and move closer together, thus causing a reduction in germ plasm diameter. If equatorial expression of XPAT-GFP can also cause this, the process might involve binding of XPAT-GFP to a cellular component. The sizes of the individual particles were not measured during this experiment, thus it will need to be repeated and granule diameter measured to confirm this hypothesis.

9.4 The effect that destruction of *Xpat* mRNA has on other germ plasm components *in vivo*

A different approach to analyse the role of *Xpat* in the germ plasm was to examine the effect degrading *Xpat* mRNA had on other germ plasm molecules. Injection of an

antisense oligo was able to specifically deplete *Xpat* mRNA from stage VI oocytes. This depletion appeared to have a specific effect on *DEADSouth* and *XVLG1* mRNAs, causing their levels to decrease; this was the exact opposite to the effect on these mRNAs following *Xpat* overexpression. Since the gene dosage in an oocyte is too small to have a significant impact on maternal mRNAs (Woodland, 1982), the only reasonable explanation for the observed changes in mRNA levels is that *Xpat* mRNA, or the protein it encodes, has a specific stabilising effect on *DEADSouth* and *XVLG1*. As XPAT protein can bind RNAs *in vitro*, it is perhaps more likely that XPAT protein could bind to *DEADSouth* and *XVLG1* transcripts and prevent their normal degradation by nucleases in the oocyte. Testing for sequence specific RNA binding properties of XPAT would confirm this hypothesis.

9.5 Does germ plasm contain different sorts of granules?

Data obtained whilst performing overexpression and depletion studies with *Xpat* suggest that there are different sorts of granules within the germ plasm of stage VI oocytes; *Xcat-2* appeared to have a significantly smaller RNA expression domain than both *Xpat* and *Xdazl*. To confirm this hypothesis double *in situ* hybridisation analysis of *Xcat-2* and *Xpat/Xdazl* would need to be performed. The localisation of *Xcat-2* to the periphery of the mitochondrial cloud during stage I of oogenesis has been reported previously (Kloc and Etkin, 1995; Kloc *et al.*, 2000a). This is in contrast to the distribution of both *Xlsirts* and *Xpat* RNAs, which cover the entire mitochondrial cloud area (Kloc and Etkin, 1995; Hudson and Woodland, 1998). Thus, both the early expression patterns of *Xcat-2* and *Xpat* and the diameter of the disc of RNA distribution at stage VI are different. These data indicate that *Xcat-2* and *Xpat* do not localise to the same granules, although a second possibility is that the individual granules, which formed in different domains in oogenesis aggregate to form the germ granules seen in fertilised eggs and embryos. *Xlsirts* are thought to have a structural role in the germ plasm, but are not found in the germinal granules (Kloc and Etkin, 1995). Hudson and Woodland (1998) suggested that *Xpat* might also have a structural role in the germ plasm. Although the similar patterns of localisation of *Xpat* and *Xlsirts* may support this hypothesis, after stage II their expression domains are different. Unlike *Xlsirts*, which is non-granular (Kloc *et al.*, 1998), *Xpat* is found as defined granules in a disc at the vegetal pole (Hudson and Woodland, 1998). However, the XPAT-GFP expression data do point to a role for

XPAT protein in forming, and perhaps structurally supporting, the germ granules during late oogenesis and/or supporting aggregation in early embryogenesis.

9.6 Roles of RNA-binding proteins

The RNA binding ability of XPAT protein was shown in an *in vitro* assay. The protein bound mostly to poly(C) suggesting that XPAT might also bind to C-rich RNAs *in vivo*. The ability of XPAT to bind RNA may be necessary for its function and could involve germ line-specific regulation of RNA processing, translation, storage or transport. It is not unexpected to find that the localised mRNA *Xpat* encodes a putative RNA-binding protein. RNAs for Nanos and Vasa, both implicated in RNA-binding and in establishing the germ cell lineage, are long-studied components of *Drosophila* pole plasm (reviewed in Rongo and Lehmann, 1996). Specifically in *Xenopus,* a *nanos*-like gene (*Xcat-2;* Mosquera *et al.,* 1993), a translation initiation factor-like putative RNA helicase *(DEADSouth*; MacArthur *et al.*, 2000) and *Xdazl*, an RNA encoding a putative RNA-binding protein (Houston *et al.,* 1998) are also expressed in the germ plasm. Thus, the presence of RNAs coding for RNA-binding proteins seems to be a common theme in germ cell determination by maternal cytoplasmic localisation. How the inheritance of these molecules establishes the germ line is still unknown, but the mechanism may involve translational inhibition or germ cell-specific regulation of mRNA splicing or stability.

Recently, it was shown that translational suppression by *nanos* is essential for entry of PGCs into the *Drosophila* gonad (Kobayashi *et al.,* 1996). The maternal RNA localisation of *Xpat*, combined with its continued presence in the PGCs after all other known markers cease to be expressed, suggest that it may function to specify the PGCs. However, *Xpat* may not be translated until after specification has occurred and may function in the later aspects of germ cell differentiation.

RNA-binding proteins in germ plasm could control gene expression at the post-transcriptional level. Analysis of *nanos* and *pos-1* mutants supports this hypothesis and indicates that translational regulation is important for the formation of PGCs (Tabara *et al.*, 1999). Similarly, Vasa (Carrera *et al.*, 2000) and Xdazl (Houston and King, 2000b) have been implicated in regulation of translation. Moreover, *cyclinB*

and *gcl*, both localised to *Drosophila* pole plasm (reviewed in Williamson and Lehmann, 1996), and *Xcat-2* (MacArthur *et al.*, 1999) and *Xdazl* (Houston and King, 2000b), germ plasm-specific RNAs in *Xenopus,* are under translational repression. It is thought that suppression of translation in the germ plasm prevents the expression of specific proteins, thus allowing the germ-line to be established.

An essential mechanism of post-transcriptional regulation of gene expression, utilised by germ cells of vertebrates and invertebrates, is the packaging of maternal mRNAs into stable non-translated cytoplasmic messenger ribonucleoprotein particles (Yurkova and Murray, 1997). Indeed there are specific germ line proteins responsible for packaging and repressing these RNAs (Standart and Jackson, 1994; Yurkova and Murray, 1997). Thus, a possible role for XPAT could be in binding to and packaging RNAs, such as *Xcat-2* or *Xdazl,* and preventing their translation. It will be necessary to obtain an antibody capable of detecting XPAT, and thus determine the spatial and temporal distribution of XPAT protein. Unfortunately, attempts to generate antisera capable of detecting endogenous levels of XPAT have so far been unsuccessful.

9.7 Summary: A role for XPAT?

In summary, the expression pattern of endogenous XPAT protein remains unknown, but the protein is likely to be a constituent of germ granules and to be important in the aggregation of germ plasm to form large granules. It could also be involved in the formation of the disc of granules of germ plasm mRNAs during late stages of oogenesis as the protein itself can form granules. Ultimately, the protein probably has functions in the nucleus of *Xenopus* oocytes or PGCs involving RNA binding. XPAT forms large aggregates in the cytoplasm, but not in the nucleus, so this process probably involves interactions with other abundant cytoplasmic components. It also interacts with the cytoskeleton, its long-range transport involving microtubules. Etkin (2000) has reported that *Xpat* mRNA is peripheral on the granules whereas *Xcat-2* is central. It is conceivable that the mRNA itself has no essential role after oocyte maturation, but that previously synthesised XPAT protein does. Obviously, light would be shed on this by knowing when *Xpat* is translated.

Bibliography

Ainger, K., Avossa, D., Morgan, F., Hill, S. J., Barry, C., Barbarese, E. and Carson, J. H. (1993). Transport and localization of exogenous myelin basic protein mRNA microinjected into oligodendrocytes. *J. Cell Biol.* **123**, 431-441.

Al-Mukhtar, K. A. K., and Webb, A. C. (1971). An ultrastructural study of primordial germ cells, oogonia and early oocytes in *Xenopus laevis*. *J. Embryol. Exp. Morphol.* **26**, 195-217.

Amikura, R., Kobayashi, S., Saito, H. and Okada, M. (1996). Changes in subcellular localization of mtlrRNA outside mitochondria in oogenesis and early embryogenesis of *Drosophila melanogaster*. *Dev. Growth Differ.* **38**, 489-498.

Amikura, R., Hanyu, K., Kashikawa, M. and Kobayashi, S. (2001a). Tudor protein is essential for the localization of mitochondrial RNAs in polar granules of *Drosophila* embryos. *Mech. Dev.* **107**, 97-104.

Amikura, R., Kashikawa, M., Nakamura, A. and Kobayashi, S. (2001b). Presence of mitochondria-type ribosomes outside mitochondria in germ plasm of *Drosophila* embryos. *Proc. Natl. Acad. Sci. USA* **98**, 9133-9138.

Balinsky, B. I., and Devis, R. J. (1963). Origin and differentiation of cytoplasmic structures in the oocytes of *Xenopus laevis*. *Acta Embryol. Morph. Exp.* **6**, 5-108.

Bardsley, A., McDonald, K., and Boswell, R. E. (1993). Distribution of tudor protein in the *Drosophila* embryo suggests separation of functions based on site of localization. *Development* 119, 207-219.

Barker, D.D., Wang, C., Moore, J., Dickinson, L.K. and Lehmann, R. (1992). Pumilio is essential for function but not for distribution of the *Drosophila* abdominal determinant Nanos. *Genes Dev.* **6**, 2312-2326.

Bashirullah, A., Cooperstock, R. L. And Lipshitz, H. D. (1998). RNA localisation in development. *Annu. Rev. Biochem.* **67**, 335-394.

Bassez, T., Paris, J., Omilli, F., Dorel, C., and Osborne, H. B. (1990). Posttranscriptional regulation of ornithine decarboxylase in *Xenopus* oocytes. *Development* **110**, 955-962.

Batchelder, C., Dunn, M. A., Choy, B., Suh, Y., Cassie, C., Shim, E. Y., Shin, T. H., Mello, C., Seydoux, G. and Blackwell, T. K. (1999). Transcriptional repression by the *Caenorhabditis elegans* germ-line protein PIE-1. *Genes Dev.* **13**, 202-212.

Bergsten, S.E. and Gavis, E.R. (1999). Role for mRNA localization in translational activation but not spatial restriction of *nanos* RNA. *Development* **126**, 659-669.

Billet, F. S., and Adam, E. (1976). The structure of the mitochondrial cloud of *Xenopus laevis* oocytes. *J. Embryol. Exp. Morphol.* **33**, 697-710.

Bonner, W.M. (1975). Protein migration into nuclei. I: Frog oocyte nuclei in vivo accumulate microinjected histones, allow entry to small proteins, and exclude large proteins. *J. Cell Biol.* **64**, 421-430.

Boswell, R. E., and Mahowald, A. P. (1985). *tudor,* A Gene Required for Assembly of the Germ Plasm in *Drosophila melanogaster*. Cell **43**, 97-104.

Braddock, M., Chambers, A., Wilson, W., Esnouf, M.P., Adams, S.E., Kingsman, A.J. and Kingsman, S.M. (1989). HIV-1 TAT "activates" presynthesized RNA in the nucleus. *Cell* **58**, 269-279.

Braddock, M., Muckenthaler, M., White, M.R., Thorburn, A.M., Sommerville, J., Kingsman, A.J. and Kingsman, S.M. (1994). Intron-less RNA injected into the nucleus of *Xenopus* oocytes accesses a regulated translation control pathway. *Nucleic Acids Res.***22**, 5255-5264.

Bradley, J.T., Kloc, M., Wolfe, K.G., Estridge, B.H. and Bilinski, S.M. (2001). Balbiani bodies in cricket oocytes: development, ultrastructure, and presence of localized RNAs. *Differentiation* **67**, 117-127.

Breitwieser, W., Markussen, F., Horstmann, H., and Ephrussi, A. (1996). Oskar protein interaction with Vasa represents an essential step in polar granules assembly. *Genes and Dev.* **10**, 2179-2188.

Brejc, K., Sixma, T.K., Kitts, P.A., Kain, S.R., Tsien, R.Y., Ormo, M. and Remington, S.J. (1997). Structural basis for dual excitation and photoisomerization of the *Aequorea victoria* green fluorescent protein. *Proc. Natl. Acad. Sci. USA* **94**, 2306-2311.

Bubunenko, M. and King, M.L. (2001). Biochemical characterization of a cellular structure retaining vegetally localized RNAs in *Xenopus* late stage oocytes. *J. Cell. Biochem.* **80**, 560-570.

Canman, J. C. and Bement, W. M. (1997). Microtubules suppress actinomycin-based cortical flow in *Xenopus* oocytes. *J. Cell Sci.* **110**, 1907-1917.

Carrera, P., Johnstone, O., Nakamura, A., Casanova, J., Jäckle, H. and Lasko, P. (2000). VASA mediates translation through interaction with a *Drosophila* yIF2 homolog. *Mol. Cell* **5**, 181-187.

Chalfie, M., Tu, Y., Euskirchen, G., Ward, W.W. and Prasher, D.C. (1994). Green fluorescent protein as a marker for gene expression. *Science* **263**, 802-805.

Chan, A. P., Kloc, M and Etkin, L. D. (1999). *fatvg* encodes a new localized RNA that uses a 25-nucleotide element (FVLE-1) to localize to the vegetal cortex of *Xenopus* oocytes. *Development* **126**, 4943-4953.

Chan, A.P., Kloc, M., Bilinski, S. and Etkin, L.D. (2001). The vegetally localized mRNA *fatvg* is associated with the germ plasm in the early embryo and is later expressed in the fat body. *Mech. Dev.* **100**, 137-140.

Chapell, R., Bueno, O. F., Alvarez-Hernandez, X., Robinson, L. C. and Leidenheimer, N. J. (1998). Activation of protein kinase C induces γ-aminobutyric acid type A receptor internalisation in *Xenopus* oocytes. *J. Biol. Chem.* **273**, 32595-32601.

Clark, I., Giniger, E., Ruohola-Baker, H., Jan, L. Y., and Jan, Y. N. (1994). Transient posterior localisation of a kinesin fusion protein reflects anteroposterior polarity of the *Drosophila* oocyte. *Curr. Biol.* **4**, 289-300.

Cody, C.W., Prasher, D.C., Westler, W.M., Prendergast, F.G. and Ward, W.W. (1993). Chemical structure of the hexapeptide chromophore of the *Aequorea* green-fluorescent protein. *Biochemistry* **32**, 1212-1218.

Coggins, L. W. (1973). An ultrastructural and radioautographic study of early oogenesis in the toad *Xenopus laevis*. *J. Cell Sci.* **12**, 71-93.

Colman, A., Morser, J., Lane, C., Besley, J., Wylie, C. and Valle, G. (1981). Fate of secretory proteins trapped in oocytes of *Xenopus laevis* by disruption of the cytoskeleton or by imbalanced subunit synthesis. *J. Cell Biol.* **91**, 770-780.

Cook, J.P., Savage, P.M., Lord, J.M. and Roberts, L.M. (1993). Biologically-active interleukin 2-ricin a-chain fusion proteins may require intracellular proteolytic cleavage to exhibit a cytotoxic effect. *Bioconj. Chem.* **4**, 440-447.

Cote, C.A., Gautreau, D., Denegre, J.M., Kress, T.L., Terry, N.A. and Mowry, K.L. (1999). A *Xenopus* protein related to hnRNP I has a role in cytoplasmic RNA localization. *Mol. Cell* **4**, 431-437.

Dahanukar, A. and Wharton, R.P. (1996). The Nanos gradient in *Drosophila* embryos is generated by translational regulation. *Genes Dev.* **10**, 2610-2620.

Dahanukar, A., Walker, J.A. and Wharton, R.P. (1999). Smaug, a novel RNA-binding protein that operates a translational switch in *Drosophila*. *Mol Cell.* **4**, 209-218

Danos, M.C. and Yost, H. J. (1995) Linkage of cardiac left-right asymmetry and dorsal-anterior development in *Xenopus*. *Development* **121**, 1467-1474.

Denegre, J. M., Ludwig, E. R. and Mowry, K. L. (1997). Localized maternal proteins in *Xenopus* revealed by subtractive immunization. *Dev. Biol.* **192**, 446-454.

Deshler, J. O., Highett, M. I., Abramson, T. and Schnapp, B. J. (1998). A highly conserved RNA-binding protein for cytoplasmic mRNA localization in vertebrates. *Curr. Biol.* **8**, 489-496.

Deshler, J. O., Highett, M. I. and Schnapp, B. J. (1997). Localization of *Xenopus* Vg1 mRNA by vera protein and the endoplasmic reticulum. *Science* **276**, 1128-1131.

Ding, D., Whittaker, K. L., and Lipshitz, H. D. (1994). Mitochondrially encoded 16S large ribosomal RNA is concentrated in the posterior polar plasm of early *Drosophila* embryos but is not required for pole cell specification. *Dev. Biol.* **163,** 503-515.

Dingwall, C. and Laskey, R.A. (1991). Nuclear targeting sequences – a consensus? *Trends Biochem. Sci.* **16,** 478-481.

Dingwall, C., Sharnick, S.V. and Laskey, R.A. (1982). A polypeptide domain that specifies migration of nucleoplasmin into the nucleus. *Cell* **30,** 449-458.

Dixon, K. E. (1994). Evolutionary aspects of primordial germ cell formation. *Ciba Found. Symp.* **182,** 92-120.

Drummond, D.R., McCrae, M.A. and Colman, A. (1985). Stability and movement of mRNAs and their encoded proteins in *Xenopus* oocytes. *J. Cell Biol.* **100,** 1148-1156.

Dumont, J. N. (1972). Oogenesis in *Xenopus laevis* (Daudin). I. Stages of oocyte development in laboratory maintained animals. *J. Morphol.* **136,** 153-180.

Dziadek, M., and Dixon, K. E. (1977). An autoradiographic analysis of nucleic acid synthesis in the presumptive primordial germ cells of *Xenopus laevis*. *J. Embryol. Exp. Morphol.* **37,** 13-31.

Eddy, E. M., and Ito, S. (1971). Fine structural and radioautographic observations of dense perinuclear cytoplasmic material in tadpole oocytes. *J. Cell. Biol.* **49,** 90-108.

Elinson, R. P., King, M. L. and Forristall, C. (1993). Isolated vegetal cortex from *Xenopus* oocytes selectively retains localized mRNA. *Dev. Biol.* **160,** 554-562.

Elisha, Z., Havin, L., Ringel, I. and Yisraeli, J. K. (1995). Vg1 RNA binding protein mediates the association of Vg1 RNA with microtubules in *Xenopus* oocytes. *EMBO J.* **14,** 5109-5114.

Ephrussi, A. and Lehmann, R. (1992). Induction of germ cell formation by *oskar*. *Nature* **358,** 387-392.

Ephrussi, A., Dickinson, L. K. and Lehmann, R. (1991). *oskar* organizes the germ plasm and directs localization of the posterior determinant *nanos*. *Cell* **66,** 37-50.

Erdelyi, M., Michon, A.M., Guichet, A., Glotzer, J.B. and Ephrussi, A. (1995). Requirement for *Drosophila* cytoplasmic tropomyosin in *oskar* mRNA localization. *Nature* **377,** 524-527.

Etkin, L.D. (1997). A new face for the endoplasmic reticulum: RNA localization. *Science* **276,** 1092-1093.

Etkin, L. R. (2000). Role of maternal gene products in embryonic patterning. In *6th Intenational Xenopus conference,* Colorado USA.

Evans Bergsten, S., Huang, T., Chatterjee, S. and Gavis, E.R. (2001). Recognition and long-range interactions of a minimal *nanos* RNA localization signal element. *Development* **128**, 427-435.

Feng, W., Benko, A.L., Lee, J.H., Stanford, D.R. and Hopper, A.K. (1999). Antagonistic effects of NES and NLS motifs determine *S. cerevisiae* Rna1p subcellular distribution. *J. Cell Sci.* **112**, 339-347.

Fire, A., Xu, S., Montgomery, M. K., Kostas, S. A., Driver, S. E. and Mello, C. C. (1998). Potent and specific genetic interference by double-stranded RNA in *Caenorhabditis elegans. Nature* **391**, 806-811.

Forbes, A. and Lehmann, R. (1998). Nanos and Pumilio have critical roles in the development and function of *Drosophila* germline stem cells. *Development* **125**, 679-690.

Forristall, C., Pondel, M., Chen, L. and King, M. L. (1995). Patterns of localization and cytoskeletal association of two vegetally localized RNAs, *Vg1* and *Xcat-2*. *Development* **121**, 201-208.

Fox, L. A., and Sale, W. S. (1987). Direction of force generated by the inner row of dynein arms on flagellar microtubules. *J. Cell. Biol.* **105**, 1781-1788.

Gard, D. L. (1991). Organization, nucleation, and acetylation of microtubules in *Xenopus laevis* oocytes: A study by confocal immunofluorescence microscopy. *Dev. Biol.* **143**, 346-363.

Gard, D.L. (1993). Confocal immunofluorescence microscopy of microtubules in amphibian oocytes and eggs. *Methods Cell Biol.* **38**, 241-264.

Gard, D. L. (1994). γ-tubulin is asymmetrically distributed in the cortex of Xenopus oocytes. *Dev. Biol.* **161**, 131-140.

Gard, D.L. (1995). Axis formation during amphibian oogenesis: reevaluating the role of the cytoskeleton. *Curr. Top. Dev. Biol.* **30**, 215-252.

Gard, D. L., Cha, B. J. and King, E. (1997). The organization and Animal-Vegetal asymmetry of cytokeratin filaments in Stage VI *Xenopus* oocytes is dependent upon F-actin and microtubules. *Dev. Biol.* **184**, 95-114.

Gard, D. L., Cha, B. J. and Schroeder, M. M. (1995). Confocal immunofluorescence microscopy of microtubules, microtubule-associated proteins, and microtubule-organizing centers during amphibian oogenesis and early development. *Curr. Top. Dev. Biol.* **31**, 383-431.

Gautreau, D., Cote, C. A. and Mowry, K. L. (1997). Two copies of a subelement from the *Vg1* RNA localization sequence are sufficient to direct vegetal localization in *Xenopus* oocytes. *Development* **124**, 5013-5020.

Gavis, E. R. (1997). Expeditions to the pole: RNA localization in *Xenopus* and *Drosophila. Trends Cell Biol.*7, 485-492.

Gavis, E.R. and Lehmann, R. (1992). Localization of *nanos* RNA controls embryonic polarity. *Cell* **71**, 301-313.

Gavis, E.R. and Lehmann, R. (1994). Translational regulation of *nanos* by RNA localization. *Nature* **369**, 315-8.

Gavis, E. R., Lunsford, L., Bergsten, S. E., and Lehmann, R. (1996). A conserved 90 nucleotide element mediates translational repression of *nanos* RNA. *Development* **122**, 2791-2800.

Gerhart, J., Danilchik, M., Roberts, J., Rowning, B., and Vincent, J. P. (1986). *Gametogenesis and the early embryo*, pp. 305-319. New York: Alan R. Liss, Inc.

Glotzer, J. B. and Ephrussi, A. (1996). mRNA localization and the cytoskeleton. *Sem. Cell Dev. Biol.* **7**, 357-365.

Glotzer, J.B., Saffrich, R., Glotzer, M. and Ephrussi, A. (1997). Cytoplasmic flows localize injected *oskar* RNA in *Drosophila* oocytes. *Curr Biol.* **7**, 326-337.

Godsave, S.F., Wylie, C.C., Lane, E.B. and Anderton, B.H. (1984). Intermediate filaments in the *Xenopus* oocyte: the appearance and distribution of cytokeratin-containing filaments. *J Embryol Exp Morphol.* **83**, 157-167.

Golumbeski, G. S., Bardsley, A., Tax, F., and Boswell, R. E. (1991). *tudor*, a posterior-group gene of *Drosophila melanogaster*, encodes a novel protein and an mRNA localised during mid-oogenesis. *Genes and Dev.* **5**, 2060-2070.

Gottlieb, E. (1992). The 3' untranslated region of localised maternal messages contains a conserved motif involved in mRNA localization. *Proc. Natl. Acad. Sci. USA* **89**, 7164-7168.

Guo, S. and Kemphues, K.J. (1995). *par-1*, a gene required for establishing polarity in *C. elegans* embryos, encodes a putative Ser/Thr kinase that is asymmetrically distributed. *Cell* **81**, 611-620.

Harland, R.M. (1991). In-situ hybridisation- an improved whole-mount method for *Xenopus* embryos. *Meth. Cell Biol.* **36**, 685-695.

Harris, A.N. and Macdonald, P.M. (2001). *Aubergine* encodes a *Drosophila* polar granule component required for pole cell formation and related to eIF2C. *Development* **128**, 2823-2832.

Hausen, P., and Riebesell, M. (1991) *The Early Development of Xenopus laevis. An Atlas of the Histology*. New York: Springer-Verlag.

Havin, L., Git, A., Elisha, Z., Oberman, F., Yaniv, K., Schwartz, S. P., Standart, N. and Yisraeli, J. K. (1998). RNA-binding protein conserved in both microtubule- and microfilament-based RNA localization. *Gen. Dev.* **12**, 1593-1598.

Hay, B., Ackerman, L., Barbel, S., Yan, L. Y., and Jan, Y. N. (1988a). Identification of a component of *Drosophila* polar granules. *Development* **103**, 625-640.

Hay, B., Jan, L. Y., and Jan, Y. N. (1988b). A protein component of *Drosophila* polar granules is encoded by *vasa* and has extensive similarity to ATP-dependent helicases. *Cell* **55**, 577-587.

Hay, B., Jan, L. Y., and Jan, Y. N. (1990). Localization of vasa, a component of *Drosophila* polar granules, in maternal-effect mutants that alter embryonic anteroposterior polarity. *Development* **109**, 425-433.

Heasman, J., and Wylie, C. C. (1983). Amphibian primordial germ cells- what can they tell us about directed cell migration? In *Current problems in germ cell differentiation. British Society for Developmental Biology: Symposium 7*, pp. 73-90. Edited by A. McLaren and C.C. Wylie. Cambridge University Press.

Heasman, J., Holwill, S. and Wylie, C.C. (1991). Fertilization of cultured *Xenopus* oocytes and use in studies of maternally inherited molecules. In *Methods in Cell Biology*, pp. 685-695. Edited by B.K. Kay and H.B. Peng. New York: Academic Press.

Heasman, J., Kofron, M. and Wylie, C. (2000). β-catenin signalling activity dissected in the early *Xenopus* embryo: a novel antisense approach. *Dev. Biol.* **222**, 124-134.

Heasman, J., Quarmby, J., and Wylie, C. C. (1984). The mitochondrial cloud of *Xenopus* oocytes: The source of the germinal granule material. *Dev. Biol.* **105**, 458-469.

Heidemann, S. R. and Gallas, P. T. (1980). The effect of taxol on living eggs of *Xenopus laevis*. *Dev. Biol.* **80**, 489-494.

Heim, R., Prasher, D.C., and Tsien, R.Y. (1994). Wavelength mutations and posttranslational autoxidation of green fluorescent protein. *Proc. Natl. Acad. Sci. USA* **91**, 12501-12504.

Horb, M. E. and Thomsen, G. H. (1997). A vegetally localized T-box transcription factor in *Xenopus* eggs specifies mesoderm and endoderm and is essential for embryonic mesoderm formation. *Development* **124**, 1689-1698.

Houston, D. W. and King, M. L. (2000a). Germ plasm and molecular determinants of germ cell fate. *Curr. Top. Dev. Biol.* **50**, 155-181.

Houston, D. W. and King, M. L. (2000b). A critical role for *Xdaz*l, a germ plasm-localized RNA, in the differentiation of primordial germ cells in *Xenopus*. *Development* **127**, 447-456.

Houston, D. W., Zhang, J., Maines J. Z., Wasserman, S. A. and King, M. L. (1998). A *Xenopus DAZ*-like gene encodes an RNA component of germ plasm and is a functional homologue of *Drosophila boule*. *Development* **125**, 171-180.

Hudson, C. and Woodland, H. R. (1998). *Xpat*, a gene expressed specifically in germ plasm and primordial germ cells of *Xenopus laevis*. *Mech. Dev.* **73**, 159-168.

Hudson, J. W., Alarcon, V. B., and Elinson, R. P. (1996). Identification of new localized RNAs in the Xenopus oocyte by differential display PCR. *Dev. Genet.* **19**, 190-198.

Hyatt, B.A. and Yost, H.J. (1998). The left-right coordinator: the role of Vg1 in organizing left-right axis formation. *Cell* **93**, 37-46.

Hyatt, B., Lohr, J., and Yost, H. J. (1996). Initiation of vertebrate left-right axis formation by maternal Vg1. *Nature* **384**, 62-65.

Iida, T. and Kobayashi, S. (1998). Essential role of mitochondrially encoded large rRNA for germ-line formation in *Drosophila* embryos. *Proc. Natl. Acad. Sci. USA* **95**, 11274-11278.

Ikenishi, K., and Tanaka, T. S. (1997). Involvement of the protein of *Xenopus vasa* homolog (*Xenopus vasa*-like gene 1, *XVLG1*) in the differentiation of primordial germ cells. *Develop. Growth Differ.* **39**, 625-633.

Ikenishi, K. and Tanaka, T. S. (2000). Spatio-temporal expression of *Xenopus vasa* homolog, *XVLG1*, in oocytes and embryos: The presence of *XVLG1* RNA in somatic cells as well as germline cells. *Develop. Growth Differ.* **42**, 95-103.

Ikenishi, K., Tanaka, T. S. and Komiya, T. (1996). Spatio-temporal distribution of the protein *of Xenopus vasa* homologue (*Xenopus vasa*-like gene 1, *XVLG1*) in embryos. *Develop. Growth Differ.* **38**, 527-535.

Inouye, S. and Tsuji, F.I. (1994). *Aequorea* green fluorescent protein. Expression of the gene and fluorescence characteristics of the recombinant protein. *FEBS Lett.* **341**, 277-280.

Islam, N. and Moss, T. (1996). Technical Tips: Enzymatic removal of vitelline membranes and other protocol modifications for whole mount in situ hybridization of *Xenopus* embryos. *TIG* **12**, 459.

Jeffery, W. R., Tomlinson, C. R. and Brodeur, R. D. (1983). Localization of actin messenger RNA during early ascidian development. *Dev. Biol.* **99**, 408-420.

Jessus, C., Thibier, C., Huchon, D. and Ozon, R. (1988). Taxol reveals cortical sites of microtubule assembly in *Xenopus* oocytes. Role of the nucleus. *Cell. Differ. Dev.* **25**, 57-63.

Jongens, T., Ackerman, L., Swedlow, J., Ian, L., and Jan, Y. (1994). *Germ cell-less* encodes a cell type-specific nuclear pore associated protein and functions early in the germ-cell specification pathway of *Drosophila. Genes Dev.* **8**, 2123-2136.

Jongens, T. A., Hay, B., Jan, L. Y., and Jan, Y. N. (1992). The germ cell-less gene product: A posteriorly localized component necessary for germ cell development in *Drosophila. Cell* **70**, 569-584.

Joseph, E.M. and Melton, D.A. (1998). Mutant Vg1 ligands disrupt endoderm and mesoderm formation in *Xenopus* embryos. *Development* **125**, 2677-2685

Kashikawa, M., Amikura, R. and Kobayashi, S. (2001) Mitochondrial small ribosomal RNA is a component of germinal granules in *Xenopus* embryos. *Mech. Dev.* **101**, 71-77.

Kashikawa, M., Amikura, R., Nakamura, A. and Kobayashi, S. (1999). Mitochondrial small ribosomal RNA is present on polar granules in early cleavage embryos of *Drosophila melanogaster. Develop. Growth Differ.* **41**, 495-502.

Kennerdell, J. R. and Carthew, R. W. (1998). Use of dsRNA-mediated genetic interference to demonstrate that *frizzled* and *frizzled 2* act in the wingless pathway. *Cell* **95**, 1017-1026.

Kim-Ha, J., Kerr, K. and Macdonald, P.M. (1995). Translational regulation of *oskar* mRNA by bruno, an ovarian RNA-binding protein, is essential. *Cell* **81**, 403-412.

King, M. L. (1995). mRNA localization during frog oogenesis. In *Localized RNAs*, pp 137-148. Edited by H. D. Lipshitz. Austin: Landes Publishing.

King, M. L. (1996). Molecular basis for cytoplasmic localization. *Dev. Gen.* **19**, 183-189.

King, M. L., and Barklis, E. (1985). Regional distribution of maternal messenger RNA in the amphibian oocyte. *Dev. Biol.* **112**, 203-212.

King, M. L., Zhou, Y. and Bubunenko, M. (1999). Polarizing genetic information in the egg: RNA localization in the frog oocyte. *BioEssays* **21**, 546-557.

Kloc, M. and Etkin, L. D. (1994). Delocalization of *Vg1* mRNA from the vegetal cortex in *Xenopus* oocytes after destruction of *Xlsirt* RNA. *Science* **265**, 1101-1103.

Kloc, M. and Etkin, L. D. (1995). Two distinct pathways for the localization of RNAs at the vegetal cortex in *Xenopus* oocytes. *Development* **121**, 287-297.

Kloc, M. and Etkin, L. D. (1998). Apparent continuity between the messenger transport organizer and late RNA localization pathways during oogenesis in *Xenopus*. *Mech. Dev.* **73**, 95-106.

Kloc, M. and Etkin, L. D. (1999). Analysis of localized RNAs in *Xenopus* oocytes. In *A comparative methods approach to the study of oocytes and embryos*, pp. 256-267. Edited by J. D. Richter. New York: Oxford University Press.

Kloc, M., Bilinski, S., Chan, A. P.-Y. and Etkin, L. D. (2000a). The targeting of *Xcat2* mRNA to the germinal granules depends on a *cis*-acting germinal granule localization element within the 3′UTR. *Dev. Biol.* **217**, 221-229.

Kloc, M., Bilinski, S., Chan, A.P. and Etkin, .D. (2000b). Mitochondrial ribosomal RNA in the germinal granules in *Xenopus* embryos revisited. *Differentiation* **67**, 80-83.

Kloc, M., Bilinski, S., Chan, A.P., Allen, L.H., Zearfoss, N.R. and Etkin, L.D. (2001). RNA localization and germ cell determination in Xenopus. *Int. Rev. Cytol.* **203**, 63-91.

Kloc, M., Larabell, C. and Etkin, L. D. (1996). Elaboration of the messenger transport organizer pathway for localization of RNA to the vegetal cortex of *Xenopus* oocytes. *Dev. Biol.* **180**, 119-130.

Kloc, M., Larabell, C., Chan, A. P.-Y. and Etkin, L. D. (1998). Contribution of METRO pathway localized molecules to the organization of the germ cell lineage. *Mech. Dev.* **75**, 81-93.

Kloc, M., Spohr, G., and Etkin, L. D. (1993). Translocation of repetitive RNA sequences with the germ plasm in *Xenopus* oocytes. *Science* **262**, 1712-1714.

Klug, S.J. and Famulok, M. (1994). All you wanted to know about SELEX. *Mol. Biol. Rep.* **20**, 97-107.

Klymkowsky, M.W. (1995). Intermediate filament organization, reorganization, and function in the clawed frog *Xenopus*. *Curr. Top. Dev. Biol.* **310**, 455-486.

Klymkowsky, M.W., Maynell, L.A. and Polson, A.G. (1987). Polar asymmetry in the organization of the cortical cytokeratin system of *Xenopus laevis* oocytes and embryos. *Development* **100**, 543-557.

Kobayashi, S., Amikura, R. and Mukai, M. (1998). Localization of mitochondrial large ribosomal RNA in germ plasm of *Xenopus* embryos. *Curr. Biol.* **8**, 1117-1120.

Kobayashi, S., Amikura, R. and Okada, M. (1993). Presence of mitochondrial large ribosomal RNA outside mitochondria in germ plasm of *Drosophila melanogaster*. *Science* **260**, 1521-1524.

Kobayashi, S., Amikura, R. and Okada, M. (1994). Localization of mitochondrial large rRNA in germinal granules and the consequent segregation of germ line. *Int. J. Dev. Biol.* **38**, 193-199.

Kobayashi, S., Amikura, R., Nakamura, A., Saito, H., and Okada, M. (1995). Mislocalizaton of *oskar* product in the anterior pole results in ectopic localization of mitochondrial large ribosomal RNA in *Drosophila* embryos. *Dev. Biol.* **169,** 384-386.

Kobayashi, S., and Okada, M. (1989). Restoration of pole-cell-forming ability to UV-irradiated *Drosophila* embryos by injection of *mitochondrial 1rRNA. Development* **107,** 733-742.

Kobayashi, S., Yamada, M., Asaoka, M., and Kitamura, T. (1996). Essential role of the posterior morphogen *nanos* for germline development in *Drosophila. Nature* **380,** 708-711.

Kofron, M., Spagnuolo, A., Klymkowsky, M., Wylie, C. and Heasman, J. (1997). The roles of maternal alpha-catenin and plakoglobin in the early Xenopus embryo. *Development* **124**, 1553-1560.

Komiya, T., Itoh, K., Ikenishi, K. and Furusawa, M. (1994). Isolation and characterization of a novel gene of the DEAD box protein family which is specifically expressed in germ cells of *Xenopus laevis. Dev. Biol.* **162,** 354-363.

Ku, M., and Melton, D. A. (1993). *Xwnt-11:* A maternally expressed *Xenopus* wnt gene. *Development* **119,** 1161-1173.

Lasko, P., and Ashburner, M. (1988). The product of the *Drosophila* gene *vasa* is very similar to eukaryotic initiation factor-4A. *Nature* **335,** 611-617.

Lasko, P.F. and Ashburner, M. (1990). Posterior localization of vasa protein correlates with, but is not sufficient for, pole cell development. *Genes Dev.* **4**, 905-921.

Lemaire, P. and Gurdon, J.B. (1994) A role for cytoplasmic determinants in mesoderm patterning: cell-autonomous activation of the goosecoid and Xwnt-8 genes along the dorsoventral axis of early *Xenopus* embryos. *Development* **120**, 1191-1199.

Liang, L., Diehl-Jones, W. and Lasko, P. (1994). Localization of vasa protein to the *Drosophila* pole plasm is independent of its RNA-binding and helicase activities. *Development* **120,** 1201-1211.

Lie, Y.S. and Macdonald, P.M. (1999). Translational regulation of *oskar* mRNA occurs independent of the cap and poly(A) tail in *Drosophila* ovarian extracts. *Development* **126**, 4989-4996.

Litman, P., Behar, L., Elisha, Z., Yisraeli, J. K. and Ginzburg, I. (1996). Exogenous Tau RNA is localized in oocytes: possible evidence for evolutionary conservation of localization mechanisms. *Dev. Biol.* **176**, 86-94.

Lohr, J. L., Danos, M. C. and Yost, H. J. (1997) Left-right asymmetry of a nodal-related gene is regulated by dorsoanterior midline structures during Xenopus development. *Development* **124**, 1465-1472

Long, R. M., Singer, R. H., Meng, X., Gonzalez, I., Nasmyth, K. And Jansen, R.-P. (1997). Mating type switching in yeast is controlled by asymmetric localization of ASH1 mRNA. *Science* **277**, 383-387.

Ludin, B., Doll, T., Meili, R., Kaech, S. and Matus, A. (1996). Application of novel vectors for GFP-tagging of proteins to study microtubule-associated proteins. *Gene* **173**, 107-111.

Lustig, K. D., Kroll, K. L., Sun, E. E. and Kirschner, M. W. (1996). Expression of a *Xenopus* T-related gene (*Xombi*) involved in mesodermal patterning and blastopore lip formation. *Dev.*, **122**, 4001-4012.

MacArthur, H., Bubunenko, M., Houston, D. W. and King, M. L. (1999). Xcat2 RNA is a translationally sequestered germ plasm component in *Xenopus. Mech. Dev.* **84**, 75-88.

MacArthur, H., Houston, D. W., Bubunenko, M., Mosquera, L. and King, M. L. (2000). *DEADsouth* is a germ plasm specific DEAD-box RNA helicase in *Xenopus* related to eIF4A. *Mech. Dev.* **95**, 291-295.

Mahowald, A. P. (1971). Polar granules of *Drosophila.* IV. Cytochemical studies showing loss of RNA from polar granules during early stages of embryogenesis. *J. Exp. Zool.* **176**, 345-52.

Mahowald, A. P., and Hennen, S. (1971). Ultrastructure of the "germ plasm" in eggs and embryos of *Rana pipiens. Dev. Biol.* **24**, 37-53.

Markussen, F.-H., Michon, A.-M., Breitwieser, W. and Ephrussi, A. (1995). Translational control of *oskar* generates Short OSK, the isoform that induces pole plasm assembly. *Development* **121**, 3723-3732.

Matus, A. (2001). GFP moves on. *Trends Cell Biol.* **11**, 183.

Mello, C. C., Schubert, C., Draper, B., Zhang, W., Label, R., and Priess, J. R. (1996). The PIE-l protein and germline specification in *C. elegans* embryos. *Nature* **382**, 710-712.

Melton, D. A. (1987). Translocation of a localized maternal mRNA to the vegetal pole of *Xenopus* oocytes. *Nature* **328**, 80-82.

Micklem, D. R. (1995). Review: mRNA localisation during development. *Dev. Biol.* **172**, 377-395.

Micklem, D.R., Adams, J., Grunert, S. and St Johnston, D. (2000). Distinct roles of two conserved Staufen domains in *oskar* mRNA localization and translation. *EMBO J.* **19**, 1366-1377.

Miller, J. R., Rowning, B. A., Larabell, C. A., Yang-Snyder, J. A., Bates, R. L. and Moon, R. T. (1999). Establishment of the Dorsal-Ventral axis in *Xenopus* embryos coincides with the dorsal enrichment of dishevelled that is dependent on cortical rotation. *J. Cell Biol.* **146**, 427-437.

Mimori-Kiyosue, Y., Shiina, N. and Tsukita, S. (2000). Adenomatous Polyposis Coli (APC) protein moves along microtubules and concentrates at their growing ends in epithelial cells. *J. Cell Biol.* **148**, 505-517.

Mishima, M. and Nishida, E. (1999). Coronin localizes to leading edges and is involved in cell spreading and lamellipodium extension in vertebrate cells. *J. Cell Sci.* **112**, 2833-2842.

Montgomery, M.K., Xu, S. and Fire, A. (1998). RNA as a target of double-stranded RNA-mediated genetic interference in *Caenorhabditis elegans*. *Proc. Natl. Acad. Sci. USA* **95**, 15502-15507.

Morise, H., Shimomura, O., Johnson, F.H. and Winant, J. (1974). Intermolecular energy transfer in the bioluminescent system of *Aequorea*. *Biochemistry* **13**, 2656-2662.

Mosquera, L., Forristall, C., Zhou, Y. and King, M. L. (1993). An mRNA localized to the vegetal cortex of *Xenopus* oocytes encodes a protein with a *nanos*-like zinc finger domain. *Development* **117**, 377-386.

Mowry, K.L. (1996). Complex formation between stage-specific oocyte factors and a *Xenopus* mRNA localization element. *Proc. Natl. Acad. Sci. USA* **93**, 14608-14613.

Mowry, K. L. and Melton, D. A. (1992). Vegetal messenger RNA localization directed by a 340-nt RNA sequence element *in Xenopus* oocytes. *Science* **255**, 991-994.

Mukai, M., Kashikawa, M. and Kobayashi, S. (1999). Induction of indora expression in pole cells by the mesoderm is required for female germ-line development in *Drosophila melanogaster*. *Development* **126**, 1023-1029.

Murata, Y. and Wharton, R.P. (1995). Binding of pumilio to maternal *hunchback* mRNA is required for posterior patterning in *Drosophila* embryos. *Cell* **80**, 747-756.

Nakahata S, Katsu Y, Mita K, Inoue K, Nagahama Y, Yamashita M. (2001). Biochemical identification of *Xenopus* Pumilio as a sequence-specific *cyclin B1* mRNA-binding protein that physically interacts with a Nanos homolog, Xcat-2, and a cytoplasmic polyadenylation element-binding protein. *J. Biol. Chem.* **276**, 20945-20953.

Nakamura, A., Amikura, R., Mukai, M., Kobayashi, S. and Lasko, P.F. (1996). Requirement for a noncoding RNA in *Drosophila* polar granules for germ cell establishment. *Science* **274**, 2075-2079.

Nakatani, J., Mizuseki, K., Tsuda, H., Nakanishi, S. and Sasai, Y. (2000). *Xenopus* Xenf; an early endodermal nuclear factor that is regulated in a pathway distinct from Sox17 and Mix-related gene pathways. *Mech. Dev.* **91**, 81-89.

Nakielny S. and Dreyfuss, G. (1997). Nuclear export of proteins and RNAs. *Curr. Opin. Cell Biol.* **9**, 420-429.

Nieuwkoop, P. D. and Faber, J. (1967). *Normal Table of Xenopus laevis (Daudin).* Amsterdam: North Holland.

Nieuwlandt, D., Wecker, M. and Gold, L. (1995). In vitro selection of RNA ligands to substance P. *Biochemistry* 34, 5651-5659.

Oates, A. C., Bruce, A. E. E. and Ho, R. K. (2000). Too much interference: injection of double-stranded RNA has non-specific effects in the zebrafish embryo. *Dev. Biol.* **224**, 20-28.

Okabe, S. and Hirokawa, N. (1989). Axonal transport. *Curr. Opin. Cell Biol.* **1**, 91-97.

Ormo, M., Cubitt, A.B., Kallio, K., Gross, L.A., Tsien, R.Y. and Remington, S.J. (1996). Crystal structure of the *Aequorea victoria* green fluorescent protein. *Science* **273**, 1392-1395.

Palacek, J. and Ubbels, G. A. (1997). Dynamic changes in the tubulin cytoskeleton during oogenesis and early development in the anuran amphibian *Xenopus laevis* (Daudin). *Folia Hist. Cytobiol.* **35**, 3-18.

Palecek, J., Habrova, V., Nedvidek, J. and Romanovsky, A. (1985). Dynamics of tubulin structures in *Xenopus laevis* oogenesis. *J. Embryol. Exp. Morphol.* **87**, 75-86.

Paschal, B. M., and Vallee, R. B. (1987). Retrograde transport by the microtubule-associated protein MAP 1C. *Nature* **330**, 181-183.

Paschal, B. M., Shpetner, H. S., and Vallee, R. B. (1987). MAP 1C is a microtubule-activated ATPase which translocates microtubules in vitro and has dynein-like properties. *J. Cell. Biol.* **105**, 1273-1282.

Peter, A.B., Schittny, J.C., Niggli, V., Reuter, H. and Sigel, E. (1991). The polarized distribution of poly(A+)-mRNA-induced functional ion channels in the *Xenopus* oocyte plasma membrane is prevented by anticytoskeletal drugs. *J. Cell. Biol.* **114**, 455-464.

Pfeiffer, D. C., and Gard, D. L. (1999). Microtubules in Xenopus oocytes are oriented with their minus-ends toward the cortex. *Motil. Cytoskel.* **44**, 34-43.

Pitt, J. N., Schisa, J. A. and Priess, J. R. (2000). P granules in the germ cells of *Caenorhabditis elegans* adults are associated with clusters of nuclear pores and contain RNA. *Dev. Biol.* **219**, 315-333.

Pokrywka, N. J., and Stephenson, E. C. (1995). Microtubules are a general component of mRNA localization systems in *Drosophila* oocytes. *Dev. Biol.* **167**, 363-370.

Pondel, M. D. and King, M. L. (1988). Localized maternal mRNA related to transforming growth factor mRNA is concentrated in a cytokeratin-enriched fraction from *Xenopus* oocytes. *Proc. Natl. Acad. Sci. USA* **85**, 7612-7616.

Pownall, M. E., Isaacs, H. V. and Slack, J. M. W. (1998). Two phases of *Hox* gene regulation during early *Xenopus* development. *Curr. Biol.* **8**, 673-676.

Prasher, D.C., Eckenrode, V.K., Ward, W.W., Prendergast, F.G. and Cormier, M.J. (1992). Primary structure of the *Aequorea victoria* green-fluorescent protein. *Gene* **111**, 229-233.

Raff, J.W. and Glover, D.M. (1989). Centrosomes, and not nuclei, initiate pole cell formation in *Drosophila* embryos. *Cell* **57**, 611-619.

Rebagliati, M. R., Weeks, D. L., Harvey, R. P. and Melton, D. A. (1985). Identification and cloning of localized maternal RNAs from *Xenopus* eggs. *Cell* **42**, 769-777.

Ressom, R. E. and Dixon, K. E. (1988). Relocation and reorganization of germ plasm in *Xenopus* embryos after fertilization. *Development* **103**, 507-518.

Robb, D. L., Heasman, J., Raats, J. and Wylie, C. (1996). A kinesin-like protein is required for germ plasm aggregation in *Xenopus. Cell* **87**, 823-831.

Robbins, J., Dilworth, S.M., Laskey, R.A. and Dingwall, C. (1991). Two interdependent basic domains in nucleoplasmin nuclear targeting sequence: identification of a class of bipartite nuclear targeting sequence. *Cell* **64**, 615-623.

Robertson, S. E., Dockendorff, T. C., Leatherman, J. L., Faulkner, D. F., and Jongens, T. A. (1999). *germ cell-less* is required only during the establishment of the germ cell lineage of *Drosophila* and has activities which are dependent and independent of its localization to the nuclear envelope. *Dev. Biol.* **215**, 288-297.

Roeder, A.D. and Gard, D.L.(1994) Confocal microscopy of F-actin distribution in *Xenopus* oocytes. *Zygote* **2**, 111-124.

Rongo, C., and Lehmann, R. (1996). Regulated synthesis, transport and assembly of the *Drosophila* germ plasm. *Trends Genet.* **12**, 102-109.

Rongo, C., Broihier, H.T., Moore, L., Van Doren, M., Forbes, A. and Lehmann, R. (1997). Germ plasm assembly and germ cell migration in *Drosophila. Cold Spring Harb. Symp. Quant. Biol.* **62**, 1-11.

Rongo, C., Gavis, E. R., and Lehmann, R. (1995). Localization of *oskar* RNA regulates oskar translation and requires oskar protein. *Development* **121**, 2737-2746.

Ross, A. F., Oleynikov, Y., Kislauskis, E. H., Taneja, K. L., and Singer, R. H. (1997). Characterization of a β-actin mRNA Zipcode-Binding Protein. *Mol. Cell. Biol.* **17**, 2158-2165.

Saffman, E. E. and Lasko, P. (1999). Germline development in vertebrates and invertebrates. *Cell. Mol. Life Sci.* **55**, 1141-1163.

Saffman, E.E., Styhler, S., Rother, K., Li, W., Richard, S. and Lasko, P. (1998). Premature translation of *oskar* in oocytes lacking the RNA-binding protein bicaudal-C. *Mol. Cell. Biol.* **18**, 4855-4862.

Sambrook, J., Fritsch, E.F. and Maniatis, T. (1989). *Molecular Cloning: A Laboratory Manual, 2nd edition.* New York: Cold Spring Harbor Laboratory Press.

Savage, R. M. and Danilchik, M. V. (1993). Dynamics of germ plasm localization and its inhibition by ultraviolet irradiation in early cleavage *Xenopus* embryos. *Dev. Biol.* **157**, 371-382.

Sayers, L. G., Miyawaki, A., Muto, A., Takeshita, H., Yamamoto, A., Michikawa, T., Furuichi, T. and Mikoshiba, K. (1997). Intracellular targeting and homotetramer formation of a truncated inositol 1,4,5-triphosphate receptor – green fluorescent protein chimera in *Xenopus laevis* oocytes: evidence for the involvement of the transmembrane spanning domain in endoplasmic reticulum targeting and homotetramer complex formation. *Biochem. J.* **323**, 273-280.

Schnapp, B. J. (1999). RNA localization: A glimpse of the machinery. *Curr. Biol.* **9**, R725-R727.

Schnapp, B. J., and Reese, T. S. (1989). Dynein is the motor for retrograde axonal transport of organelles. *Proc. Natl. Acad. Sci. USA*. **86**, 1548-1552.

Schnapp, B. J., Arn, E. A., Deshler, J. O. and Highett, M. I. (1997). RNA localization in *Xenopus* oocytes. *Sem. Cell. Dev. Biol.* **8**, 529-540.

Schroer, T. A., Steuer, E. R., and Sheetz, M. P. (1989). Cytoplasmic dynein is a minus end-directed motor for membranous organelles. *Cell* **56**, 937-946.

Schwartz, S. P., Aisenthal, L., Elisha, Z. Oberman, F. and Yisraeli, J. K. (1992). A 69-kDA RNA-binding protein from *Xenopus* oocytes recognizes a common motif in two vegetally localized maternal mRNAs. *Proc. Natl. Acad. Sci. USA* **89**, 11895-11899.

SenGupta, D.J., Zhang, B., Kraemer, B., Pochart, P., Fields, S. and Wickens, M. (1996). A three-hybrid system to detect RNA-protein interactions in vivo. *Proc. Natl. Acad. Sci. USA* **93**, 8496-8501.

Seydoux, G. and Dunn, M.A. (1997). Transcriptionally repressed germ cells lack a subpopulation of phosphorylated RNA polymerase II in early embryos of *Caenorhabditis elegans* and *Drosophila melanogaster*. *Development* **124**, 2191-2201.

Seydoux, G. and Strome, S. (1999). Launching the germline in *Caenorhabditis elegans*: regulation of gene expression in early germ cells. *Development* **126**, 3275-3283.

Seydoux, G., Mello, C. C., Pettitt, J., Wood, W. B., Priess, J. R., and Fire, A. (1996). Repression of gene expression in the embryonic germ lineage of *C. elegans*. *Nature* **382**, 713-716.

Sharp, P. A. (1999). RNAi and double-strand RNA. *Gen. Dev.* **13**, 139-141.

Shimomura, O., Johnson, F. H. and Saiga, Y. (1962). Extraction, purification and properties of aequorin, a bioluminescent protein from the luminous hydromedusan, *Aequorea*. *J. Cell. Comp. Physiol.* **59**, 223-239.

Shulman, J.M., Benton, R. and St Johnston, D. (2000). The *Drosophila* homolog of *C. elegans* PAR-1 organizes the oocyte cytoskeleton and directs *oskar* mRNA localization to the posterior pole. *Cell* **101**, 377-388.

Siomi, H., Matunis, M.J., Michael, W.M. and Dreyfuss, G. (1993). The pre-mRNA binding K protein contains a novel evolutionary conserved motif. *Nuc. Acid Res.* **21**, 1193-1198.

Sive, H. L., Grainger, R.M. and Harland, R. M. (2000). *Early Development of Xenopus laevis: A Laboratory Manual.* New York: Cold Spring Harbor Laboratory Press.

Smibert, C.A., Wilson, J.E., Kerr, K. and Macdonald, P.M. (1996). Smaug protein represses translation of unlocalized *nanos* mRNA in the *Drosophila* embryo. *Genes Dev.* **10**, 2600-2609.

Smith, L. D. and Williams, M. A. (1975). Germinal plasm and determination of the primordial germ cells. In *The Developmental Biology of Reproduction*, pp 3-24. New York: Academic Press, Inc.

Smith, J. L., Wilson, J. E. and Macdonald, P. M. (1992). Overexpression of *oskar* directs ectopic activation of *nanos* and presumptive pole cell formation in *Drosophila* embryos. *Cell* **70**, 849-859.

Standart, N., and Jackson, R. J. (1994). Regulation of translation by specific protein/mRNA interactions. *Biochimie* **76**, 867-879

Stearns, T., Evans, L. and Kirschner, M. (1991). Gamma-tubulin is a highly conserved component of the centrosome. *Cell* **65**, 825-836.

Stennard, F., Carnac, G. and Gurdon, J.B. (1996). The *Xenopus* T-box gene, *Antopodean*, encodes a vegetally localised maternal mRNA and can trigger mesoderm formation. *Development* **122**, 4179-4188.

St Johnston, D. (1995). The intracellular localization of messenger RNAs. *Cell* **81**, 161-170

Strome, S., and Wood, W. B. (1982). Immunofluorescence visualization of germ-line-specific cytoplasmic granules in embryos, larvae and adults of *Caenorhabditis elegans. Proc. Natl. Acad. Sci.USA* **79**, 1558-1562.

Strome, S., and Wood, W. B. (1983). Generation of asymmetry and segregation of germ-line granules in early *C. elegans* embryos. *Cell* **35**, 15-25.

Styhler, S., Nakamura, A., Swan, A., Suter, B. and Lasko, P. (1998). *vasa* is required for GURKEN accumulation in the oocyte, and is involved in oocyte differentiation and germline cyst development. *Development* **125**, 1569-1578.

Summerton, J. and Weller, D. (1997). Morpholino antisense oligomers: design, preparation, and properties. *Antisense Nuc. acid drug dev.* **7**: 187-195.

Sundell, C.L. and Singer, R.H. (1991). Requirement of microfilaments in sorting of actin messenger RNA. *Science* **253**, 1275-1277.

Swanson, M. S. and Dreyfuss, G. (1988). Classification and purification of proteins of heterogeneous nuclear ribonucleoprotein particles by RNA-binding specificities. *Mol. Cell. Biol.* **8**, 2237-2241.

Tabara, H., Hill, R. J., Mello, C. C., Priess, J. R. and Kohara, Y. (1999). *pos-1* encodes a cytoplasmic zinc-finger protein essential for germline specification in *C. elegans. Development* **126**, 1-11.

Tautz, D. and Pfeifle, C. (1989). A non-radioactive *in situ* hybridization method for the localization of specific RNAs in *Drosophila* embryos reveals translational control of the segmentation gene hunchback. *Chromosoma* **98**, 81-85.

Taylor, M., Paulauskis, J., Weller, D., Kobzik, L. (1996). In vitro efficacy of Morpholino-modified antisense oligomers directed against tumor necrosis factor-alpha mRNA. *J. Biol. Chem.* **271**, 17445-17452.

Theurkauf, W. E., Alberts, B. M., Jan, Y. N. and Jongens, T. A. (1993). A central role for microtubules in the differentiation of *Drosophila* oocytes. *Development* **118**, 1169-1180.

Theurkauf, W. E., Smiley, S., Wong, M. L. and Alberts, B. M. (1992). Reorganization of the cytoskeleton during *Drosophila* oogenesis: implications for axis specification and intercellular transport. *Development* **115**, 923-936.

Thomsen, G. H., and Melton, D. (1993). Processed Vg1 protein is an axial mesoderm inducer in Xenopus. *Cell* **74**, 433-441.

Tomancak ,P., Guichet, A., Zavorszky, P. and Ephrussi, A. (1998). Oocyte polarity depends on regulation of *gurken* by Vasa. *Development* **125**, 1723-1732.

Torpey, N.P., Heasman, J. and Wylie, C.C. (1992). Distinct distribution of vimentin and cytokeratin in *Xenopus* oocytes and early embryos. *J Cell Sci.* **101**, 151-160.

Tourte, M., Mignotte, F., and Mounolou, J.-C. (1984). Heterogeneous distribution and replication activity of mitochondria in *Xenopus laevis* oocytes. *Eur. J. Cell. Biol.* **34**, 171-178.

Tsien, R.Y. (1998). The green fluorescent protein. *Annu. Rev. Biochem.* **67**, 509-544.

Tuschl, T., Zamore, P.D., Lehmann, R., Bartel, D.P. and Sharp, P.A. (1999). Targeted mRNA degradation by double-stranded RNA *in vitro*. *Genes Dev.* **13**, 3191-3197.

Vallee, R.B. and Bloom, G.S. (1991). Mechanisms of fast and slow axonal transport. *Ann. Rev. Neurosci.* **14**, 59-92.

Van Doren, M., Williamson, A.L. and Lehmann, R. (1998). Regulation of zygotic gene expression in *Drosophila* primordial germ cells. *Curr. Biol.* **8**, 243-246.

van Eeden, F.J., Palacios, I.M., Petronczki, M., Weston, M.J. and St Johnston, D. (2001). Barentsz is essential for the posterior localization of *oskar* mRNA and colocalizes with it to the posterior pole. *J. Cell Biol.* **154**, 511-523.

Wang, C. and Lehmann, R. (1991) Nanos is the localized posterior determinant in *Drosophila*. *Cell* **66**, 637-647.

Wang, C., Dickinson, L.K. and Lehmann, R. (1994). Genetics of *nanos* localization in *Drosophila*. *Dev Dyn.* **199**, 103-115.

Wargelius, A., Ellingsen, S. and Fjose, A. (1999). Double-stranded RNA induces specific developmental defects in zebrafish embryos. *Biochem. Biophys. Res. Commun.* **263**, 156-161.

Webster, P.J., Liang, L., Berg, C.A., Lasko, P. and Macdonald, P.M. (1997). Translational repressor bruno plays multiple roles in development and is widely conserved. *Genes Dev.* **11**, 2510-2521.

Weeks, D. L. and Melton, D. A. (1987). A maternal mRNA localized to the vegetal hemisphere in *Xenopus* eggs codes for a growth factor related to TGF-β. *Cell* **51**, 861-867.

Wharton, R.P. and Struhl, G. (1991) RNA regulatory elements mediate control of *Drosophila* body pattern by the posterior morphogen nanos. *Cell* **67**, 955-967

Whitington, P. M. and Dixon, K. E. (1975). Quantitative studies of germ plasm and germ cells during early embryogenesis of *Xenopus laevis*. *J. Embryol. Exp. Morphol.* **33**, 57-74.

Wianny, F. and Zernicka-Goetz, M. (2000). Specific interference with gene function by double-stranded RNA in early mouse development. *Nat. Cell Biol.* **2**, 70-75.

Williamson, A., and Lehmann, R. (1996). Germ cell development in *Drosophila. Annu. Rev. Cell Dev. Biol.* **12**, 365-91.

Wilson, J.E., Connell, J.E. and Macdonald, P.M. (1996). aubergine enhances *oskar* translation in the *Drosophila* ovary. *Development* **122**, 1631-1639.

Woodland, H. (1982).The translational control phase of early development. *Biosci. Rep.* **2**, 471-491.

Woodland, H.R. and Adamson, E.D. (1977). The synthesis and storage of histones during the oogenesis of *Xenopus laevis. Dev. Biol.* **57**, 118-135.

Wylie, C. (1999). Germ cells. *Cell* **96**, 165-174.

Wylie, C. C., and Heasman, J. (1976). The formation of the gonadal ridge in *Xenopus laevis.* I. A. light and transmission electron microscope study. *J. Embryol. Exp. Morphol.* **35**, 125-138.

Yang, F., Moss, L.G. and Phillips, G.N. Jr. (1996). The molecular structure of green fluorescent protein. *Nat. Biotechnol.* **14**, 1246-1251.

Yisraeli, J. K. and Melton, D. A. (1988). The maternal mRNA Vg1 is correctly localized following injection into *Xenopus* oocytes. *Nature* **336**, 592-595.

Yisraeli, J. K., Sokol, S. and Melton, D. A. (1990). A two-step model for the localization of maternal mRNA in *Xenopus* oocytes: Involvement of microtubules and microfilaments in the translocation and anchoring of Vg1 mRNA. *Development* **108**, 289-298.

Yurkova, M. S., and Murray, M. T. (1997). A translation regulatory particle containing the Xenopus oocyte Y box protein mRNP3+4. *J. Biol. Chem.* **272**, 10870-10876.

Zamore, P.D., Williamson, J.R. and Lehmann, R. (1997). The Pumilio protein binds RNA through a conserved domain that defines a new class of RNA-binding proteins. *RNA* **3**, 1421-1433.

Zhang, J., and King, M. L. (1996). *Xenopus VegT* RNA is localized to the vegetal cortex during oogenesis and encodes a novel T-box transcription factor involved in mesoderm patterning. *Development* **122**, 4119-4129.

Zhang, J., Houston, D. W., King, M. L., Payne, C., Wylie, C. and Heasman, J. (1998). The role of maternal VegT in establishing the primary germ layers in *Xenopus* embryos. *Cell* **99**, 515-524

Zhao, W.M., Jiang, C., Kroll, T.T. and Huber, P.W. (2001a). A proline-rich protein binds to the localization element of *Xenopus Vg1* mRNA and to ligands involved in actin polymerization. *EMBO J.* **20**, 2315-2325.

Zhao, Z., Cao, Y., Li, M. and Meng, A. (2001b). Double-stranded RNA injection produces nonspecific defects in Zebrafish. *Dev. Biol.* **229**, 215-223.

Zhou, Y. and King, M. L. (1996a). Localization of *Xcat-2* RNA, a putative germ plasm component, to the mitochondrial cloud in *Xenopus* stage I oocytes. *Development* **122**, 2947-2953.

Zhou, Y. and King, M. L. (1996b). RNA transport to the vegetal cortex of *Xenopus* oocytes. *Dev. Biol.* **179**, 173-183.

Appendix 1

Raw data: diameters of expression domain of germ plasm RNAs

Diameter of expression domain of each germ plasm RNA was measured using an eye-piece graticule in a dissecting stereomicroscope. Numbers correspond to diameter of RNA expression domain per oocyte, measured in epu (eye-piece units).

In each case 40 epu=1mm; 1epu =25μm

For Section 7.2.4

CONT= control (uninjected) oocytes; XPAT= oocytes injected with *Xpat* mRNA. *Xcat-2= in situ* hybridisation to *Xcat-2; Xdazl= in situ* hybridisation to *Xdazl; DEADSouth= in situ* hybridisation to *DEADSouth; Xpat ORF= in situ* hybridisation to *Xpat.*

CONT *Xcat-2:*	23, 20, 18, 20, 25, 18, 19, 21, 27, 24, 16, 22, 19, 21.
XPAT *Xcat-2:*	20, 19, 19, 17, 18, 20, 27, 16, 16, 16, 20, 20, 18, 17, 16
CONT *Xdazl:*	25, 25, 23, 31, 26, 31, 30, 24.
XPAT *Xdazl:*	30, 31, 31,28, 31, 22, 27, 27, 33, 28, 26, 22, 34, 33, 28, 31, 28, 30, 29, 31, 29
CONT *DEADSouth:*	30, 23
XPAT *DEADSouth:*	22, 21, 17, 19, 22, 20, 21, 21, 22, 19
CONT *XpatORF:*	35, 25, 33, 31, 30, 31, 30, 22, 20, 27, 24, 27, 29, 23, 25, 26, 23, 23, 30, 26

For Section 3.6

Diameters of *Xcat-2* RNA expression domain in stage VI *Xenopus* oocytes.

GFP= oocytes injected with GFP, XGeq= oocytes expressing XPAT-GFP equatorially in particles, XGgran= oocytes expressing XPAT-GFP in granules at the vegetal pole.

GFP:	22, 23, 30, 20, 24, 18, 15, 20, 22, 22, 19, 18, 21, 19.
XGeq:	19, 22, 18, 17, 19, 15, 15, 20, 14, 18, 20
XGgran:	14, 15, 12

Appendix 2

Sequences of XPAT in deletion variants of XPAT-GFP

The numbers correspond to the amino acid residue positions in wild-type XPAT.

A) XPAT-GFP

```
MALKAEDSFD  IYSQLIQSFC  RYAENTTVSE  SQSPAFNAQK  EFQTCQDHAC  CTHSEAHTHI   60
LMQQWQLLEE  QWEYIDHLKT  DVAALKQLLH  GFMNSLSGTD  SGMEGTNHFL  PPHQNPTLLK  120
DEEIVASALN  RPSVDINGFE  ENITTGAQIH  AAFTKSPKKM  PATSTPRKSE  VLWSCSPTLA  180
TDGYFMLPDI  ILNPLDGKKL  VSMLRSSNYE  PHRFAELLFQ  HHVPHSLFQL  WANKVNFDGS  240
RGKLGLPRNL  MIDILHQTSK  RFVLGPKEKR  KIKTRLNLLL  RTRQDRAWWD  VGL
```

B) ΔN1

```
MQQWQLLEE  QWEYIDHLKT  DVAALKQLLH  GFMNSLSGTD  SGMEGTNHFL  PPHQNPTLLKD  121
EEIVASALN  RPSVDINGFE  ENITTGAQIH  AAFTKSPKKM  PATSTPRKSE  VLWSCSPTLAT  181
DGYFMLPDI  ILNPLDGKKL  VSMLRSSNYE  PHRFAELLFQ  HHVPHSLFQL  WANKVNFDGSR  241
GKLGLPRNL  MIDILHQTSK  RFVLGPKEKR  KIKTRLNLLL  RTRQDRAWWD  VGL
```

C) ΔN2

```
MNSLSGTDSG  MEGTNHFLPP  HQNPTLLKDE  EIVASALNRP  SVDINGFEEN  ITTGAQIHAA  152
FTKSPKKMPA  STPRKSEVLW  SCSPTLATDG  YFMLPDIILN  PLDGKKLVSM  LRSSNYEPHR  212
FAELLFQHHV  PHSLFQLWAN  KVNFDGSRGK  LGLPRNLMID  ILHQTSKRFV  LGPKEKRKIK  272
TRLNLLLRTR  QDRAWWDVGL
```

D) ΔN3

```
MPATSTPRKS  EVLWSCSPTL  ATDGYFMLPD  IILNPLDGKK  LVSMLRSSNY  EPHRFAELLF  219
QHHVPHSLFQ  LWANKVNFDG  SRGKLGLPRN  LMIDILHQTS  KRFVLGPKEK  RKIKTRLNLL  279
LRTRQDRAWW  DVGL
```

E) ΔC1

```
MALKAEDSFD  IYSQLIQSFC  RYAENTTVSE  SQSPAFNAQK  EFQTCQDHAC  CTHSEAHTHI   61
LMQQWQLLEE  QWEYIDHLKT  DVAALKQLLH  GFMNSLSGTD  SGMEGTNHFL  PPHQNPTLLK  121
DEEIVASALN  RPSVDINGFE  ENITTGAQIH  AAFTKSPKKM  PATST
```